

Characteristics and Seasonality of Particulate and Dissolved Organic Matter Discharged by the Lena River to the Arctic Coast

Dissertation

submitted in fulfilment of the requirements for the degree of
Doctor of Natural Science (Dr. rer. nat.)

by

Olga Ogneva

Doctoral colloquium: 20 February 2025

Faculty of Geosciences
University of Bremen

The work on this PhD thesis was carried out within the Marine Geochemistry and Permafrost sections of the Alfred Wegener Institute Helmholtz Centre for Polar and Marine Research (AWI) in Bremerhaven and Potsdam in Germany between August 2018 and December 2022. This work was conducted as a part of the German–British scientific research project “Changing Arctic carbon cycle in the COastal Ocean Near-shore (CACOON)”, which has been supported by the Bundesministerium für Bildung und Forschung (grant no. 03F0806A) and the Natural Environment Research Council (grant no. NE/R012806/1).

First reviewer:

Prof. Dr. Gesine Mollenhauer

Alfred Wegener Institute Helmholtz Centre for Polar and Marine Research,
Marine Geochemistry section, Bremerhaven, Germany
University of Bremen, Faculty of Geosciences, Bremen, Germany

Second reviewer:

Prof. Dr. Cindy De Jonge

Federal Institute of Technology Zurich (ETH), Department of Earth and Planetary
Sciences, Zurich, Switzerland

Supervisors:

Prof. Dr. Gesine Mollenhauer

Alfred Wegener Institute Helmholtz Centre for Polar and Marine Research,
Marine Geochemistry section, Bremerhaven, Germany
University of Bremen, Faculty of Geosciences, Bremen, Germany

Dr. Jens Strauss

Alfred Wegener Institute Helmholtz Centre for Polar and Marine Research,
Permafrost Research Section, Potsdam, Germany



"Omnia fluunt, omnia mutantur"
(*"Everything flows, everything changes"*)
- Heraclitus, ~535–475 BCE

"The future is in the past! Onwards, Aoshima!"
- Mable Pines. *Gravity Falls*, 2015

Abstract

Permafrost is considered to be a resting titan, exceptionally vulnerable to the impact of ongoing climate change. Warming temperatures intensify permafrost thawing, leading to the release of previously stored and frozen organic matter (OM) back into the active biogeochemical cycle. Once released from permafrost, OM eventually appears in lakes, streams and rivers, which carry their waters into larger water bodies. In this study, I aimed to investigate particulate and dissolved organic carbon (POC and DOC) discharged by the one of largest Arctic rivers—the Lena River—into the Arctic Ocean. While writing this work, I was deeply curious and focused on the major question: what is the composition and fate of organic matter that the Lena River transports across the continent, through its delta, to the Arctic coast?

This thesis was written to resolve this research curiosity as a part of the German–British scientific research project “Changing Arctic Carbon cycle in the COastal Ocean Near-shore (CACOON)”. The main body of this thesis comprises three manuscripts, each focusing on specific research themes.

The first manuscript, a scientific publication titled “*Particulate organic matter in the Lena River and its delta: from the permafrost catchment to the Arctic Ocean,*” was published in the journal *Biogeosciences* (DOI: <https://doi.org/10.5194/bg-20-1423-2023>). Here, the dynamics of POC were studied in the Lena River delta and compared with those in the river’s main stem using C isotopic composition to define the sources of organic matter. This study reveals that total suspended matter and POC concentrations decreased by 70 % during transit from the main stem to the delta and Arctic Ocean. Dual-carbon ($\Delta^{14}\text{C}$ and $\delta^{13}\text{C}$) isotope mixing model analyses revealed a dominant phytoplankton contribution to deltaic POC and also demonstrated an additional input of permafrost-derived OM. These results highlight the importance of deltaic and estuarine processes in shaping OM dynamics in Arctic nearshore zones.

The second manuscript “*Dissolved and Particulate Organic Carbon Characteristics in Summer and Winter Waters of the Lena Delta*” was submitted to *Permafrost and Periglacial Processes* journal. It aimed to identify sources and seasonality of organic C at the Lena delta. C isotopes ($\Delta^{14}\text{C}$ and $\delta^{13}\text{C}$) were measured in DOC and POC along a 140 km transect of the Lena delta. The study showed that DOC concentrations in the Lena delta were unexpectedly higher in winter than in summer. Isotopic analyses revealed that winter DOC showed a greater contribution of older C compared to summer DOC. These findings provide valuable insights into carbon dynamics in the largest Arctic delta, contributing to the understanding of how climate warming affects the critical interface between land and ocean.

Finally, the third manuscript "*Exploring the mysteries of GDGTs in the Arctic: Insights from the Lena Delta and Laptev Sea Nearshore*" is a draft focused on glycerol dialkyl glycerol tetraethers (GDGTs)—biomarkers used as proxies for environmental conditions. Isoprenoidal (isoGDGT), hydroxylated (OH-GDGT), branched (brGDGT), and H-shaped brGDGTs (H-brGDGTs) were extracted from POC to analyse their distribution in the Lena delta in winter and summer and along a transect to the Laptev Sea (only in summer). The result showed that IsoGDGT and OH-GDGT reflected marine influence - salinity and water temperatures. BrGDGTs, largely soil-derived, were more concentrated in winter, indicating higher terrestrial input, whereas summer levels reflected dilution by vegetation and aquatic microorganisms. H-brGDGTs, associated with peat, showed enhanced deposition near the coast, likely due to flocculation in saline waters. Additionally, this study highlighted the unique geochemical signature of Arctic river systems such as brGDGT signature with the dominance of 6-methyl isomers (IIIa', IIa') and the predominance of 5-methyl isomers (IIIa, IIa). These findings reveal how temperature, salinity, and organic matter sources shape the distribution of GDGTs in Arctic riverine and coastal systems.

Supporting the findings of my research, I added three published and co-authored manuscripts to the appendix of this thesis. First, the paper "Organic matter characteristics of a rapidly eroding permafrost cliff in NE Siberia" by Haugk et al. (2022) demonstrates how permafrost thaw and coastal erosion mobilize significant quantities of organic carbon and nitrogen, driving changes in the biogeochemistry of Arctic nearshore waters. Second, "Degrading permafrost river catchments and their impact on the Arctic Ocean nearshore processes" by Mann et al. (2022) explores the transformations and ecological impacts of permafrost-derived organic matter as it is transported from land to the ocean, highlighting its role in shaping nearshore ecosystem dynamics. Third, "Seasonal nitrogen fluxes of the Lena River Delta" by Sanders et al. (2022) expands on these insights by examining the broader implications of these processes for Arctic carbon fluxes and nutrient cycling, emphasizing the importance of nearshore zones as hotspots of change under ongoing climate warming.

Overall, this thesis provides comprehensive and multifaceted research on dissolved and particulate organic carbon in the Lena delta, including their origin, transformation during transport from the source to the Arctic nearshore zone, and seasonal changes.

Kurzfassung

Der Permafrost ist als „schlafender Riese“ bekannt, der außergewöhnlich anfällig für die Auswirkungen des fortschreitenden Klimawandels ist. Steigende Temperaturen beschleunigen das Auftauen des Permafrosts, was zur Freisetzung zuvor gespeicherten und eingefrorenen organischen Materials (OM) in den biogeochemischen Kreislauf führt. Sobald OM aus dem Permafrost freigesetzt wird, gelangt es schließlich in Seen, Bäche und Flüsse, die diese Stoffe in größere Gewässer transportieren. In dieser Studie wurde untersucht, wie partikulärer und gelöster organischer Kohlenstoff (POC und DOC) von einem der größten arktischen Flüsse – dem Lena-Fluss – in den Arktischen Ozean eingetragen wird. Dabei stand die zentrale Frage im Vordergrund: Wie setzt sich die organische Substanz zusammen, die der Lena-Fluss über den Kontinent, durch sein Delta bis zur arktischen Küste transportiert, und was wird daraus?

Diese Dissertation wurde im Rahmen des deutsch-britischen Forschungsprojekts „Changing Arctic Carbon cycle in the COastal Ocean Near-shore (CACOON)“ verfasst. Der Hauptteil dieser Arbeit besteht aus drei Manuskripten, die jeweils auf spezifische Forschungsthemen eingehen.

Das erste Manuskript, ein wissenschaftlicher Artikel mit dem Titel „*Particulate organic matter in the Lena River and its delta: from the permafrost catchment to the Arctic Ocean,*“ wurde in der Zeitschrift *Biogeosciences* veröffentlicht (DOI: <https://doi.org/10.5194/bg-20-1423-2023>). Darin wurden die Dynamiken von POC im Lena-Delta untersucht und mit denen im Hauptstrom des Flusses verglichen. Hierbei wurde die Zusammensetzung von C-Isotopen verwendet, um die Quellen der organischen Substanz zu bestimmen. Die Studie zeigt, dass die Konzentrationen von Gesamtpartikeln und POC während des Transports vom Hauptstrom über das Delta in den Arktischen Ozean um 70 % abnahmen. Die Untersuchung der Kohlestoffisotope ($\Delta^{14}\text{C}$ und $\delta^{13}\text{C}$) ergaben einen dominanten Beitrag von Phytoplankton zum POC im Delta sowie einen zusätzlichen Eintrag organischer Substanz aus Permafrost Ablagerungen. Diese Ergebnisse unterstreichen die Bedeutung deltaischer und ästuarer Prozesse für die Dynamik der organischen Substanz in den arktischen Küstenregionen.

Das zweite Manuskript „*Dissolved and Particulate Organic Carbon Characteristics in Summer and Winter Waters of the Lena Delta*“ wurde zur Veröffentlichung in der Zeitschrift *Permafrost and Periglacial Processes* eingereicht. Es hatte zum Ziel, die Quellen und die Saisonalität von organischem Kohlenstoff im Lena-Delta zu untersuchen. Kohlestoffisotope ($\Delta^{14}\text{C}$ und $\delta^{13}\text{C}$) wurden in DOC und POC entlang eines 140 km langen Transektes des Lena-Deltas gemessen. Die Studie zeigte, dass die DOC-Konzentrationen im Lena-Delta im Winter unerwartet höher waren als im Sommer.

Isotopenanalysen offenbarten, dass DOC im Winter einen größeren Anteil älteren Kohlenstoffs aufwies als im Sommer. Diese Ergebnisse liefern wertvolle Einblicke in die Kohlenstoffdynamik des größten arktischen Deltas und tragen zum Verständnis bei, wie die Klimaerwärmung die kritische Schnittstelle zwischen Land und Ozean beeinflusst.

Das dritte Manuskript „*Exploring the mysteries of GDGTs in the Arctic: Insights from the Lena Delta and Laptev Sea Nearshore*“ ist ein Entwurf eines Manuskriptes, der sich auf Glycerol-Dialkyl-Glycerol-Tetraether (GDGTs) konzentriert – Biomarker, die als Proxy für Umweltbedingungen verwendet werden. Isoprenoidale (isoGDGT), hydroxylierten (OH-GDGT), verzweigte (brGDGT) und H-förmige brGDGTs (H-brGDGTs) wurden aus POC extrahiert, um deren Verteilung im Lena-Delta im Winter und Sommer sowie entlang eines Transektes zur Laptev-See (nur an Proben aus dem Sommer) zu analysieren. Die Ergebnisse zeigen, dass isoGDGT und OH-GDGT marine Einflüsse – Salzgehalt und Wassertemperaturen – widerspiegeln. BrGDGTs, die größtenteils in Böden an Land produziert werden, waren im Winter stärker konzentriert, was auf einen höheren terrestrischen Eintrag hinweist, während die Sommerwerte eine Verdünnung durch Vegetation und aquatische Mikroorganismen zeigten. H-brGDGTs, die mit Torf assoziiert sind, zeigten eine verstärkte Ablagerung in Küstennähe, wahrscheinlich aufgrund von Flokkulation in salzhaltigem Wasser. Darüber hinaus hob die Studie die einzigartige geochemische Signatur arktischer Flusssysteme hervor, einschließlich einer brGDGT-Signatur mit einer Dominanz von 6-Methyl-Isomeren (IIIa', IIa') und der Vorherrschaft von 5-Methyl-Isomeren (IIIa, IIa). Diese Erkenntnisse zeigen, wie Temperatur, Salzgehalt und organische Substanzquellen die Verteilung von GDGTs in arktischen Fluss- und Küstensystemen prägen.

Zur Unterstützung der Ergebnisse meiner Forschung habe ich drei veröffentlichte und von mir mitverfasste Manuskripte in den Anhang dieser Dissertation aufgenommen: Der Artikel „Organic matter characteristics of a rapidly eroding permafrost cliff in NE Siberia“ von Haugk et al. (2022) zeigt, wie Permafrosttauen und Küstenerosion erhebliche Mengen organischen Kohlenstoffs und Stickstoffs mobilisieren und dadurch Veränderungen in der Biogeochemie arktischer Küstengewässer bewirken. Der Beitrag „Degrading permafrost river catchments and their impact on Arctic Ocean nearshore processes“ von Mann et al. (2022) untersucht die Transformationen und ökologischen Auswirkungen von organischen Stoffen aus dem Permafrost während ihres Transports vom Land ins Meer und hebt deren Rolle bei der Gestaltung von Küstenökosystemen hervor. Der Artikel „Seasonal nitrogen fluxes of the Lena River Delta“ von Sanders et al. (2022) knüpft an diese Erkenntnisse an, indem er die weiterreichenden Auswirkungen dieser Prozesse auf die Kohlenstoffflüsse und den Nährstoffkreislauf in der Arktis untersucht und die Bedeutung von Küstenzonen als Hotspots des Wandels im Zuge der fortschreitenden Klimaerwärmung betont.

Kurzfassung

Insgesamt liefert diese Dissertation umfassende und vielseitige Forschungsergebnisse zu gelöstem und partikulärem organischem Kohlenstoff im Lena-Delta, einschließlich deren Herkunft, Transformation während des Transports von der Quelle bis zur arktischen Küstenzone und saisonaler Veränderungen.

Contents

Abstract.....	i
Kurzfassung	iii
Contents.....	vi
List of important abbreviations	viii
1 Introduction.....	1
1.1 Permafrost in the changing climate	1
1.2 Arctic nearshore	3
1.3 Arctic rivers and organic matter discharge	5
1.4 Organic matter in waters	8
1.5 Objectives	9
1.6 Declaration of (co-) author contributions	11
2 Materials and Methods	14
2.1 The Lena River study region.....	14
2.2 Into the Arctic: field campaigns and sampling.....	15
2.3 Laboratory analyses.....	20
3 Particulate organic matter in the Lena River and its delta: from the permafrost catchment to the Arctic Ocean	24
Abstract.....	25
3.1 Introduction	26
3.2 Materials and Methods	29
3.3 Results	36
3.4 Discussion	42
3.5 Summary and Conclusions	59
References	62
Supplement.....	69
4 Dissolved and particulate organic carbon characteristics in summer and winter waters of the Lena Delta	72
Abstract.....	74
4.1 Introduction	75
4.2 Materials and Methods	77
4.3 Results	84
4.4 Discussion	89
4.5 Conclusion	96
References	97
Supporting Information	103

5	Exploring the mysteries of GDGTs in the Arctic: Insights from the Lena Delta and Laptev Sea Nearshore	105
	Abstract.....	106
	5.1 Introduction	107
	5.2 Materials and Methods	109
	5.3 Results	113
	5.4 Discussion	115
	5.5 Conclusion	125
	References	126
	Supplement.....	131
6	Synthesis and Outlook	134
	Acknowledgements.....	142
	References.....	144
	Versicherung an Eides Statt.....	151
	Appendix.....	A
	Organic matter characteristics of a rapidly eroding permafrost cliff in NE Siberia (Lena Delta, Laptev Sea region).....	A-1
	Degrading permafrost river catchments and their impact on Arctic Ocean nearshore processes..	A-18
	Seasonal nitrogen fluxes of the Lena River Delta	A-36

List of important abbreviations

AWI – Alfred Wegener Institute Helmholtz Centre for Polar and Marine Research

DOC – dissolved organic carbon

DOM – dissolved organic matter

GDGTs – glycerol dialkyl glycerol tetraether lipids

OC – organic carbon

OM – organic matter

POC – particulate organic carbon

POM – particulate organic matter

SPM – suspended particulate matter

TSM – total suspended matter

Introduction

1.1 Permafrost in the changing climate

Permafrost is a unique formation mostly spread predominately in Northern hemisphere. The permafrost region underlies approximately 22% of the Earth's exposed land surface (Obu et al., 2019), covering an estimated 21×10^6 km² of our planet. Permafrost is simply defined as ground that remains at or below 0°C for at least two consecutive years (French, 2007). Yet, this concise definition encompasses the most extensive component of the cryosphere, with its distribution spanning high-latitude regions, high mountain terrains, and elevated plateaus in mid- and low-latitude environments (Zhang et al., 2008).

Permafrost stores an enormous reservoir of carbon on Earth; it essentially freezes organic material in place, slowing microbial decomposition, which could be described as nature's own freezer. Composed largely of organic matter, including plant and animal remains (Figure 1-1b), this reservoir stores approximately 1460–1600 gigatons of carbon in the soils and permafrost of high-latitude ecosystems (within the upper 25 m of depth), which is nearly double the carbon currently present in the atmosphere (Hugelius et al., 2014, Strauss et al., 2021a).

Today, the ancient carbon reserves in permafrost are under increasing threat as global temperatures continue to rise especially in northern high-latitude regions (Rantanen et al., 2022). The vulnerability of permafrost and its stored carbon to ongoing climate change has been a major concern in numerous studies over the past 25 years (for example Schuur et al., 2015, 2022; Strauss et al, 2013, 2021 a, b and others and others referenced in this study and beyond). The permafrost is thawing from both the surface downwards and in deeper ground layers, sometimes causing ground collapse (Turetsky

et al., 2020). As permafrost soils warm, dormant microbial communities are reactivated, accelerating the decomposition of previously preserved organic matter (Figure 1-1). Although often viewed as distant and isolated, the environmental changes occurring within these permafrost zones carry global consequences, as warming enables previously locked carbon stocks to enter the atmosphere. This process releases substantial amounts of greenhouse gases—carbon dioxide (CO₂), methane (CH₄), and nitrous oxide (N₂O)—which have severe implications for global climate change (Voigt et al., 2020; Schuur et al., 2015) (Figure 1-1a). Extensive research on this topic (for example recent Oliva & Fritz, 2018; Mann et al., 2022; Schuur et al., 2022; Strauss et al., 2024) highlight the degradation of permafrost and ongoing intensification of hydrological cycles which enhance the amount and alter the type of organic carbon (OC) delivered from land to Arctic nearshore environments.

Terrestrial permafrost thaw in river catchments can release peat and permafrost-derived OC from soils into inland aquatic ecosystems (Frey & McClelland, 2009; Wild et al., 2019). Permafrost mobilized from catchments entering a river can undergo various processes, including transformation and modification during transport (Semiletov et al., 2011). Depending on environmental conditions and its inherent reactivity, it may either be re-buried through sedimentation (Vonk et al., 2019) or rapidly re-mineralized by microorganisms (Mann et al., 2015) (Figure 1-1a). This is particularly true for ice- and organic-rich Yedoma permafrost, which is considered to be of 'high quality' for microbial communities, likely due to its rapid formation during the Late Pleistocene, which limited prior processing (Mann et al., 2015, 2022; Strauss et al., 2022). Thus, the influence of thawing permafrost is not confined to terrestrial ecosystems. As organic matter is mobilized from permafrost regions, rivers play a crucial role in transporting this material downstream to Arctic coastal zones. Here, organic matter undergoes further

transformations, contributing to marine carbon cycling and reshaping coastal ecosystem dynamics.

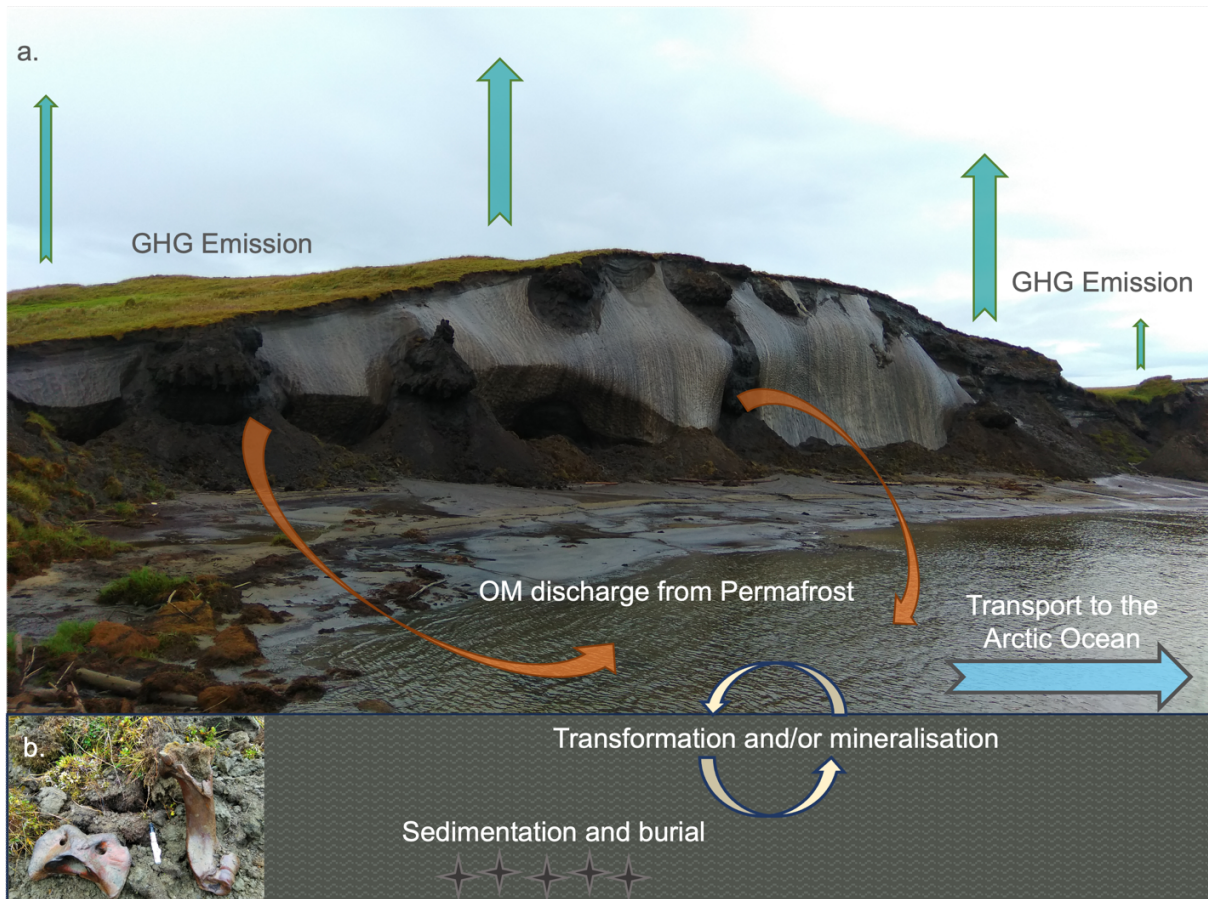


Figure 1-1. (a) Key processes occurring in the Lena River delta, illustrating the fate of organic matter mobilized from thawing Yedoma permafrost on Sobo-Sise Island. Freshly mobilized organic matter can follow multiple pathways: it may be decomposed in the terrestrial environment, contributing to GHG emissions, or, if discharged into the Lena River, it may be transported to the Arctic Ocean, or transformed/mineralized, or deposited and buried in deltaic sediments. (b) Evidence of freshly mobilized Pleistocene organic material from Yedoma deposits, including bones and plant remains.

1.2 Arctic nearshore

The Arctic coast, represents the world's largest continental shelf, (Lantuit et al., 2012), serving as a critical interaction zone between land, ocean, and atmosphere. The

nearshore zone shapes Arctic Ocean water characteristics, boundary currents, and biogeochemical profiles (Wassmann, 2015; Dethier & Harper, 2012). This area, rich in biodiversity and human activity, is among the most dynamic in the circumpolar landscape (Forbes, 2011). Despite its ecological importance, the term “coast” lacks a consistent definition. Here, we adopt Forbes et al. (2011) and ICARP’s (2007) broad definition, encompassing marine and terrestrial systems influenced by the land-ocean interface, which includes nearshore marine areas in benthic and pelagic zones as well as adjacent terrestrial areas impacted by marine processes (Forbes, 2011; ICARP-II, 2007).

Despite its volume being only 1% of the global ocean, Arctic coasts receive disproportionately high inputs of freshwater and organic matter, with around 10% of global river discharge entering the Arctic Ocean (Rachold et al., 2000). This includes contributions from 20 of the world’s 100 longest rivers, with drainage basins storing more than half of the global soil organic carbon (Shiklomanov et al., 2021). The Arctic nearshore zone is a focal area for terrestrial organic matter (OM) transformation due to high nutrient and freshwater influx.

This vital region, however, is increasingly threatened by climate change. Rising temperatures, diminishing sea ice, and extended open-water seasons in the Arctic have led to increased storm frequency and intensity, particularly in the fall (Krumpfen et al., 2019; IPCC, 2021). These changes significantly affect coastal geomorphology, infrastructure, and ecosystems. The National Snow and Ice Data Center (NSIDC) highlights that the loss of sea ice allows larger waves to reach shorelines, accelerating coastal erosion (NSIDC, 2023). Additionally, a study by Vermaire et al. (2013) discussed how Arctic warming and sea ice declines contribute to more frequent and intense storms, which further affecting coastal regions.

The Arctic coast is profoundly affected by permafrost thaw, which intensifies coastal erosion and reshapes its fragile systems (Rachold et al., 2000; Jones et al., 2020; Nielsen

et al., 2020). Erosion rates vary widely across the region, averaging 0.5 m/year but exceeding 3 m/year in areas such as the Laptev, East Siberian, and Beaufort Seas (Lantuit et al., 2012). This process increases sediment discharge and releases significant amounts of previously sequestered terrestrial organic carbon into nearshore environments (Jones et al., 2020; Tanski et al., 2019). Combined with rising temperatures, prolonged open-water seasons, and shifting hydrological patterns, permafrost thaw contributes to the disruption of sedimentation processes and the increased availability of permafrost-derived carbon, fundamentally altering the Arctic coast's role as a dynamic interface between land and sea (Tanski et al., 2019; Jong et al., 2020; Haugk et al., 2022).

Shifting hydrological cycles, such as increased river discharge and altered seasonal flow patterns, further enhance the delivery of organic inputs to nearshore waters (Juhls et al., 2020; Wang et al., 2021). These changes disrupt sedimentation processes, reducing the physical stability of coastlines and altering carbon burial efficiency (Charkin et al., 2011; Vonk et al., 2014; Bristol et al., 2024). At the same time, the increased availability of carbon and nutrients enhances phytoplankton productivity, facilitated by the extended growing season and expanded open water (Lewis et al., 2020) and subsequently alters food web dynamics, and potentially can lead to eutrophication in some areas (Back et al., 2021). Rivers act as pathways, transporting carbon and nutrients from terrestrial sources - especially from thawing permafrost - into the Arctic Ocean. This crucial role of rivers as conduits for carbon and nutrient transport underscores their significance in shaping Arctic coastal and oceanic ecosystems, warranting a closer examination of their hydrological and biogeochemical dynamics.

1.3 Arctic rivers and organic matter discharge

Arctic rivers become ice-free in early summer, discharging over 90% of their annual flow into the Arctic Ocean between May and July (Back et al., 2021). This seasonal flow regime highlights the crucial role of Arctic rivers in delivering large quantities of freshwater and

dissolved organic matter to the Arctic Ocean. In fact, the Arctic Ocean receives a disproportionately high input of freshwater and dissolved organic matter compared to other oceans (Opsahl et al., 1999), making the Arctic freshwater cycle a key driver of biological and geochemical processes. Through the transport of dissolved and particulate materials from terrestrial sources to coastal regions, these rivers exert significant influence on the Arctic's unique environmental and ecological systems.

One of the critical concerns related to the Arctic freshwater cycle is the freshening of Arctic Ocean waters due to strong continental runoff (Dittmar & Kattner, 2003; Gordeev et al., 2006;). The magnitude of this runoff is underscored by reports of significant increases in Arctic river discharge in recent decades (Bring et al., 2016; Feng et al., 2021; McClelland et al., 2016; Wang et al., 2021). This intensification is not only a result of natural hydrological processes but also driven by anthropogenic activities such as logging, mining, and dam construction, which have particularly influenced sediment discharge patterns in major river systems like the Ob and Yenisei Rivers (Bobrovitskaya et al., 2003). These alterations in sediment dynamics further underscore the complex interplay between human activity and Arctic hydrology.

The impacts of climate change have further compounded these shifts in Arctic river discharge. Substantial increases in discharge patterns have been observed across regions such as eastern Siberia, Alaska, and central Canada, pointing to a broader trend of hydrological intensification in response to warming temperatures. Expanding observation networks in these areas could significantly enhance our understanding of the Arctic freshwater cycle and its implications for the global climate system (Forryan et al., 2019). Additionally, rising temperatures are causing earlier snowmelt and river ice breakup, which prolongs and intensifies streamflow during the thawing season. This phenomenon contributes directly to permafrost degradation, a feedback loop with

serious implications for carbon release and ecosystem stability in the Arctic (Clark et al., 2001; Zheng et al., 2019; Connolly et al., 2020; Wang et al., 2021).

Among the eight largest Arctic rivers by annual discharge, six are located in Eurasia (Kolyma, Yenisei, Lena, Ob, Pechora, and Severnaya Dvina), while the remaining two (Mackenzie and Yukon) flow through North America. Together, the watersheds of these rivers span approximately 70% of the pan-Arctic drainage basin, contributing the bulk of freshwater inflow to the Arctic Ocean. Of these, the Ob, Yenisei, and Lena Rivers are particularly notable, discharging approximately 1,500 km³ of freshwater annually into the Kara Sea and an additional 800 km³ into the Laptev Sea, collectively accounting for about half of the total Arctic river runoff (Guay et al., 2001; Osadchiev et al., 2020). Among this the Lena River, in particular, stands out as the second-largest Arctic river by annual discharge. Since 1936, its discharge has grown by 15.6%, largely attributed to a striking 93% rise in winter flow rates (Ye et al., 2003; Tananaev, 2016a). In 2021, the combined discharge from the six Eurasian rivers between January and October reached 1850 km³, which represents an increase of 81 km³, or roughly 5%, compared to the 1981–2010 average (Holmes et al., 2021). The hydrological changes observed across these rivers highlight their critical role in sustaining Arctic marine ecosystems under the pressures of climate change and increasing freshwater inflow. As an Arctic River - Lena River is particularly significant due to its dramatic rise in discharge, its vast permafrost-dominated basin, and the presence of extensive Yedoma deposits, all of which make it a key system for investigating how increasing freshwater flows affect organic matter fluxes to the Arctic Ocean.

Since 2003, the hydrology and biogeochemistry of the greatest (largest) Arctic rivers (Ob, Yenisei, Lena, Kolyma, Yukon, and Mackenzie) have been measured as part of the Arctic Great Rivers Observatory (ArcticGRO; <https://arcticgreatrivers.org/>, last access: 25 November 2024). Within the framework of the ArcticGRO, depending on the year,

between four and six samples were collected per year by the ArcticGRO consortium (Holmes et al., 2021).

Although ArcticGRO provides critical data on upstream river dynamics, sampling efforts have predominantly focused on main channels, leaving processes within delta regions, such as the Lena River delta, less studied. This gap limits understanding of the biogeochemical transformations that organic matter undergoes as it transitions through deltas to the Arctic Ocean, where it may significantly alter marine carbon cycles and ecosystem functioning. Thus, sampling from the Lena River took place ~ 800 km upstream from the Lena River delta at the town of Zhigansk. This long distance from the sampling site to the areas where the river enters the Arctic Ocean, along with the deficit of information about the delta and the potential biogeochemical processes taking place there (OM transformation, sedimentation, and enrichment), may lead to a distortion or a lack of information about the final state of OM reaching the Arctic Ocean.

1.4 Organic matter in waters

The total organic matter in terrestrial and aquatic ecosystems consists of two operationally defined phases: particulate organic matter (POM) and dissolved organic matter (DOM). DOM consists of organic compounds small enough to pass through a 0.45 or 0.07 μm filter (Ma et al., 2019), while POM refers to larger organic particles that are retained by this filter. These two forms of OM differ not only in size but also in origin, composition, and reactivity, each contributing uniquely to the Arctic nearshore environment (Ewing et al., 2015).

The chemical properties of DOM and POM reflect their origins. OM may have either allochthonous (terrigenous) or autochthonous (aquatic) origins (S. Zhang et al., 2023). Allochthonous OM usually originates mainly from the runoff or leaching of organic matter from soils and higher plants in the terrestrial system (Derrien et al., 2015). This type of

DOM is typically rich in complex molecules like lignin and tannins, making it less reactive and more resistant to microbial decomposition (Amon et al., 2012). In contrast, autochthonous DOM is produced within the aquatic environment itself, primarily through the metabolic activities of aquatic organisms like algae, bacteria, plankton, and macrophytes. This form of OM is more labile and includes simpler compounds such as sugars, proteins, and organic acids, which are more readily available for microbial use (Derrien et al., 2018).

1.5 Objectives

This research aims to elucidate the sources, transformations, and seasonal dynamics of organic carbon as it transitions from Arctic river systems to coastal waters, focusing on the Lena River and its delta. By analysing both particulate and dissolved organic carbon in varying conditions, this work investigates how deltaic processes and seasonal shifts influence carbon composition, concentration, and isotopic signatures. Additionally, through the study of specific biomarkers, including glycerol dialkyl glycerol tetraethers (GDGTs), this research examines how environmental changes impact particulate organic matter and microbial indicators within the Arctic nearshore zone. Overall, this thesis contributes to a deeper understanding of the role Arctic river systems play in coastal carbon cycling and their response to environmental variability.

The core of this thesis consists of three chapters, each representing a separate publication (published, submitted, or in draft form). The specific objectives of each chapter are outlined below.

1.5.1 Objectives of manuscript 1

The aim of the study “Particulate organic matter in the Lena River and its delta: from the permafrost catchment to the Arctic Ocean” was to determine the dominant sources of particulate organic carbon (POC) within the Lena River and its delta, and investigate how

deltaic processes influence the composition and concentration of POC in the transition from the river to the Arctic Ocean. The specific research questions were:

Q1.1: What transformations does POC undergo during the transport from the Lena River catchment to the delta, and how do these processes influence its spatial distribution and concentration?

Q1.2: What is the composition of POC in the Lena delta and how does this differ from the POC composition in the river's main stem?

1.5.2 Objective of manuscript 2

In "Dissolved and Particulate Organic Carbon Characteristics in Summer and Winter Waters of the Lena Delta", it was the aim to decipher how the supply, sources, and composition of dissolved and particulate organic carbon (DOC and POC) in the Lena River Delta differ between winter and summer, and how these seasonal conditions influence carbon modifications during transit through the delta. The specific research questions were:

Q2.1: How do DOC and POC concentrations vary between winter and summer in the Lena delta?

Q2.2: What are the primary sources and seasonal transformation processes for DOC in the Lena delta?

1.5.3 Objective of manuscript 3

The manuscript draft "Exploring the mysteries of GDGTs in the Arctic: Insights from the Lena Delta and Laptev Sea Nearshore" aims to examine the seasonal and spatial patterns of OM in the Lena delta and Arctic nearshore. Therefore, I have chosen to investigate glycerol dialkyl glycerol tetraether (GDGT) biomarkers in particulate organic matter within the Lena delta and Arctic nearshore, focusing on how these patterns reflect

environmental shifts and highlight distinctive Arctic river influences. The specific research questions were:

Q3.1: What are the seasonal and spatial distribution dynamics of glycerol dialkyl glycerol tetraethers (GDGTs) in the Lena delta and the Laptev Sea nearshore zone?

Q3.2: What do dynamics of GDGTs distribution across the delta-to-nearshore transect reveal about the role of Arctic rivers in modulating particulate organic matter and microbial biomarkers in Arctic coastal systems?

The objectives of this thesis are strongly connected to key questions in permafrost carbon research, particularly addressing how much carbon is released from permafrost systems, the pools from which it originates, and the processes following its release. By investigating both particulate and dissolved organic carbon through spatial, seasonal, and biomarker analyses, this work provides new insights into carbon dynamics in Arctic river systems and contributes to a broader understanding of how Arctic deltas mediate the release, transport, and transformation of carbon, addressing fundamental questions about the fate of permafrost carbon in a changing climate.

1.6 Declaration of (co-) author contributions

This cumulative dissertation comprises three first-author manuscripts. The following sections outline the individual (co-)author contributions to each scientific paper and provide the status of the manuscripts.

1st manuscript: *Particulate organic matter in the Lena River and its delta: from the permafrost catchment to the Arctic Ocean*

Olga Ogneva, Gesine Mollenhauer, Bennet Juhls, Tina Sanders, Juri Palmtag, Matthias Fuchs, Hendrik Grotheer, Paul J. Mann, and Jens Strauss

Published on 12 April 2023 in *Biogeosciences* (DOI: 10.5194/bg-20-1423-2023)

OO, GM, JS designed and planned the study. TS, MF, JP, JS, and OO carried out the fieldwork and collected the samples in the Arctic. OO carried out laboratory analyses. BJ designed the maps. HG provided R code for endmember analysis. OO performed data analysis and wrote the paper with the key contributions and guidance of GM and JS. All co-authors contributed to the editing processes.

2nd manuscript: “Dissolved and Particulate Organic Carbon Characteristics in Summer and Winter Waters of the Lena Delta”

Olga Ogneva, Gesine Mollenhauer, Tina Sanders, B. Juhls, J. Palmtag, M. Fuchs, J. Hammes, H. Grotheer, P. J. Mann, S. Opfergelt and J. Strauss

Submitted to *Permafrost and Periglacial Processes* journal on June 27 2024.

OO, GM, JS designed and planned the study. TS, MF, JP, JS, and OO carried out the fieldwork and collected the samples in the winter and summer Arctic. OO carried out laboratory analyses, including radio C measurements, with the help of HG. OO performed data analysis and wrote the paper with the key contributions and guidance of GM and JS. SO and BJ provided insightful advice and suggestions. All co-authors contributed to the editing processes.

3rd manuscript “Exploring the mysteries of GDGTs in the Arctic: Insights from the Lena Delta and Laptev Sea Nearshore”

Introduction

Olga Ogneva, Gesine Mollenhauer, Jens Hefter, Bingbing Wei, Tina Sanders, Juri Palmtag, Matthias Fuchs Laura Kattein and Jens Strauss

Complete draft

OO, GM, JS designed and planned the study. TS, MF, JP, JS, and OO carried out the fieldwork and collected the samples in the winter and summer Arctic. LK and JH assisted with biomarkers extraction. OO performed data analysis including biomarker quantification and interpretation, with the guidance of JH. BW helped with the interpretation of GDGTs indexes and proxy. OO wrote the paper with the key contributions of GM and JS. All co-authors contributed to the editing processes.

Materials and Methods

In this chapter, I aim to provide an overview of the study area and methodological aspects of this dissertation, focusing on the field campaigns and sampling efforts, while also touching upon the laboratory methods, whose details are covered in the relevant manuscripts. However, the journeys that brought this dissertation to life—our expeditions—often remain in the shadows, despite undoubtedly deserving to be illuminated.

2.1 The Lena River study region

Originating at 53° N near Lake Baikal and flowing northward to 71° N, where it reaches the Laptev Sea, the Lena River stretches approximately 4,400 km. Its vast basin covers an area of about 2.61 million km², the majority of which is characterized by permafrost—predominantly continuous permafrost, accounting for 70.5% (Obu et al., 2019; Juhls et al., 2020). The landscape of the Lena River basin is dominated by taiga forests (72%) and tundra ecosystems (12%) (Amon et al., 2012). As it traverses eastern Siberia, the river collects organic material from a variety of sources, including Pleistocene and Holocene Yedoma deposits. These ancient deposits, though occupying just 3.5% of the basin, represent an important reservoir of organic matter susceptible to mobilization under changing environmental conditions (Strauss et al., 2013, 2021b). Further downstream, the Lena River delta spans an area of 28,500 km², making it the largest delta in the Arctic

and one of the largest in the world (Semiletov et al., 2011a). The presence of Yedoma in the delta highlights its critical role in organic matter transformation, sedimentation, and nutrient cycling as the river delivers material to the Arctic Ocean.

To summarize, the Lena River was chosen for this study due to its significant role in shaping Arctic freshwater and organic matter dynamics. Its large discharge, increasing due to climate-induced changes, and its unique basin composition—including extensive permafrost and Yedoma deposits—make it a critical system for understanding how rising river flows influence the transport and transformation of organic matter to the Arctic Ocean.

2.2 Into the Arctic: field campaigns and sampling

During the CACOON project, two field campaigns were conducted in the Lena delta. The first, referred to as the "winter" campaign, took place in late March to early April, a time when the Lena River and the Laptev Sea remained covered in ice and cold, but the return of the sun made the work easier and more enjoyable (Figure 2-1). The second, a summer campaign, aimed to resample the same locations from the winter expedition to capture the seasonal variations in the studied parameters.

Starting from Tiksi—a tiny port town on the edge of East Siberia,—we set out with the ambitious goal of reaching as far as possible on the sea ice and then into the Lena delta. The aim was to capture the widest possible salinity gradient from the river to the shelf. Our camp was a mobile sledge caravan, consisting of a house on sledges used for accommodation and laboratory work, pulled by a caterpillar tractor with a freight sledge carrying our tools and samples (Figure 2-1a). A "Vezdekhod"—a caterpillar all-terrain vehicle—led the way, scouting the ice conditions and atmosphere ahead of the journey. There were ten of us in total: five crewmembers and five scientists. The scientific team

from AWI included O. Ogneva, M. Fuchs, J. Palmtag, and our expedition & project leader, J. Strauss (Figure 2-1b).

Our planned sampling route spanned a 100 km east-to-west transect, beginning offshore and ending at the mouth of the Sardakhskaya channel. However, right on our way, on day four, in the vastness of the mighty Arctic desert, we reached a place that our crew—locals—told us was the southern border of polar bear territory, a spot where we might have been lucky (or unlucky) to encounter these awe-inspiring creatures. But there, at 72.5255°N; 129.8648°E, an unbreachable crack awaited us (Figure 2-1b), stretching to the north and east. Around 5 meters wide, with ice so thin it revealed open water beneath, it stopped us in our tracks, making it impossible to complete the transect on the shelf.

We had to adapt to these circumstances, and we did so with great success—not losing the spark of the research but striking a new one. Instead of the original plan, we shifted to an alternative sampling strategy and focused on a transect upstream, targeting a heavily eroding Yedoma permafrost cliff ~40 km upstream of the Sardakhskaya channel, with sampling locations spaced every 5 km.

At each site, we drilled a borehole through the ice and collected environmental data using a Multiparameter Water Quality Sonde (measuring water depth, salinity, pH, dissolved oxygen, conductivity, and more). We also retrieved 20 L of water through multiple deployments of a 5 L water sampler (UWITEC, Austria). Sampling was performed at one to three depths per station, depending on the site's bottom depth. Water was always collected directly beneath the ice (approximately 2 m). For sites with river depths exceeding 4–7 m, we collected an additional sample just above the bottom (4–7 m). At sites with depths >7 m, we also collected a sample from the mid-depth between the under-ice and bottom samples.



Figure 2-1. Winter campaign in the Lena delta. (a) Our mobile caravan consisting of "Vezdekhod"—a caterpillar all-terrain vehicle, a house on sledges, a tractor and a freight sledge. (b) The team in front of an ice crack (from left to right: O.Ogneva, J.Palmtag, M.Fuchs & J. Strauss). (c) Transportation of water samples between locations during sampling. (d) Yedoma cliff at Sobo-Sise Island in winter.

To meet the broader project requirements—though not used for this dissertation—we also collected three ice cores using a Kovacs Mark II ice corer and up to two UWITEC (gravity corer) short cores from surface sediments at selected locations. Additionally, gas samples (CO_2 , N_2O , or CH_4), snow samples, and snow depth measurements were taken at each site. The expedition spanned from 25 March 2019 to 10 April 2019, with active water sampling conducted between 29 March and 5 April.

The second sampling campaign was carried out in summer from 28.7.2019 to 23.08.2019. It included three parts – the first part (was a sea cruise on the Laptev Sea

with the vessel *Anatoliy Zhilinskiy*, the second part was a river cruise on the Sardakhskaya channel with the ship *Merzlotoved* and the third part included intensive laboratory work on Samoylov Research Station. The first part of the “CACOON Sea” expedition took us to the Laptev Sea nearshore zone, where we managed to sample as planned —no ice cracks stopped us, thanks to the absence of ice, nor did the rolling seas, driven away by our strong sampling motivation and the team’s adventurous spirit (O. Ogneva, T. Sanders, M. Fuchs, and W. Schneider).

We began the cruise on 2 August 2019 at 18:00, leaving Bykov Mys and heading south along the Bykovsky Peninsula, following the shipping channel. At the southern tip of the peninsula, we turned east until we reached the 12-mile zone border. From there, we travelled northeast and reached the first sampling site on 3 August 2019 at 06:30, where we started sampling right away. We worked our way west along the planned transect, stopping every 10 km for sampling, until the shallow waters brought us to the last station—the *Anatoliy Zhilinskiy* could not go any further.

Our return journey took us south to the 12-mile zone, then west to the southern tip of the Bykovsky Peninsula, and finally north back to Bykov Mys. However, as fate would have it, the *Anatoliy Zhilinskiy* was stuck in the shallow waters near Bykov Mys. Luckily, the *Merzlotoved*, our freshwater vessel, came to the rescue and pulled us from the seaboard.

The second route of the expedition began on 7 August 2019, with the CACOON crew departing from Samoylov Island aboard the ship *Merzlotoved*. *Merzlotoved* mean ‘Permafrost researcher’ in English, a very fitting name for the aim of this expedition. On the first day, we sailed all the way to Sobo-Sise Island, where we spent the evening under the soft glow of the polar night. We watched the eroding Yedoma cliff, searched for

Pleistocene animal bones (Figure 1-1b), and listened to the sound of falling chunks from the Yedoma wall—a surreal and humbling experience.

The next day, the cruise continued as we reached the edge of the delta. From there, we began sampling our way back, stopping every 5 km to revisit our winter sampling locations. Some locations (at the edge of the delta) were very shallow, preventing Merzlotoved from accessing them. In these cases, we used a flat bottom boat to reach the sites (Figure 2-2c). That night, the ship returned to the base of the Sobo-Sise cliff. On the final day, Merzlotoved made its way back to Samoylov Island, sampling stations at intervals of 10 km, and later 20 km, as we completed our journey.

Like in the winter, during sampling in summer both sea and river we also retrieved 20 L of water through multiple deployments of a 5 L water sampler (UWITEC, Austria) (Figure 2-2b). Sampling was performed at one to three depths per station, depending on the site's bottom depth. Also at every site we deployed CTD (conductivity, temperature, depth) instrument (Figure 2-2a).

The final part of the expedition involved preliminary water sampling preparation in the laboratory at the Samoylov Island station, where we stayed during the expedition. There, I filtered the collected water to separate organic matter, preparing samples with DOC only and filters for further POC and biomarker analysis (see next chapter).



Figure 2-2. Summer campaign in the Lena delta. (a) Conductivity, Temperature, and Depth (CTD) instrument used for measurements. (b) A 5 L water sampler filled with collected water. (c) Using a flat-bottom boat to access distant sampling locations.

2.3 Laboratory analyses

2.3.1 Total Suspended Matter (TSM), Particulate Organic Carbon (POC), and Dissolved Organic Carbon (DOC)

Water samples were filtered either immediately on-site during the winter campaign or within 10 days at the Samoylov Island research station during the summer campaign (10

days water was stored at 4°C). For TSM and POC, 400 mL of water was filtered through pre-weighed and pre-combusted (4.5 h at 450°C) glass fibre filters (GF/F Whatman, 0.7 µm nominal pore size, 25 mm diameter). Filters with TSM/POC were stored frozen at -18°C in pre-combusted glass petri dishes, and later dried at 40°C for 24 hours to determine TSM concentration. The difference in filter weights before and after filtration was used to calculate TSM concentration per unit volume of water (mg L⁻¹).

For POC analysis, selected filters were acidified with 10% HCl to remove inorganic carbon. After drying again at 40°C, the filters were packed into tin boats. POC content (mg C) was measured using a Sercon 20–20 isotope ratio mass spectrometer (IRMS) coupled to an automated nitrogen carbon analyser (ANCA). POC concentration (mg L⁻¹) was then calculated by dividing the total POC content per filter by the volume of water filtered through that filter.

For DOC, filtered water (GF/F Whatman, 0.7 µm) was stored frozen at -18°C until analysis. DOC concentrations (mg C L⁻¹) were measured using a high-temperature catalytic oxidation analyser (TOC-VHPH Shimadzu) at the Alfred Wegener Institute (AWI) in Potsdam. Calibration was conducted using five certified standards covering a range from 1.26 to 27.31 mg C L⁻¹, with a precision of ±10%.

2.3.2 Radiocarbon ($\Delta^{14}\text{C}$) and stable Carbon ($\delta^{13}\text{C}$) isotopes

Radiocarbon analyses ($\Delta^{14}\text{C}$) were conducted using a Mini Carbon Dating System (MICADAS) at the Alfred Wegener Institute (AWI) in Bremerhaven, following the procedure described by Mollenhauer et al. (2021). MICADAS, a state-of-the-art accelerator mass spectrometer, allows precise measurements of radiocarbon in small sample sizes, making it particularly suitable for environmental and geochemical studies. Samples were prepared by removing inorganic carbon through acidification, followed by

drying and packing into tin capsules. Radiocarbon data were normalized against international standards, including oxalic acid II (OxAll, NIST SRM4990C), and corrected for sampling time and $\delta^{13}\text{C}$ to account for isotopic fractionation. To ensure accuracy, blank corrections were applied using five empty combusted filters that underwent identical preparation as the samples. The $\Delta^{14}\text{C}$ results were expressed in ‰ relative to the absolute international standard (reference year 1950) and classified into three categories for interpretation: “ancient” ($\Delta^{14}\text{C} < -900$ ‰ or $\sim 18,500$ radiocarbon years), “old” (-50 ‰ $\geq \Delta^{14}\text{C} \geq -900$ ‰ or ~ 400 – $18,500$ radiocarbon years), and “young/modern” ($\Delta^{14}\text{C} > -50$ ‰ or < 400 radiocarbon years; Stuiver & Polach, 1977).

Stable carbon isotope ($\delta^{13}\text{C}$) analyses were performed on a Sercon 20–20 isotope ratio mass spectrometer (IRMS) coupled with an automated nitrogen carbon analyser (ANCA). $\delta^{13}\text{C}$ values were expressed in per mil (‰) relative to the Pee Dee Belemnite (PDB) standard. Calibration was conducted using in-house and certified standards (isoleucine, NIST RM 8573, USGS40), ensuring a precision of ± 0.2 ‰. POC content per filter was divided by the volume of water filtered to determine POC concentrations.

2.3.3 Biomarkers: Glycerol Dialkyl Glycerol Tetraethers (GDGTs)

Water samples for GDGT analysis were filtered through pre-combusted (4.5 h at 450°C) glass fiber filters (GF/F Whatman, $0.7\ \mu\text{m}$ nominal pore size, 142 mm diameter, Figure 2-3) during the winter campaign or within 10 days of collection during the summer campaign at the Samoylov Island research station. Filters were stored frozen at -18°C in pre-combusted aluminium foil envelopes until processing.

For analysis, filters were dried at 45°C , cut into small pieces, and lipids were extracted three times using ultra sonication in a dichloromethane (9:1, v/v) solvent mixture, with a C46-GDGT standard added. Extracted lipids were fractionated using silica gel

chromatography, and the GDGT-containing polar fraction was eluted with methanol (1:1, v/v), dried, and re-dissolved in 2-propanol (99:1, v/v).

GDGTs were analysed using an Agilent 1260 Infinity II UHPLC-MS system following established methods (Hopmans et al., 2016). Chromatographic separation was achieved using two UPLC silica columns under controlled temperature and gradients (see manuscript 3 for further details). GDGTs were detected using atmospheric pressure chemical ionization-mass spectrometry (APCI-MS) in positive ion mode. Selective ion monitoring (SIM) was applied to detect key GDGT ions, including 5- and 6-methyl isomers of branched GDGTs (brGDGTs) and isoprenoidal GDGTs. The APCI-MS settings included a nebulizer pressure of 50 psi, vaporizer and drying gas temperatures of 350°C, a capillary voltage of 4 kV, and a corona current of +5 μ A. Quantification was performed relative to the internal C46-GDGT standard (Schouten et al., 2007).



Figure 2-3. Glass fibre filters (GF/F Whatman, 0.7 μ m nominal pore size, 142 mm diameter) containing suspended matter, just taken out from the filtration system after filtering 12 L of water. The filtration was conducted in the laboratory at the Samoylov Research Station in the Lena Delta for subsequent biomarker analyses.

Particulate organic matter in the Lena River
and its delta: from the permafrost
catchment to the Arctic Ocean

Particulate organic matter in the Lena River and its Delta: From the permafrost catchment to the Arctic Ocean

Olga Ogneva^{1,2,3}, Gesine Mollenhauer^{1,3}, Bennet Juhls², Tina Sanders⁴, Juri Palmtag^{5,a}, Matthias Fuchs², Hendrik Grotheer¹, Paul J. Mann⁵ and Jens Strauss²

¹Marine Geochemistry Section, Alfred Wegener Institute Helmholtz Centre for Polar and Marine Research, Bremerhaven, 27570, Germany

²Permafrost Research Section, Alfred Wegener Institute Helmholtz Centre for Polar and Marine Research, Potsdam, 14473, Germany

³Faculty of Geosciences, University of Bremen, Bremen, 28359, Germany

⁴Institute for Carbon Cycles, Helmholtz Centre Hereon, Geesthacht, 21502, Germany

⁵Department of Geography and Environmental Sciences, Northumbria University, Newcastle-upon-Tyne, NE1 8ST, UK

^anow at: Department of Human Geography, Stockholm University, Stockholm, Sweden

Correspondence to: Olga Ogneva (Olga.Ogneva@awi.de), Gesine Mollenhauer (Gesine.Mollenhauer@awi.de) and Jens Strauss (Jens.Strauss@awi.de)

Abstract

Rapid Arctic warming accelerates permafrost thaw, causing an additional release of terrestrial organic matter (OM) into rivers, and ultimately, after transport via deltas and estuaries, to the Arctic Ocean nearshore. The majority of our understanding of nearshore OM dynamics and fate has been developed from freshwater rivers, despite the likely impact of highly dynamic estuarine and deltaic environments on transformation, storage, and age of OM delivered to coastal waters. Here, we studied particulate organic carbon (POC) dynamics in the Lena Delta and compared it with POC dynamics in the Lena River main stem along a ~1600 km transect long from Yakutsk, downstream to the delta. We measured POC, total suspended matter (TSM), and carbon isotopes ($\delta^{13}\text{C}$ and $\Delta^{14}\text{C}$) in POC to compare riverine and deltaic OM composition and changes in OM source and fate during transport offshore. We found that TSM and POC concentrations decreased by 70 %, during transit from the main stem to the delta and Arctic Ocean. We found deltaic POC to be strongly depleted in ^{13}C relative to fluvial POC. Dual-carbon ($\Delta^{14}\text{C}$ and $\delta^{13}\text{C}$) isotope mixing model analyses indicated a significant phytoplankton contribution to deltaic POC (~68 ± 6 %) and suggested an additional input of permafrost-derived OM into deltaic waters (~18 ± 4 % of deltaic POC originates from Pleistocene deposits vs ~

5 ±4% in the river main stem). Despite the lower concentration of POC in the delta than in the main stem (0.41 ±0.10 vs. 0.79 ±0.30 mg L⁻¹, respectively), the amount of POC derived from Yedoma deposits in deltaic waters was almost twice as large as POC of Yedoma origin in the main stem (0.07 ±0.02 and 0.04 ±0.02 mg L⁻¹, respectively). We assert that estuarine and deltaic processes require consideration in order to correctly understand OM dynamics throughout Arctic nearshore coastal zones and how these processes may evolve under future climate-driven change.

3.1 Introduction

Arctic rivers contribute substantial quantities of freshwater and organic matter (OM) to the Arctic Ocean, thereby influencing coastal patterns of stratification, ocean chemistry, and biogeochemistry. These freshwater and OM loads originate from an extensive accumulated pan-Arctic watershed area larger than the Arctic Ocean itself (Terhaar et al., 2021). Arctic rivers, therefore, provide an integrated signature of processes and changes occurring across Arctic watersheds. In these Arctic watersheds, soils and permafrost contain between 1460 - 1600 gigatons of organic carbon (C: within the upper 25 m depth) (Hugelius et al., 2014; Strauss et al., 2021a), corresponding to about 2.5 times as much C as in the current atmosphere and more than half of the organic C stored in soils globally (Köchy et al., 2015). Annual Arctic air temperatures have risen by more than four times the magnitude of the global mean air temperature rise (Rantanen et al., 2022), with warming in winter being four times greater than in summer (Ballinger et al., 2020). Precipitation is increasing as well and is projected to be >50 % higher by 2100 (Overland et al., 2014). In response to warming air temperatures, permafrost is thawing (Biskaborn et al., 2019; Fox-Kemper et al., 2021).

Permafrost can modify fluvial processes and their functioning, for example via the occurrence of surface runoff from hillslopes and sediment erosion in river valleys and channels (Tananaev & Lotsari, 2022). Permafrost thaw has consequences for river

discharge in several ways. Deepening of the seasonal active layer and release of waters from melting ground ice result in intensified summer river runoff and increased groundwater storage (Walvoord & Striegl, 2007). In addition, the delayed active layer freeze-up increases winter river runoff (Walvoord & Kurylyk, 2016; Lamontagne-Hallé et al., 2018; Wang et al., 2021a). Enhanced terrestrial permafrost thaw and intensification of hydrological cycles have the potential to enrich Arctic rivers with remobilised OM and nutrients, modifying food web dynamics and changing the connectivity between terrestrial landscapes and nearshore ecosystems (Brown et al., 2019; Terhaar et al., 2021; Mann et al., 2022). Thus, together with rising temperatures, precipitation, and changes in evapotranspiration, permafrost degradation alters the biogeochemical cycle of the rivers and the freshwater cycle of the Arctic and ultimately modifies river discharge (Carmack et al., 2016; Lique et al., 2016; Vihma et al., 2016; Oliva & Fritz, 2018; Brown et al., 2019; Yang et al., 2021). Permafrost degradation and associated active layer thickening accelerates riverine carbonate, nitrogen, and phosphorus exports (Zhang et al., 2021) and provides additional C of permafrost origin, especially in summer, fall, and winter (Wild et al., 2019). The permafrost mobilised from catchments that enters a river can subsequently undergo a variety of processes. Once mobilised, OM from permafrost is susceptible to transformation and modification during transport (Vonk et al., 2019). Upon discharge into, and offshore transport within, the Arctic Ocean (Bröder et al., 2018) it is re-buried in marine sedimentary depo-centres, where it is either being removed from the active C cycle or re-mineralised further (Grotheer et al., 2020).

The nearshore coastal zone of the Arctic Ocean (including deltas, estuaries, and coasts) is of great importance as a location of terrestrial organic matter burial (Lisitzin, 1994), but also as a biogeochemically active area where major transformation processes of terrestrial material are expected to take place (Tanski et al., 2019; Jong et al., 2020; Sanders et al., 2022). Despite the importance of Arctic estuarine and deltaic

environments in OM biogeochemistry, their functioning is still poorly understood; coastal ocean dynamics are inferred from freshwater endmembers based purely on riverine OM properties. Since 2003, the hydrology and biogeochemistry of the greatest (largest) Arctic rivers (Ob, Yenisei, Lena, Kolyma, Yukon, and Mackenzie) have been measured as part of the Arctic Great Rivers Observatory (ArcticGRO; <https://arcticgreatrivers.org/>). Historical records together with ArcticGRO data have demonstrated that the long-term increasing freshwater discharge trend has been most pronounced for rivers across the Eurasian Arctic, constituting the strongest evidence of Arctic freshwater cycle intensification (Feng et al., 2021; Shiklomanov et al., 2021a).

Within the framework of the ArcticGRO, depending on the year, between 4 and 6 samples per year were collected by ArcticGRO consortium (Holmes et al., 2021). Samples characterising the OM from the largest Arctic rivers are taken directly from the rivers' main stems rather than from their deltas and estuaries. For example, sampling from the Lena River, the river which transports the largest amount of particulate organic C (POC) of all Arctic rivers (McClelland et al., 2016) to the Arctic Ocean and has one of the world's biggest deltas (Fedorova et al., 2015), took place ~800 km upstream from the Lena Delta at the town of Zhigansk. This long distance from the sampling site to the areas where the river enters the Arctic Ocean, and the deficit of information about the delta and the potential biogeochemical processes taking place there (OM transformation/sedimentation/enrichment) may lead to a distortion or a lack of information about the final state of OM reaching the Arctic Ocean.

In this study, we aim to bridge this gap by characterizing POC along the Lena River over a transect from the upper reaches of the Lena River near Yakutsk (approximately 1640 km from the coast) north to the Lena Delta in order to decipher the distribution, main sources, and transformation of particulate organic matter (POM) on its way from the permafrost catchment to the Arctic Ocean. Our findings show that the concentration and

composition of the POC pool are highly dynamic during transport and that the transformation and storage of riverine OM need to be accounted for when examining contemporary and projecting future changes in coastal processes.

3.2 Materials and Methods

3.2.1 Study area

The Lena River is one of the greatest Arctic rivers. It discharges approximately $543 \text{ km}^3 \text{ yr}^{-1}$ of water into the Laptev Sea, (mean annual discharge in the period 1936 – 2019) (Wang et al., 2021b) which is the second-largest amount of water discharged into the Arctic Ocean of all Arctic rivers (Gordeev, 2006; Holmes et al., 2018). The Laptev Sea is a marginal sea of the Arctic Ocean and is a key region controlling the sea-ice formation and drift patterns (Krumpfen et al., 2019). Together with the East Siberian Sea and the Russian part of the Chukchi Sea it constitutes the largest shelf system in the Arctic: The East Siberian Arctic Shelf.

The Lena River is 4400 km long from its origin at 53°N , north of Lake Baikal, to 71°N , where it reaches the Laptev Sea. It drains an area of $\sim 2.61 \times 10^6 \text{ km}^2$, of which more than 94 % is assumed to be underlain by permafrost (mainly continuous: 70.5 %) (Obu et al., 2019; Juhls et al., 2020) and is covered by taiga forest (72 % coverage) and tundra ecosystems (12 %) (Amon et al., 2012). Running from the south to the north of East Siberia, the Lena River receives OM from various sources within its basin such as Holocene and Pleistocene deposits (Yedoma), which are widespread across the region and cover approximately 3.5 % of the Lena watershed area (Strauss et al., 2013, 2021b). The Lena River watershed was subdivided into the Aldan and Vilyuy catchments, Upper and the Lower Lena, which contribute differently to the TSM and water discharge into the Lena River and are characterised by distinct morphologies (Figure 3-1a). Here, we define the Aldan and Vilyuy catchments, the Upper and Lower Lena River by the area of

subcatchments of the Lena River using the HydroSheds database (Lehner & Grill, 2013) and follow the terminology for the subcatchments of Kutscher et al. (2017) and Liu et al. (2005). The separation between the Upper and Lower Lena was defined approximately 150 km downstream from Yakutsk (Figure 3-1a). The Upper Lena includes the southern limits of the river and the catchment upstream of the Aldan junction. Its watershed covers an extensive area between Lake Baikal and Yakutsk and includes dozens of tributaries including creeks and small rivers. The Lower Lena consists of the catchment area downstream of the Aldan junction excluding the catchments of Aldan and Vilyuy. It flows from downstream of Yakutsk into the Laptev Sea and receives waters from catchments including the Verkchoyansk Range (Figure 3-1a). The delta of the Lena River occupies an area of $28.5 \times 10^3 \text{ km}^2$; it is the largest delta in the Arctic on the Eurasian continent, and one of the biggest deltas in the world (Semiletov et al., 2011). The Lena main stem reaches Stolb Island at the apex of the Lena Delta (Figure 3-1a); there it divides into numerous branches and more than 800 transverse channels with a total length of 6500 km, forming the delta (Fedorova et al., 2015). About 80-90 % of Lena River derived water and 85 % of sediments enter the eastern Laptev Sea along two major branches: the Sardakhskaya-Trofimovskaya system (accounting for 60-75 % of Lena River water and up to 70 % of sediment discharge, with the Sardakhskaya branch itself transporting 23-33 %) and the Bykovskaya branch (20-25 % of water and up to 15 % of sediment discharge) (Ivanov & Piskun, 1999; Charkin et al., 2011). The other two main branches are the Olenekskaya and Tumanskaya (together transporting 5-10 % of water and 10 % of sediment discharge) which flow towards the western and central Laptev Sea (Charkin et al., 2011).

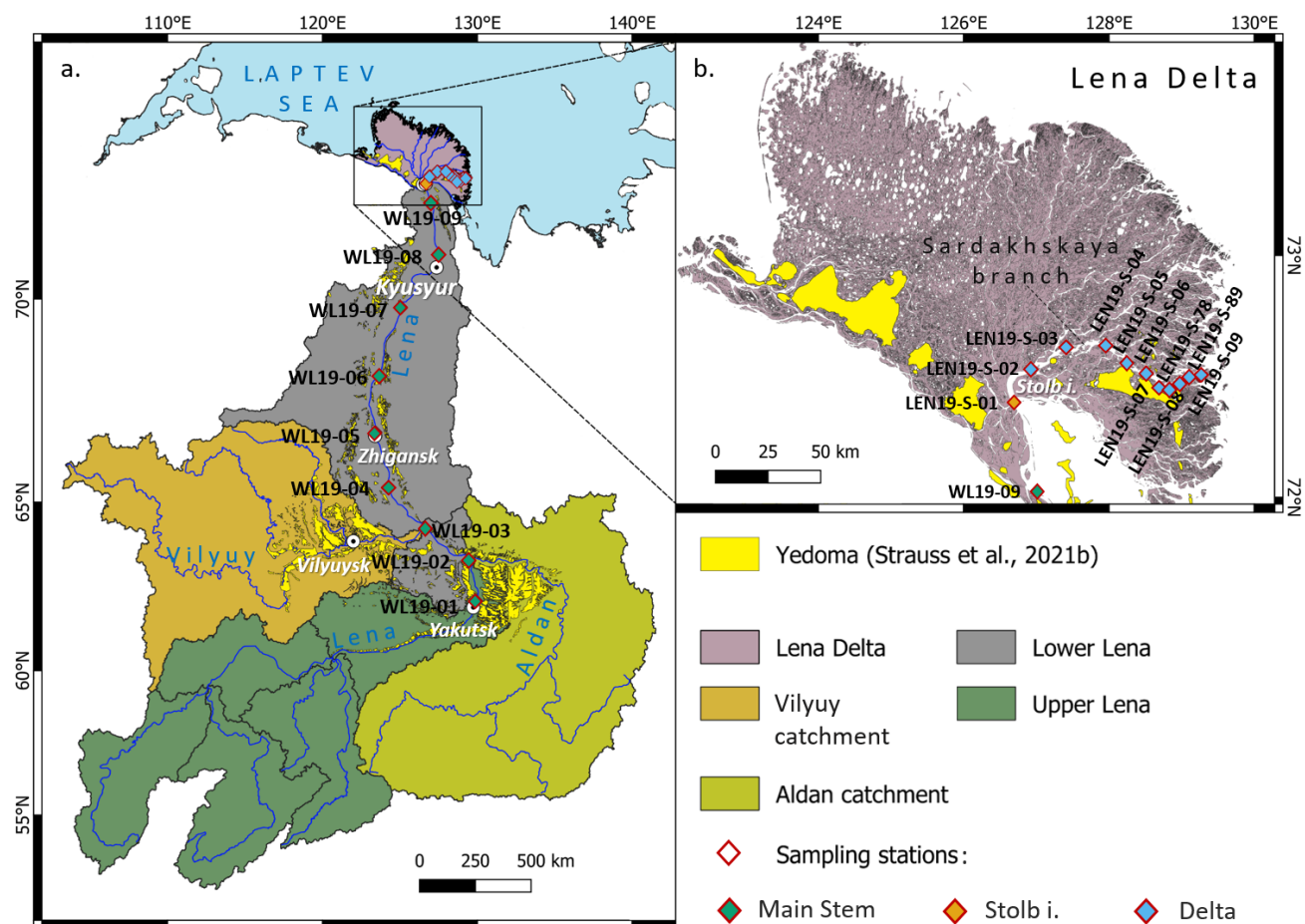


Figure 3-1. The Lena River catchment and its Delta with Yedoma distribution (Strauss et al., 2021b) in the catchment area. a) Sampling locations along the Lena River main stem ($n = 9$) and the Lena River catchment area; b) Sampling locations at Stolb Island ($n = 3$) and in the Lena Delta along the Sardakhskaya branch ($n = 20$).

Nowadays, constant patterns of shifting temperature and precipitation regimes are observed in the Lena watershed (Pohl et al., 2020) which is characterised by permafrost and is particularly sensitive to climate change. Thus, over the past 84 years, the discharge of the Lena River has increased by 22 % (Wang et al., 2021b) and reached as much as $626 \text{ km}^3 \text{ yr}^{-1}$ for the years 2016-2018 compared to an average of $557 \text{ km}^3 \text{ yr}^{-1}$ in the years 1981-2010 (Holmes et al., 2019). Nevertheless, characteristics of OM discharged from the Lena River are measured by ArcticGRO, which collects water samples near Zhigansk,

located ~800 km upstream from the Lena Delta. It is also known that a significant fraction of suspended matter carried by the Lena River is deposited before the Lena reaches Kyusyur, along a narrow part of the Lena main stem so-called "Lena Pipe" (Semiletov et al., 2011 Fedorova et al., 2015). Since the ArcticGRO sampling site is far from where the Lena runoff enters the Arctic Ocean, biogeochemical processes taking place downstream from Zhigansk and particularly in the delta are not reflected in the ArcticGRO data. Thus, the properties of water and suspended materials sampled at Zhigansk may in fact not be entirely representative of the discharge to the ocean.

3.2.2 Sampling

In this study, we sampled along the Lena main stem from Yakutsk to Stolb Island and then onward through the Sardakhskaya branch. Samples from the Lena main stem and its Delta were taken separately during two independent expeditions in 2019. The first sampling campaign took place between 20 June and 30 June 2019 and covered a transect along the Lena main stem. Surface water was taken along a 1300 km long transect from Yakutsk to the Lena Delta (Figure 3-1a) on-board the vessel *Merzlotoved*. Sampling took place at nine sites approximately every 150 km on the way to the Lena Delta. This transect intersects the location of the perennial ArcticGRO observation program and includes a sampling station downstream of the town of Zhigansk (station WL19-05). Water samples were taken from the surface (~1 m water depth) using a pre-cleaned plastic bucket. The water sample was stored in 500 ml high-density polyethylene (HDPE) bottles (pre-cleaned with 10 % HCl for 3 days) and immediately frozen at -10 °C for preservation. The second sampling campaign started on 7 August 2019. The aim of the expedition was a detailed investigation along the Sardakhskaya branch, from Stolb Island to the eastern Laptev Sea (Fuchs et al., 2021). The distance between the sampling locations varied between ~20 km and ~5 km, with coarser sampling at the beginning of

the transect near Stolb Island and increasing spatial resolution towards the Laptev Sea (Figure 3-1b).

We used a 5-litre water sampler (UWITEC, Austria) to collect water from one to three depths per station (depending on the bottom depth at the sampling location). We took surface water (0-1 m) at each sampling site. If the river depth at a location was 3-7 m, two depths were sampled: surface water and above the bottom depth (0-1 m and 3-7 m). When water depth exceeded 7 m, water was sampled at three depths: 1) surface (0-1 m), 2) mid-depth in the water column (3-7 m), and 3) just above the river bottom (8-18 m). The water samples were collected in 20 L plastic canisters, which were pre-cleaned with 10 % HCL and kept cool until return to the laboratory on Samoylov Island, where the samples were further analysed.

Additionally, samples from previous Lena Delta expeditions were used for this study. Those samples were taken near Stolb Island in 2016 (8 August and 15 August) and in 2017 (11 July and 25 July). This collection of samples and further analyses were conducted in the same way as for the samples from the riverine deltaic transects obtained in 2019.

3.2.3 Laboratory analyses

3.2.3.1 Total suspended matter concentration

Directly after sampling (delta transect) or after 40 days of freezing (Yakutsk-delta transect), samples were delivered to the Samoylov Island research station laboratory, where they were processed for further analyses. Water was filtered through pre-combusted (4.5 hours, 450 °C) and pre-weighed glass fibre filters (GF/F Whatman, 0.75 µm membrane, Ø 2.5 cm) for total suspended matter (TSM) content, POC concentration, and C isotope analysis. Filters were stored frozen in pre-combusted glass petri dishes. After filtration, the filters were dried for 24 hours at 40 °C and weighed. We used the

difference in weights between dried filters with TSM and pre-weighed empty filters to calculate TSM concentration per unit volume of water (mg L^{-1}).

2.3.2 Particulate organic carbon concentration, carbon isotope analyses ($\Delta^{14}\text{C}$, $\delta^{13}\text{C}$), and relative organic carbon content in total suspended matter

After calculation of TSM, selected filters (different replicates from the same water sample) were further processed 1) to determine total POC concentration (mg L^{-1}) together with stable C isotopes, and 2) to determine $\Delta^{14}\text{C}$ of POC. For this purpose, in both cases filters were acidified with 10 % HCl to remove inorganic C (sufficient HCl to wet the filter surface including its sediment). Then they were dried again for 24 hours at 40 °C and packed/rolled into small tin boats (6x6x12 mm) (Mollenhauer et al., 2021). For filters with TSM concentrations above 20 mg L^{-1} , it was expected that C contents on the filter exceeded 100 μg . For those samples, only a subsample of the filter was used.

POC content on the filter and its $\delta^{13}\text{C}$ signature were measured on a Sercon - 20-20 isotope ratio mass spectrometer (IRMS) coupled to an Automated Nitrogen Carbon Analyser (ANCA). Stable C isotope values were expressed as $\delta^{13}\text{C}$ in per mil (‰) and normalised against the Pee Dee Belemnite (PDB) standard.

Precision and accuracy of the isotope ratios and C masses were assessed by repeated analysis of in-house standards (Isoleucine, *National Institute of Standards & Technology*, RM 8573, USGS40) with known isotopic composition (-26.39 ± 0.09 ‰). The precision of $\delta^{13}\text{C}$ measurements was better than ± 0.2 ‰, the mean uncertainty for POC was ± 3.34 μg , and the concentrations were determined by dividing the POC content per filter by the volume of water filtered through that filter.

The relative organic carbon (OC) content of the TSM (OC_{TSM} , wt%) was calculated by dividing the sample POC content by the TSM content (Eq. 1)

$$OC_{TSM} = \frac{POC}{TSM} \cdot 100\% \quad (1)$$

Radiocarbon dating by accelerator mass spectrometer (AMS) was achieved on a Mini Carbon Dating System (MICADAS) following Mollenhauer et al. (2021). We report radiocarbon data as $\Delta^{14}C$ values in ‰, which expresses the relative difference in ^{14}C activity between the absolute international standard (reference year 1950) and the sample activity corrected for sampling time and normalised to $\delta^{13}C=25$ ‰ (Stuiver & Polach, 1977). Blank sample was determined by five empty combusted blank filters (GF/F, 2.5 cm Ø) treated identically to the samples (Mollenhauer et al., 2021).

Since radiocarbon analysis is commonly used as a method for determining OM age (Stuiver & Polach, 1977), for discussion of the results, we referred to more ^{14}C -depleted samples as "ancient" C from "ancient" OM sources (less than -900 ‰ or $\sim 18,500$ $\Delta^{14}C$ years), then to more ^{14}C -enriched samples (in the range between -50 and -900 ‰ or $\sim 400 - 18,500$ $\Delta^{14}C$ years) we referred as "old" and to the samples with $\Delta^{14}C$ above -50 ‰ as "young".

3.2.3.3 Data representation and calculations

The data used in this study were subdivided into three groups according to the sampling locations and differences in the hydrological regime and studied parameters: 1) samples from the Lena River main channel along the sampling transect from Yakutsk to the Lena Delta, 2) samples from near Stolb Island at the apex of the Lena River main stem and Lena Delta, and 3) samples from the Sardakhszkaya branch in the Lena Delta itself. We

discuss our data in the context of a compilation of summer data obtained by the ArcticGRO initiative (group 4). This dataset includes parameters measured from 2004 to 2019 (Holmes et al., 2021) in the summer between 15 June and 31 August. This subset of ArcticGRO samples was chosen to allow direct comparison of the published results with data presented here and to avoid extreme events of the hydrologic system like the spring – early summer ice breakup (maximum water and TSM discharge) and winter ice-cover (minimum water and TSM discharge) (Magritsky et al., 2018).

The discharge data are provided by the Russian Federal Service for Hydrometeorology and Environmental Monitoring (Roshydromet, published by Shiklomanov et al., 2021b) for the Lena River at Kyusyur (70.68°N, 127.39°E, see Figure 3-1a).

The groups of data defined for this study are described in Figures 3-2 to 3-5 and Table 3-2 as “Main Stem”, “Delta”, “Stolb” and “ArcticGRO”.

Endmember modelling analysis was performed to derive quantitative estimates of the relative input of a potential C source endmember into the POC pool of every water sample and described in detail in 4.2.3.

3.3 Results

3.3.1 Depth distribution

We sampled water in the delta from different depths to investigate the distribution of OM through the water profile in the deltaic ecosystem. We did not observe systematic and significant differences between TSM, POC concentration, OC content, or carbon isotopes of POC for different water depths. Previous measurements using a Conductivity, Temperature and Depth (CTD) probe during the sampling campaign showed no temperature or conductivity stratification of the water profile (Fuchs et al., 2022). Thus, to characterise other studied parameters in the Lena Delta, we considered all the data

measured in the delta from all water depths as one dataset without further subdividing the values into depth groups.

3.3.2 Total suspended matter; particulate organic carbon and its content in total suspended matter

3.3.2.1 Total suspended matter

TSM concentration varied strongly between the river main stem with high spatial variability, and the Lena Delta, where TSM was distributed homogeneously (Figure 3-2a). The concentration of TSM from the main stem decreased from the upstream catchment to the delta, from 34.5 to 15.0 mg L⁻¹, with an average of 22.7 ±6.3 mg L⁻¹ (mean ±stdev). We measured the highest TSM concentration at a station 150 km downstream from Yakutsk (WL19-02), where the largest Lena tributary (Aldan) flows into the main stem (Figure 3-1a; 3-2a). From there on, TSM concentrations consistently decreased, reaching a minimum at the two stations closest to the delta near Stolb Island (WL19-08 and -09).

Compared to the Lena River main stem transect, the TSM concentrations in the delta were lower and rather homogeneous, displaying no obvious trends in spatial distribution. The highest TSM concentrations in the delta were found for several samples along the entire transect; 20.0 mg L⁻¹ 40 km downstream from Stolb Island (LEN19-S-03), 16.4 mg L⁻¹ in the middle of the Sardakhskaya branch (LEN19-S-05), and 19.4 mg L⁻¹ and 18.8 mg L⁻¹ closer to the delta outlet (LEN19-S-08 and -89). The mean concentration of TSM for the delta was 9.3 ±5.2 mg L⁻¹, which is lower than in the river main stem. The mean TSM concentrations at Stolb Island (transition zone between the Lena main stem and the delta) was 8.6 ±3.7 mg L⁻¹ with a maximum up to 13.8 mg L⁻¹ in the middle of the profile, which is within the range of the lowest values measured in the main stem transect and the average deltaic values (Figure 3-1a).

TSM reported in the ArcticGRO dataset varied within a greater range than our main stem samples result (7.6 and 51.0 mg L⁻¹) nevertheless, the average TSM (27.8 ±11.3 mg L⁻¹) was similar to that of our main stem sample result.

3.3.2.2 Particulate organic carbon and its content in total suspended matter

The distribution pattern of POC concentrations along the Lena River main stem was similar to that of TSM concentrations (Figure 3-2b). POC decreased by ~70 % downstream, from 1.32 mg L⁻¹ at Yakutsk (WL19-01) to 0.40 mg L⁻¹ at the last station (WL19-09). The mean POC concentration in the Lena River was 0.79 ±0.30 mg L⁻¹. The highest POC concentration was measured at the two southernmost sites (WL19-01, WL19-02) (1.32 and 1.28 mg L⁻¹, respectively).

Deltaic POC concentration was on average lower than riverine POC with a mean of 0.41 ±0.10 mg L⁻¹ (range 0.26-0.66 mg L⁻¹). The samples with high TSM had high POC concentrations as well. These values were similar to the range of POC concentrations found for the second half of the river main channel transect.

Like TSM, POC concentrations provided by the ArcticGRO database were very similar to the values we obtained in this study. The average POC concentration from ArcticGRO is 0.86 ±0.41 mg L⁻¹, within the range of 0.52-1.46 mg L⁻¹.

The POC content in TSM (OC_{TSM}, wt%) from main stem samples was relatively constant along the complete river transect with a mean OC_{TSM} of 3.4 ±0.2 wt%. The southernmost station (WL19-01; Yakutsk) was an exception, being enriched in suspended matter and especially in POC (TSM: 26.5 mg L⁻¹ and POC: 1.28 mg L⁻¹) and OC_{TSM} was slightly higher than the transect average (4.8 wt%) (Figure 3-2c). In the deltaic waters, OC_{TSM} was significantly higher than in main stem samples, and the values within the delta increased from Stolb Island (4.3 ±0.7 wt%; LEN19-S-01) toward the river mouth (up to 7.1 wt% for LEN19-S-09, sampled at 5 m depth). The average OC_{TSM} in the delta was 5.2 ±1.5 wt%,

with a minimum as low as 2.8 wt% for stations with the highest TSM and POC concentrations (40 km downstream from Stolb Island, LEN19-S-03).

OC_{TSM} at Zhigansk from ArcticGRO was in a similar range as the values we found in the main Lena River channel. The average value was 3.5 ± 1.3 wt%. The two lowest values of 1.9 wt% were measured for samples with very high TSM and POC concentrations. Two high values stood out from the other values and were measured in the sample with the lowest POC and TSM concentrations. The mean OC_{TSM} within ArcticGRO was not significantly different from the mean POC content in the river transect data, with values of 3.6 % and 3.4 %, respectively.

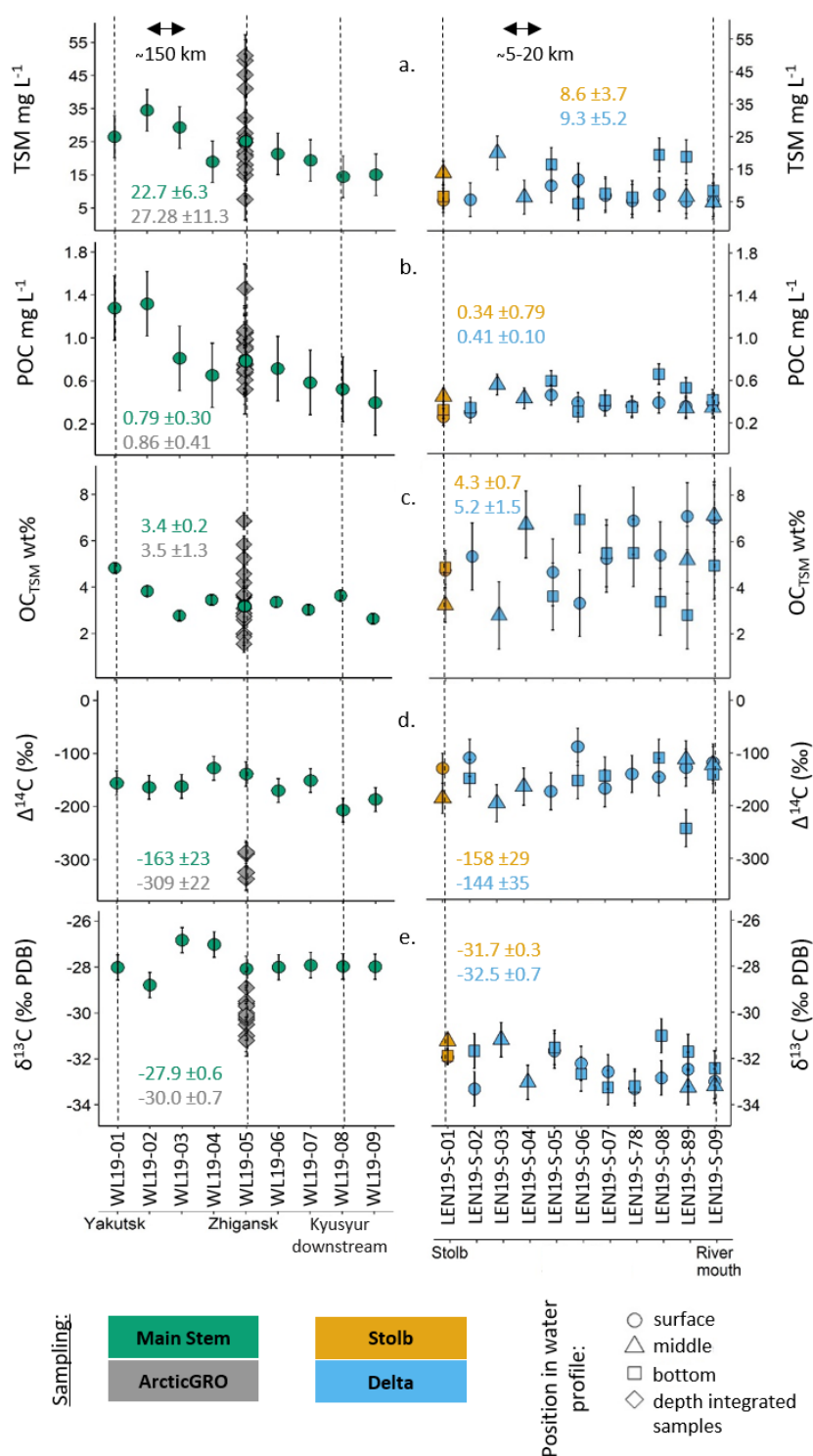


Figure 3-2. Distribution of studied parameters along the transect in the Lena main stem, the Lena Delta, and for the ArcticGRO dataset (mean ±stdev), discrete values displayed on each panel represent the average (±stdev) for every sampling group: a. TSM mg L⁻¹; b. POC, mg L⁻¹; c) OC_{TSM}, wt%; d) Δ¹⁴C of POC, ‰; e) δ¹³C of POC, ‰.

3.3.3 Isotopic composition of particulate organic carbon

3.3.3.1 $\Delta^{14}\text{C}$ of particulate organic carbon

Radiocarbon levels of POC varied within a wide range between -243 and -88 ‰ (between 2236 and 740 $\Delta^{14}\text{C}$ years mean age, respectively) along the entire transect (Figure 3-2d), and did not differ substantially between river main stem and delta samples. The mean radiocarbon value for the main stem part of the transect was -163 ± 23 ‰ (range from -207 to -128 ‰). The $\Delta^{14}\text{C}$ of POC at the first three upstream main stem stations (WL19-01, -02, and -03) were similar at -160 ± 3 ‰. Further downstream $\Delta^{14}\text{C}$ increased to -128 ‰ at the station ~ 150 km upstream Zhigansk (WL19-04) and decreased to -207 ‰ at station WL19-08 on the way to Stolb Island (LEN19-S-01), where it was -158 ‰. In the delta, the mean $\Delta^{14}\text{C}$ ‰ was -144 ± 35 ‰ with a minimum of -243 ‰ at station LEN19-S-89 before the delta discharges into the sea and a maximum of -88 ‰ at LEN19-S-06 in the middle of the delta transect. Thus, Lena Delta POC in 2019 was within the same age as, or younger (higher $\Delta^{14}\text{C}$ concentration) than POC in the Lena River main stem.

ArcticGRO reported significantly lower $\Delta^{14}\text{C}$ values than what we found. The average $\Delta^{14}\text{C}$ value was -309 ‰, while our value for Zhigansk in 2019 was -164 ‰ (WL19-05), which was similar to the average for the entire transect in 2019 (-163 ± 23 ‰).

3.3.3.2 $\delta^{13}\text{C}$ of particulate organic carbon

A strong difference was noted on the $\delta^{13}\text{C}$ of POC. In the main stem $\delta^{13}\text{C}$ values were significantly higher than in the delta and at Stolb, with means of -27.9 ± 0.6 ‰ in the main stem and -31.7 ± 0.3 and -32.5 ± 0.7 ‰ at Stolb and in the delta, respectively (Figure 3-2e). Values within the main stem part of the transect ranged between -28.8 and -26.8 ‰, with higher values for stations WL19-03 (-26.8 ‰) and WL19-04 (-27.0 ‰) after the Aldan and Vilyuy Lena tributaries exit the Lena main stem. The $\delta^{13}\text{C}$ values of POC within the delta and at Stolb displayed slightly more spatial variation, with values between -

33.1 and -31.0 ‰ and no specific distribution trend; thus, the lowest value of -33.3 ‰ was measured at several deltaic stations (LEN19-S-02, LEN19-S-07, LEN19-S-78, and LEN19-S-89) (Figure 3-2e). The $\delta^{13}\text{C}$ of POC reported by ArcticGRO was -30.0 ± 0.7 ‰, which was in between the values measured by us in 2019 at the Lena main stem and delta.

3.4 Discussion

3.4.1 Organic carbon load in the Lena main stem and the Lena Delta

The TSM and POC concentrations measured in 2019 displayed generally higher and more variable values along the Lena River main stem than in the Delta, while the OC content of TSM was higher in the Lena Delta (Figure 3-2c). This pattern could be explained by a) the local flow regime and its hydrological changes such as flow velocity, water and sources distribution, and mean catchment slope along the Lena main stem and its Delta, or b) the time of sampling relative to the annual spring-summer flooding and the discharge fluctuations, or c) a combination of both factors. In the following, we discuss these factors in detail.

3.4.1.1 Discharge and sampling time

The Lena River is characterised by a nival hydrograph regime with a distinct flood event taking place in the beginning of summer during the snowmelt and ice breakup period (May-June) and a very low water flow in winter (Yang et al., 2002). Discharge has a strong effect on the amount of solids and OM released by a river (Magritsky et al., 2018). The peak of annual POC concentrations in the Lena River ($>3.6 \text{ mg L}^{-1}$, McClelland et al., 2016) and TSM concentrations ($>150 \text{ mg L}^{-1}$, ArcticGRO) occur right after the flooding following ice breakup in late May–early June.

The peak water yield in 2019 took place on 2 June and reached $83,000 \text{ m}^3 \text{ s}^{-1}$, then it decreased and varied in the range of $49,200\text{--}45,999 \text{ m}^3 \text{ s}^{-1}$ during the time interval when the main stem transect was sampled (Shiklomanov et al., 2021b). During the sampling in the Delta (2019/08/07–2019/08/09) the discharge was $19,600\text{--}19,000 \text{ m}^3 \text{ s}^{-1}$, which was less than half the discharge during main stem sampling.

We assessed all ArcticGRO data on TSM and POC for the Lena River to demonstrate that TSM and POC concentrations were correlated with discharge (Figure 3-S1). However, when considering a discharge ranging between $15,000$ and $50,000 \text{ m}^3 \text{ s}^{-1}$, (the typical range of discharge values in summer (including 2019) and in September), there is no significant relationship between discharge and TSM and POC concentrations (Figure 3-S2). Thus, the strong relationship between discharge and TSM/POC appears to be driven by the large difference between maxima in all parameters (observed during the spring flood) and their minima (found during low flow in winter).

Average surface water TSM and POC concentrations in the Lena River in 2019 agree with reported average TSM and POC concentrations observed by ArcticGRO during periods with discharge within the mentioned range (TSM in this study: 21.29 mg L^{-1} as compared with 22.66 mg L^{-1} for ArcticGRO, and POC 0.77 mg L^{-1} and 0.79 mg L^{-1} , respectively). TSM and POC concentrations in the Lena Delta in summer 2019 were 2 and 1.5 times lower, respectively, than values reported by ArcticGRO for a comparable time of year and under similar discharge conditions (TSM: $9.3 \pm 5.2 \text{ mg L}^{-1}$, POC: $0.41 \pm 0.10 \text{ mg L}^{-1}$) (Figure 3-2a & b). On the other hand, our deltaic POC concentrations are similar to previously published POC data for the Lena Delta (Winterfeld et al., 2015) (Figure 3-3). This shows that the difference we observe between river and delta is a persistent feature that is not biased by sampling time or depth but is mostly caused by other factors such as, e.g., flow and velocity.

3.4.1.2 Hydrology of the Lena River

The first station of our main stem transect was situated at the Upper Lena and the second station marks the transition from Upper to Lower Lena. According to Kutscher et al. (2017), Upper and Lower areas of the Lena account for the following fractions of the total watershed area and POC discharge: Upper Lena (37 % of the entire Lena River watershed, 2.9 Tg C yr⁻¹ of TSM), Aldan, the watershed of the Lena River's main tributary (29 %, 1.8 Tg C yr⁻¹), Lower Lena (15 %, 1.1 Tg C yr⁻¹) and Vilyuy, the second big tributary of the Lena (19 %, 0.6 Tg C yr⁻¹).

Surface river water concentrations of TSM and POC in 2019 display a decreasing trend from Yakutsk to Kysuyur downstream along the Lena River (Figure 3-2a & b). The highest TSM and POC concentrations (34.5 mg L⁻¹ and 1.32 mg L⁻¹, respectively) were found at the location close to where the Aldan tributary flows into the Lena River (WL19-02); downstream from where the Vilyuy tributary feeds into the Lena (WL19-03), TSM and POC concentrations steadily decrease. Several factors may account for this observation.

OM concentrations in the Lower Lena were lower compared to the Upper Lena. It has been suggested that this is related to the difference in the geological setting in the northern part of the catchment compared to the southern part (Kutscher et al., 2017) and to the mean slope of the Upper Lena sub catchment, which is reflected by OM concentrations in the river (Mulholland, 1997). The Upper Lena is sourced from regions with higher precipitation (Chevychelov & Bosikov, 2010), smaller extent of continuous permafrost (Obu et al., 2019), and more productive forests (Stone & Schlesinger, 2003). In contrast, the Lower Lena receives a considerable part of the water flowing from the steeply sloped mountainous areas of the Verkhoyansk Range. The water catchment area of the Lower Lena is covered by shallow, OM-poor soils: Gleyzems, which are Al-Fe-humic soils, and shallow, weakly developed soils that develop in mountainous areas

(Stolbovoi, 2002). OM from the Upper Lena catchment may reach the Lower Lena, as we measured at the beginning of the riverine transect. TSM and POC concentrations decreased in the Lower Lena regime because local tributaries carry less OM, with possibly relatively more mineral compounds, which, for example, is reflected in the decrease in OC_{TSM} from the south to the north of the main stem transect (Figure 3-2c).

The lower TSM and POC downstream from the Vilyuy could also result from the hydrological change, which takes place inside the Lower Lena itself. Kääb et al. (2013) reported that the velocity of the Lena River decreases downstream from south to north along the 620 km long Lena River transect between 67.00° and $71.58^\circ N$ (corresponding to the river stretch between our stations WL19-05 (Zhigansk) and WL19-09 (the nearest to the delta), reaching the lowest values approximately 40 km south of Kyusyur. This is a result of the topography of the region, where the base slope elevation of the river flattens near 150 km south of Kyusyur. It is also known that the majority of TSM brought by the Lena River from the water catchment is deposited before the Lena reaches the stream north of Kyusyur, which is known as the “Lenskaya Truba” (which means “Lena pipe”) (Antonov, 1960). This is the narrowest (sometimes less than 2 km) and deepest (more than 20 m) part of the river (Fedorova et al., 2015) where the TSM sedimentation takes place. The preferential sedimentation of mineral particles may also affect the isotopic composition of transported OM. As it was shown by Vonk (2014) contemporary terrestrial OM is dispersed mainly by horizontal transport, while mineral-associated (i.e., heavier), older OC from topsoil and Yedoma is affected mainly by vertical transport and seem to settle rapidly. Thus, decreasing velocity in the Lower Lena (from 2.5 m s^{-1} to 0.8 m s^{-1} in May (Kääb et al., 2013)) and in the Lena Delta itself (from 1.3 to 0.9 m s^{-1} in August (Nigamatzyanova et al., 2015)) allows for further sedimentation of TSM and old C, resulting in a decrease of its concentration.

The Lena Delta was characterised by the lowest TSM and POC values in 2019, as previously described. Several factors may account for these findings. It is known that the sediment transport from the Lena Delta to the Laptev Sea is controlled by the distribution of water and sediment discharge along the different deltaic branches (Rachold et al., 1996). According to Rachold et al. (1996), the Trofimovskaya-Sardakhskaya branch system receives 61 % of the annual water volume registered at Stolb station. These channels have complex structures and contain several different regional sub-delta systems. As a result, only 7 to 8 % of the initial water volume reaches the mouth of the Trofimovskaya channel (Rachold et al., 1996). The water, loaded with suspended matter, is distributed into the numerous channels; this affects the amount of TSM detected in the big channels. Due to the extensive branching of the channels in the delta, velocity decreases, allowing for settling and sedimentation of TSM, mostly on flood plains (Sanders et al., 2022) following the high-water flooding season.

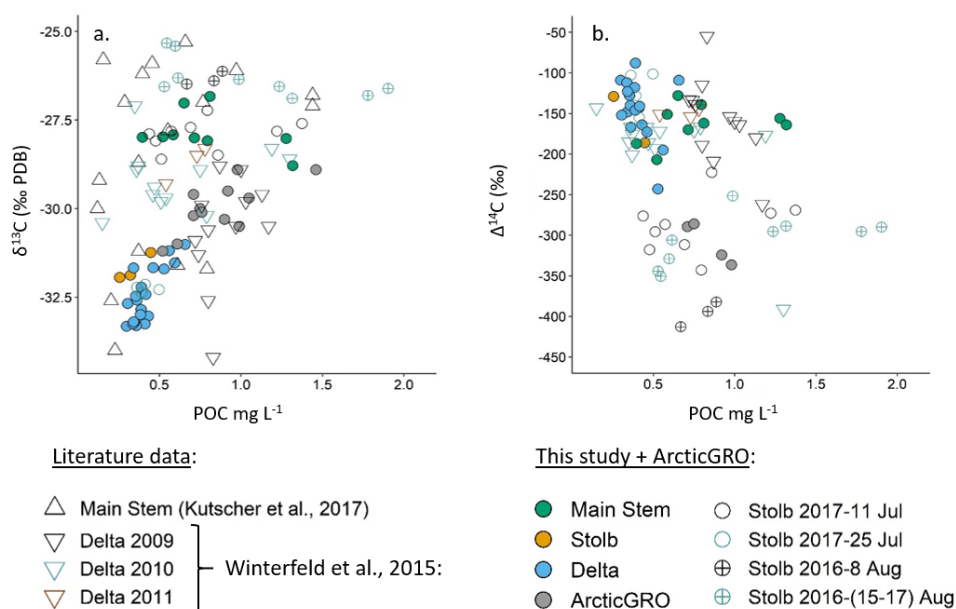


Figure 3-3. Stable and radiocarbon isotopic values and POC concentration for the Lena Delta and the Lena River main stem. Values were taken from this study and from the literature (Kutscher et al., 2017 and Winterfeld et al., 2015).

The OM_{TSM} is much higher in the delta compared to the Lena main stem, which may be a result of preferential settling of denser mineral-rich particles between the main stem

and the delta. Further input of OM originates from the islands, supplied by bank erosion and degradation of ice-rich permafrost deposits such as Yedoma; both processes take place in the delta (Stettner et al., 2018; Fuchs et al., 2020; Haugk et al., 2022). Based on these observed patterns, we suggest that the Lena Delta should be distinguished as the third hydrographically and sedimentologically distinct part of the Lena River system.

3.4.2 Potential sources of particulate organic carbon

3.4.2.1 Stable carbon isotope sources

The $\delta^{13}\text{C}$ values of POC in the Lena main stem surface water ranged between -28.8 and -26.8 ‰ with a mean of -27.9 ± 0.6 ‰, comparable to a typical $\delta^{13}\text{C}$ of terrestrial C3 plants (about -27 ‰) (Finlay & Kendall, 2008). C3 plants are dominant in the Lena catchment area and account for most of the soil OM (SOM) (from -28.4 to -27.0 ‰), including that of Yedoma deposits (-27.5 ‰) that have been described for the Lena watershed (Vonk et al., 2017, Schirrmeister et al., 2011), and for the terrestrial primary production (-27.7 ‰) such as organic and litter layers (Wild et al., 2019). The observed $\delta^{13}\text{C}$ values also overlap with the range of $\delta^{13}\text{C}$ values determined for soils from the first terrace of Lena Delta soils (from -27.0 to -25.1 ‰) (Winterfeld et al., 2015).

In contrast to main stem POC, deltaic POC was more depleted in ^{13}C (mean -32.5 ± 0.7 ‰) (Figure 3-2e; 3a). Similarly low values were found in the delta in 2016 and 2017 and were previously reported in several publications for the Lena Delta (e.g. Winterfeld et al., 2015), the Lena River (Kutscher et al., 2017) (Figure 3-3), and the Kolyma River (Bröder et al., 2020). Those authors related riverine POC depleted in ^{13}C to the influence of aquatic primary production and suggested a phytoplankton contribution to explain the isotopic composition of POM. However, in these studies reported POC $\delta^{13}\text{C}$ values below -30 ‰ were the exception rather than the rule. This is in contrast to our set of deltaic

samples from 2019, where POC is consistently strongly depleted in ^{13}C , showing $\delta^{13}\text{C}$ values between -33.3 and -31 ‰.

Unfortunately, neither of the cited publications reports the phytoplankton biomass and/or chlorophyll-a data for the studied water samples, nor were these measurements part of our sampling campaign. This lack of quantitative observational data requires a theoretical estimation of phytoplankton input into POC.

According to the data from Finlay and Kendal (2008), $\delta^{13}\text{C}$ from phytoplankton in river POC ranges from -42 to -25 ‰. However, these authors stress that the range of isotopic values is smaller within each single river. Regardless, low $\delta^{13}\text{C}$ of POC, as observed in our deltaic samples, is consistent with substantial contributions of POC from aquatic production during phytoplankton bloom.

In the Arctic, 2019 was a warm and dry year when mean annual surface air temperature over the Arctic land mass was the second highest in the observational period (1900–present) (Richter-Menge et al., 2019). Our Lena Delta sampling period was between 20 July and 10 August, which is the season when the highest water temperatures were observed by Liu et al. (2005). Higher water temperatures induce higher metabolic rates and thus increased aquatic primary production as well as heterotrophic activity (Paczkowska et al., 2019; Bosco-Galazzo et al., 2018; Allen et al., 2005). The average water temperature in the delta in 2019 according to the CTD measurements was 15.2 °C (Fuchs et al., 2022). Liu et al. (2005) reported a decrease of water temperatures from the Upper Lena to the north. Average Lena water temperatures at Kyusyur (the northernmost station of that study) were 3-5 °C lower in mid-open water season (end of June–end of August) compared to the Aldan and Upper Lena basins and barely reached 15 °C (Liu et al., 2005). Likewise, ArcticGRO reports a water temperature of 15.0 °C on 2 August 2019. Thus, the water temperatures in the Lena Delta during our sampling campaign (7-8

August) were higher than in Zhigansk (~800 km to the south of the delta) despite the latitudinal gradient in water temperatures observed by Liu et al. (2005). A heat wave in 2019 may have had further consequences in the Lena Delta, such as the formation of isolated small deltaic channels, which were separated due to extremely low water conditions. These channels may represent favourable habitats for the development of high numbers of algae despite the absence of an additional nutrient flux, as temperature and velocity appear to exert a stronger positive influence on phytoplankton growth, outbalancing the lack of nutrients (Li et al., 2013). From this, it follows that the delta provided more favourable thermal conditions for phytoplankton than did the main stem; this was particularly true in the very warm year of 2019. We suggest that sampling during potential algal blooms took place in earlier years as well. For example, in 2017 we observed a $\delta^{13}\text{C}$ decrease from -27.9 ‰ to -32.3 ‰ within only two weeks (11 July – 25 July 2017), suggesting that an algal bloom developed between the two sampling dates (Figure 3-3a).

Additional support for the increase of aquatic production in August 2019 is provided by gradients in nitrate ($1.5 \mu\text{mol L}^{-1}$ to $0.25 \mu\text{mol L}^{-1}$) and silicate ($50 \mu\text{mol L}^{-1}$ to $18 \mu\text{mol L}^{-1}$) observed by Sanders et al. (2022) on the way along the sampling transect from Stolb Island further into the delta (LEN19-S-01, -02 and -03). Sanders et al. (2022) suggest that phytoplankton such as diatoms may be responsible for this uptake, as described in Hawkings et al. (2017).

The C isotopic fractionation during photosynthesis is not constant and may depend on the environmental conditions, but isotopic composition of phytoplankton generally strongly correlates with the isotopic composition of dissolved inorganic C (DIC) (Rounick and James, 1984). In the Lena Delta, the $\delta^{13}\text{C}$ of DIC has not been measured, but the low $\delta^{13}\text{C}$ of POC suggests a ^{13}C -depleted DIC pool. Low $\delta^{13}\text{C}$ in DIC can be caused by several processes as shown for riverine DIC in the rivers of Patagonia: degradation of

dissolved OC (DOC) containing soil organic C will result in low $\delta^{13}\text{C}$ of DIC, and $\delta^{13}\text{C}$ of DIC was found to be negatively correlated with DOC concentration (Brunet et al., 2005). It is conceivable that DOC remineralisation leads to similarly reduced $\delta^{13}\text{C}$ of DIC in the Lena Delta, which is in agreement with observations of rapid remineralisation of DOC released from thawing permafrost as reported for the Kolyma catchment (Mann et al., 2015) and for thaw creeks on an island in the Lena Delta (Stolpmann et al., 2022).

The fact that the lowest $\delta^{13}\text{C}$ values tend to be in samples with the lowest POC concentrations offers another interesting perspective (Figure 3-3a). As discussed above, TSM content (and POC from terrestrial sources) appears to be related to flow velocity. It is known that velocity exerts a strong negative effect on Chlorophyll-a concentration (Li et al., 2013). Together with other hydrological properties such as increasing suspended matter and turbidity, velocity could be one of the critical forcing factors regulating phytoplankton biomass, high velocity dilutes phytoplankton cells, reduces light availability, and changes the entire dynamic of aquatic production (Salmaso & Braioni, 2008). In turn, low flow velocities in the deltaic channels, as suggested by low POC values, could provide more favourable conditions for aquatic production while at the same time, larger or denser mineral-bearing particles might be settling.

The combined factors of low flow velocity in the shallow delta channels, where sunlight penetrates much of the water column which contains only small amounts of suspended particles, and the extremely warm summer conditions during our sampling campaign might have resulted in high primary production providing larger relative amounts of POC than in the main stem and during previous years.

$\delta^{13}\text{C}$ from ArcticGRO was lower than the $\delta^{13}\text{C}$ of POC we measured in the main stem, which may indicate more phytoplankton contribution to ArcticGRO samples. This may have resulted from potential higher C3 plant contribution to POC in the main stem in

2019 instead of contributions from phytoplankton, which was very likely higher for ArcticGRO samples due to the sampling time (nine of 12 $\delta^{13}\text{C}$ ArcticGRO records were measured in samples taken in August and at the end of July), and/or from less DOC recycling in June (main stem sampling 2019) than at the end of July–August (ArcticGRO).

3.4.2.2 $\Delta^{14}\text{C}$ in particulate organic matter

$\Delta^{14}\text{C}$ of POC sampled in 2019 was homogeneous along the studied transect, both along the Lena River main stem and within the Lena Delta (Figure 3-2d). In contrast to this, $\Delta^{14}\text{C}$ values reported by ArcticGRO were strongly depleted in ^{14}C compared to our 2019 transect data, although the values found in this study for the Lena Delta and nearby Stolb Island fit within the range of other previously published data from the Lena Delta (Figure 3-3b; 4). Values published by Winterfeld et al. (2015) for multiple summer seasons in the Lena Delta vary between -145 and -194 ‰; Karlsson et al. (2016) reported values in the range of -433 to -97 ‰ (Figure 3-4). This comparison reveals that the 2019 deltaic transect data are not atypical, as they are similar to the values for August 2009 and very close to July-August 2010 and June-July 2011.

The $\Delta^{14}\text{C}$ of POC from Stolb in 2016 and 2017 were relatively similar to ArcticGRO values or sometimes lower (Figure 3-3b; 4). It is important to highlight that $\Delta^{14}\text{C}$ in POC may change strongly within a relatively short period. For example, sampling in the summers of 2016 and 2017 was done twice with only one (2016) or two (2017) weeks in between. $\Delta^{14}\text{C}$ in 2017 increased over the course of two weeks (11-25 July) by almost 170 ‰ causing values to jump from -288 ‰ to -122 ‰ (Figure 3-3b). The data from 2016 also showed a distinct but less pronounced increase in $\Delta^{14}\text{C}$ within one weeks (8-15 August) from -387 ‰ up to -306 ‰. Thus, $\Delta^{14}\text{C}$ of POC is a parameter that exhibits large variability along the Lena main stem and inside its Delta. This variability makes this parameter hard

to interpret and suggests that local and short-term effects exert strong control (e.g., collapse of a bluff along the channel bank, or rain events).

The difference between ArcticGRO and the 2019 data may also be explained by the rather small number of ArcticGRO observations used for this comparison. The mean $\Delta^{14}\text{C}$ value of the entire Lena dataset from ArcticGRO is -275 ‰ and ranges from -398 to -164 ‰, which includes our $\Delta^{14}\text{C}$ values observed in 2019. We did not consider the entire ArcticGRO dataset for Lena River samples as we expect that during the discharge peak following the ice breakup in spring, POC might be of distinctly different origin than during the summer. We thus selected only values obtained for samples collected in the summer season after 15 June until 31 August. As a result, the reduced ArcticGRO dataset consists of only four samples with a mean $\Delta^{14}\text{C}$ value of -309 ‰ (min/max -336/-286 ‰) sampled in August of 2004 and 2005, similar to the time of the year when our deltaic campaign took place.

Another explanation for the difference in $\Delta^{14}\text{C}$ of POC between ArcticGRO and our riverine transect may be the fact that ArcticGRO samples are depth-integrated, since potentially river water masses may be stratified (e.g. Mackenzie: Hilton et al., 2015). We did not collect samples from different water depths along the river transect from Yakutsk to Stolb Island but instead were only able to sample surface waters, and from discrete water depths for the samples from the Lena Delta. The Lena River itself is deep along its main stem (up to 20 m downstream from Yakutsk); thus, pronounced and systematic differences between water mass properties like temperature, light penetration, could prevail, in turn influencing the composition of POC. We speculate that surface water POM might be biased towards more phytoplankton contribution in the sunlit surface waters and/or toward the contribution of vascular plants floating in the surface waters of the stream, resulting in apparently younger POM than at depth. This might explain why our 2019 river samples are systematically younger than the ArcticGRO values.

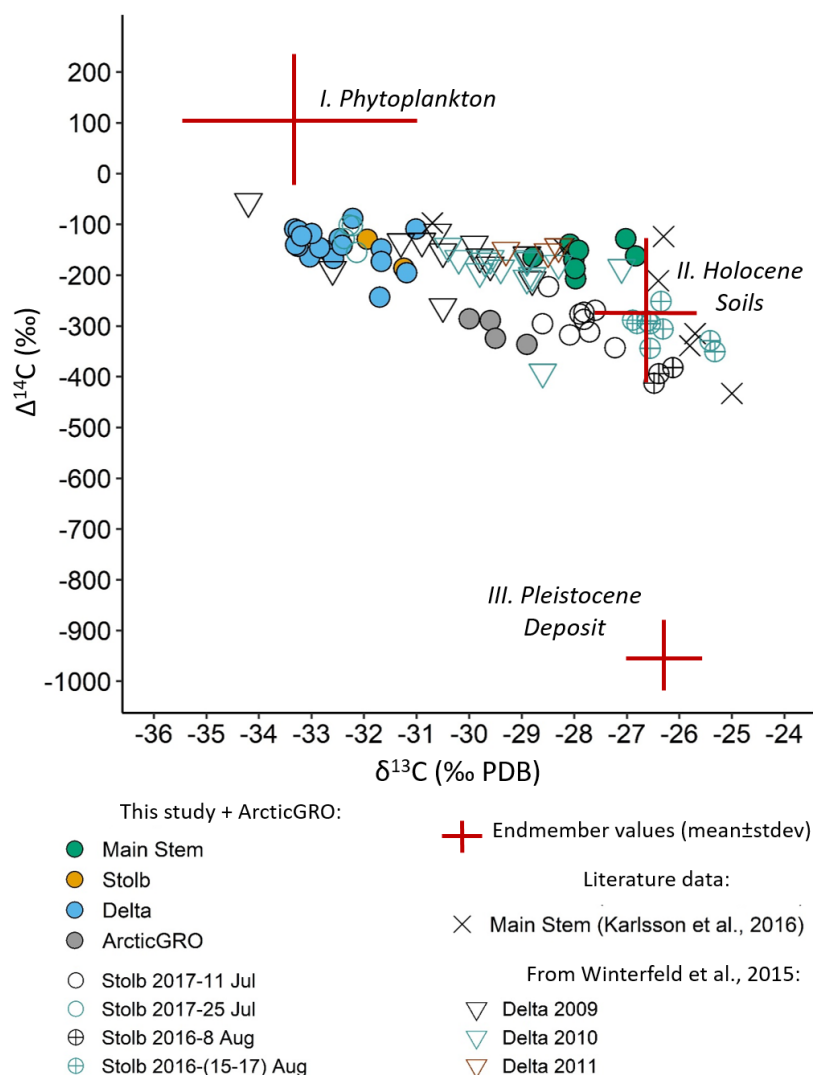


Figure 3-4. The origin of the POC in the Lena River and the Lena Delta. Endmember values (red crosses) were combined after Galimov et al., 2006, Wild et al., 2019, and Winterfeld et al., 2015; additional previously published data were added from Winterfeld et al., 2015 and Karlsson et al., 2016.

Samples with lower POC concentrations tend to display higher $\Delta^{14}\text{C}$ values and vice versa (Figure 3-3b). We suggests that conditions with low suspended particle load promote phytoplankton growth, while highly turbid waters contain substantial amounts of POC derived from riverbank erosion or cliff failure.

4.2.3 Estimation of organic matter sources based on endmember modelling

Combined radiocarbon and stable C isotope compositions are used to investigate the origin of OM. The difference in OM origin for POC measured along the transects in 2019 was illustrated by stable C isotope variations. $\delta^{13}\text{C}$ values in the delta suggest an aquatic origin of POC, and those samples also display comparatively high $\Delta^{14}\text{C}$ values. On the other hand, $\Delta^{14}\text{C}$ of POC in the delta and in the main stem are similar, but differ in $\delta^{13}\text{C}$ values from the river samples, which are less depleted in ^{13}C . If the delta samples contain substantial amounts of aquatically produced OM, isotope mass balance considerations require that some of the POC collected from delta waters still derive from terrestrial sources, which are older than the sources supplying POC to the main stem. To examine this hypothesis, we applied an endmember model.

Riverine POM is regarded as originating, to variable degrees, from autochthonous production of phytoplankton and from allochthonous sources such as vegetation and soils (Ittekkot & Laane, 1991). Terrestrial allochthonous sources for the Lena River catchment may be divided into two pools with different ages and origins: Holocene permafrost soils and organic-rich Pleistocene deposits. To illustrate possible sources of OM, we used a dual-carbon-isotope ($\Delta^{14}\text{C}$, $\delta^{13}\text{C}$) three-endmember mixing model. Endmembers for the OM sources in the Lena main stem and its Delta were defined as phytoplankton (I), Holocene soils (II), and Pleistocene deposits (III), and the respective endmember isotope values were taken from previously published studies (Table 3-1). For Holocene soils, endmember values were taken from Winterfeld et al. (2015). This study focused on the Lena Delta, and Holocene soil endmembers were combined from data measured directly for deltaic soils by this group of authors in 2009, 2010, 2011 and from a literature review. $\delta^{13}\text{C}$ values which we chose to use as endmember values were measured for Holocene soils which resemble soils in Lena River ecosystems, for example

from the Yenisey watershed, and $\Delta^{14}\text{C}$ values were measured mostly within the Lena Delta in different years (Winterfeld et al., 2015).

Endmember values for ancient permafrost Yedoma have also been measured. We use endmember values from Wild et al. (2019). In this study $\Delta^{14}\text{C}$ and $\delta^{13}\text{C}$ values of Pleistocene deposits were constrained using observations from Yedoma deposits from multiple researchers which were combined together for, in total, 329 observations for $\Delta^{14}\text{C}$ and 374 for $\delta^{13}\text{C}$.

The determination of phytoplankton endmembers required further consideration. The $\delta^{13}\text{C}$ endmember values for phytoplankton assumed in previous studies (e.g., Mann et al., 2015; Vonk et al., 2010; Wild et al., 2019; Winterfeld et al., 2015) are higher than the range of $\delta^{13}\text{C}$ measured by us in the 2019 samples. The $\delta^{13}\text{C}$ values reported by Galimov et al. (2006) for phytoplankton, however, are in the same range as ours from the Lena Delta and Stolb Island (-32.4 ‰). Those authors determined $\delta^{13}\text{C}$ values of phytoplankton in the Yenisey estuary ranging from -27.8 to -37.0 ‰, where phytoplankton is dominated by species of the phylum Bacillariophyta, which is the dominant phylum in the Lena Delta as well (42.3 % of all the species; Gabyshev et al., 2019). Therefore, we use the endmember value of -33.3 ± 2.3 ‰ for $\delta^{13}\text{C}$ of phytoplankton.

We determined the $\Delta^{14}\text{C}$ endmember value for phytoplankton based on the assumption that recent terrestrial and aquatic vegetation contains mostly modern C from the atmosphere, potentially even carrying elevated levels of ^{14}C affected by nuclear weapons testing during the 1960s and 1970s; thus, values from organic litter from Russia, Scandinavia, and Alaska were included (Wild et al., 2019).

Table 3-1. Possible sources of C used for the endmember modelling, and their isotopic composition (after Winterfeld et al., 2015, Wild et al., 2019, and Galimov et al., 2006).

Endmember:	$\delta^{13}\text{C}$ (‰)	$\pm\delta^{13}\text{C}$	Source	$\Delta^{14}\text{C}$ (‰)	$\pm\Delta^{14}\text{C}$	Source
Phytoplankton	-33.3	2.3	Galimov et al., 2006	97	125	Wild et al., 2019
Holocene soils	-26.6	1.0	Winterfeld et al., 2015	-282	133	Winterfeld et al., 2015
Pleistocene deposits	-26.3	0.7	Wild et al., 2019	-955	66	Wild et al., 2019

Proposing phytoplankton as one of three main sources of POC does not exclude the input of contemporary vegetation into the riverine and deltaic OM. $\Delta^{14}\text{C}$ signals from both modern vegetation and phytoplankton sources may in many cases be identical, and similar to the atmosphere (Winterfeld et al., 2015, Wild et al. 2019), while their $\delta^{13}\text{C}$ values are likely different. Moreover, modern plant material may display variable $\Delta^{14}\text{C}$ values between leaves, stems and roots. Therefore, phytoplankton was proposed as a modern OM source based on evidence from $\delta^{13}\text{C}$ values of POC corresponding to algal input (see section 4.2.1) and suggesting sufficiently lower input of plant debris into POC. Modern plants likely contributed as well, but due to their rather constant $\delta^{13}\text{C}$ signature paired with variable $\Delta^{14}\text{C}$ values (plant debris vs roots and litter) they cannot be distinguished from Holocene soils and must be regarded to be a contributor to this endmember.

Isotope mass balance endmember modelling was based on the following equations:

$$f_{\text{phytoplankton}} + f_{\text{holocene soils}} + f_{\text{pleistocene deposit}} = 1 \quad (2)$$

$$\delta^{13}\text{C}_{\text{sample}} = f_{\text{phytoplankton}} \delta^{13}\text{C}_{\text{phytoplankton}} + f_{\text{holocene soils}} \delta^{13}\text{C}_{\text{holocene soils}} + f_{\text{pleistocene deposit}} \delta^{13}\text{C}_{\text{Pleistocene deposit}} \quad (3)$$

$$\Delta^{14}\text{C}_{\text{sample}} = f_{\text{phytoplankton}} \Delta^{14}\text{C}_{\text{phytoplankton}} + f_{\text{holocene soils}} \Delta^{14}\text{C}_{\text{holocene soils}} + f_{\text{pleistocene deposit}} \Delta^{14}\text{C}_{\text{Pleistocene deposit}} \quad (4)$$

where $f_{\text{phytoplankton}}$, $f_{\text{holocene soils}}$, and $f_{\text{pleistocene deposit}}$ are the fractions contributed to the samples by phytoplankton, Holocene soils, and Pleistocene deposits, respectively. We applied the random sampling computer simulation (Monte Carlo simulation), which is based on the assumption that the endmember values are represented by a normal distribution, where the mean and a standard deviation were taken from previously published studies (Galimov et al., 2006; Wild et al., 2019; Winterfeld et al., 2015). Calculations were conducted using random sampling from this distribution while simultaneously applying the random sample to mass balance equations (Eq., 2, 3, 4) with repeated random sampling (5,000,000 times). Modelling was carried out in R studio using the code published by Andersson (2011) in a modified version (Grotheer et al., 2020).

Based on this endmember model, the phytoplankton contribution is highest in deltaic samples with a mean of 68 ± 6 % (Table 3-2, Table 3-S1 and Figure 3-4; 5), whereas main stem POC consists of approximately 39 ± 8 % aquatically produced material. In contrast, Holocene soils account for 13 ± 10 % in the delta versus 56 ± 12 % in riverine POC. Moreover, dual-carbon-isotope ($\Delta^{14}\text{C}$, $\delta^{13}\text{C}$) three-endmember mixing model results are consistent with input from an additional old permafrost source into deltaic POC. Thus, the Pleistocene contribution to the Lena Delta POC was estimated as 18 ± 4 % which is

almost four times higher compared to the main stem POC which held less than 5 % of ancient permafrost C in 2019 (Table 3-2, Table 3-S1, and Figure 3-5). This demonstrates an additional source of permafrost derived C, particularly in deltaic waters.

Our estimation of permafrost input into POC in the Lena main stem differs from that of Wild et al. (2019) who estimated pre-aged material input to the Lena River in summer as 62 ± 0.5 %. Such a large variation is explained by the different approaches applied. Wild et al. (2019) divided endmember sources into 1) recent terrestrial primary production (vegetation, phytoplankton), and 2) pre-aged OM, which included all terrestrial OM: active layer, Holocene peat and thermokarst Pleistocene deposits. Phytoplankton was not included as a potential source, but it is likely included in the recent primary production category. In our study, we did not consider Holocene soils to be ancient C, but emphasised Pleistocene deposits (Yedoma) as the contribution of ancient C in riverine and deltaic POC. The combined contribution to main stem POC from both Holocene soils and Pleistocene deposits was estimated by us to be ~ 61 %, which is similar to the contribution from a pre-aged OM source measured by Wild et al. (2019).

Table 3-2. Relative OM source contribution to water sample POC in 2019 (mean \pm std).

	I. Phytoplankton, %	\pm std	II. Holocene soils, %	\pm std	III. Pleistocene deposit, %	\pm std
Lena main stem	39	8	56	12	5	4
Delta*	68	6	13	10	18	4

**For this model samples from Stolb Island were included with the deltaic samples and contributed to the final mean \pm std values for potential POC sources.*

The estimated contributions of different OM sources to the actual average POC concentration measured for the Lena main stem and delta (Figure 3-5) showed that POC derived from Holocene soils decreased from 0.44 to 0.05 mg L⁻¹ due to sedimentation,

which takes place in the Lower Lena, particularly downstream from Kyusyur station, and in the delta itself as explained in section 4.1.2. POC derived from Pleistocene deposits almost doubles from 0.04 ± 0.02 (main stem) to $0.07 \pm 0.02 \text{ mg L}^{-1}$ (Lena Delta). This is the case despite the lower concentration of POC in the delta than in the main stem and the lower discharge during the sampling time in the delta. This suggests that the Lena Delta receives POC from an additional ancient permafrost deposit source, which is specific to the Lena Delta. These observations support a finding from Karlsson et al. (2016), who estimated the contribution of carbon derived from Pleistocene deposits to surface coastal surface sediments for the East Siberian Arctic Shelf to be $\sim 53 \%$ with surface soil contribution estimated to be only $\sim 0.23 \%$. Thus, the type of material that reaches the sea floor in the coastal zone reflects Yedoma deltaic origin.

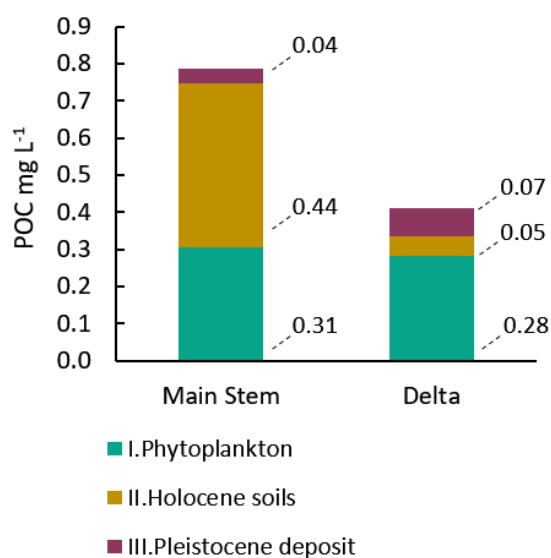


Figure 3-5. Contributions of different OM sources to the POC measured in the Lena River main stem and the Lena Delta along the transect in 2019

3.5 Summary and Conclusions

We found a significant difference between the two investigated parts of the Lena River system, the main stem and the delta. TSM and POC in the main stem were significantly

higher than in the delta. At the same time, TSM and POC concentrations along the main stem remained within the range of values registered by ArcticGRO for the years 2009–2019, while deltaic values of TSM and POC hardly reached the lowest values measured for Zhigansk. Conversely, the OM_{TSM} is higher in the delta than in the river, likely resulting from a different composition of the suspended matter.

The distribution pattern of TSM along the main stem decreases downstream to Stolb Island, which is the apex of the Lena Delta. This suggests that the major enrichment in TSM (mass wise) of the Lena main stem takes place along the main channel in the Upper Lena catchment. This TSM is rich in mineral compounds, which tend to settle out on the way to the ocean where river velocity decreases. Settling is even more pronounced in the delta, where flow velocity is lower because in the delta the main stem divides into multiple branches.

Modern OM, possibly from phytoplankton primary production, dominates in the delta, combined with a higher input of ancient permafrost, while riverine OM is predominantly derived from soil OM. The actual concentration of ancient permafrost-derived POC in the delta exceeds the concentration in the main stem ($\sim 0.07 \pm 0.02$ and 0.04 ± 0.02 mg L^{-1} , respectively) despite the lower concentration of POC (0.79 ± 0.30 mg L^{-1} in the river main stem and 0.41 ± 0.10 mg L^{-1} in the delta).

Our findings suggest that if an estimation of Lena OM discharge to the coastal zone is based only on the data from the Lena main stem, it may overestimate the load of TSM and underestimate its sedimentation, which takes place in the Lower Lena and its delta. In order to predict the effects on coastal waters of changes in permafrost due to climate change, additional and concurrent sampling from the river delta and the river main stem is needed. Particles that are mobilised from thawing permafrost in the Lena catchment may be deposited and decomposed on the way to the ocean. Therefore, investigating

permafrost fingerprints only in samples from the main stem may lead to incorrect conclusions and a biased perspective of permafrost carbon release to the coastal zone and the Arctic Ocean. The Lena Delta provides an additional source of permafrost carbon; Yedoma-derived OM, as part of the total permafrost carbon, could be then discharged into the Arctic coastal waters. The Lena Delta as the interface between the Lena River and the Arctic Ocean plays a crucial role in determining the qualitative and quantitative composition of OM discharged into the Arctic Ocean.

Data availability. The data presented in this study are freely available in the PANGAEA data repository: <https://doi.org/10.1594/PANGAEA.950668>.

Author contributions. OO, GM, and JS designed the concept of the study. OO drafted a first version of the manuscript and carried out laboratory analyses of TSM and POC including radio C analyses together with HG. BJ designed the maps. HG provided R code for endmember analysis. TS, MF, JP, JS, and OO carried out the field work and collected the samples. All co-authors contributed to the manuscript writing and editing processes.

Financial support. This research is part of the 'Changing Arctic Carbon cycle in the COastal Ocean Near-shore (CACOON)' project funded by the Bundesministerium für Bildung und Forschung (grant no. 03F0806A) and the Natural Environment Research Council (grant no. NE/R012806/1). BJ was funded by the European Space Agency (ESA) as part of the Climate Change Initiative (CCI) fellowship (ESA ESRIN/Contract No. 4000133761/21/I-NB)

Competing Interests. The authors declare that they have no conflict of interest.

Acknowledgments. We are grateful to everyone who helped and supported the CACOON project and the joint Russian-German "Lena 2019" expeditions, particularly

Volkmar Aßmann (AWI) for logistics during the summer expedition and the Samoylov Research Station for hospitality. We would particularly like to thank Waldemar Schneider (AWI) for invaluable help with sampling along the Lena River main stem.

References

- Allen, A. P., Gillooly, J. F., and Brown, J. H.: Linking the global carbon cycle to individual metabolism. *Functional Ecology*, 19(2), 202–213, <https://doi.org/10.1111/j.1365-2435.2005.00952.x>, 2005
- Amon, R. M. W., Rinehart, A. J., Duan, S., Louchouart, P., Prokushkin, A., Guggenberger, G., Bauch, D., Stedmon, C., Raymond, P. A., Holmes R. M., McClelland, J. W., Peterson, B. J., Walker S. A., Zhulidov, A. V.: Dissolved organic matter sources in large Arctic rivers. *Geochimica et Cosmochimica Acta*, 94, 217–237, <https://doi.org/10.1016/j.gca.2012.07.015>, 2012
- Andersson, A.: A systematic examination of a random sampling strategy for source apportionment calculations. *Science of the Total Environment*, 412–413, 232–238, <https://doi.org/10.1016/j.scitotenv.2011.10.031>, 2011
- Antonov, V.S.: The Lena River Delta.- Works of oceanographic committee of the Acad. Sci. USSR Vol. VI: 25-34, 1960 (in Russian)
- Ballinger, T. J., Overland, J. E., Wang, M., Bhatt, U. S., Hanna, E., Hanssen-Bauer, I., Kim, S. -J., Thoman, R. L., Walsh, J. E.: Arctic Report Card 2020: Surface Air Temperature, <https://doi.org/10.25923/gcw8-2z06>, 2020
- Biskaborn, B. K., Smith, S. L., Noetzli, J., Matthes, H., Vieira, G., Streletskiy, D. A., Schoeneich, P., Romanovsky, V. E., Lewkow, A. G., Abramov, A., Allard, M., Boike, J., Cable, W. L., Christiansen, H. H., Delaloye, R., Diekmann, B., Drozdov, D., Etzelmüller, B., Grosse, G., Guglielmin, M., Thomas Ingeman-Nielsen, T., Ketil Isaksen, K., Ishikawa, M., Johansson, M., Johannsson, H., Joo, A., Kaverin, D., Kholodov, A., Konstantinov, P., Kröger, T., Lambiel, C., Lanckman, J.-P., Luo, D., Malkova, G., Meiklejohn, I., Moskalenko, N., Oliva, M., Phillips, M., Ramos, M., Sannel, A. B. K., Sergeev, D., Seybold, C., Skryabin, P., Vasiliev, A., Wu, Q., Yoshikawa, K., Zheleznyak, M., and Lantuit, H.: Permafrost is warming at a global scale, *Nat. Commun.*, 95 10, 264, <https://doi.org/10.1038/s41467-018-08240-4>, 2019.
- Boscolo-Galazzo, F., Crichton, K. A., Barker, S., and Pearson, P. N.: Temperature dependency of metabolic rates in the upper ocean: A positive feedback to global climate change? *Global and Planetary Change*, 170(August), 201–212, <https://doi.org/10.1016/j.gloplacha.2018.08.017>, 2018
- Bröder, L., Tesi, T., Andersson, A., Semiletov, I., and Gustafsson, Ö.: Bounding cross-shelf transport time and degradation in Siberian-Arctic land-ocean carbon transfer. *Nature Communications*, (February), <https://doi.org/10.1038/s41467-018-03192-1>, 2018
- Bröder, L., Davydova, A., Davydov, S., Zimov, N., and Haghypour, N.: Particulate Organic Matter Dynamics in a Permafrost Headwater Stream and the Kolyma River Mainstem *Journal of Geophysical Research: Biogeosciences*. 1–16, <https://doi.org/10.1029/2019JG005511>, 2020
- Brown, N. J., Nilsson, J., and Pemberton, P.: Arctic Ocean freshwater dynamics: Transient response to increasing river runoff and precipitation. *Journal of Geophysical Research: Oceans*, 124, 5205– 5219, <https://doi.org/10.1029/2018JC014923>, 2019

- Brunet, F., Gaiero, D., Probst, J. L., Depetris, P. J., Lafaye, F. G., and Stille, P.: $\delta^{13}\text{C}$ tracing of dissolved inorganic carbon sources in patagonian rivers (Argentina). *Hydrological Processes*, 19(17), 3321–3344, <https://doi.org/10.1002/hyp.5973>, 2005
- Carmack, E. C., Yamamoto-Kawai, M., Haine, T. W. N., Bacon, S., Bluhm, B. A., Lique, C., Melling, H., Polyakov, I. V., Straneo, F., Timmermans, M.-L., Williams, W. J.: Freshwater and its role in the Arctic Marine System: Sources, disposition, storage, export, and physical and biogeochemical consequences in the Arctic and global oceans. *Journal of Geophysical Research G: Biogeosciences*, 121(3), 675–717, <https://doi.org/10.1002/2015JG003140>, 2016
- Charkin, A. N., Dudarev, O. V., Semiletov, I. P., Kruhmalev, A. V., Vonk, J. E., Sánchez-García, L., Karlsson, E., and Gustafsson, Ö.: Seasonal and interannual variability of sedimentation and organic matter distribution in the Buor-Khaya Gulf: the primary recipient of input from Lena River and coastal erosion in the southeast Laptev Sea, *Biogeosciences*, 8, 2581–2594, <https://doi.org/10.5194/bg-8-2581-2011>, 2011
- Chevychelov, A. P., Bosikov, N. P.: Natural conditions. In: Troeva E. I., Isaev A. P., Cherosov M. M., Karpov N. S. (eds) *The far north: plant biodiversity and ecology of Yakutia. Plant and Vegetation 3*. Springer, Dordrecht, pp 1–23, https://doi.org/10.1007/978-90-481-3774-9_1, 2010
- Fedorova, I., Chetverova, A., Bolshiyarov, D., Makarov, A., Boike, J., Heim, B., Morgenstern, A., Overduin, P. P., Wegner, C., Kashina, V., Eulenburg, A., Dobrotina, E., and Sidorina, I.: Lena Delta hydrology and geochemistry: long-term hydrological data and recent field observations, *Biogeosciences*, 12, 345–363, <https://doi.org/10.5194/bg-12-345-2015>, 2015.
- Feng, D., Gleason, C. J., Lin, P., Yang, X., Pan, M., and Ishitsuka, Y.: Recent changes to Arctic river discharge. *Nature Communications*, 12(1), 1–9, <https://doi.org/10.1038/s41467-021-27228-1>, 2021
- Finlay, J. C., and Kendall, C.: Stable Isotope Tracing of Temporal and Spatial Variability in Organic Matter Sources to Freshwater Ecosystems. In *Stable Isotopes in Ecology and Environmental Science* (eds Michener R. and Lajtha K.), <https://doi.org/10.1002/9780470691854.ch10>, 2008
- Fox-Kemper, B., Hewitt, H. T., Xiao, C., Aðalgeirsdóttir, G., Drijfhout, S. S., Edwards, T. L., Golledge, N. R., Hemer, M., Kopp, R. E., Krinner, G., Mix, A., Notz, D., Nowicki, S., Nurhati, I. S., Ruiz, L., Sallée, J.-B., Slangen, A. B. A., and Yu, Y.: Ocean, Cryosphere and Sea Level Change. In *Climate Change 2021: The Physical Science Basis. Contribution of Working Group I to the Sixth Assessment Report of the Intergovernmental Panel on Climate Change* [Masson-Delmotte, V., Zhai, P., Pirani, A., Connors, S. L., Péan, C., Berger, S., Caud, N., Chen, Y., Goldfarb, L., Gomis, M. I., Huang, M., Leitzell K., Lonnoy E., Matthews, J. B. R., Maycock, T. K., Waterfield, T., Yelekçi, O., Yu, R., and Zhou B. (eds.)]. Cambridge University Press, Cambridge, United Kingdom and New York, NY, USA, pp. 1211–1362, <https://doi:10.1017/9781009157896.011>, 2021
- Fuchs, M., Nitze, I., Strauss, J., Günther, F., Wetterich, S., Kizyakov, A., Fritz, M., Opel, T., Grigoriev, M.N., Maksimov, G.T. and Grosse, G.: Rapid Fluvio-Thermal Erosion of a Yedoma Permafrost Cliff in the Lena River Delta. *Front. Earth Sci.* 8:336, <https://doi: 10.3389/feart.2020.00336>, 2020
- Fuchs, M., Ogneva, O., Sanders, T., Schneider, W., Polyakov, V., Becker, O. O., Bolshiyarov, D., Mollenhauer, G., and Strauss, J.: CACOON Sea – water sampling along the Sardakhskaya channel and near shore of the Laptev Sea, in: Fuchs, M., Bolshiyarov, D., Grigoriev, M. N., Morgenstern, A., and Dill, A. (eds.). *Reports on Polar and Marine Research, Russian-German Cooperation: Expeditions to Siberia in 2019*, Bremerhaven, Alfred Wegener Institute, Chapter 3.26, pp. 141-149, ISBN: 1866-3192, https://doi.org/10.48433/BzPM_0749_2021, 2021
- Fuchs, M., Palmtag, J., Juhls, B., Overduin, P. P., Grosse, G., Abdelwahab, A., Bedington, M., Sanders, T., Ogneva, O., Fedorova, I. V., Zimov, N. S., Mann, P. J., and Strauss, J.: High-resolution bathymetry models for the Lena Delta and Kolyma Gulf coastal zones, *Earth Syst. Sci. Data*, 14, 2279–2301, <https://doi.org/10.5194/essd-14-2279-2022>, 2022

- Gabyshev, V. A., Tsarenko, P. M. and Ivanova, A. P.: Diversity and Features of the Spatial Structure of Algal Communities of Water Bodies and Watercourses in the Lena River Estuary. *Inland Water Biol* 12, 1–9, <https://doi.org/10.1134/S1995082919050067>, 2019
- Galimov, E. M., Kodina, L. A., Stepanets, O. V., and Korobenik, G. S. Biogeochemistry of the Russian Arctic. Kara Sea: Research results under the SIRRO project, 1995–2003. *Geochem. Int.* 44, 1053–1104, <https://doi.org/10.1134/S0016702906110012>, 2006
- Gordeev, V. V.: Fluvial sediment flux to the Arctic Ocean. *Geomorphology*, 80(1–2), 94–104, <https://doi.org/10.1016/j.geomorph.2005.09.008>, 2006
- Grotheer, H., Meyer, V., Riedel, T., Pfalz, G., Mathieu, L., Hefter, J., Gentz, T., Mollenhauer, G., Fritz, M.: Burial and origin of permafrost-derived carbon in the nearshore zone of the southern Canadian Beaufort Sea. *Geophysical Research Letters*, 47, e2019GL085897, <https://doi.org/10.1029/2019GL085897>, 2020
- Haugk, C., Jongejans, L. L., Mangelsdorf, K., Fuchs, M., Ogneva, O., Palmtag, J., Mollenhauer, G., Mann, P. J., Overduin, P. P., Grosse, G., Sanders, T., Tuerena, R. E., Schirrmeister, L., Wetterich, S., Kizyakov, A., Karger, C., and Strauss, J.: Organic matter characteristics of a rapidly eroding permafrost cliff in NE Siberia (Lena Delta, Laptev Sea region), *Biogeosciences*, 19, 2079–2094, <https://doi.org/10.5194/bg-19-2079-2022>, 2022
- Hawkings, J., Wadham, J., Benning, L. Hendry, K. R., Tranter, M., Tedstone, A., Nienow, P., Raiswell, R.: Ice sheets as a missing source of silica to the polar oceans. *Nat Commun* 8, 14198 (2017), <https://doi.org/10.1038/ncomms14198>, 2017
- Hilton, R., Galy, V., Gaillardet, J., Dellinger, M., Bryant, C., O'Regan, M., Gröcke, D.R., Coxall, H., Bouchez, J. & Calmels, D. Erosion of organic carbon in the Arctic as a geological carbon dioxide sink. *Nature* 524, 84–87, <https://doi.org/10.1038/nature14653>, 2015
- Holmes R. M., Shiklomanov A. I., Suslova A., Tretiakov M., McClelland J. W., Spencer R. G. M., Tank S. E.: Arctic Report Card 2018: River Discharge, <https://doi.org/10.25923/zevf-ar65>, 2018
- Holmes, R. M., Shiklomanov, A. I., Suslova, A., Tretiakov, M., McClelland, J. W., Spencer, R. G. M. and Tank, S. E.: River Discharge [in "State of the Climate in 2018"]. *Bull. Amer. Meteor. Soc.*, 100 (9), 161–163, <https://doi:10.1175/2019BAMSStateoftheClimate.1>, 2019
- Holmes, R.M., McClelland, J.W., Tank, S.E., Spencer, R.G.M., and Shiklomanov A.I.: Arctic Great Rivers Observatory. Water Quality Dataset, Version 20210319. <https://www.arcticgreatrivers.org/data>, 2021
- Hugelius, G., Strauss, J., Zubrzycki, S., Harden, J. W., Schuur, E. A. G., Ping, C.-L., Schirrmeister, L., Grosse, G., Michaelson, G. J., Koven, C. D., O'Donnell, J. A., Elberling, B., Mishra, U., Camill, P., Yu, Z., Palmtag, J., and Kuhry, P.: Estimated stocks of circumpolar permafrost carbon with quantified uncertainty ranges and identified data gaps, *Biogeosciences*, 11, 6573–6593, <https://doi.org/10.5194/bg-11-6573-2014>, 2014
- Ittekkot, V., and Laane, R. W. P. M.: Fate of riverine particulate organic matter. In: Degens, E. T., Kempe, S., Richey, J. E. (Eds.), *Biogeochemistry of Major World Rivers*. Wiley, New York, pp. 233–242, <https://doi.org/10.1002/aqc.3270010209>, 1991
- Ivanov, V.V., Piskun, A.A. (1999). Distribution of River Water and Suspended Sediment Loads in the Deltas of Rivers in the Basins of The Laptev and East-Siberian Seas, in *Land-Ocean Systems in the Siberian Arctic: Dynamics and History*, edited by H. Kassens et al., pp. 239-250, Springer, Berlin, Heidelberg, https://doi.org/10.1007/978-3-642-60134-7_22, 1999
- Jong, D., Bröder, L., Tanski, G., Fritz, M., Lantuit, H., Tesi, T., Haghypour, N., Eglinton, T.I. and Vonk, J.E. (2020), Nearshore Zone Dynamics Determine Pathway of Organic Carbon From Eroding Permafrost Coasts, *Geophys. Res. Lett.*, 47: e2020GL088561, <https://doi.org/10.1029/2020GL088561>, 2020
- Juhls, B., Stedmon, C. A., Morgenstern, A., Meyer, H., Hölemann, J., Heim, B., Povazhnyi, V., and Overduin P. P.: Identifying Drivers of Seasonality in Lena River Biogeochemistry and Dissolved Organic Matter Fluxes. *Front. Environ. Sci.* 8:53, <https://doi:10.3389/fenvs.2020.00053>, 2020

- Kääb, A., Lamare, M., and Abrams, M.: River ice flux and water velocities along a 600 km-long reach of Lena River, Siberia, from satellite stereo, *Hydrol. Earth Syst. Sci.*, 17, 4671–4683, <https://doi.org/10.5194/hess-17-4671-2013>, 2013.
- Karlsson, E., Gelting, J., Tesi, T., van Dongen, B., Andersson, A., Semiletov, I., Charkin, A., Dudarev, O., and Gustafsson, Ö.: Different sources and degradation state of dissolved, particulate, and sedimentary organic matter along the Eurasian Arctic coastal margin, *Global Biogeochem. Cycles*, 30, 898– 919, <https://doi:10.1002/2015GB005307>, 2016
- Köchy, M., Hiederer, R., and Freibauer, A.: Global distribution of soil organic carbon – Part 1: Masses and frequency distributions of SOC stocks for the tropics, permafrost regions, wetlands, and the world, *SOIL*, 1, 351–365, <https://doi.org/10.5194/soil-1-351-2015>, 2015
- Krumpen, T., Belter, J., Boetius, A., Damm, E., Haas, C., Hendricks, S., Nicolaus, M., Nöthig, E. M. , Paul, S., Peeken, I., Ricker, R., and Stein, R.: Arctic warming interrupts the Transpolar Drift and affects long range transport of sea ice and ice-rafted matter, *Sci. Rep.*, 9, 5459, <https://doi.org/10.1038/s41598-019-41456-y>, 2019
- Kutscher, L., Mörth, C.-M., Porcelli, D., Hirst, C., Maximov, T. C., Petrov, R. E., and Andersson, P. S.: Spatial variation in concentration and sources of organic carbon in the Lena River, Siberia, *J. Geophys. Res. Biogeosci.*, 122, 1999– 2016, <https://doi:10.1002/2017JG003858>, 2017
- Lamontagne-Hallé, P., McKenzie, J. M., Kurylyk, B. L., and Zipper, S. C.: Changing groundwater discharge dynamics in permafrost regions, *Environmental Research Letters*, 13(8), <https://doi.org/10.1088/1748-9326/aad404>, 2018
- Lehner, B. and Grill, G.: Global river hydrography and network routing: baseline data and new approaches to study the world's large river systems. *Hydrol. Process.*, 27: 2171–2186. <https://doi.org/10.1002/hyp.9740>, 2013
- Li, F., Zhang, H., Zhu, Y., Xiao, Y., and Chen, L.: Effect of flow velocity on phytoplankton biomass and composition in a freshwater lake. *Science of the Total Environment*, 447, 64–71, <https://doi.org/10.1016/j.scitotenv.2012.12.066>, 2013
- Lique, C., Holland, M. M., Dibike, Y. B., Lawrence, D. M., and Screen, J. A.: Modeling the Arctic freshwater system and its integration in the global system: Lessons learned and future challenges. 540–566, <https://doi.org/10.1002/2015JG003120>.Received, 2016
- Lisitzin, A. P.: A marginal Filter of the Ocean. *Okeanologiya*, 34 (5), 735-747, 1994, (In Russian)
- Liu, B., Yang, D., Ye, B., and Berezovskaya, S.: Long-term open-water season stream temperature variations and changes over Lena River Basin in Siberia. *Global and Planetary Change*, 48(1-3 SPEC. ISS.), 96–111, <https://doi.org/10.1016/j.gloplacha.2004.12.007>, 2005
- Magritsky, D., Alexeevsky, N., Aybulatov, D., Fofonova, V., and Gorelkin, A.: Features and Evaluations of Spatial and Temporal Changes of Water Runoff, Sediment Yield and Heat Flux in the Lena River Delta. *Polarforschung*, 87(2), 89-110, <https://doi.org/10.2312/polarforschung.87.2.89>, 2018
- Mann, P. J., Eglinton, T. I., McIntyre, C. P., Zimov, N., Davydova, A., Vonk, J. E., Holmes, R. M., and Spencer, R. G. M.: Utilization of old permafrost carbon in headwaters of Arctic fluvial networks, *Nat. Commun.*, 6, 7856, <https://doi:10.1038/ncomms8856>, 2015
- Mann, P.J., Strauss, J., Palmtag, J., Dowdy, K., Ogneva, O., Fuchs, M., Bedington, M., Torres, R., Polimene, L., Overduin, P., Mollenhauer, G., Grosse, G., Rachold, V., Sobczak, W.V., Spencer, R.G.M., and Juhls, B.: Degrading permafrost river catchments and their impact on Arctic Ocean nearshore processes. *Ambio* 51, 439–455, <https://doi.org/10.1007/s13280-021-01666-z>, 2022
- McClelland, J. W., Holmes, R. M., Peterson, B. J., Raymond, P. A., Striegl, R. G., Zhulidov, A. V., Zimov, S. A., Zimov N., Tank, S. E., Spencer, R. G. M., Staples, R., Gurtovaya, T. Y., and Griffin C. G.: Particulate organic carbon and nitrogen export from major Arctic rivers, *Global Biogeochem. Cycles*, 30, 629– 643, <https://doi:10.1002/2015GB005351>, 2016

- Mollenhauer, G., Grotheer, H., Gentz, T., Bonk, E., and Hefter, J.: Standard operation procedures and performance of the MICADAS radiocarbon laboratory at Alfred Wegener Institute (AWI), Germany. *Nuclear Instruments and Methods in Physics Research, Section B: Beam Interactions with Materials and Atoms*, 496 (April), 45–51, <https://doi.org/10.1016/j.nimb.2021.03.016>, 2021
- Mulholland, P. J.: Dissolved organic matter concentration and flux in streams. *Journal of the North American Benthological Society*, 16(1), 131–141, <https://doi.org/10.2307/1468246>, 1997
- Nigamatzyanova, G.R., Frolova, L.A., Chetverova, A.A., Fedorova, I.V.: Hydrobiological investigation of channels in the mouth region of the Lena River, *Uchenye Zapiski Kazanskogo Universiteta. Seriya Estestvennye Nauki*, vol. 157, no. 4, pp. 96–108, 2015, (In Russian)
- Obu, J., Westermann, S., Bartsch, A., Berdnikov, N., Christiansen, H.H., Dashtseren, A., Delaloye, R., Elberling, B., Etzelmüller, B., Kholodov, A., Khomutov, A., Kääh, A., Leibman, M.O., Lewkowicz, A.G., Panda, S.K., Romanovsky, V., Way, R.G., Westergaard-Nielsen, A., Wu, T., Yamkhin, J., Zou, D.: Northern Hemisphere permafrost map based on TTOP modelling for 2000–2016 at 1 km² scale. *Earth-Science Reviews*, 193(October 2018), 299–316, <https://doi.org/10.1016/j.earscirev.2019.04.023>, 2019
- Oliva, M., and Fritz, M.: Permafrost degradation on a warmer Earth: Challenges and perspectives. *Current Opinion in Environmental Science and Health*, 5, 14–18, <https://doi.org/10.1016/j.coesh.2018.03.007>, 2018
- Overland, J. E., Wang, M., Walsh, J. E., and Stroeve, J. C.: Future Arctic climate changes: Adaptation and mitigation time scales. *Earth's Future*, 2(2), 68–74, <https://doi.org/10.1002/2013ef000162>, 2014
- Paczkowska, J., Rowe, O. F., Figueroa, D., and Andersson, A.: Drivers of phytoplankton production and community structure in nutrient-poor estuaries receiving terrestrial organic inflow. *Marine Environmental Research*, 151(August), 104778, <https://doi.org/10.1016/j.marenvres.2019.104778>, 2019
- Pohl, E., Grenier, C., Vrac, M., and Kageyama, M.: Emerging climate signals in the Lena River catchment: a non-parametric statistical approach. *Hydrology and Earth System Sciences*, 24(5), 2817–2839, <https://doi.org/10.5194/hess-24-2817-2020>, 2020
- Rachold, V., Alabyan, A., Hubberten, H.-W., Korotaev, V.N. and Zaitsev, A.A.: Sediment transport to the Laptev Sea—hydrology and geochemistry of the Lena River. *Polar Research*, 15: 183-196, <https://doi.org/10.1111/j.1751-8369.1996.tb00468.x>, 1996
- Rantanen, M., Karpechko, A. Y., Lipponen, A., Nordling, K., Hyvärinen, O., Ruosteenoja, K., Vihma, T., and Laaksonen, A.: The Arctic has warmed nearly four times faster than the globe since 1979, *Communications Earth and Environment*, 3, 168, <https://doi:10.1038/s43247-022-00498-3>, 2022.
- Richter-Menge, J., Druckenmiller, M. L., and Jeffries, M. Eds.: *Arctic Report Card 2019*, <https://www.arctic.noaa.gov/Report-Card>, 2019
- Rounick, J. S., James, M. R.: Geothermal and cold springs faunas: Inorganic carbon sources affect isotope values, *Limnology and Oceanography*, 2, <https://doi: 10.4319/lo.1984.29.2.0386>, 1984
- Salmaso, N., and Braioni, M. G.: Factors controlling the seasonal development and distribution of the phytoplankton community in the lowland course of a large river in Northern Italy (River Adige), *Aquatic Ecology*, 42(4), pp. 533–545, <https://doi.org/10.1007/s10452-007-9135-x>, 2008
- Sanders, T., Fiencke, C., Fuchs, M., Haugk, C., Juhls, B., Mollenhauer, G., Ogneva, O., Overduin, P., Palmtag, J., Povazhniy, V., Strauss, J.: Seasonal nitrogen fluxes of the Lena River Delta. *Ambio* 51, 423–438 (2022), <https://doi.org/10.1007/s13280-021-01665-0>, 2022
- Schirmer, L., Grosse, G., Wetterich, S., Overduin, P. P., Strauss, J., Schuur, E. A. G., and Hubberten, H.-W.: Fossil organic matter characteristics in permafrost deposits of the northeast Siberian Arctic, *Journal of Geophysical Research: Biogeosciences*, 116, G00M02, <https://doi:10.1029/2011jg001647>, 2011.
- Semiletov, I. P., Pipko, I. I., Shakhova, N. E., Dudarev, O. V., Pugach, S. P., Charkin, A. N., McRoy, C. P., Kosmach, D., and Gustafsson, Ö.: Carbon transport by the Lena River from its headwaters to the Arctic

- Ocean, with emphasis on fluvial input of terrestrial particulate organic carbon vs. carbon transport by coastal erosion, *Biogeosciences*, 8, 2407–2426, <https://doi.org/10.5194/bg-8-2407-2011>, 2011
- Shiklomanov, A., Déry, S., Tretiakov, M., Yang, D., Magritsky, D., Georgiadi A., Tang W.: River Freshwater Flux to the Arctic Ocean. In: Yang, D., Kane, D.L. (eds) *Arctic Hydrology, Permafrost and Ecosystems*. Springer, Cham., https://doi.org/10.1007/978-3-030-50930-9_24, 2021a
- Shiklomanov, A.I., R.M. Holmes, J.W. McClelland, S.E. Tank, and R.G.M. Spencer. Arctic Great Rivers Observatory. Discharge Dataset, Version 20220630. <https://www.arcticrivers.org/data>, 2021b
- Stettner, S.; Beamish, A. L.; Bartsch, A.; Heim, B.; Grosse, G.; Roth, A.; Lantuit, H.: Monitoring Inter- and Intra-Seasonal Dynamics of Rapidly Degrading Ice-Rich Permafrost Riverbanks in the Lena Delta with TerraSAR-X Time Series. *Remote Sens.* 10, 51, <https://doi.org/10.3390/rs10010051>, 2018
- Stolbovoi, V.: Carbon in Russian soils. *Climatic Change*, 55(1–2), 131–156, <https://doi.org/10.1023/A:1020289403835>, 2002
- Stolpmann, L., Mollenhauer, G., Morgenstern, A., Hammes, J. S., Boike, J., Overduin, P. P. and Grosse, G.: Origin and Pathways of Dissolved Organic Carbon in a Small Catchment in the Lena River Delta, *Frontiers in Earth Science*, 9. <https://doi.org/10.3389/feart.2021.759085>, 2022
- Stone, T. A., and Schlesinger P.: RLC Forest Cover Map of the Former Soviet Union, 1990. ORNL DAAC, Oak Ridge, Tennessee, USA, <https://doi.org/10.3334/ORNLDAAC/691>, 2003
- Strauss, J., Schirrmeister, L., Grosse, G., Wetterich, S., Ulrich, M., Herzsuh, U., and Hubberten, H.-W.: The deep permafrost carbon pool of the Yedoma region in Siberia and Alaska, *Geophys. Res. Lett.*, 40, 6165– 6170, <https://doi.org/10.1002/2013GL058088>, 2013
- Strauss, J., Abbott, B., Hugelius, G., Schuur, E. A. G., Treat, C., Fuchs, M., Schädel, C., Ulrich, M., Turetsky, M. R., Keuschnig, M., Biasi, C., Yang, Y., and Grosse, G.: Permafrost., in: *Recarbonizing global soils – A technical manual of recommended management practices*, edited by: Food and Agriculture Organization of the United Nations (FAO), Rome, Italy, 127-147, . <https://doi.org/10.4060/cb6386en>, 2021a
- Strauss, J., Laboor, S., Schirrmeister, L., Fedorov, A. N., Fortier, D., Froese, D., Fuchs, M., Günther, F., Grigoriev, M., Harden, J., Hugelius, G., Jongejans, L. L., Kanevskiy, M., Kholodov, A., Kunitsky, V., Kraev, G., Lozhkin, A., Rivkina, E., Shur, Y., Siegert, C., Spektor, V., Streletskaya, I., Ulrich, M., Vartanyan, S., Veremeeva, A., Anthony, K.W., Wetterich, S., Zimov, N., and Grosse, G.: Circum-Arctic Map of the Yedoma Permafrost Domain. *Front. Earth Sci.* 9:758360, <https://doi.org/10.3389/feart.2021.758360>, 2021b
- Stuiver, M., and Polach, H. A.: Discussion Reporting of ¹⁴C Data. *Radiocarbon*, 19(3), 355–363, <https://doi.org/10.1017/S0033822200003672>, 1977
- Tananaev, N., and Lotsari, E.: Defrosting northern catchments: Fluvial effects of permafrost degradation. *Earth-Science Reviews*, 228(March), 103996, <https://doi.org/10.1016/j.earscirev.2022.103996>, 2022
- Tanski, G., Wagner, D., Knoblauch, C., Fritz, M., Sachs, T., and Lantuit, H.: Rapid CO₂ release from eroding permafrost in seawater. *Geophysical Research Letters*, 46, 11244–11252, <https://doi.org/10.1029/2019GL084303>, 2019
- Terhaar, J., Lauerwald, R., Regnier, P., Gruber, N., and Bopp, L.: Around one third of current Arctic Ocean primary production sustained by rivers and coastal erosion. *Nature Communications*, 12(1), 1–10, <https://doi.org/10.1038/s41467-020-20470-z>, 2021
- Vihma, T., Screen, J., Tjernström, M., Newton, B., Zhang, X., Popova, V., Deser, C., Holland, M., and Prowse, T.: The atmospheric role in the Arctic water cycle: A review on processes, past and future changes, and their impacts, *J. Geophys. Res. Biogeosci.*, 121, 586– 620, <https://doi.org/10.1002/2015JG003132>, 2016
- Vonk, J. E., Sánchez-García, L., Semiletov, I., Dudarev, O., Eglinton, T., Andersson, A., and Gustafsson, Ö.: Molecular and radiocarbon constraints on sources and degradation of terrestrial organic carbon

- along the Kolyma paleoriver transect, East Siberian Sea, *Biogeosciences*, 7, 3153–3166, <https://doi.org/10.5194/bg-7-3153-2010>, 2010
- Vonk, J. E., Semiletov, I. P., Dudarev, O. V., Eglinton, T. I., Andersson, A., Shakhova, N., Charkin, A., Heim, B., and Gustafsson, Ö.: Preferential burial of permafrost-derived organic carbon in Siberian-Arctic shelf waters, *J. Geophys. Res. Oceans*, 119, 8410–8421, <https://doi.org/10.1002/2014JC010261>, 2014
- Vonk, J. E., Tesi, T., Bröder, L., Holmstrand, H., Hugelius, G., Andersson, A., Dudarev, O., Semiletov, I., and Gustafsson, Ö.: Distinguishing between old and modern permafrost sources in the northeast Siberian land–shelf system with compound-specific $\delta^2\text{H}$ analysis, *The Cryosphere*, 11, 1879–1895, <https://doi.org/10.5194/tc-11-1879-2017>, 2017
- Vonk, J. E., Tank, S. E., and Walvoord, M. A.: Integrating hydrology and biogeochemistry across frozen landscapes. *Nature Communications*, 10(1), 3–6, <https://doi.org/10.1038/s41467-019-13361-5>, 2019
- Walvoord, M. A. and Striegl, R. G.: Increased groundwater to stream discharge from permafrost thawing in the Yukon River basin: potential impacts on lateral export of carbon and nitrogen. *Geophysical Research Letters* 34, 1–6, L12402, <https://doi.org/10.1029/2007GL030216>, 2007.
- Walvoord, M. A., and Kurylyk, B. L.: Hydrologic Impacts of Thawing Permafrost - A Review, *Vadose Zone Journal*, 15 (6): 1-20, <https://doi.org/10.2136/vzj2016.01.0010>, 2016
- Wang, K., Zhang, T., and Yang, D.: Permafrost dynamics and their hydrologic impacts over the Russian Arctic Drainage Basin. *Advances in Climate Change Research*, <https://doi.org/10.1016/j.accre.2021.03.014>, 2021a
- Wang, P., Huang, Q., Pozdniakov, S. P., Liu, S., Ma, N., Wang, T., Zhang, Y., Yu, J., Xie, J., Fu, G., Frolova, N. L., Liu, C.: Potential role of permafrost thaw on increasing Siberian river discharge. *Environmental Research Letters*, 16(3), <https://doi.org/10.1088/1748-9326/abe326>, 2021b
- Wild, B., Andersson, A., Bröder, L., Vonk, J., Hugelius, G., and McClelland, J. W.: Rivers across the Siberian Arctic unearth the patterns of carbon release from thawing permafrost. *Proc. Natl. Acad. Sci. U.S.A.* 116, 10280–10285, <https://doi.org/10.1073/pnas.1811797116>, 2019
- Winterfeld, M., Laepple, T., and Mollenhauer, G.: Characterization of particulate organic matter in the Lena River delta and adjacent nearshore zone, NE Siberia – Part I: Radiocarbon inventories, *Biogeosciences*, 12, 3769–3788, <https://doi.org/10.5194/bg-12-3769-2015>, 2015
- Yang, D., Kane, D. L., Hinzman, L. D., Zhang, X., Zhang, T., and Ye, H.: Siberian Lena River hydrologic regime and recent change. *Journal of Geophysical Research Atmospheres*, 107(23), ACL 14-1-ACL 14-10, <https://doi.org/10.1029/2002JD002542>, 2002
- Yang, D., Park, H., Peterson, A., Liu, B.: Arctic River Water Temperatures and Thermal Regimes. In: Yang, D., Kane, D.L. (eds) *Arctic Hydrology, Permafrost and Ecosystems*. Springer, Cham. https://doi.org/10.1007/978-3-030-50930-9_10, 2021
- Zhang, S. M., Mu, C. C., Li, Z. L., Dong, W. W., Wang, X. Y., Streletskaia, I., Grebenets, V., Sokratov, S., Kizyakov, A., Wu, X. D.: Export of nutrients and suspended solids from major Arctic rivers and their response to permafrost degradation. *Advances in Climate Change Research*, 12(4), 466–474. <https://doi.org/10.1016/j.accre.2021.06.002>, 2021
- Zimov, S. A., Schuur, E. A. G., and Stuart Chapin, F.: Permafrost and the global carbon budget. *Science*, 312(5780), 1612–1613, <https://doi.org/10.1126/science.1128908>, 2006

Supplement

Particulate organic matter in the Lena River and its Delta: from the permafrost catchment to the Arctic Ocean

Correspondence to: Olga Ogneva (Olga.Ogneva@awi.de), Gesine Mollenhauer (Gesine.Mollenhauer@awi.de) and Jens Strauss (Jens.Strauss@awi.de)

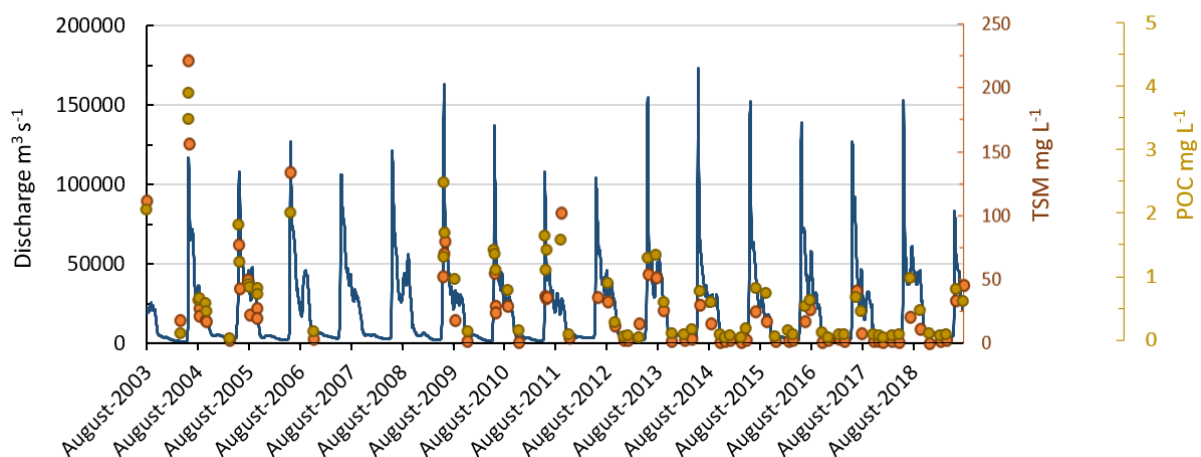


Figure 3-S1. Time series of the Lena River discharge provided by ArcticGRO for 2003-2019 and TSM, POC concentration fluctuation.

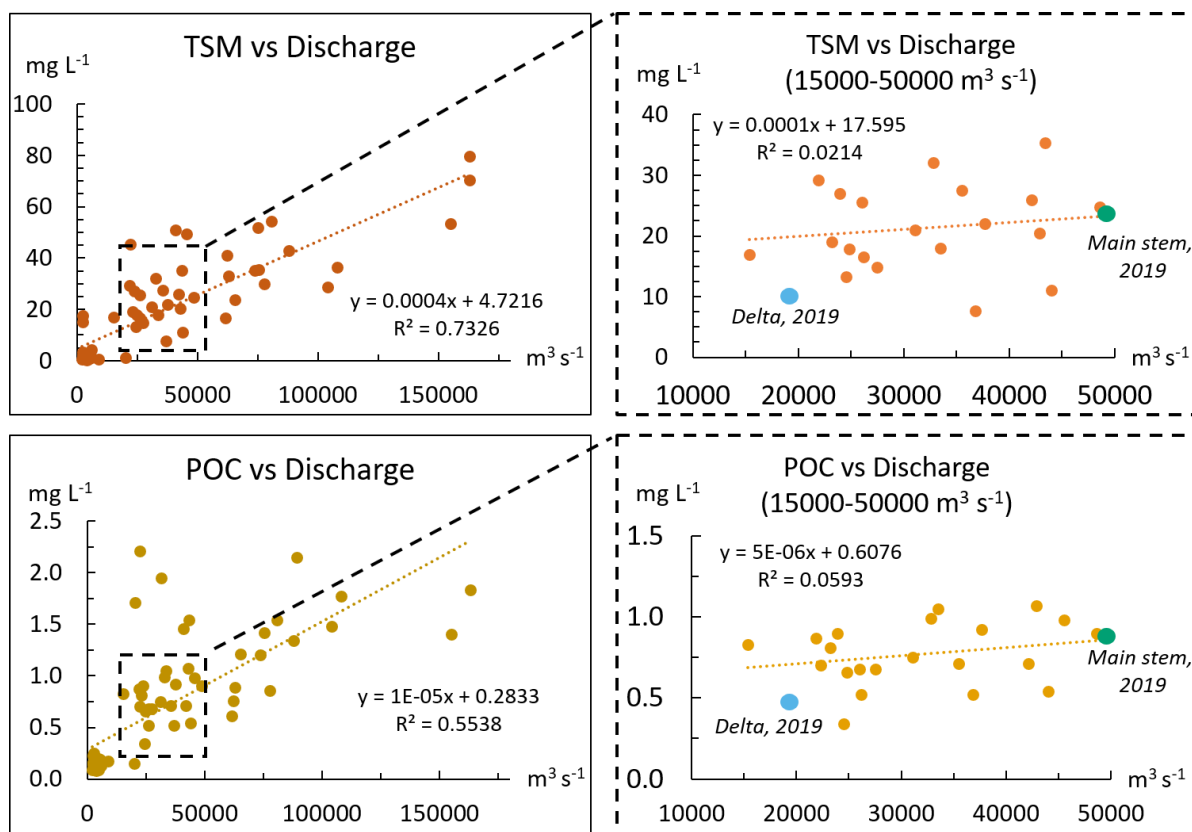


Figure 3-S2. TSM, POC concentration (outliers were removed) and the Lena River discharge provided by ArcticGRO (left hand panels) and TSM and POC concentrations within the reduced range of the Lena River discharge including TSM and POC concentrations measured for this study in 2019 (right hand panels).

Table 3-S1. Contribution of different OM sources to the composition of POC in the Lena River main stem and the Lena Delta.

Sample ID	Location	I. Phytoplankton, %	±std	II. Holocene Soils, %	±std	III. Pleistocene deposit, %	±std
LEN19-S-01-1	Stolb*	67.8	7.8	16.8	12.2	15.4	4.5
LEN19-S-01-9	Stolb*	61.2	7.9	18.8	12.4	20.1	4.5
LEN19-S-02-1	Delta	74.0	5.3	10.2	8.2	15.8	3.1
LEN19-S-02-16	Delta	65.2	7.7	18.1	12.1	16.7	4.5
LEN19-S-03-1	Delta	61.0	7.9	17.6	12.4	21.4	4.6
LEN19-S-04-1	Delta	69.7	4.6	8.7	7.0	21.6	2.6
LEN19-S-05-1	Delta	64.2	7.3	15.9	11.4	19.9	4.2
LEN19-S-06-1	Delta	71.4	7.4	17.2	11.5	11.3	4.3
LEN19-S-06-6	Delta	69.3	5.6	11.2	8.7	19.6	3.3
LEN19-S-07-1	Delta	68.3	5.4	10.5	8.4	21.2	3.1
LEN19-S-07-15	Delta	71.4	4.7	9.3	7.2	19.4	2.7
LEN19-S-78-1	Delta	72.0	4.7	8.7	7.3	19.3	2.8
LEN19-S-08-1	Delta	70.4	5.4	10.2	8.4	19.3	3.1
LEN19-S-08-6	Delta	64.0	9.0	25.6	14.0	10.3	5.1
LEN19-S-89-1	Delta	70.2	6.5	13.2	10.1	16.6	3.8
LEN19-S-89-6	Delta	73.7	5.3	10.2	8.2	16.1	3.1
LEN19-S-89-12	Delta	60.4	5.6	11.4	8.7	28.2	3.2
LEN19-S-09-1	Delta	72.5	5.7	11.2	8.9	16.3	3.3
LEN19-S-09-5	Delta	72.7	5.1	10.2	7.9	17.2	3.0
LEN19-S-09-10	Delta	68.9	6.4	13.4	10.0	17.7	3.7
MEAN		68.4	6.3	13.4	9.7	18.2	3.6
WL19-01	Main Stem	40.8	7.6	54.7	11.6	4.5	4.1
WL19-02	Main Stem	42.7	9.6	50.7	14.9	6.6	5.3
WL19-03	Main Stem	35.4	5.5	61.9	8.1	2.7	2.8
WL19-04	Main Stem	46.0	7.2	50.5	11.0	3.5	3.8
WL19-05	Main Stem	45.4	8.0	50.1	12.3	4.6	4.4
WL19-06	Main Stem	37.4	7.8	58.0	12.0	4.6	4.3
WL19-07	Main Stem	41.8	7.6	53.9	11.6	4.3	4.1
WL19-0	Main Stem	30.8	9.1	62.8	14.0	6.4	5.0
WL19-09	Main Stem	34.0	8.0	60.8	12.3	5.3	4.4
MEAN		39.4	7.8	55.9	12.0	4.7	4.2

*For this model samples from Stolb Island were included with the delta samples and contributed to the final mean ±stdv values for potential POC sources

4

Dissolved and particulate organic carbon characteristics in summer and winter waters of the Lena Delta

Dissolved and Particulate Organic Carbon Characteristics in Summer and Winter Waters of the Lena Delta

O. Ogneva^{1,2,3}, G. Mollenhauer^{1,3,4,*}, T. Sanders⁵, B. Juhls², J. Palmtag^{6,a}, M. Fuchs^{2,b}, J. Hammes^{1,c}, H. Grotheer^{1,4}, P. J. Mann⁶, S. Opfergelt⁷ and J. Strauss^{2,*}

¹Marine Geochemistry Section, Alfred Wegener Institute Helmholtz Centre for Polar and Marine Research, 27570 Bremerhaven, Germany

²Permafrost Research Section, Alfred Wegener Institute Helmholtz Centre for Polar and Marine Research, 14473 Potsdam, Germany

³Faculty of Geosciences, University of Bremen, Bremen, 28359, Germany

⁴Marum Center for Marine Environmental Sciences, University of Bremen, 28359 Bremen, Germany

⁵Institute for Carbon Cycles, Helmholtz Centre Hereon, 21502 Geesthacht, Germany

⁶Department of Geography and Environmental Sciences, Northumbria University, Newcastle-upon-Tyne, NE1 8ST, UK

⁷Earth and Life Institute, Université catholique de Louvain, Louvain-la-Neuve, Belgium

^anow at: Swedish Nuclear Fuel and Waste Management Co. (SKB), P.O. Box 3091, 169 03 Solna, Sweden

^bnow at: Renewable and Sustainable Energy Institute, University of Colorado Boulder, Boulder, USA

^cnow at: Carbon Drawdown Initiative GmbH, Fürth, Germany

*Corresponding authors: Gesine Mollenhauer (Gesine.Mollenhauer@awi.de) and Jens Strauss (Jens.Strauss@awi.de)

Emails of all co-authors: olga.ogneva@awi.de; Gesine.Mollenhauer@awi.de; tina.sanders@hereon.de; bennet.juhls@awi.de; juri.palmtag.work@gmail.com; Matthias.Fuchs@colorado.edu; Jens.Hammes@carbon-drawdown.de; hendrik.grotheer@awi.de; paul.mann@northumbria.ac.uk; sophie.opfergelt@uclouvain.be; jens.strauss@awi.de

Data availability statement

The data presented in this study is freely available in the PANGAEA data repository, Ogneva et al., 2023b (<https://doi.org/10.1594/PANGAEA.962633>). POC data are available from Ogneva et al., 2022 (<https://doi.org/10.1594/PANGAEA.950668>).

Funding statement

This research is part of the CACOON project funded by the Bundesministerium für Bildung und Forschung (BMBF, grant no. #03F0806A) and the Natural Environment Research Council (grant no. NE/R012806/1). TS was supported by the EISPAC project also funded by BMBF (grant no. #03F0809A) as a part of the joint German-UK 'Changing Arctic Ocean' effort. BJ was funded by the European Space Agency (ESA) as part of the Climate Change Initiative (CCI) fellowship (ESA ESRIN/Contract No. 4000133761/21/I-NB), and HG was funded by DFG under Germany's Excellence Strategy, no. EXC-2077–390741603.

Conflict of interest disclosure

The authors declare no conflicts of interest relevant to this study.

Acknowledgments

We are grateful to everyone who helped and supported the 'Changing Arctic Carbon cycle in the cOastal Ocean Near-shore (CACOON)' project and the joint Russian-German "Lena 2019" expedition, particularly Volkmar Aßmann (AWI) for logistics during the summer expedition and the Samoylov Research Station for hospitality.

Key Points:

- Unique dataset on DOC and POC concentrations and isotopic composition ($\Delta^{14}\text{C}$ and $\delta^{13}\text{C}$) from the largest Arctic delta, revealing differences in carbon sources delivered to the Lena Delta between summer and winter
- Summer DOC was enriched in ^{14}C , derived from leachates of modern plant debris grown in the first decade of the 21st century

Abstract

Rapid Arctic warming accelerates permafrost thaw, altering water flow and organic matter transport to aquatic ecosystems. To identify sources and seasonality of OC at the mouth of the Lena River, we measured summer and winter concentrations and C isotopes ($\Delta^{14}\text{C}$ and $\delta^{13}\text{C}$) of DOC and POC along a 140 km transect of the Lena Delta. Despite low water flow during winter, DOC concentrations in the Lena Delta were higher than those measured at the end of the summer (6.31 ± 0.60 and 5.54 ± 0.17 mg L⁻¹, respectively). We found pronounced differences in the DOC isotopic composition of waters between seasons (winter: mean = -16 ± 16 ‰ ranging between -14 and 46 ‰ and summer: mean = 41 ± 26 ‰ in the range between -47 and 79 ‰). $\Delta^{14}\text{C}$ of winter DOC suggested higher relative contributions of older carbon compared to summer DOC, which is enriched in ^{14}C . This study with its unique dataset on the largest Arctic delta will help to assess the ongoing changes with climate warming at this frontier between the land and the ocean realm.

4.1 Introduction

The Arctic is experiencing unprecedented environmental change in response to global climate change. High-latitude landscapes are susceptible to ongoing surface permafrost thaw due to warming Arctic air and soil temperatures (Biskaborn et al., 2019; Rantanen et al., 2022). Terrestrial landscape changes accelerate the release of organic matter (OM), containing organic carbon (OC) and nitrogen from peat, soil, and permafrost to inland aquatic systems (Schuur et al., 2022; Strauss et al., 2022, Strauss et al. 2024; Turetsky et al., 2020; Wild et al., 2019). Terrigenous OM and nutrients can be further transported to the Arctic coastal waters (Cole et al., 2007; Sanders et al., 2022; Tank et al., 2016) with subsequent impacts on biogeochemical cycles, primary production and dissolved inorganic carbon in the Arctic Ocean (Frey & McClelland, 2009; Terhaar et al., 2021). Contributions of permafrost-derived OC in aquatic and Arctic coastal waters are affected by changing river discharge regimes (Bröder et al., 2020; McGuire et al., 2009; Ogneva et al., 2023a), and supply from rapidly eroding river banks (Bröder et al., 2021; Fuchs et al., 2020; Kanevskiy et al., 2016) and coastlines (Tanski et al., 2019). Once mobilized into inland or coastal waters, permafrost and peat-derived OC from deepening active layers may be rapidly utilized by aquatic microorganisms and emitted to the atmosphere as carbon dioxide or methane (Bertin et al., 2023, Miner et al., 2022; Polimene et al., 2022; Schädel et al., 2016) enhancing riverine C emissions from river basins and nearshore waters (Vonk & Gustafsson, 2013). Permafrost OC inputs to Arctic rivers and streams, particularly dissolved organic carbon (DOC) from ice- and organic-rich Yedoma permafrost, are highly labile and preferentially utilized by aquatic microorganisms, leading to patterns of decreasing permafrost contributions in OC pools with increasing water residence times (Mann et al., 2015; Mann et al., 2022; Stolpmann et al., 2022).

Nearshore regions across the Arctic (including deltas, estuaries, and coasts) are biogeochemically active areas and hotspots for environmental change (Mann et al., 2022) where major transformation processes of terrestrial material are expected to take place (Jong et al., 2020; Sanders et al., 2022; Tanski et al., 2021; Tanski et al., 2019; Fuchs et al, in review). Estuarine and deltaic regions can be regarded as filters for riverine inputs and solute fluxes to the coastal waters and the open ocean (Smith et al., 2005; Emmerton et al., 2008; Kipp et al., 2020; Novak et al., 2022). Despite the importance of Arctic estuarine and deltaic environments in OM biogeochemistry (Ogneva et al., 2023a), their functioning is still poorly understood and the number of studies and therewith datasets that consider the supply, composition and transformation of terrestrial OM during transport from river-to-shelf is limited. Moreover, studies comparing the different seasons are lacking for OC or scarce for other nutrients (Knights et al., 2023), limiting the ability to predict the impact of shifting seasonality and of intensification of the Arctic freshwater cycle. In the specific context of the Lena River, one of the Arctic's largest rivers with increasing winter water discharge, total carbon entering the sea with the Lena discharge is estimated to be almost 10 Tg C yr⁻¹. Lena River discharge rates have increased over the last decade by around 10% (relative to 1971-2000 baseline) and are expected to continue to increase (+25% by 2100; Mann et al. 2022 and references herein). River ice break-up is generally occurring earlier, and freeze up later (Juhls et al., 2020), shortening the period of winter base flow. Moreover, the delayed active layer freeze-up increases winter river runoff (Feng et al., 2021; Lamontagne-Hallé et al., 2018; Shiklomanov et al., 2021a; Walvoord & Kurylyk, 2016; Wang et al., 2021). Changing connectivity between terrestrial landscapes and coastal waters has potentially significant ramifications for coastal carbon budgets and ecosystem structure, but depends upon how OM is transformed with estuarine and deltaic environments.

In this study, we examine how the supply and composition of DOC and POC (using $\Delta^{14}\text{C}$, $\delta^{13}\text{C}$) in the Lena River delta varied between winter and summer seasons. Further, we examine how dissolved and particulate OC loads vary during transit using seasonal transects across the Lena Delta. Our aim was to identify the dominant sources of DOC and POC to deltaic waters, and to consider how OC modification differs between dominant seasons.

4.2 Materials and Methods

4.2.1 Study area

The Lena Delta is the largest delta in the Arctic and represents one of the largest in the world. It occupies an area of $29,17 \times 10^3 \text{ km}^2$ (Fuchs et al., in review) and combines more than 800 transverse channels and branches with a total length of 6500 km (Fedorova et al., 2015). The delta receives approximately $543 \text{ km}^3 \text{ yr}^{-1}$ of freshwater (mean discharge for 1936 – 2019 at the upstream Kyusyur discharge station; Wang et al. (2021)). The Lena River catchment drains an area covering $\sim 2.61 \times 10^6 \text{ km}^2$, of which, more than 94 % contains permafrost and $\sim 70.5 \%$ of the catchment area is underlain by continuous permafrost (Juhls et al., 2020; Obu et al., 2019). Pleistocene-aged permafrost deposits (Yedoma) cover approximately 3.5 % of the Lena watershed area (Strauss et al., 2022; Strauss et al., 2017). Yedoma cliffs are actively eroding along the Lena River and delta banks (Fuchs et al., 2020; Haugk et al., 2022).

In this study, we sampled the Sardakhskaya channel (Figure 4-1), which together with the Trofimovskaya channel, form a system through which about 60-75 % of Lena freshwater export (Fedorova et al., 2015) and up to 70 % of sediments are routed to the Arctic Ocean coastline (Charkin et al., 2011; Ivanov & Piskun, 1999).

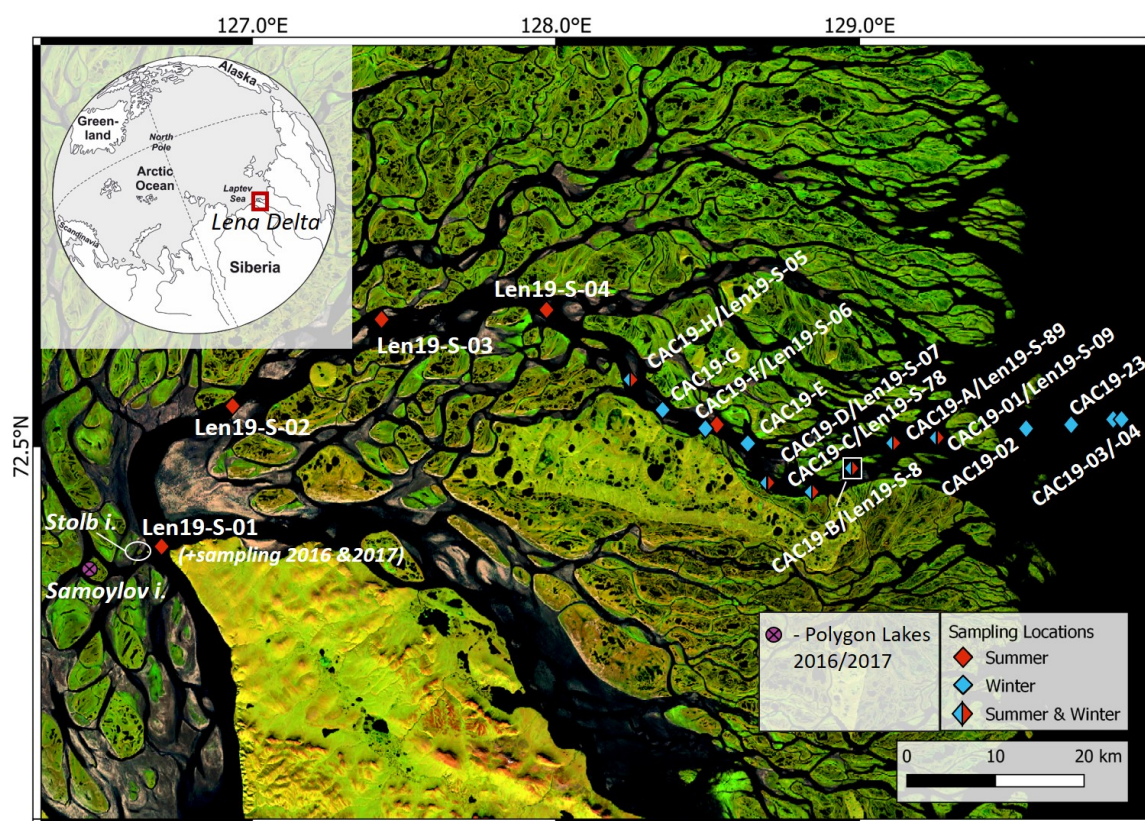


Figure 4-1. Sampling transect in the Lena Delta along the Sardakhskaya branch in 2019 and sampling locations in the Lena Delta in previous years near Stolp Island. ‘CAC’ samples represent on-ice winter sampling during the CACOON project, while ‘Len’, the Lena summer (S) ship-based sampling. 19 includes the year of sampling (2019). Adapted from M. Fuchs et al. (2021a) and Strauss et al. (2021).

4.2.1.1 Sample campaigns and water collection

Two sampling campaigns to the Lena Delta were conducted during the winter and summer months of 2019. Sites Len-19-S-# were sampled in summer, while CAC-19-# sites were sampled in winter.

The winter campaign took place between 26th March - 8th April, during which river, delta and coastal waters were fully ice-covered. Sampling was conducted using an on-ice camp comprising a cabin, a freight sled, a tractor and a caterpillar all-terrain vehicle, enabling unprecedented sampling across the difficult to access land-to-ocean region during the

highly data lean winter period (Figure 4-2). Sampling took place approximately every 5 km, starting at the easternmost location upon sea-ice (Figure 4-1; CAC19-03/-04). Sampling continued westward along a transect toward the delta, and then up ~40 km into the Sardakhszkaya channel (the last sampling site LEN19-S-01, Table 4-1).



Figure 4-2. Sampling vehicles in winter and summer. a) all terrain caterpillar vehicle in the Lena Delta on the Lena Delta river ice for reaching field sites further from the camp; b) Working process on ice in the Lena Delta in winter: drilling and water sampling; c) The research vessel "Merzlotoved" with the Sobo-Sise Yedoma cliff in the background; d) Water sampling at the back of the research vessel in the Lena Delta in summer 2019.

At each site, a borehole was drilled through the ice and 20 L of water collected using multiple deployments of a 5 L water sampler (UWITEC, Austria). Water was collected

from between one to three depths per station depending on the bottom depth at the sampling location. Waters were collected directly under the ice (around 2 m) at each sampling site. When river depths exceeded 4-7 m at a site, an additional water sample was collected from just above the bottom (4-7 m). At water depths >7 m, an additional water sample was collected from the mid-depth between the under-ice and bottom samples (Table 4-1). Winter water samples ($n = 21$) were stored in 20 L plastic canisters (pre-cleaned with 10 % HCl for 3 days) and kept cool until returning to the mobile laboratory in the camp, where it was further processed.

The summer sampling campaign was conducted between the 7th - 28th August 2019. Sampling by ship started in the West at Stolb Island, near the transition point between the Lena River and Delta (Figure 4-1). Sampling subsequently took place at locations along the Sardakhs kaya branch out into the Eastern Laptev Sea, and stations previously sampled during the winter campaign were re-occupied. Distances between sample sites varied between ~5 km along the channel, increasing to ~20 km within the Laptev Sea coast. Summer water sampling and collection ($n = 23$) was conducted identically to that of winter samples, except surface samples were taken from between 0 - 1m depth. At LEN19-S-06, we passed a rapidly eroding Yedom a Cliff (Figure 4-2c) previously studied by Fuchs et al. (2020) and Wetterich et al. (2020; 2021).

4.2.1.2 Archive samples and datasets

In addition to samples from the two sampling campaigns described above, we also include previously unpublished datasets from samples collected during similar expeditions from 2016-2017. These include water samples from near the island of Stolb at the Apex of the delta ($n = 32$), as well as water samples from small ponds on Samoylov Island ($n = 6$), which were collected in August 2016 and July 2017 (see also Stolpmann et al., 2022). The collection of these water samples and subsequent DOC concentration

and isotope analyses (described below) were identical to our summer sampling campaign approach.

4.2.2 Laboratory analyses

Water samples were filtered immediately on-site during the winter sampling campaign, or in summer, after less than 10 days storage, at the laboratory at the Samoylov Island Research Station. Waters were passed through a pre-combusted (4.5 hours, 450 °C) and pre-weighed glass fiber filter (GF/F Whatman, 0.7 µm nominal pore-size, Ø 2.5 cm) to separate POC (remaining on the filter) and DOC (dissolved in water which passed through the filter). Filters were packed into pre-combusted glass petri dishes, and waters were collected into 150 mL HDPE bottles (pre-cleaned with 10% HCl), and both kept frozen at -18 °C until further analyses.

4.2.2.1 Dissolved organic carbon concentration and carbon isotope analyses ($\Delta^{14}\text{C}$, $\delta^{13}\text{C}$)

DOC concentrations (mgC L^{-1}) were measured using a high temperature catalytic oxidation analyser (TOC- VHPH Shimadzu) at Alfred Wegener Institute (AWI) Potsdam. After every tenth sample, one blank (Milli-Q water) and one standard were measured. Five different certified standards covering a range between 1.26 mgC L^{-1} (SUPER_05_1) and 27.31 mgC L^{-1} (Std. US-QC) were used to calibrate the instrument. The results of standards provided a precision $\pm 10\%$.

Radiocarbon analyses by accelerator mass spectrometry (AMS) was carried out on a Mini Carbon Dating System (MICADAS) at AWI Bremerhaven, following the standard operation procedures described in detail by Mollenhauer et al. (2021). Filtered water samples (GF/F Whatman, 0.7 µm membrane) were acidified to pH ~ 1-2 with HCl. The aliquot for analyses (a volume containing approximately 100 µgC) was dried using a rotary-evaporator. Isolated DOC was transferred in an aqueous solution into 50 µL liquid tin capsules. After complete drying at 40 °C in a desiccator under vacuum (500-600 bar),

capsules with DOC were folded, combusted in an elemental analyser (Elementar Analysensysteme) connected via the Gas Interface System (Wacker et al., 2013) to the MICADAS and analysed using the option to obtain ^{14}C results on CO_2 gas. The radiocarbon data were normalized against CO_2 gas produced from oxalic acid II (OxAll, NIST SRM4990C) and blank corrected against ^{14}C -free CO_2 gas. Additionally, the processing blank was determined following Sun et al. (2020) and raw radiocarbon data were subsequently blank corrected following Wacker et al. (2010). We report radiocarbon data as $\Delta^{14}\text{C}$ values in ‰, which expresses the relative difference in ^{14}C activity between the absolute international standard (base year 1950) corrected for sampling time and normalized to $\delta^{13}\text{C}=25$ ‰ (Stuiver & Polach, 1977). To facilitate the discussion of the results, we refer to the most ^{14}C -depleted samples (less than -900 ‰ or older than $\sim 18,500$ ^{14}C years) as “ancient”, samples with $\Delta^{14}\text{C}$ ranging between -50 and -900 ‰ (corresponding to ~ 400 - 18,500 ^{14}C years) are referred to as “old”, and samples with $\Delta^{14}\text{C}$ above -50 ‰ to 0‰ are identified as “young” and “modern” (above 0 ‰).

The preparation for the stable C isotope analyses was the same as for $\Delta^{14}\text{C}$, but samples were measured on a Sercon-20-20 isotope ratio mass spectrometer (IRMS) coupled to an Automated Nitrogen Carbon Analyser (ANCA) at AWI Bremerhaven. Stable C isotope values were expressed as $\delta^{13}\text{C}$ in per mil (‰) and normalized against the Pee Dee Belemnite (PDB) standard. The analyser was calibrated using Isoleucine (NIST, RM 8573, USGS40) with a known isotopic composition. The precision of $\delta^{13}\text{C}$ measurements was better than ± 0.2 ‰.

4.2.2.2 Particulate organic carbon concentration and carbon isotope analyses ($\delta^{13}\text{C}$, $\Delta^{14}\text{C}$)

To determine total POC concentration (mgC L^{-1}) together with stable C isotopes, and to determine $\Delta^{14}\text{C}$ of POC, filters were dried for 24 hours at 40 °C, then acidified with drops of 10 % HCl (sufficient to wet the filter surface including its sediment) to remove inorganic

C. If the amount of C exceeded 100 µg, only a subsample of the filter was used. After carbonate removal, the filters were oven-dried under the same conditions and packed/rolled into tin boats (8x8x15 mm; IVA Analysentechnik Part no.: IVA2213742001). POC content on the filter and its $\delta^{13}\text{C}$ signature were measured on a Sercon-20-20 IRMS. The mean uncertainty for POC was ± 3.34 µgC, and concentrations were determined by dividing the POC content per filter by the volume of water filtered through that filter. The isotope ratios and C masses were evaluated for precision and accuracy by conducting multiple analyses of in-house standards (isoleucine, NIST, RM 8573, USGS40) with known isotopic composition (-26.39 ± 0.09 ‰). The $\delta^{13}\text{C}$ measurements exhibited a precision better than ± 0.2 ‰, while the average uncertainty for POC was ± 3.34 µg. The concentrations were determined by dividing the POC content per filter by the volume of water filtered through that filter.

Radiocarbon analyses of POC like for DOC were carried out on a Mini Carbon Dating System (MICADAS) following the procedure described in detail in Mollenhauer et al. (2021). The processing blank was determined by analysing five empty combusted blank filters (GF/F, 2.5 cm Ø) treated identically to the samples (Mollenhauer et al., 2021). POC data for the summer transect only have previously been described in Ogneva et al. (2023a, 2023b).

4.2.3 Statistics

We used the Welch t-test to examine whether differences between parameters measured in 2019 in the Lena Delta in winter and in summer were statistically significant. The significance level (alpha) was set at 0.01.

4.3 Results

4.3.1 Organic matter transformation within the Delta: Winter vs Summer

4.3.1.1 Concentrations of DOC and POC

Concentrations of DOC and POC were not significantly different by sample depth, so here we only present results separated by sampling period and study site. Deltaic POC and DOC concentrations differed between summer and winter campaigns (Figures 3 and 4). Winter DOC concentrations displayed a greater range (mean $6.31 \pm 0.61 \text{ mgC L}^{-1}$, $n = 21$, ranging between 5.82 and 8.54 mgC L^{-1}), than summer month samples (average: $5.54 \pm 0.18 \text{ mgC L}^{-1}$, range of 5.28 to 5.92 mgC L^{-1}). Two specific winter locations had markedly higher DOC concentrations than the winter mean concentration. One of these samples from the middle of the sampling transect (LEN19-S-07/ CAC19-F), was collected from a station 1-2 km downstream from an eroding Yedomá bank (Sobo-Sise cliff; Figure 4-3 and 4), and contained a DOC concentration of 8.54 mgC L^{-1} . A second higher DOC concentration of 7.30 mgC L^{-1} was also found at the Delta mouth (CAC19-02). DOC concentrations in the Lena Delta were significantly higher during winter months, relative to summer, even when the influence of CAC19-F (erosion-influenced) was removed (Welch t-test; $t(42)=5.8$, $p < 0.001$ or $t(41)=8.0$, $p < 0.001$). In general, no clear trends in DOC concentrations were observed with distance downstream and offshore, across either season.

POC concentrations differed significantly between seasons ($t(42)= -11.2$, $p < 0.001$ or $t(41)=-12.7$, $p < 0.001$, when the very high value measured at site CAC19-F was excluded from the calculation), displaying an inverse seasonal pattern relative to the DOC pool (Figures 3a and 3d). Mean summer POC concentrations are ~3 times higher ($0.40 \pm 0.10 \text{ mgC L}^{-1}$) than those measured during winter ($0.13 \pm 0.06 \text{ mgC L}^{-1}$). The highest winter POC concentration was recorded at the same station as the highest DOC concentration,

namely at station LEN19-S-07/CAC19-F (Figures 3 and 4 – Sobo-Sise cliff), where the winter POC value is as high as in summer and reach 0.36 mgC L^{-1} . In summer, this location is not characterized by high OM concentrations either in POC) or in DOC. We find winter POC concentration to be distributed relatively homogeneously along the Lena Delta (except LEN19-S-07/CAC19-F site), while in summer POC concentration values are more variable along the channel.

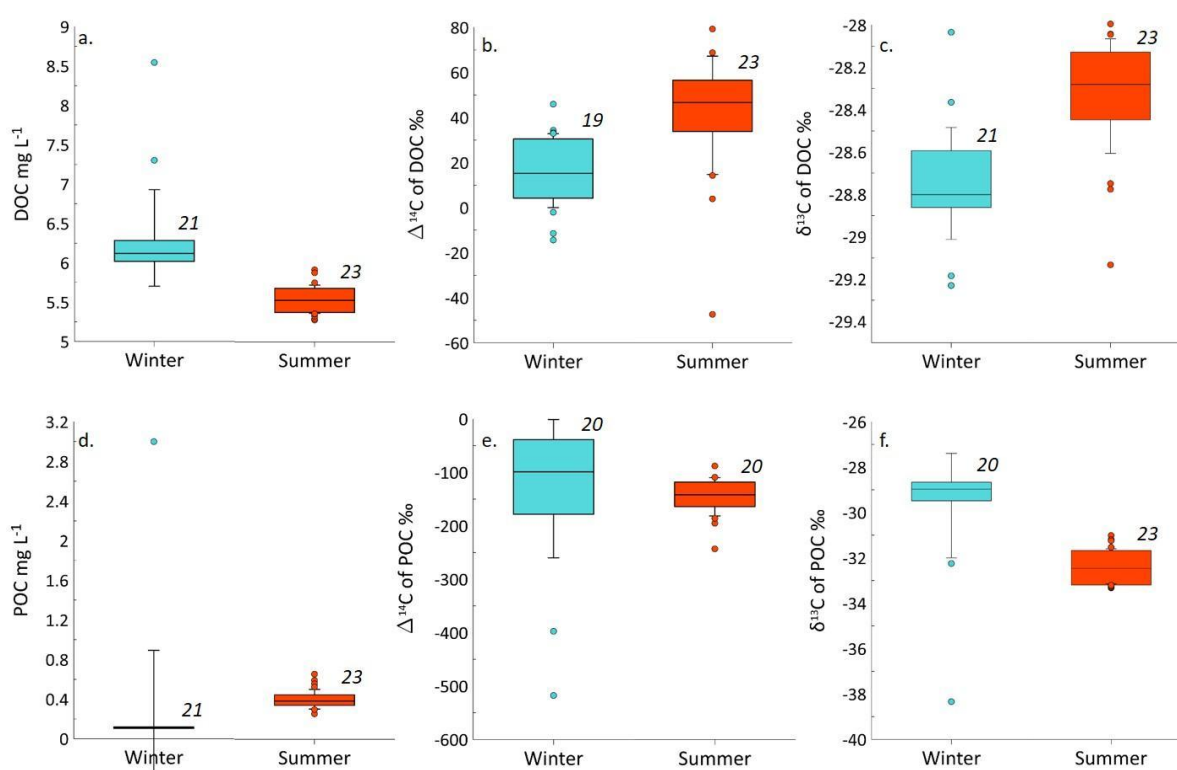


Figure 4-3. Box-whisker plots displaying the variability in dissolved (DOC, top row: a, b, c) and particulate (POC, bottom row: d, e, f) organic carbon concentration and isotopic composition ($\Delta^{14}\text{C}$ and $\delta^{13}\text{C}$) (for all sampling depths) between winter and summer in the Lena Delta in 2019. Central lines in plots represent the median, boxes are defined by the lower and upper quartiles and whiskers indicate the standard deviation, numbers denote sample count.

4.3.1.2 Carbon isotopic composition of DOC and POC

The mean $\Delta^{14}\text{C}$ of DOC were significantly lower in winter samples than summer ($t(40)=-3.5$, $p=0.001$), yet summer values varied over a larger range (summer: mean = 41 ± 26

‰, range - 47 to 79 ‰; winter: mean = -16 ± 16 ‰ ranging between -14 and 46 ‰; Figures 3 and 4). One sample (LEN19-S-02) drove the large variance in summer DOC values $\Delta^{14}\text{C}$ (-47 ‰), representing a highly depleted DOC sample within deeper Lena River main stem waters. $\Delta^{14}\text{C}$ of DOC decreased at the three most seaward sampling locations (LEN19-S-08, -89 and -09, respectively). By contrast, winter $\Delta^{14}\text{C}$ DOC values were found to be homogeneously distributed along the transect. No distinct patterns of difference in $\Delta^{14}\text{C}$ of POC ($t(38)=0.5$, $p=.61$) or any particular trends in distribution are obvious, neither for the winter season, nor for the summer (Figure 4-4).

Stable C isotopic composition varied between seasons for both DOC and POC (Figure 4-3 and 4). DOC concentrations in summer were slightly more enriched in ^{13}C compared to winter DOC (summer mean: -28.3 ± 0.3 ‰ in the range of -29.1 and -28.0 ‰; winter mean: -28.8 ± 0.3 ‰ in the range between -29.2 and -28.0 ‰; $t(42)=-5.1$, $p<.001$ or $t(41)=-6.0$, $p<0.001$, when very high value measured at site CAC19-F is removed from calculation). The highest $\delta^{13}\text{C}$ of DOC (-28.0 ‰) is measured in summer at station LEN19-S-08/CAC19-B and in winter (-28.0 ‰) at station LEN19-S-07/CAC19-F displaying the highest DOC and POC concentrations, and the lowest value (-29.1 ‰) is measured in summer at the Stolb island (LEN19-S-01).

$\delta^{13}\text{C}$ of POC is lower in summer (-32.4 ± 0.8 ‰) and higher in winter (-29.7 ± 2.2 ‰) ($t(41)=5.3$, $p<.001$ or $t(40)=10.8$, $p<0.001$, when very low value measured at site CAC19-F is removed from calculation). There are no discernible spatial patterns observed in $\delta^{13}\text{C}$ of POC along the transect in both seasons.

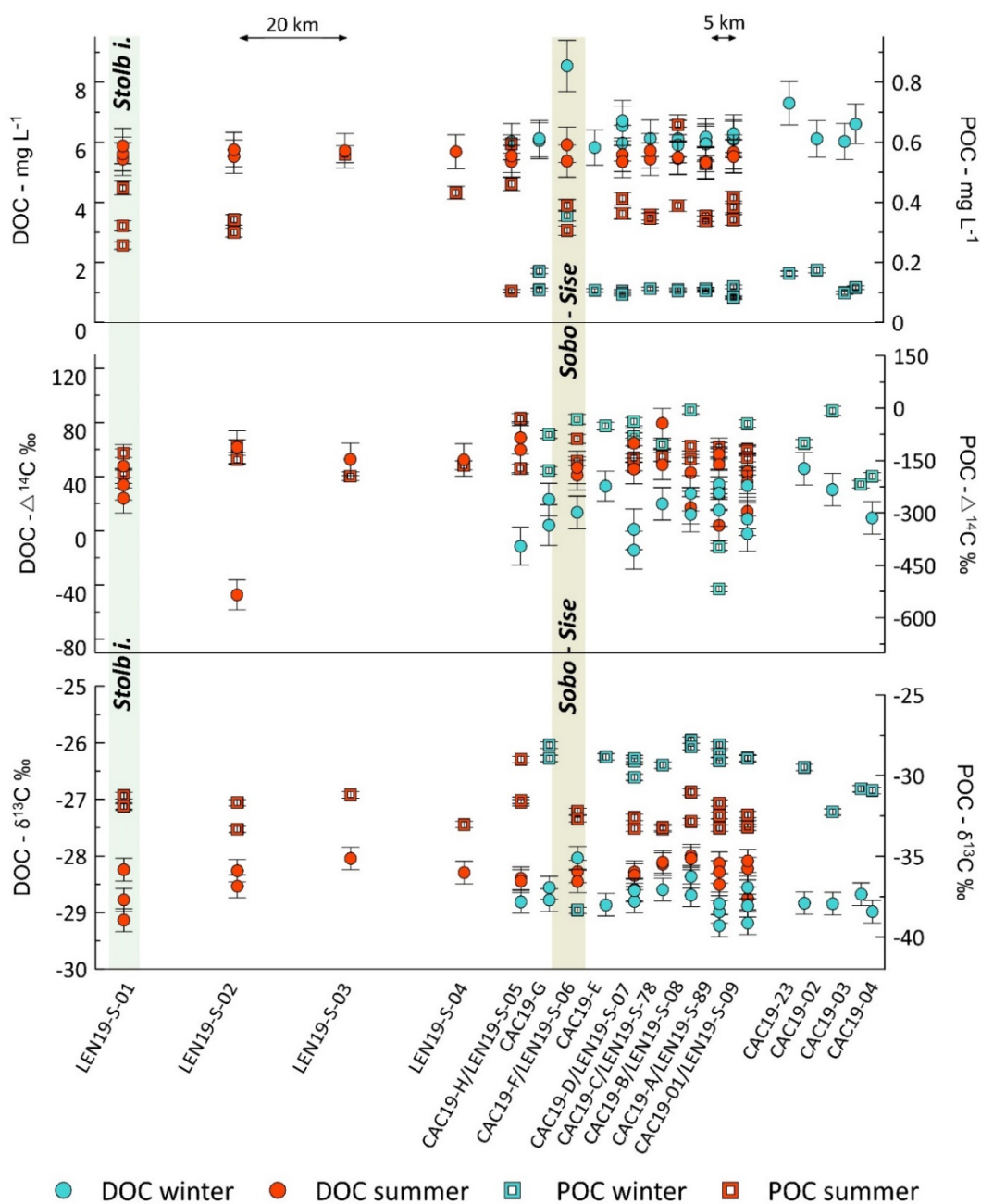


Figure 4-4. Variability of DOC and POC concentration (a) and isotope composition: $\Delta^{14}\text{C}$ (b) and $\delta^{13}\text{C}$ (c) (for all sampling depths) along the transects across the Sardakhskaya branch in the Lena Delta in summer and winter 2019. The relative distance on the x – axis represents the actual distance between sampling sites, except for sites CAC19-03 and CAC19-04, where the actual distance between them is 1 km, but the larger distance (5 km) on x-axis was kept on the figure to avoid overlapping.

4.3.2 DOC concentration and isotope composition in polygonal tundra lakes and at Stolb in 2016-2017

The DOC concentration in the polygon lakes at Samoylov island varied between 3.71 and 7.63 mgC L⁻¹, with a mean of 5.01 ±1.24 mgC L⁻¹, which is slightly lower than in winter and in summer 2019 within the Lena Delta (6.31 ±0.60 and 5.54 ±0.17 mgC L⁻¹, respectively). Average $\Delta^{14}\text{C}$ is 45 ±19 ‰, similar to the $\Delta^{14}\text{C}$ for DOC in deltaic waters in summer 2019 and higher than in winter (41 ±26 ‰ mean in summer and -16 ±16 ‰ in winter). No ¹³C stable isotope data are available for this sample set.

DOC concentrations at Stolb Island in the Lena Delta in 2016-2017 varied within a broader range than in 2019 between 3.17 and 8.45 mgC L⁻¹ with the mean of 7.16 ±1.33 mgC L⁻¹ in 2016 and 6.29 ±1.07 mgC L⁻¹ in 2017. DOC levels in the summers of 2017 and 2016 are higher than in the summer of 2019 (5.54 ± 0.17 mgC L⁻¹). Additionally, DOC levels in 2016 are higher, while in 2017 they are comparable to the levels in winter 2019 (6.31 ± 0.60 mgC L⁻¹).

The $\Delta^{14}\text{C}$ of DOC in 2016-2017 at Stolb varied between 35 and 69 ‰. There is no difference between the two years, with an average 54 ±8 ‰ in both years. This is statistically similar to $\Delta^{14}\text{C}$ of DOC in the delta in summer 2019 ($t(52)=-2.7$, $p=0.01$) and higher than in winter 2019 ($t(48)=-10.9$, $p<.001$), thus supporting the trend of winter DOC being more depleted in ¹⁴C as we observed in 2019.

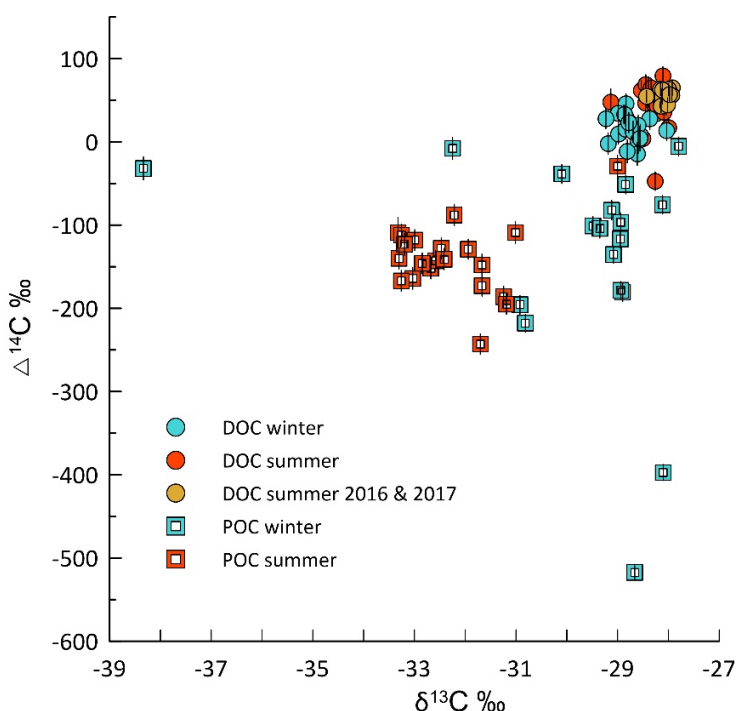


Figure 4-5. Isotopic composition ($\Delta^{14}\text{C}$ and $\delta^{13}\text{C}$) of dissolved (DOC) and particulate (POC) organic C in the Lena Delta in summer (August 2019) and in winter (April 2019). Additional data are shown for water samples taken at Stolb Island in summers of 2016 and 2017.

The $\delta^{13}\text{C}$ values of DOC at Stolb in 2016-2017 vary between -28.4 and -27.9 ‰ and in 2016 do not differ statistically from values in 2017 (with a mean for both years of -28.1 ± 0.1 ‰). Thus, $\delta^{13}\text{C}$ values of DOC in 2016-2017 are slightly higher than in 2019 ($t(33)=-2.9, p=.007$) and higher than in winter 2019 ($t(31)=-7.9, p<.001$).

4.4 Discussion

4.4.1 Seasonal and spatial differences of organic carbon released from the Lena Delta to the Arctic Ocean

In our data set for the Lena Delta, we find DOC concentrations in winter to be higher than in summer. It has been reported at Zhigansk (ArcticGRO) and Samoylov Island in the Lena Delta from 2014-2019, DOC concentrations in April (at the end of the winter season) were the lowest (Juhls et al. (2020) or were the same as at the end of the summer (Behnke et al. 2021, Liu et al., 2022). We propose several reasons causing this difference between our observations and the published data.

On the one hand, the hydrology of the Lena delta differs from the Lena River main stem (Rachold et al., 1996). In the Lena Delta, the extensive branching of channels results in a decrease in velocity, leading to the settling and sedimentation of total suspended matter, predominantly occurring on floodplains during the high-water flooding season (Sanders et al., 2022). In the main stem of the Lena River, active enrichment of suspended matter with subsequent sedimentation occurs on the way to the delta, but before reaching it (Semiletov et al., 2011; Fedorova et al., 2015). It is conceivable that DOC concentrations also vary spatially from the river main stem (Zhigansk ~ 800 km south of the delta) to the delta, like spatial patterns of POC (Ogneva et al., 2023a), making a comparison between our transect and the published data from a single site difficult. In fact, DOC concentrations Delta measured by us in 2019 in the Lena River were lower than average winter (November – April) DOC reported by ArcticGRO ($7.2 \pm 1.9 \text{ mg L}^{-1}$; McClelland et al., 2023), supporting a systematic difference between DOC concentrations at Zhigansk and Delta. In addition, the carbon isotopic differences we observe between winter and summer imply that DOC in the delta derives from different sources during the two seasons. Lastly, the year 2019 was extremely warm and dry in summer, August 2019 was the record low on an almost 90 years time series (Richter-Menge et al., 2020), resulting in unusually low water discharge ($\sim 19000 \text{ m}^3 \text{ s}^{-1}$) (Roshydromet, published by Shiklomanov et al. (2021b)) and subsequently lower DOC concentrations may have been additionally reduced by higher rates of photo-oxidation in the summer compared to winter.

Our POC results demonstrated opposing patterns relative to the DOC pool. We confirmed an established pattern, where POC flux, as well as water yield and total suspended matter in Arctic rivers, was seen to be lower in winter than summer (McClelland et al., 2016). Thus, winter POC concentrations were approximately 3 times lower than in summer (0.13 ± 0.06 and $0.40 \pm 0.10 \text{ mg L}^{-1}$, respectively). Compared to

samples measured upstream in the Lena River (ArcticGRO data, McClelland et al., 2023) deltaic POC concentrations during summer months are generally lower (< 50%) and contain a greater contribution of autochthonous-derived (phytoplankton) OM (more enriched in ^{13}C) (Ogneva et al., 2023a). As discussed by these authors, more efficient settling of particles in slower flowing waters of the delta compared to the Lena River can be a simple explanation. Nevertheless, POC in the Lena Delta in winter 2019 did not differ from average winter (November – April) POC concentration reported by ArcticGRO ($0.14 \pm 0.4 \text{ mg L}^{-1}$) (McClelland et al., 2023).

The highest winter concentrations of DOC (8.54 mg L^{-1}) and POC (0.36 mg L^{-1} , almost three times higher than the average value of $0.13 \pm 0.06 \text{ mg L}^{-1}$), were observed downstream from the Sobo–Sise Yedomia cliff (station CAC19-F). Sanders et al. (2022) showed that at this station, water temperature, ammonium, phosphate and silicon concentrations were likewise higher than at any other sampling station. These combined data indicate strong exchange between water and sediment and suggest a disturbance of river bottom sediment. Meanwhile, all the sediments taken in summer in the delta were very sandy (97.8-99.7 %) with very low content of total organic C (0.1-0.2 %) (Sanders et al., 2022) which makes direct mixing with a sediment an unlikely explanation for the unusual values of the CAC19-F sample, but it could have been an erosional source from the cliff instead of sediment from upwelling.

4.4.2 Main sources and transformation patterns of organic carbon in the Lena Delta

Generally, sources of DOC can be categorized into three groups based on the seasonal hydrological shifts. During the spring freshet, DOC is reported to primarily originate from surface runoff including leached components from fresh litter of angiosperm and gymnosperm plants, which have young ^{14}C ages (Amon et al., 2012; Behnke et al., 2021). In late summer and winter, when the dissolved organic matter concentrations are the

lowest, dissolved organic matter sources in Arctic rivers are associated with mosses peat bogs, and the near-surface thawed soil layers, which exhibit older radiocarbon signatures indicative of drainage from deeper soil horizons (Neff et al., 2006; Spencer et al., 2008).

Using the isotopic composition of DOC measured in our samples, we investigated whether these general patterns can be confirmed also for the Lena Delta. The stable C isotopic composition of DOC was statistically indistinguishable between the sampled seasons (-28.33 ± 0.26 ‰ in summer, -28.75 ± 0.26 ‰ in winter) and remained within the range of contemporary OC pools (Mann et al., 2015), including vegetation, surface soils and surface active layer signals. Thus, $\delta^{13}\text{C}$ of DOC cannot be used as a parameter to describe the difference between summer and winter DOC. However, combined $\delta^{13}\text{C}$ and $\Delta^{14}\text{C}$ evidence reveals distinct patterns.

In summer, the DOC in the Lena River and its Delta is characterized by modern carbon and its combined $\delta^{13}\text{C}$ and $\Delta^{14}\text{C}$ values suggest that it originates from vascular plants and algae and does not contain any contributions from fossil materials, excluding Yedoma as a major source. The $\Delta^{14}\text{C}$ signal of modern plants is assumed to reflect the radiocarbon composition of the atmosphere during their growth, which was enriched in ^{14}C due to nuclear bomb testing in the 1950s and $\Delta^{14}\text{C}$ values have remained above 0 until around 2020. Atmospheric $\Delta^{14}\text{C}$ in 2016-2019 ranged between 0-13 ‰ (Emmenegger et al., 2023). The measured $\Delta^{14}\text{C}$ of 41 ± 26 ‰ for DOC in summer 2019 was above atmospheric levels of that year. Instead, these higher $\Delta^{14}\text{C}$ values for DOC from the Lena Delta correspond to the atmospheric values observed in the previous decade (2001 – 2009) (Hammer & Levin, 2017).

Water percolating through the active layer in the polygonal tundra often forms small ponds in the central depressions of the low-centred polygons. Our observations on DOC from three small polygon lakes on Samoylov Island, with $\Delta^{14}\text{C}$ values of 45 ± 19 ‰ (Figure

4-6), support our suggestion that DOC in the river is derived from leaching of the active layer, which may contain elevated ^{14}C levels inherited from the growing seasons of previous decades. The sampling of these ponds took place in the time of the year when the active layer in the Lena Delta reaches its maximum thickness (Boike et al., 2019). This might suggest that during late summer, the oldest DOC from the thawing permafrost would be expected. However, due to nuclear weapons testing, atmospheric ^{14}C levels in recent decades were higher than they are now, which explains why “young” or even “above modern” values are obtained for DOC that might be leached from soil layers that have accumulated during previous decades. This suggests that as the active layer deepens and permafrost thaws, the ^{14}C signatures in DOC leached from these layers may initially increase and only begin to decrease when older permafrost organic matter accumulated before 1950 is released. This pattern should be considered when studying the age and composition of DOC. We acknowledge that using three lakes on one island in the delta to interpret the deltaic signal is not sufficient but may provide some insight into the terrestrial background.

Our data from Stolb in 2016-2017 and the deltaic transect in 2019 do not show clear differences in $\Delta^{14}\text{C}$ values of DOC. Because the active layer on Samoylov Island in 2019 was only 16 and 14 cm thicker than in 2016 and 2017 (Pfeiffer et al., 2020), respectively. Differences in the mean ^{14}C content of the active layers of the respective years are thus likely too small to be resolved within our measurement uncertainty.

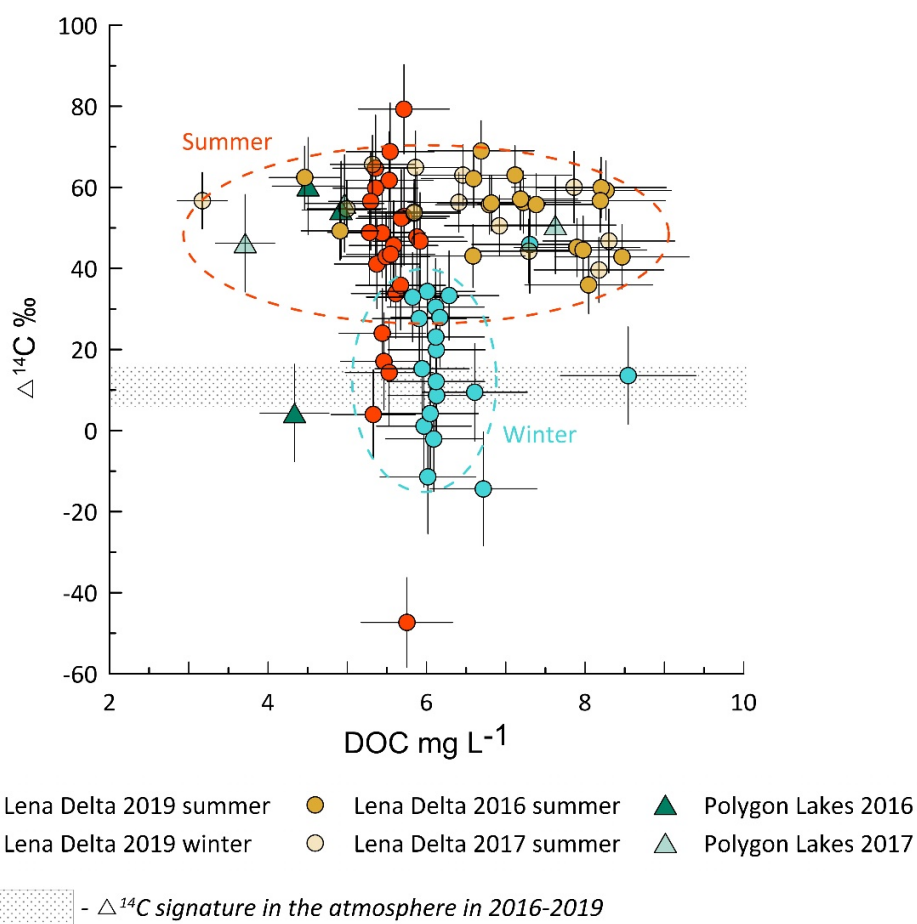


Figure 4-6. DOC concentration and its radiocarbon content in the Lena Delta (2016, 2017, 2019) and in the Polygon Lakes (2016, 2017) at Samoylov Island. The atmospheric $\Delta^{14}\text{C}$ signature in 2016-2019 is based on Emmenegger et al. (2023).

A distinct contrast between the seasons was found for the $\Delta^{14}\text{C}$ of DOC in the Lena Delta, with winter DOC exhibiting older ages (lower $\Delta^{14}\text{C}$) compared to summer ($\Delta^{14}\text{C}$: -16 ± 16 ‰ and 41 ± 26 ‰, respectively). This finding aligns with some previous studies (Liu et al., 2022; Wild et al., 2019), but differs from others such as Behnke et al. (2021), who reported minimal differences between winter and summer $\Delta^{14}\text{C}$ signals for DOC in the Lena River. During the low discharge period in winter, DOC is reported to be mainly transported by groundwater (Amon et al., 2012; Douglas et al., 2013, Juhls et al. 2020), suggesting an input of aged carbon from terrestrial sources. The majority of the Lena River catchment is underlain by continuous permafrost (70.5 %) (Juhls et al., 2020; Obu

et al., 2019) making intra-permafrost groundwater (Woo, 2012) draining taliks (Behnke et al., 2021), the more likely type of groundwater for the Lena Delta. If this permafrost contributed to the Lena deltaic DOC in winter, an older radiocarbon signal would be expected. However, the DOC $\Delta^{14}\text{C}$ values in winter resemble those of the atmosphere during the time of sampling, suggesting that a considerable proportion of this DOC derives from organic matter that was photosynthetically produced during the respective years. The potential influence of inter-annually and seasonally pooled waters from the Vilyuy reservoir (Juhls et al., 2020), which accounts for a significant percentage of the water that is discharged via the Lena River in winter (Tananaev et al., 2016), further complicates the interpretation.

POC in summer was depleted in ^{13}C ($\delta^{13}\text{C}$: $-32.4 \pm 0.8 \text{ ‰}$), likely due to contributions from aquatic organisms and the potential effect of an algal bloom taking place at the end of the summer in August (Ogneva et al., 2023a). Algal blooms in rivers can result in low $\delta^{13}\text{C}$ values of POC as the DIC pool is drawn down by photosynthesis and then replenished by respiration and transport of DIC from upstream (Finlay and Kendall, 2008). In winter, different sources of POM would be expected. Winter $\delta^{13}\text{C}$ of POC in the Lena Delta is higher than in summer (mean $-29.7 \pm 2.2 \text{ ‰}$) and corresponds to the typical terrestrial $\delta^{13}\text{C}$ values according to Vonk et al. (2010). However, it was lower than the $\delta^{13}\text{C}$ values directly measured for Holocene soils ($-26.6 \pm 1.0 \text{ ‰}$) and Yedoma ($-26.3 \pm 0.7 \text{ ‰}$) in the region (Wild et al., 2019; Winterfeld et al., 2015). In contrast to our findings, analyses of POC annual fluxes provided by the ArcticGRO initiative (McClelland et al., 2023) revealed that unlike in the Lena Delta winter POC in Arctic rivers is more depleted in $\delta^{13}\text{C}$ than summer POC. These authors reported winter and summer mean $\delta^{13}\text{C}$ values of POC at Zhigansk in the Lena River as $-32.8 \pm 1 \text{ ‰}$ and $-29.0 \pm 0.4 \text{ ‰}$, respectively, showing the opposite contrast between seasons. As discussed in Ogneva et al. (2023a) for the summer, this discrepancy could be attributed to the combined factors of low flow

velocity in the shallow delta channels, where sunlight penetrates much of the water column containing smaller amounts of suspended particles, and the extremely warm summer conditions during our sampling campaign in 2019, leading to high primary production and low $\delta^{13}\text{C}$ values of POC in the Lena Delta. By contrast, McClelland et al. (2016) reported lower winter $\delta^{13}\text{C}$ than ours, which was explained by contributions from bacterial communities, particularly methanotrophs, a process that appears to be less active in the shallow delta channels.

We found no significant difference between the summer and winter $\Delta^{14}\text{C}$ signals of POC, contrary to our expectation of a more ^{14}C -depleted signal in winter indicative of less phytoplankton contribution in winter. The lack of a radiocarbon age difference might also suggest that aquatic production uses the same carbon source as is contained in POC. This suggests an additional modern source of POC in winter, potentially aquatic bacterial communities. Since the concentration of POC in winter is very low ($0.13 \pm 0.06 \text{ mg L}^{-1}$) contributions from methanogenic bacteria may have a significant impact on the composition of winter POC.

4.5 Conclusion

We found that the amount and composition of dissolved organic carbon (DOC) and particulate organic carbon (POC) in the Lena Delta vary between the summer and winter seasons. Surprisingly, despite lower water flow in winter, the concentration of DOC in the Lena Delta is higher during this season as compared to the end of summer. The sources of DOC also differ between the two seasons. In summer, the DOC is enriched in $\Delta^{14}\text{C}$, likely due to plant debris from the post-1950s period. In contrast, winter DOC contains slightly older carbon. This study provides a unique dataset on the largest Arctic delta, which will be key to assess the ongoing changes with climate warming at this frontier between the land and the ocean realm.

Supporting Information

Supporting information (Table 4-S1, including the sample location descriptions) accompanies this manuscript

References

- Amon, R. M. W., Rinehart, A. J., Duan, S., Louchouart, P., Prokushkin, A., Guggenberger, G., et al. (2012). Dissolved organic matter sources in large Arctic rivers. *Geochimica et Cosmochimica Acta*, 94, 217-237, <https://doi.org/10.1016/j.gca.2012.07.015>.
- Behnke, M. I., McClelland, J. W., Tank, S. E., Kellerman, A. M., Holmes, R. M., Haghypour, N., et al. (2021). Pan-Arctic Riverine Dissolved Organic Matter: Synchronous Molecular Stability, Shifting Sources and Subsidies. *Global biogeochemical cycles*, 35(4), e2020GB006871, <https://doi.org/10.1029/2020GB006871>.
- Bertin, C., Carroll, D., Menemenlis, D., Dutkiewicz, S., Zhang, H., Matsuoka, A., et al. (2023). Biogeochemical River Runoff Drives Intense Coastal Arctic Ocean CO₂ Outgassing. *Geophysical Research Letters*, 50(8), e2022GL102377, <https://doi.org/10.1029/2022GL102377>.
- Biskaborn, B. K., Smith, S. L., Noetzli, J., Matthes, H., Vieira, G., Streletskiy, D. A., et al. (2019). Permafrost is warming at a global scale. *Nature Communications*, 10(1), 264, <https://doi.org/10.1038/s41467-018-08240-4>.
- Boike, J., Nitzbon, J., Anders, K., Grigoriev, M., Bolshiyarov, D., Langer, M., et al. (2019). A 16-year record (2002–2017) of permafrost, active-layer, and meteorological conditions at the Samoylov Island Arctic permafrost research site, Lena River delta, northern Siberia: an opportunity to validate remote-sensing data and land surface, snow, and permafrost models. *Earth Syst. Sci. Data*, 11(1), 261-299, <https://doi.org/10.5194/essd-11-261-2019>.
- Bröder, L., Davydova, A., Davydov, S., Zimov, N., Haghypour, N., Eglinton, T. I., & Vonk, J. E. (2020). Particulate Organic Matter Dynamics in a Permafrost Headwater Stream and the Kolyma River Mainstem. *J Geophys Res Biogeosci*, 125(2), e2019JG005511, <https://doi.org/10.1029/2019JG005511>.
- Bröder, L., Keskitalo, K., Zolkos, S., Shakil, S., Tank, S. E., Kokelj, S. V., et al. (2021). Preferential export of permafrost-derived organic matter as retrogressive thaw slumping intensifies. *Environmental Research Letters*, 16(5), 054059, <https://doi.org/10.1088/1748-9326/abee4b>.
- Charkin, A. N., Dudarev, O. V., Semiletov, I. P., Kruhmaliev, A. V., Vonk, J. E., Sánchez-García, L., et al. (2011). Seasonal and interannual variability of sedimentation and organic matter distribution in the Buor-Khaya Gulf: the primary recipient of input from Lena River and coastal erosion in the southeast Laptev Sea. *Biogeosciences*, 8(9), 2581-2594, <https://doi.org/10.5194/bg-8-2581-2011>.
- Cole, J. J., Prairie, Y. T., Caraco, N. F., McDowell, W. H., Tranvik, L. J., Striegl, R. G., et al. (2007). Plumbing the global carbon cycle: Integrating inland waters into the terrestrial carbon budget. *Ecosystems*, 10(1), 171-184, <https://doi.org/10.1007/s10021-006-9013-8>.
- Douglas, T. A., Blum, J. D., Guo, L., Keller, K., & Gleason, J. D. (2013). Hydrogeochemistry of seasonal flow regimes in the Chena River, a subarctic watershed draining discontinuous permafrost in interior Alaska (USA). *Chemical Geology*, 335, 48-62, <https://doi.org/10.1016/j.chemgeo.2012.10.045>.
- Emmenegger, L., Leuenberger, M., & Steinbacher, M. (2023). ICOS ATC/CAL 14C Release, Jungfraujoch (13.9 m), 2015-09-21–2022-08-07. Retrieved from: <https://hdl.handle.net/11676/mZZZOIWKAZq-nWd1saWzVNuG>

- Emmerton, C. A., Lesack, L. F. W., & Vincent, W. F. (2008). Mackenzie River nutrient delivery to the Arctic Ocean and effects of the Mackenzie Delta during open water conditions. *Global Biogeochem. Cycles*, 22, GB1024, doi:10.1029/2006GB002856.
- Fedorova, I., Chetverova, A., Bolshiyarov, D., Makarov, A., Boike, J., Heim, B., et al. (2015). Lena Delta hydrology and geochemistry: long-term hydrological data and recent field observations. *Biogeosciences*, 12(2), 345-363, <https://doi.org/10.5194/bg-12-345-2015>.
- Feng, D., Gleason, C. J., Lin, P., Yang, X., Pan, M., & Ishitsuka, Y. (2021). Recent changes to Arctic river discharge. *Nature Communications*, 12(1), 6917, <https://doi.org/10.1038/s41467-021-27228-1>.
- Frey, K. E., & McClelland, J. W. (2009). Impacts of permafrost degradation on arctic river biogeochemistry. *Hydrological Processes*, 23(1), 169-182, <https://doi.org/10.1002/hyp.7196>.
- Fuchs M., Sachs T., Jongejans L.L., et al. Large stocks of permafrost soil organic carbon and nitrogen in Arctic river deltas. *Nature Geoscience*. in review;
- Fuchs, M., Nitze, I., Strauss, J., Gunther, F., Wetterich, S., Kizyakov, A., et al. (2020). Rapid Fluvio-Thermal Erosion of a Yedoma Permafrost Cliff in the Lena River Delta. *Frontiers in Earth Science*, 8, 336, <https://doi.org/10.3389/feart.2020.00336>.
- Fuchs, M., Ogneva, O., Sanders, T., Schneider, W., Polyakov, V., Becker, O. O., et al. (2021a). CACOON Sea - water sampling along the Sardakhskaya channel and near shore of the Laptev Sea (chapter 3.26) In M. Fuchs, D. Bolshiyarov, M. N. Grigoriev, A. Morgenstern, L. A. Pestryakova, L. Tsibizov, & A. Dill (Eds.), *Reports on Polar and Marine Research - Russian-German Cooperation: Expeditions to Siberia in 2019*. Bremerhaven: Alfred Wegener Institute, https://doi.org/10.48433/BzPM_0749_2021.
- Fuchs, M., Palmtag, J., Ogneva, O., Sanders, T., Aksenov, A., Polyakov, V. I., & Strauss, J. (2021b). Conductivity, temperature and depth (CTD) measurements during the CACOON cruises in 2019 in the Lena Delta region.
- Hammer, S., & Levin, I. (2017). Monthly mean atmospheric D14CO2 at Jungfraujoch and Schauinsland from 1986 to 2016 [atmospheric observations].
- Haugk, C., Jongejans, L. L., Mangelsdorf, K., Fuchs, M., Ogneva, O., Palmtag, J., et al. (2022). Organic matter characteristics of a rapidly eroding permafrost cliff in NE Siberia (Lena Delta, Laptev Sea region). *Biogeosciences*, 19(7), 2079-2094, <https://doi.org/10.5194/bg-19-2079-2022>.
- Ivanov, V., & Piskun, A. (1999). Distribution of river water and suspended sediment loads in the deltas of rivers in the basins of the Laptev and East-Siberian Seas. In *Land-ocean systems in the Siberian Arctic: dynamics and history* (pp. 239-250). Berlin, Heidelberg: Springer, https://doi.org/10.1007/978-3-642-60134-7_22.
- Jong, D., Bröder, L., Tanski, G., Fritz, M., Lantuit, H., Tesi, T., et al. (2020). Nearshore Zone Dynamics Determine Pathway of Organic Carbon From Eroding Permafrost Coasts. *Geophysical Research Letters*, 47(15), e2020GL088561, <https://doi.org/10.1029/2020GL088561>.
- Juhls, B., Stedmon, C. A., Morgenstern, A., Meyer, H., Holemann, J., Heim, B., et al. (2020). Identifying Drivers of Seasonality in Lena River Biogeochemistry and Dissolved Organic Matter Fluxes. *Frontiers in Environmental Science*, 8(53), <https://doi.org/10.3389/fenvs.2020.00053>.
- Kanevskiy, M., Shur, Y., Strauss, J., Jorgenson, T., Fortier, D., Stephani, E., & Vasiliev, A. (2016). Patterns and rates of riverbank erosion involving ice-rich permafrost (yedoma) in northern Alaska. *Geomorphology*, 253, 370-384, <https://doi.org/10.1016/j.geomorph.2015.10.023>.
- Kipp, L.E., Henderson, P.B., Wang, Z.A. et al. Deltaic and Estuarine Controls on Mackenzie River Solute Fluxes to the Arctic Ocean. *Estuaries and Coasts* 43, 1992–2014 (2020). <https://doi.org/10.1007/s12237-020-00739-8>
- Knights, D., Piliouras, A., Schwenk, J., Hariharan, J., & Russoniello, C. (2023). Seasonal and Morphological Controls on Nitrate Retention in Arctic Deltas. *Geophysical Research Letters*, 50(7), e2022GL102201, <https://doi.org/10.1029/2022GL102201>.

- Lamontagne-Hallé, P., McKenzie, J. M., Kurylyk, B. L., & Zipper, S. C. (2018). Changing groundwater discharge dynamics in permafrost regions. *Environmental Research Letters*, 13(8), 084017, <https://doi.org/10.1088/1748-9326/aad404>.
- Liu, S., Wang, P., Huang, Q., Yu, J., Pozdniakov, S. P., & Kazak, E. S. (2022). Seasonal and spatial variations in riverine DOC exports in permafrost-dominated Arctic river basins. *Journal of Hydrology*, 612, 128060, <https://doi.org/10.1016/j.jhydrol.2022.128060>.
- Mann, P. J., Eglinton, T. I., McIntyre, C. P., Zimov, N., Davydova, A., Vonk, J. E., et al. (2015). Utilization of ancient permafrost carbon in headwaters of Arctic fluvial networks. *Nat Commun*, 6, 7856, <https://doi.org/10.1038/ncomms8856>.
- Mann, P. J., Strauss, J., Palmtag, J., Dowdy, K., Ogneva, O., Fuchs, M., et al. (2022). Degrading permafrost river catchments and their impact on Arctic Ocean nearshore processes. *AMBIO*, 51, 439–455, <https://doi.org/10.1007/s13280-021-01666-z>.
- McClelland, J. W., Holmes, R. M., Peterson, B. J., Raymond, P. A., Striegl, R. G., Zhulidov, A. V., et al. (2016). Particulate organic carbon and nitrogen export from major Arctic rivers. *Global biogeochemical cycles*, 30(5), 629–643, <https://doi.org/10.1002/2015gb005351>.
- McClelland, J. W., Tank, S., Spencer, R. G. M., Shiklomanov, A. I., Zolkos, S., & Holmes, R. M. (2023). Arctic Great Rivers Observatory. Water Quality Dataset, Version 20230314. Retrieved from: <https://www.arcticgreatrivers.org/data>
- McGuire, A. D., Anderson, L. G., Christensen, T. R., Dallimore, S., Guo, L. D., Hayes, D. J., et al. (2009). Sensitivity of the carbon cycle in the Arctic to climate change. *Ecological Monographs*, 79(4), 523–555, <https://doi.org/10.1890/08-2025.1>.
- Miner, K. R., Turetsky, M. R., Malina, E., Bartsch, A., Tamminen, J., McGuire, A. D., et al. (2022). Permafrost carbon emissions in a changing Arctic. *Nature Reviews Earth & Environment*, 3(1), 55–67, <https://doi.org/10.1038/s43017-021-00230-3>.
- Mollenhauer, G., Grotheer, H., Torben, G., Bonk, E., & Hefter, J. (2021). Standard operation procedures and performance of the MICADAS radiocarbon laboratory at Alfred Wegener Institute (AWI), Germany. *Nuclear Instruments and Methods in Physics Research Section B: Beam Interactions with Materials and Atoms*, 496, 45–51, <https://doi.org/10.1016/j.nimb.2021.03.016>.
- Neff, J. C., Finlay, J. C., Zimov, S. A., Davydov, S. P., Carrasco, J. J., Schuur, E. A. G., & Davydova, A. I. (2006). Seasonal changes in the age and structure of dissolved organic carbon in Siberian rivers and streams. *Geophysical Research Letters*, 33(23), <https://doi.org/10.1029/2006GL028222>.
- Novak, M. G., Mannino, A., Clark, J. B., Hernes, P., Tzortziou, M., Spencer, R. G. M., Kellerman, A. M. and Grunert, B. (2022) Arctic biogeochemical and optical properties of dissolved organic matter across river to sea gradients. *Front. Mar. Sci.* 9:949034. doi: 10.3389/fmars.2022.949034.
- Obu, J., Westermann, S., Bartsch, A., Berdnikov, N., Christiansen, H. H., Dashtseren, A., et al. (2019). Northern Hemisphere permafrost map based on TTOP modelling for 2000–2016 at 1 km² scale. *Earth-Science Reviews*, 193, 299–316, <https://doi.org/10.1016/j.earscirev.2019.04.023>.
- Ogneva, O., Mollenhauer, G., Fuchs, M., Sanders, T., Palmtag, J., Grotheer, H., et al. (2023b). Dissolved and Particulate Organic Carbon and its isotopic composition in the Lena Delta in winter 2019 and in summer 2019, 2017 and 2016 [dataset]. PANGAEA. <https://doi.org/10.1594/PANGAEA.962633>
- Ogneva, O., Mollenhauer, G., Juhls, B., Sanders, T., Palmtag, J., Fuchs, M., et al. (2023a). Particulate organic matter in the Lena River and its delta: from the permafrost catchment to the Arctic Ocean. *Biogeosciences*, 20(7), 1423–1441, <https://doi.org/10.5194/bg-20-1423-2023>.
- Ogneva, O., Mollenhauer, G., Juhls, B., Sanders, T., Palmtag, J., Fuchs, M., et al. (2022). Total suspended matter, particulate organic carbon and its isotopic composition in the Lena River and its Delta. [Dataset]. PANGAEA. <https://doi.org/10.1594/PANGAEA.950668>

- Pfeiffer, E., Eckhardt, T., Kutzbach, L., Fedorova, I., Tsibizov, L., & Beer, C. (2020). Focus Siberian Permafrost–Terrestrial Cryosphere and Climate Change: International Symposium. Paper presented at the Berichte zur Polar-und Meeresforschung = Reports on Polar and Marine Research, Institute of Soil Science, Universität Hamburg, https://doi.org/10.2312/BzPM_0739_2020.
- Polimene, L., Torres, R., Powley, H. R., Bedington, M., Juhls, B., Palmtag, J., et al. (2022). Biological lability of terrestrial DOM increases CO₂ outgassing across Arctic shelves. *Biogeochemistry*, 160(3), 289-300, <https://doi.org/10.1007/s10533-022-00961-5>.
- Rachold, V., Alabyan, A., Hubberten, H. W., Korotaev, V., & Zaitsev, A. (1996). Sediment transport to the Laptev Sea—hydrology and geochemistry of the Lena River. *Polar Research*, 15(2), 183-196, <https://doi.org/10.3402/polar.v15i2.6646>.
- Rantanen, M., Karpechko, A. Y., Lipponen, A., Nordling, K., Hyvärinen, O., Ruosteenoja, K., et al. (2022). The Arctic has warmed nearly four times faster than the globe since 1979. *Communications Earth & Environment*, 3(1), <https://doi.org/10.1038/s43247-022-00498-3>.
- Raymond, P. A., McClelland, J. W., Holmes, R. M., Zhulidov, A. V., Mull, K., Peterson, B. J., et al. (2007). Flux and age of dissolved organic carbon exported to the Arctic Ocean: A carbon isotopic study of the five largest arctic rivers. *Global biogeochemical cycles*, 21(4), <https://doi.org/10.1029/2007GB002934>.
- Richter-Menge, J., Druckenmiller, M. L., Andersen, J. K., Andreassen, L. M., Baker, E. H., Ballinger, T. J., et al. (2020). The Arctic. *Bulletin of the American Meteorological Society*, 101(8), <https://doi.org/10.1175/BAMS-D-20-0086.1>.
- Sanders, T., Fiencke, C., Fuchs, M., Haugk, C., Juhls, B., Mollenhauer, G., et al. (2022). Seasonal nitrogen fluxes of the Lena River Delta. *AMBIO*, 51, 423–438, <https://doi.org/10.1007/s13280-021-01665-0>.
- Schädel, C., Bader, M. K. F., Schuur, E. A. G., Biasi, C., Bracho, R., Capek, P., et al. (2016). Potential carbon emissions dominated by carbon dioxide from thawed permafrost soils. *Nature Climate Change*, 6, 950–953, <https://doi.org/10.1038/nclimate3054>.
- Schuur, E. A. G., Abbott, B. W., Commane, R., Ernakovich, J., Euskirchen, E., Hugelius, G., et al. (2022). Permafrost and Climate Change: Carbon Cycle Feedbacks From the Warming Arctic. *Annual Review of Environment and Resources*, 47(1), 343-371, <https://doi.org/10.1146/annurev-environ-012220-011847>.
- Semiletov, I. P., Pipko, I. I., Shakhova, N. E., Dudarev, O. V., Pugach, S. P., Charkin, A. N., et al. (2011). Carbon transport by the Lena River from its headwaters to the Arctic Ocean, with emphasis on fluvial input of terrestrial particulate organic carbon vs. carbon transport by coastal erosion. *Biogeosciences*, 8(9), 2407-2426, <https://doi.org/10.5194/bg-8-2407-2011>.
- Shiklomanov, A., Déry, S., Tretiakov, M., Yang, D., Magritsky, D., Georgiadi, A., & Tang, W. (2021a). River Freshwater Flux to the Arctic Ocean. In D. Yang & D. L. Kane (Eds.), *Arctic Hydrology, Permafrost and Ecosystems* (pp. 703-738). Cham: Springer International Publishing, https://doi.org/10.1007/978-3-030-50930-9_24.
- Shiklomanov, A. I., Holmes, R. M., McClelland, J. W., Tank, S. E., & Spencer, R. G. M. (2021b). Arctic Great Rivers Observatory. Discharge Dataset, Version 20210319. [Dataset] <https://www.arcticrivers.org/data>
- Smith, S. V., Buddemeier, R. W., Wulff, F., Swaney, D. P., Camacho-Ibar, V. F., David, L. T., et al. (2005). C, N, P fluxes in the coastal zone. In *Coastal Fluxes in the Anthropocene: The Land-Ocean Interactions in the Coastal Zone Project of the International Geosphere-Biosphere Programme* (pp. 95-143). Berlin, Heidelberg: Springer
- Spencer, R. G. M., Aiken, G. R., Wickland, K. P., Striegl, R. G., & Hernes, P. J. (2008). Seasonal and spatial variability in dissolved organic matter quantity and composition from the Yukon River basin, Alaska. *Global biogeochemical cycles*, 22(4), <https://doi.org/10.1029/2008GB003231>.
- Stolpmann, L., Mollenhauer, G., Morgenstern, A., Hammes, J. S., Boike, J., Overduin, P. P., & Grosse, G. (2022). Origin and Pathways of Dissolved Organic Carbon in a Small Catchment in the Lena River Delta. *Frontiers in Earth Science*, 9, <https://doi.org/10.3389/feart.2021.759085>.

- Strauss J, Fuchs M, Hugelius G, et al. Organic matter storage and vulnerability in the permafrost domain. In: Elias S, ed. *Encyclopedia of Quaternary Science*. 3rd ed. Elsevier; 2024a, <https://doi.org/10.1016/B978-0-323-99931-1.00164-1>.
- Strauss J, Marushchak ME, van Delden L, et al. Potential nitrogen mobilisation from the Yedoma permafrost domain. *Environmental Research Letters*. 2024b; 19(4):043002. <https://doi.org/10.1088/1748-9326/ad3167>
- Strauss, J., Biasi, C., Sanders, T., Abbott, B. W., von Deimling, T. S., Voigt, C., et al. (2022). A globally relevant stock of soil nitrogen in the Yedoma permafrost domain. *Nature Communications*, 13(1), 6074, <https://doi.org/10.1038/s41467-022-33794-9>.
- Strauss, J., Ogneva, O., Palmtag, J., & Fuchs, M. (2021). CACOON Ice: Spring campaign NERC-BMBF project 'Changing Arctic Carbon Cycle in the Coastal Ocean Near-Shore (CACOON) (chapter 2.1). In M. Fuchs, D. Bolshiyarov, M. N. Grigoriev, A. Morgenstern, L. A. Pestryakova, L. Tsibizov, & A. Dill (Eds.), *Reports on Polar and Marine Research - Russian-German Cooperation: Expeditions to Siberia in 2019*. Bremerhaven: Alfred Wegener Institute, https://doi.org/10.48433/BzPM_0749_2021.
- Strauss, J., Schirrmeister, L., Grosse, G., Fortier, D., Hugelius, G., Knoblauch, C., et al. (2017). Deep Yedoma permafrost: A synthesis of depositional characteristics and carbon vulnerability. *Earth-Science Reviews*, 172, 75-86, <https://doi.org/10.1016/j.earscirev.2017.07.007>.
- Stuiver, M., & Polach, H. A. (1977). Discussion: reporting of 14 C data. *Radiocarbon*, 19(3), 355-363, <https://doi.org/10.1017/S0033822200003672>.
- Sun, S., Meyer, V. D., Dolman, A. M., Winterfeld, M., Hefter, J., Dumann, W., et al. (2020). 14C blank assessment in small-scale compound-specific radiocarbon analysis of lipid biomarkers and lignin phenols. *Radiocarbon*, 62(1), 207-218, <https://doi.org/10.1017/RDC.2019.108>.
- Tananaev, N. I., Makarieva, O. M., & Lebedeva, L. S. (2016). Trends in annual and extreme flows in the Lena River basin, Northern Eurasia. *Geophysical Research Letters*, 43(20), 10,764-710,772, <https://doi.org/10.1002/2016GL070796>.
- Tank, S. E., Striegl, R. G., McClelland, J. W., & Kokelj, S. V. (2016). Multi-decadal increases in dissolved organic carbon and alkalinity flux from the Mackenzie drainage basin to the Arctic Ocean. *Environmental Research Letters*, 11(5), 054015, <https://doi.org/10.1088/1748-9326/11/5/054015>.
- Tanski, G., Bröder, L., Wagner, D., Knoblauch, C., Lantuit, H., Beer, C., et al. (2021). Permafrost Carbon and CO2 Pathways Differ at Contrasting Coastal Erosion Sites in the Canadian Arctic. *Frontiers in Earth Science*, 9(207), <https://doi.org/10.3389/feart.2021.630493>.
- Tanski, G., Wagner, D., Knoblauch, C., Fritz, M., Sachs, T., & Lantuit, H. (2019). Rapid CO2 Release From Eroding Permafrost in Seawater. *Geophysical Research Letters*, 46(20), 11244-11252, <https://doi.org/10.1029/2019GL084303>.
- Terhaar, J., Lauerwald, R., Regnier, P., Gruber, N., & Bopp, L. (2021). Around one third of current Arctic Ocean primary production sustained by rivers and coastal erosion. *Nature Communications*, 12(1), 169, <https://doi.org/10.1038/s41467-020-20470-z>.
- Terhaar, J., Orr, J. C., Ethé, C., Regnier, P., & Bopp, L. (2019). Simulated Arctic Ocean Response to Doubling of Riverine Carbon and Nutrient Delivery. *Global biogeochemical cycles*, 33(8), 1048-1070, <https://doi.org/10.1029/2019GB006200>.
- Turetsky, M. R., Abbott, B. W., Jones, M. C., Anthony, K. W., Olefeldt, D., Schuur, E. A. G., et al. (2020). Carbon release through abrupt permafrost thaw. *Nature Geoscience*, 13(2), 138-143, <https://doi.org/10.1038/s41561-019-0526-0>.
- Vonk, J. E., & Gustafsson, Ö. (2013). Permafrost-carbon complexities. *Nature Geoscience*, 6(9), 675-676, <https://doi.org/10.1038/ngeo1937>.
- Vonk, J. E., Sánchez-García, L., Semiletov, I., Dudarev, O., Eglinton, T., Andersson, A., & Gustafsson, Ö. (2010). Molecular and radiocarbon constraints on sources and degradation of terrestrial organic carbon

- along the Kolyma paleoriver transect, East Siberian Sea. *Biogeosciences*, 7(10), 3153-3166, <https://doi.org/10.5194/bg-7-3153-2010>.
- Wacker, L., Christl, M., & Synal, H. A. (2010). Bats: A new tool for AMS data reduction. *Nuclear Instruments and Methods in Physics Research Section B: Beam Interactions with Materials and Atoms*, 268(7), 976-979, <https://doi.org/10.1016/j.nimb.2009.10.078>.
- Wacker, L., Fahrni, S., Hajdas, I., Molnar, M., Synal, H.-A., Szidat, S., & Zhang, Y. (2013). A versatile gas interface for routine radiocarbon analysis with a gas ion source. *Nuclear Instruments and Methods in Physics Research Section B: Beam Interactions with Materials and Atoms*, 294, 315-319, <https://doi.org/10.1016/j.nimb.2012.02.009>.
- Walvoord, M. A., & Kurylyk, B. L. (2016). Hydrologic Impacts of Thawing Permafrost - A Review. *Vadose Zone Journal*, 15(6), vzj2016.2001.0010, <https://doi.org/10.2136/vzj2016.01.0010>.
- Walvoord, M. A., & Striegl, R. G. (2007). Increased groundwater to stream discharge from permafrost thawing in the Yukon River basin: Potential impacts on lateral export of carbon and nitrogen. *Geophysical Research Letters*, 34(12), <https://doi.org/10.1029/2007GL030216>.
- Wang, P., Huang, Q., Pozdniakov, S. P., Liu, S., Ma, N., Wang, T., et al. (2021). Potential role of permafrost thaw on increasing Siberian river discharge. *Environmental Research Letters*, 16(3), 034046, <https://doi.org/10.1088/1748-9326/abe326>.
- Wetterich S, Kizyakov A, Fritz M, et al. The cryostratigraphy of the Yedoma cliff of Sobo-Sise Island (Lena delta) reveals permafrost dynamics in the central Laptev Sea coastal region during the last 52kyr. *The Cryosphere*. 2020;14(12):4525-4551. <https://doi.org/10.5194/tc-14-4525-2020>
- Wetterich S, Rudaya N, Nazarova L, et al. Paleo-Ecology of the Yedoma Ice Complex on Sobo-Sise Island (Eastern Lena Delta, Siberian Arctic). Original Research. *Frontiers in Earth Science*. 2021-June-18 2021;9(489), <https://doi.org/10.3389/feart.2021.681511>
- Wild, B., Andersson, A., Bröder, L., Vonk, J., Hugelius, G., McClelland, J. W., et al. (2019). Rivers across the Siberian Arctic unearth the patterns of carbon release from thawing permafrost. *Proceedings of the National Academy of Sciences*, 116(21), 10280-10285, <https://doi.org/10.1073/pnas.1811797116>.
- Winterfeld, M., Goñi, M. A., Just, J., Hefter, J., & Mollenhauer, G. (2015). Characterization of particulate organic matter in the Lena River delta and adjacent nearshore zone, NE Siberia – Part 2: Lignin-derived phenol compositions. *Biogeosciences*, 12(7), 2261-2283, <https://doi.org/10.5194/bg-12-2261-2015>.
- Woo, M.-k. (2012). *Permafrost hydrology*. Berlin, Heidelberg: Springer, <https://doi.org/10.1007/978-3-642-23462-0>.

Supporting Information

Dissolved and Particulate Organic Carbon Characteristics in Summer and Winter Waters of the Lena Delta

O. Ogneva^{1,2,3}, G. Mollenhauer^{1,3,4}, T. Sanders⁵, B. Juhls², J. Palmtag^{6,a}, M. Fuchs^{2,b}, J. Hammes^{1,c}, H. Grotheer^{1,4}, P. J. Mann⁶, S. Opfergelt⁷ and J. Strauss²

¹Marine Geochemistry Section, Alfred Wegener Institute Helmholtz Centre for Polar and Marine Research, 27570 Bremerhaven, Germany

²Permafrost Research Section, Alfred Wegener Institute Helmholtz Centre for Polar and Marine Research, 14473 Potsdam, Germany

³Faculty of Geosciences, University of Bremen, Bremen, 28359, Germany

⁴Marum Center for Marine Environmental Sciences, University of Bremen, 28359 Bremen, Germany

⁵Institute for Carbon Cycles, Helmholtz Centre Hereon, 21502 Geesthacht, Germany

⁶Department of Geography and Environmental Sciences, Northumbria University, Newcastle-upon-Tyne, NE1 8ST, UK

⁷Earth and Life Institute, Université catholique de Louvain, Louvain-la-Neuve, Belgium

^anow at: Swedish Nuclear Fuel and Waste Management Co. (SKB), P.O. Box 3091, 169 03 Solna, Sweden

^bnow at: Renewable and Sustainable Energy Institute, University of Colorado Boulder, Boulder, USA

^cnow at: Carbon Drawdown Initiative GmbH, Fürth, Germany

Table 4-S1. Sample station locations in the Lena Delta along the Sardakhskaya branch from 2019 and sampling locations in the Lena Delta in previous years. Sampling depth equal to 0.5 m in summer season means that samples were taken from the surface.

Station Name	Latitude	Longitude	Date	Sampling depth, m	Sampling
CAC19-01	72.50908	129.24791	30.03.2019	2.5; 6; 11	Lena Delta, 2019
CAC19-02	72.51685	129.54568	29.03.2019	2.5	Lena Delta, 2019
CAC19-03	72.52538	129.84203	30.03.2019	2.3	Lena Delta, 2019
CAC19-04	72.52548	129.86385	31.03.2019	2.5	Lena Delta, 2019
CAC19-23	72.52135	129.69305	31.03.2019	2.5	Lena Delta, 2019
CAC19-A	72.50127	129.10159	01.04.2019	2.5; 7; 12	Lena Delta, 2019
CAC19-B	72.47939	128.97108	01.04.2019	2.5; 5	Lena Delta, 2019
CAC19-C	72.45562	128.84447	02.04.2019	2.5	Lena Delta, 2019
CAC19-D	72.46153	128.69456	02.04.2019	2.5; 10; 18	Lena Delta, 2019
CAC19-E	72.50182	128.62968	03.04.2019	2.5	Lena Delta, 2019
CAC19-F	72.51871	128.49216	03.04.2019	3	Lena Delta, 2019
CAC19-G	72.53542	128.35324	04.04.2019	2.5; 7.5	Lena Delta, 2019
CAC19-H	72.56407	128.23865	04.04.2019	3	Lena Delta, 2019
LEN19-S-01	72.39936	126.69558	09.08.2019	0.5; 9; 18	Lena Delta, 2019
LEN19-S-02	72.53733	126.92917	09.08.2019	0.5; 16	Lena Delta, 2019

Manuscript 2: Dissolved and particulate organic carbon characteristics in summer and winter waters of the Lena delta

LEN19-S-03	72.62711	127.41936	09.08.2019	0.5	Lena Delta, 2019
LEN19-S-04	72.63353	127.95914	09.08.2019	0.5	Lena Delta, 2019
LEN19-S-05	72.56378	128.24464	09.08.2019	0.5; 4	Lena Delta, 2019
LEN19-S-06	72.52108	128.51558	08.08.2019	0.5	Lena Delta, 2019
LEN19-S-07	72.46139	128.69514	08.08.2019	0.5; 15	Lena Delta, 2019
LEN19-S-78	72.45311	128.84103	08.08.2019	0.5; 8	Lena Delta, 2019
LEN19-S-08	72.47706	128.97078	08.08.2019	0.5; 6	Lena Delta, 2019
LEN19-S-89	72.50167	129.10172	08.08.2019	0.5; 6; 12	Lena Delta, 2019
LEN19-S-09	72.50897	129.25089	08.08.2019	0.5; 5; 10	Lena Delta, 2019
L16-06	72.39981	126.70611	08.08.2016	0.5; 12; 21	Lena Delta, main channel at Stolb i.
L16-07	72.39979	126.7267	08.08.2016	0.5; 12; 21	Lena Delta, main channel at Stolb i.
L16-08	72.39561	126.67867	08.08.2016	0.5; 4; 8	Lena Delta, main channel at Stolb i.
L16-14	72.39978	126.72666	15.08.2016	0.5; 12; 21	Lena Delta, main channel at Stolb i.
L16-15	72.39981	126.70611	15.08.2016	0.5; 12; 21	Lena Delta, main channel at Stolb i.
L16-16	72.39561	126.67867	15.08.2016	0.5; 4; 8	Lena Delta, main channel at Stolb i.
L17-07	72.39561	126.67867	11.07.2017	0.5; 4; 8	Lena Delta, main channel at Stolb i.
L17-08	72.39981	126.70611	11.07.2017	0.5; 12; 21	Lena Delta, main channel at Stolb i.
L17-09	72.39978	126.72666	11.07.2017	0; 4; 8	Lena Delta, main channel at Stolb i.
L17-18	72.39886	126.71221	25.07.2017	0.5	Lena Delta, main channel at Stolb i.
L17-19	72.39886	126.71221	25.07.2017	0.5; 12; 21	Lena Delta, main channel at Stolb i.
L17-20	72.39886	126.72214	25.07.2017	0.5	Lena Delta, main channel at Stolb i.
L16-03	72.38394	126.48583	04.08.2016	0.5	Samoylov i.; North lake, Polygon-1
L16-04	72.38372	126.48550	04.08.2016	0.5	Samoylov i.; North Lake, Polygon-2
L16-05	72.38356	126.48560	04.08.2016	0.5	Samoylov i.; North Lake, Polygon-3
L17-10	72.38393	126.48612	14.07.2017	0.5	Samoylov i.; Polygon pond North
L17-11	72.28277	126.48544	14.07.2017	0.5	Samoylov i.; Polygon pond Mid
L17-12	72.38368	126.48508	14.07.2017	0.5	Samoylov i.; Polygon pond South

5

Exploring the mysteries of GDGTs in the Arctic: Insights from the Lena Delta and Laptev Sea Nearshore

Exploring the mysteries of GDGTs in the Arctic: Insights from the Lena Delta and Laptev Sea Nearshore

Olga Ogneva^{1,2,3}, Gesine Mollenhauer^{1,3,4}, Jens Hefter¹, Bingbing Wei^{1,4}, Tina Sanders⁴, Juri Palmtag^{5,a}, Matthias Fuchs^{2,b}, Laura Kattein^{1,3} and Jens Strauss²

¹Marine Geochemistry Section, Alfred Wegener Institute Helmholtz Centre for Polar and Marine Research, Bremerhaven, 27570, Germany

²Permafrost Research Section, Alfred Wegener Institute Helmholtz Centre for Polar and Marine Research, Potsdam, 14473, Germany

³Faculty of Geosciences, University of Bremen, Bremen, 28359, Germany

⁴MARUM - Center for Marine Environmental Sciences, University of Bremen, Bremen, Germany

⁵Institute for Carbon Cycles, Helmholtz Centre Hereon, Geesthacht, 21502, Germany

⁶Department of Geography and Environmental Sciences, Northumbria University, Newcastle-upon-Tyne, NE1 8ST, UK

^anow at: Swedish Nuclear Fuel and Waste Management Co. (SKB), Box 3091, 169 03 Solna, Sweden

^bnow at: Renewable and Sustainable Energy Institute, University of Colorado Boulder, United States

Correspondence to: Olga Ogneva (Olga.Ogneva@awi.de), Gesine Mollenhauer (Gesine.Mollenhauer@awi.de) and Jens Strauss (Jens.Strauss@awi.de)

Abstract

Permafrost thaw in the Arctic leads to the release of organic matter from terrestrial sources into inland aquatic systems and further into the Arctic Ocean. Nearshore regions, such as deltas and estuaries, are critical areas where significant transformations of terrestrial material occur, serving as natural filters for riverine inputs to the ocean. Our study focuses on glycerol dialkyl glycerol tetraethers (GDGTs), including isoprenoidal (isoGDGT), hydroxylated (OH-GDGT), branched (brGDGT), and H-shaped brGDGT (H-brGDGTs), biomarkers used in several indices that serve as proxies for a range of environmental parameters. We extracted the GDGTs from particulate organic matter (POM) within the Lena Delta waters during both summer and winter, as well as along a transect to the Laptev Sea nearshore zone sampled only in summer. Along the latter, isoGDGT and OH-GDGT concentrations increased seaward, correlating with salinity. Temperatures estimated based on the TEX₈₆L index closely matched in-situ measurements in marine environments but underestimated temperatures in the freshwater delta during winter. BrGDGTs, primarily soil-derived, showed elevated

concentrations in winter POC, reflecting relatively increased terrestrial input and reduced aquatic production. Summer BrGDGT concentrations, though higher in absolute terms, were diluted by contributions from vegetation and algae. H-brGDGTs are linked to peat and revealed a distinct pattern with a secondary peak in near-bottom nearshore sediments, indicating enhanced peat deposition through flocculation in saline environments. These findings illustrate the complex interactions between temperature, salinity, and organic matter sources in shaping the seasonal and spatial distribution of GDGTs in Arctic river and nearshore systems.

5.1 Introduction

The Arctic is experiencing rapid change with increasing air and soil temperatures (Biskaborn et al., 2019; Rantanen et al., 2022). Terrestrial permafrost thaw accelerates the release of organic matter (OM) and nitrogen from the soil to inland aquatic systems (Schuur et al., 2015; Strauss et al., 2017, 2024; Turetsky et al., 2020; Wild et al., 2019). This OM can be further transported to the Arctic coastal waters (Cole et al., 2007; Sanders et al., 2022; Tank et al., 2016), modifying significantly the biogeochemical cycles in the Arctic Ocean (Frey and McClelland, 2009; Terhaar et al., 2021).

Nearshore regions across the Arctic (including deltas, estuaries, and coasts) are biogeochemically dynamic areas and hotspots of environmental change (Mann et al., 2022) where major transformations of terrestrial material are expected to occur (Sanders et al., 2022; Tanski et al., 2019; 2021). Estuaries and deltaic regions act as natural filters for riverine inputs to coastal waters and the open ocean (Smith et al., 2002). Despite their importance in the biogeochemistry of organic matter (Ogneva et al., 2023), our understanding of how these environments function remains limited, and there are only few studies that comprehensively investigate the supply, composition, and transformation of terrestrial organic matter during its transport from rivers to the shelf (Semiletov et al., 2011; Jong et al., 2019 ; Gustafsson et al., 2020; Mann et al., 2022;

Polimene et al., 2022). Additionally, only a few studies examine different seasons, especially concerning organic carbon (OC) and other nutrients (Knights et al., 2023), which restricts our ability to predict the effects of changing seasonality and the intensification of the Arctic freshwater cycle.

A versatile tool for the investigation of the impact of permafrost thaw on these biogeochemical dynamic in the Arctic nearshore is to study lipid biomarkers (Haugk et al., 2022; Jongejans et al., 2022; Strauss et al., 2015). In this paper, we provide an analysis of glycerol dialkyl glycerol tetraethers (GDGTs).

GDGTs are membrane-spanning lipids and essential components of microbial cell membranes (Figure 5-S1). They serve as biomarkers in environmental research. GDGTs are either formed by archaea or bacteria synthesising isoprenoid alkyl chains (isoGDGTs) or methyl-branched alkyl chains (brGDGTs), respectively (Schouten et al., 2013).

IsoGDGTs are uniquely characterized by crenarchaeol and its isomer and produced by the extremophilic Thaumarchaeota archaea phylum (Schouten et al., 2013). Thus, they are useful chemotaxonomic markers for this phylogenetic group (Schouten et al., 2013).

BrGDGTs have been tentatively attributed to bacterial origin - heterotrophic Acidobacteria (Schouten et al., 2013). They have been found in natural samples such as soils, peats and lake sediments (De Jonge et al., 2014a; Naafs et al., 2017) and the relative abundance of the individual brGDGTs depends on environmental factors such as temperature and pH (Naafs et al., 2017).

These widely used archaeal and bacterial biomarkers have the potential to inform about OM origins, as well as environmental parameters at the location of their biosynthesis but remain poorly studied in the permafrost zone. Initial studies on suspended material from the Yenisey River revealed distinct characteristics in the Arctic watershed (De Jonge et

al., 2014b, 2015). A comprehensive study on various permafrost deposit types in Siberia showed promise that they might help to distinguish organic matter sources (Kusch et al., 2019). Our study is the first to characterize GDGTs in suspended matter collected in the Lena Delta and its nearshore zone.

Additionally to the commonly reported isoGDGTs and brGDGTs, in this paper, we also report about the less well-studied branched glycerol monoalkyl glycerol tetraether lipid group (called H-brGDGTs) discovered more recently (Knappy et al., 2011, Schouten et al., 2013). Moreover, we analysed the hydroxylated isoprenoid (OH)-GDGT produced by both marine and freshwater thaumarchaeota. These were used recently to decipher past sea surface temperature (Damste et al. 2022a, b).

We investigated GDGT compounds in particulate organic matter (POM) sampled in the Lena Delta during the winter and summer seasons of 2019, and we studied GDGTs along a transect from the Lena Delta to the Laptev Sea nearshore zone during the summer of the same year. Our research aims are to elucidate the seasonal and spatial dynamics of GDGT distribution within the Lena Delta, specifically examining how Arctic temperature, hydrological patterns, and organic matter sources of the Lena Delta and Laptev nearshore zone influence GDGTs, providing insights into microbial adaptation, biogeochemical processes, and the impact of environmental factors such as salinity and pH on GDGT production and distribution.

5.2 Materials and Methods

5.2.1 Study region: The Lena Delta

The Lena Delta, the largest polar delta, covers an extensive area of $28.5 \times 10^3 \text{ km}^2$ (Semiletov et al., 2011) and annually receives approximately $543 \text{ km}^3 \text{ yr}^{-1}$ of freshwater (mean discharge for 1936 – 2019 at Kyusyur station upstream of the delta; Wang et al., 2021). The Lena River catchment encompasses approximately $2.61 \times 10^6 \text{ km}^2$, with over

94% of this area containing permafrost with 70.5% underlain by continuous permafrost (Juhls et al., 2020; Obu et al., 2019). Within the Lena watershed, actively eroding Pleistocene-aged permafrost deposits known as Yedoma cover roughly 3.5% of the region (Fuchs et al., 2020; Haugk et al., 2022; Strauss et al., 2017).

In this study, we sampled the Lena delta along the Sardakhskaya channel (Figure 5- 1), which, together with the Trofimovskaya channel, constitutes a system responsible for transporting about 60-75% of the Lena's freshwater export (Fedorova et al., 2015) and up to 70% of total Lena particulate load to the Arctic Ocean coastline (Charkin et al., 2011; Ivanov & Piskun, 1999). Sampling was continued offshore along an eastward transect into the Laptev nearshore zone (Figure 5- 1).

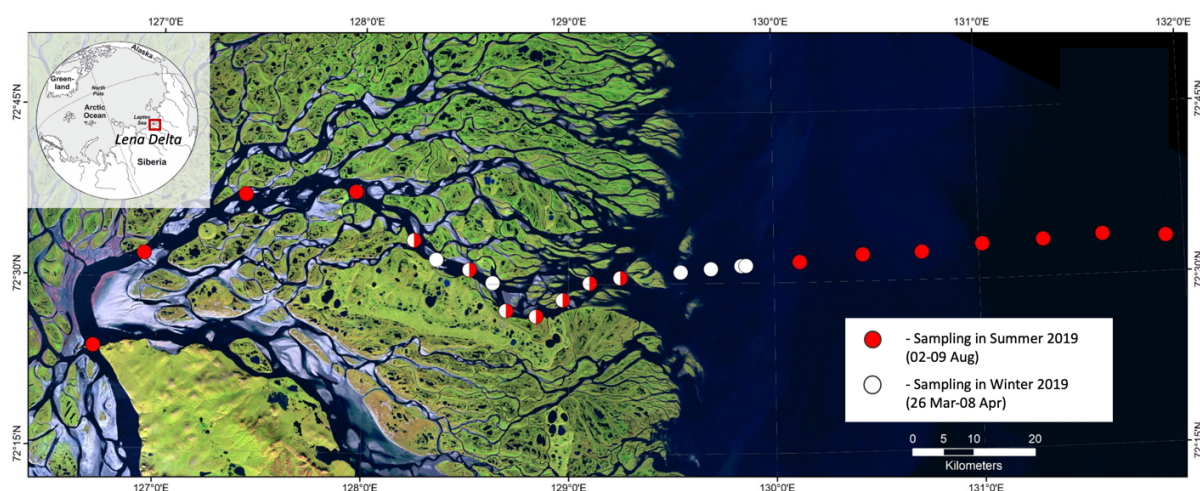


Figure 5-1. Sampling locations in the Lena delta and Laptev Sea nearshore in 2019. Red dots - sampling stations in Summer, white dots - sampling stations in Winter and red/white dots - locations, where samples have been collected in both seasons.

5.2.2 Sampling

Details of our sampling campaigns can be found in Fuchs et al., 2021, Ogneva et al., 2023 and Ogneva et al., 2024 (in review). Two distinct sampling campaigns were carried out in the Lena Delta and Laptev Sea nearshore during the winter and summer months

of 2019. The winter campaign took place from March 26th to April 8th, when the River, Delta, and Coastal waters were fully ice-covered. Water samples (n = 21) were taken at approximately 5-kilometer intervals, commencing at the easternmost sea-ice location (Figure 5- 1) (exact sampling locations are listed in Table 5-S1). The summer sampling campaign occurred from August 2nd to 28th, 2019. Started at Stolb Island in the west, near the transition point between the Lena River and the Delta (Figure 5- 1) samples were taken at locations along the Sardakhskaya branch (n= 23) previously sampled during the winter campaign. To investigate the transition from freshwater to saltwater, additional sampling in the Laptev nearshore was conducted from a sea-going vessel, employing the same methodology as in the Lena Delta (n = 20).

5.2.3 Laboratory analyses

During the winter sampling campaign, water samples were immediately filtered on-site. In the summer, filtration was carried out after storing the samples for less than 10 days at the laboratory located at the Samoylov Island Research Station. The filtration process involved passing the water (6-12 L for biomarker analyses and 400 ml for POC and TSM) through pre-combusted (for 4.5 hours at 450°C) and pre-weighed glass fiber filters (GF/F Whatman, 0.7 µm nominal pore size, with a diameter of 142 mm for biomarker study and with a diameter of 25 mm for particulate organic carbon (POC) and total suspended matter (TSM) analyses).

The filtered materials were then carefully placed into pre-combusted glass petri dishes or into pre-combusted aluminium foil envelopes and stored at -18°C until further analyses. Analyses of POC concentration were described in Ogneva et al., 2023.

To extract GDGTs, frozen filters were dried at 45° for 24 hours, then cut into pieces and extracted (3 times) after the addition of a known amount of the internal C46-GDGT standard using ultra sonication with a dichloromethane: methanol 9:1 (v: v) solvent

mixture. Total lipid extracts were combined, dried and subsequently separated into three polarity fractions using silica gel chromatography. The polar fraction containing GDGTs was eluted using 4 mL of methanol:DCM at 1:1 (v:v) ratio. Polar fractions were dried, re-dissolved in 2-propanol:n-hexane (99:1) and filtered through a polytetrafluoroethylene filter (0.45 μm pore size). Samples were brought to a concentration of 2 $\mu\text{g } \mu\text{l}^{-1}$ prior to GDGT analysis. GDGTs were analysed on an Agilent 1260 Infinity II ultrahigh-performance liquid chromatography-mass spectrometry (UHPLC-MS) system, consisting of a G1712B binary pump, a G7129A vial sampler with integrated sample thermostat, a G7116A multicolumn thermostat, and a G6125C single quadrupole mass spectrometer with an atmospheric pressure chemical ionization (APCI) ion source.

Chromatographic separation (including 5-and 6-Methyl isomers of brGDGTs) of the GDGTs was achieved by coupling two UPLC silica columns (Waters Acquity BEH HILIC, 2.1 \times 150 mm, 1.7 μm) with a 2.1 \times 5 mm pre-column as in Hopmans et al. (2016), but with the following chromatographic modifications: Mobile phases A and B consisted of n-hexane: chloroform (99:1, v/v) and n-hexane: 2-propanol: chloroform (89:10:1, v/v/v), respectively. The flow rate was set to 0.4mL/min and the columns were heated to 50°C, resulting in a maximum backpressure of 425 bar. Sample aliquots of 20 μL were injected with isocratic elution for 20 minutes using 86% A and 14% B, followed by a gradient to 30% A and 70% B within the next 20 min. After this, the mobile phase was set to 100% B, and the column was rinsed for 13 min, followed by a 7 min re-equilibration time with 86% A and 14% B before the next sample analysis. The total run time was 60 min.

GDGTs were detected using positive ion APCI-MS and selective ion monitoring (SIM) of (M + H)⁺ ions (Schouten et al., 2007) with the following settings: nebulizer pressure 50 psi, vaporizer and drying gas temperature 350°C, drying gas flow 5 L/min. The capillary voltage was 4 kV and the corona current +5 μA .

The detector was set for the following SIM ions: m/z 744 (C_{46} standard), m/z 1302.3 (GDGT-0), m/z 1300.3 (GDGT-1), m/z 1298.3 (GDGT-2), m/z 1296.3 (GDGT-3), m/z 1292.3 (crenarchaeol and crenarchaeol isomer), m/z 1022 (GDGT-Ia), m/z 1020 (GDGT-Ib), m/z 1018 (GDGT-Ic), m/z 1036 (GDGT-IIa and IIa'), m/z 1034 (GDGT-IIb and IIb'), m/z 1032 (GDGT-IIc and IIc'), m/z 1050 (GDGT-IIIa and IIIa'), m/z 1048 (GDGT-IIIb and IIIb'), m/z 1046 (GDGT-IIIc and IIIc'). The resulting scan/dwell time was 66ms.

5.3 Results

Total concentrations (the sum of all GDGTs within one GDGT class) of isoGDGT, OH-GDGT, brGRGT and H-brGDGT in summer and in winter in the Lena Delta and in summer in the Laptev nearshore zone are shown in Figure 5-2. The highest isoGDGT concentrations were measured in the sea in summer: average sum isoGDGT in the Laptev nearshore zone was $7.0 \pm 5.7 \mu\text{g g}^{-1}$ POC or $1.67 \pm 1.16 \text{ ng L}^{-1}$ ($n=18$) (Figure 5- 2.) and in the Lena Delta in both seasons concentrations were lower (0.48 ± 0.25 or $0.18 \pm 0.08 \text{ ng L}^{-1}$ in summer ($n=23$) and $2.30 \pm 0.77 \mu\text{g g}^{-1}$ POC or $0.26 \pm 0.07 \text{ ng L}^{-1}$ in winter ($n=21$)). Likewise, OH-GDGT in the Laptev nearshore zone reached $1.52 \pm 1.17 \mu\text{g g}^{-1}$ POC or $0.36 \pm 0.25 \text{ ng L}^{-1}$ and was lower in the Lena delta ($0.006 \pm 0.005 \mu\text{g g}^{-1}$ POC or $<0.01 \text{ ng L}^{-1}$ in summer and $0.022 \pm 0.041 \mu\text{g g}^{-1}$ POC or $0.26 \pm 0.07 \text{ ng L}^{-1}$ in winter) there was no statistical differences between POC normalized deltaic values in winter and summer ($p>0.05$).

Total concentrations of br-GDGTs and H-brGDGTs normalized to POC were highest in winter samples from the delta ($37.98 \pm 16.05 \mu\text{g g}^{-1}$ POC and $0.16 \pm 0.14 \mu\text{g g}^{-1}$ POC, respectively), compared to those in the summer samples from the delta (15.24 ± 8.32 and $0.06 \pm 0.01 \mu\text{g g}^{-1}$ POC) and in the nearshore zone (11.15 ± 2.69 and $0.09 \pm 0.07 \mu\text{g g}^{-1}$ POC) Non-normalized bulk concentrations (ng L^{-1}) provided different results, a slightly higher brGDGTs concentration in the delta in summer ($5.76 \pm 2.35 \text{ ng L}^{-1}$) compared to

the delta in winter ($4.29 \pm 1.23 \text{ ng L}^{-1}$) and in the Laptev Sea nearshore zone in summer ($2.99 \pm 0.79 \text{ ng L}^{-1}$) H-brGDGT concentrations statistically did not differ between stations and slightly varied around 0.02 ng L^{-1} (Figure 5-2).

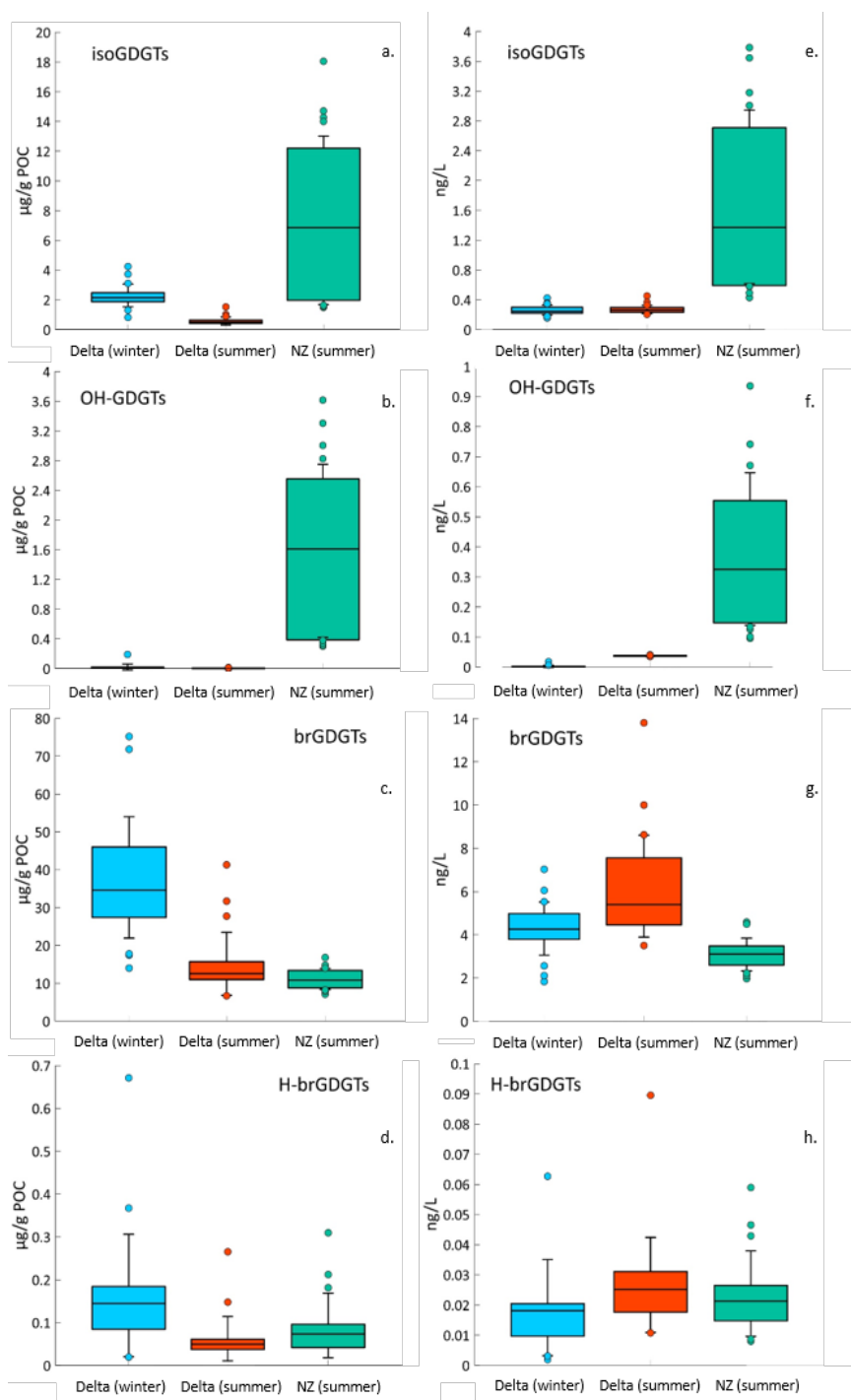


Figure 5-2. GDGT-abundances in samples of suspended particulate organic matter from the Lena Delta in winter and summer and the Laptev nearshore zone (NZ) in summer. Particulate organic matter (POC)-normalized contents – first column (a, b, c, d) and concentrations per L of water – second column (e, f, g, h). a/e)isoGDGTs, b/f)OH-GDGTs c/g) brGDGTs, d/h)H-brGDGTs. Central lines of the plots represent the median, boxes are defined by the lower and upper quartiles and whiskers indicate the standard deviation (winter delta n=21, summer delta n=23 and for nearshore zone, summer n = 18).

5.4 Discussion

5.4.1. IsoGDGTs and OH-GDGTs

The concentrations of isoprenoidal GDGTs and their hydroxylated forms in the river were consistently low during both winter and summer, particularly in comparison to levels observed in the Laptev nearshore zone (Figure 5-2). These compounds were largely absent within the delta region, however, their prevalence increased steadily as we moved seaward, with concentrations rising from the surface to deeper water layers (Figure 5-3). This observation aligns with previous studies that have documented the strong influence of salinity on GDGT distribution in Polar Regions, such as the Bering Sea and Arctic Ocean (Park et al., 2014; Damste et al., 2022b).

IsoGDGTs and OH-GDGTs are synthesized by thaumarchaea, which occur in aquatic systems, and culture experiments and in-situ observations suggest that growth temperature significantly impacts the relative abundance of IsoGDGTs and OH-GDGTs (Schouten et al., 2013). These GDGTs contain crenarchaeol, a structurally unique GDGT with one cyclohexane and four cyclopentane moieties (Holzheimer et al., 2021). Thaumarchaea adjust the number of cyclopentane moieties depending on growth temperature (Gabriel and Chong, 2000; Wuchter et al., 2004). Consequently, Schouten et al. (2002) introduced the TEX₈₆ (tetraether index of tetraethers consisting 86 carbons) as a sea surface temperature proxy. However, Kim et al. (2010) found the TEX₈₆ to be less effective in polar oceans and developed TEX_{86L}, which better correlates with SST in cooler environments. TEX_{86L}, based on GDGT ratios, links higher values to warmer waters and lower values to cooler conditions, making it a valuable tool for paleoclimate reconstructions.

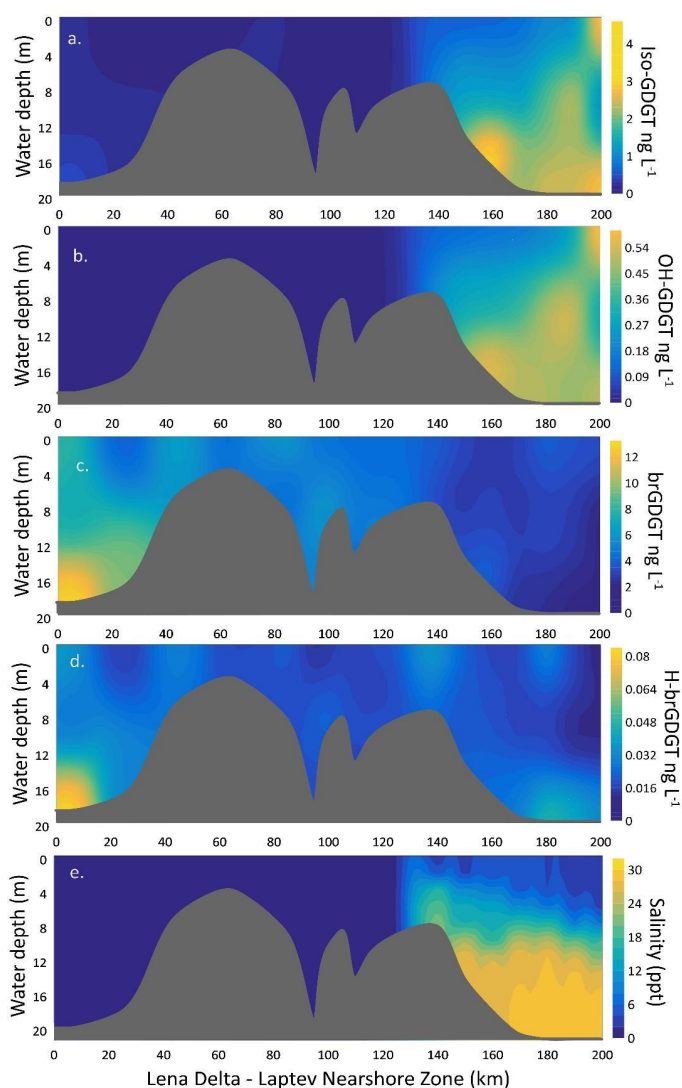


Figure 5-3. Distribution of GDGTs (per L of water) and salinity (ppt) along the transect from the Lena Delta to the Laptev Sea nearshore zone in summer. a) isoGDGTs, b) OH-GDGTs c) brGDGTs, d) H-brGDGTs, e) Salinity.

In our study, the TEX_{86L} index generally correlated with temperature, with higher TEX_{86L} values occurring at warmer temperatures, particularly in the summer deltaic samples (Figure 5-4). This pattern reflects the adaptation of thaumarchaea to warmer temperatures, consistent with their need to modulate membrane fluidity and permeability via cyclopentane rings as temperatures rise. This is consistent with the findings of Kim et al. (2010). In contrast, lower TEX_{86L} values and temperatures were recorded in the delta during winter, consistent with the seasonal temperature dependency of the index.

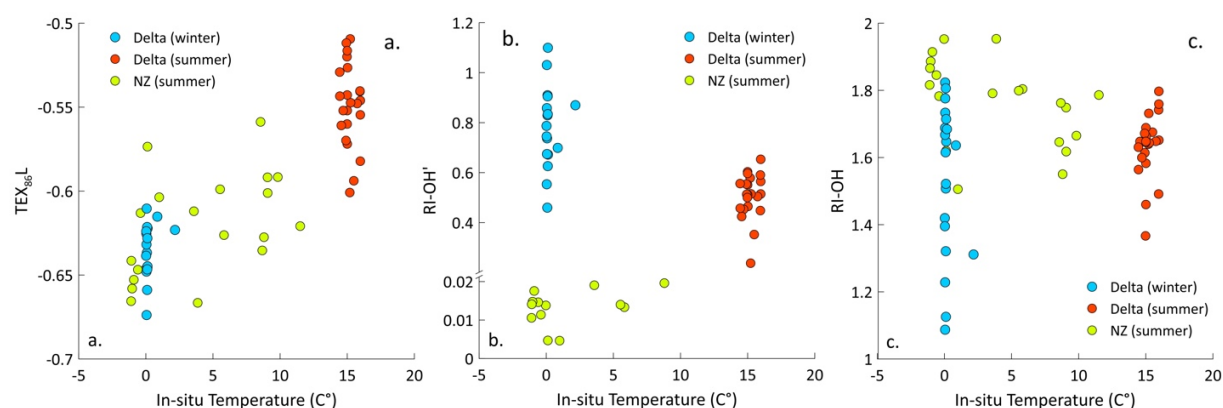


Figure 5-4. IsoGDGTs ratios in the Lena Delta in winter and summer and in Laptev nearshore zone (NZ) in summer compared to in-situ temperature: a) The TEX_{86L} index -temperature scatterplot; b) RI-OH' and in-situ temperature scatterplot; c) RI-OH temperature scatterplot.

The RI-OH and RI-OH' indices reflect the relative abundance of hydroxylated GDGTs (OH-GDGTs), which have poor correlations with in-situ temperature, particularly for delta samples (Figure 5-4b, c).

This is likely due to the low concentration of OH-GDGTs in the delta samples, which affects the calculated RI-OH and RI-OH' indices. They have been shown to vary in response to salinity levels, with higher values typically observed in more saline environments, suggesting that OH-GDGT composition is sensitive to salinity (Fietz et al., 2021). The two indices differ slightly, with RI-OH' reflecting the abundance of OH-GDGTs with a specific hydroxylation pattern, making it more sensitive to salinity variations, while RI-OH captures broader hydroxylation patterns, potentially reflecting additional factors such as temperature (Lü et al., 2015).

In our study, higher RI-OH' values were found in the delta samples, while higher RI-OH values were observed in the nearshore samples. This suggests that OH-GDGT composition was influenced by factors other than salinity alone, such as temperature or organic matter input, especially in the delta. Laptev near-shore summer samples exhibited a lower range of RI-OH' compared to deltaic samples, which contradicts the typical trend where higher values are expected in more saline environments. This may

indicate that OH-GDGT production in marine environments is not solely controlled by salinity but by additional environmental factors.

In the delta, winter samples showed higher RI-OH' values and a broader range of RI-OH values compared to summer samples, indicating that the composition of OH-GDGTs shifted in colder, low-salinity conditions rather than being reduced. These findings suggest that other factors beyond salinity, such as temperature and seasonal changes, influenced OH-GDGT distributions (Figure 5-4). This observation is consistent with other studies showing that salinity affects OH-GDGT distributions but may not be the sole driver (Damste et al., 2022b).

5.4.2 BrGDGTs

5.4.2.1 BrGDGTs and H-brGDGT from the delta to the Sea.

BrGDGTs, are a group of compounds derived from bacteria and possess 4–6 methyl substituents ('branches') on the linear C28 alkyl chains and up to two cyclopentyl moieties formed by internal cyclization (Weijers et al., 2006).

Their presence becomes progressively less pronounced along the Lena Delta transect, beginning near its starting point close to Stolb Island and gradually decreasing towards the delta's mouth (Figure 5-3). This pattern aligns with previous findings (Ogneva et al., 2023), which emphasized the behaviour of organic matter within the Lena delta. The study revealed that the Lena delta's POM originates primarily from areas near the delta, as much of the POM in the upstream Lena River settles before reaching the delta. A vast amount of organic matter is collected by the Lena River from its extensive catchment area. A significant portion of this material settles within the Lenskaya Truba (Lena pipe), a narrow and deep segment of the river, located about 200 kilometers upstream from the delta (Antonov, 1960; Fedorova et al., 2015; Ogneva et al., 2023). The Lenskaya Truba acts as a major sedimentation zone, where organic matter, including soil-derived

OM and brGDGT, is deposited. The concentration of brGDGT in the river's main channel may also be enhanced by bank soil erosion, which is more pronounced in the Lena's main channel compared to the delta (Chalov & Prokopeva, 2022).

H-brGDGTs are compounds often associated with peat origins (Naafs et al., 2018). Their distribution within the delta closely follows the brGDGT pattern, with a peak concentration observed at the delta's apex, nearest to the sediment deposition centre of the Lena pipe (Figure 5-3). However, unlike brGDGTs, H-brGDGTs display a secondary peak in the nearshore bottom sediments. This secondary peak indicates a distinct pathway for the mobilization and sedimentation of materials containing H-brGDGTs, differing from that of brGDGTs suggesting transportation and subsequent deposition of peat-derived material in the nearshore zone (Figure 5-3). The Laptev Sea Nearshore zone is characterized by a freshwater riverine layer overlaying saltwater, evident from the salinity gradient (Figure 5-3): fresh river water resides at the surface, while saltwater is situated deeper, closer to the bottom. Nevertheless, H-brGDGTs accumulate at the seabed. This observation suggests that H-brGDGTs are selectively attached to particles with a propensity to sink. For instance, they may be associated with mineral-enriched "heavy particles." A similar selectivity in mineral association was previously demonstrated by Vonk (2010) for *n*-alkanoic acids. Another explanation is that peat-indicator compounds might be part of eroded coarse plant debris that becomes waterlogged and rapidly deposited, as suggested by Van Crimpen et al. (2024). In addition, as salinity increases, it promotes the flocculation of suspended organic particles, including hydrophobic peat, by reducing electrostatic repulsion and enabling particle aggregation. This process leads to faster sedimentation of peat in saline environments compared to freshwater, where it remains suspended for longer periods (Furukawa, 2014; Mietta et al., 2009; Winkler et al., 2012). This explains the observed peat deposition in nearshore zones versus its absence in the freshwater delta.

Additionally, this process contributes to the "estuarine filter," where terrigenous materials, such as organic matter and minerals, are deposited at the river-ocean interface, reducing their transport to the open ocean (Bianchi, 2011).

5.4.2.2 (Sources) BrGDGT in winter and summer

The seasonal differences in brGDGT concentrations in the Lena Delta indicate that, while brGDGTs were more concentrated relative to POC in winter, their absolute concentrations were higher in summer (Figure 5-2). This can be attributed to the differing sources of POC between the seasons. In summer, POC was found to be primarily derived from vegetation and algae (Ogneva et al., 2023), which increases the overall suspended organic material but results in a lower relative content of brGDGTs, since these compounds predominantly originate from soil (Weijers et al., 2006). In winter, despite significantly lower POC levels, the contribution of soil material to the overall POM is likely higher (Ogneva et al., 2024, under review). This soil-derived POM contained more brGDGTs, resulting in a higher ratio of brGDGTs to POC. We hypothesize that the elevated presence of brGDGTs during winter may reflect an increased relative input of organic matter from soils or terrestrial sources and/or a decreased contribution from aquatic production. This scenario is in agreement with the fact that previous attempts to differentiate an influence of terrestrial sources (such as thermokarst, active layer, fluvial terrace, and Yedoma) on OC normalized brGDGTs concentration in the summer season did not yield significant differences (Kusch et al., 2019).

5.4.3 Unique signature or Arctic River SPM

The OC-normalized abundances of iso- and brGDGTs measured in SPM from both summer and winter deltaic samples resembled those reported by Kusch (2019), for the active layer, fluvial terrace, thermokarst, and Yedoma permafrost deposits from the same region (Figure 5-5). Both datasets revealed a dominance of pentamethylated brGDGTs,

particularly the isomers IIIa, IIIa', IIa, IIa' and Ia, which are the most abundant as well as at this study, while the isoGDGTs and tetra- and hexamethylated brGDGTs are limited suggesting that their production is less favored in the environmental conditions of the Lena Delta. (Figure 5-5). These similarities suggest that brGDGT production in both permafrost and SPM environments is influenced by common environmental factors, such as temperature and pH. This relationship has been established in previous research, particularly by De Jonge et al. (2014a, b), who demonstrated that the degree of methylation of brGDGTs correlates with mean annual temperature, while the degree of cyclization is related to soil pH (Kusch et al., 2019). The predominance of IIIa and IIa in our dataset aligns with these observations, suggesting that microbial communities in the Lena Delta produce highly methylated brGDGTs, possibly reflecting adaptation to the region's specific temperature and pH conditions, as discussed by Peterse et al. (2009) and Kusch et al. (2019).

In contrast to the samples analysed by Kusch et al. (2019), where the most abundant brGDGT isomers across the active layer, thermokarst, Yedoma, and fluvial terrace were IIIa and IIa, our analysis of SPM from the Lena Delta showed that IIIa' and IIa' (6-methyl brGDGTs) dominated over IIIa and IIa (Figure 5-5). This pattern was similar to that reported by De Jonge et al. (2014b, 2015) for SPM from the Yenisei River, where they demonstrated a consistent presence of 6-methyl brGDGTs (IIIa' and IIa') throughout the river's flow, suggesting in-situ production within the freshwater column rather than input from terrestrial sources or influence from salt/brackish water—where these isomers were nearly absent (similar to our findings, Figure 5-6).

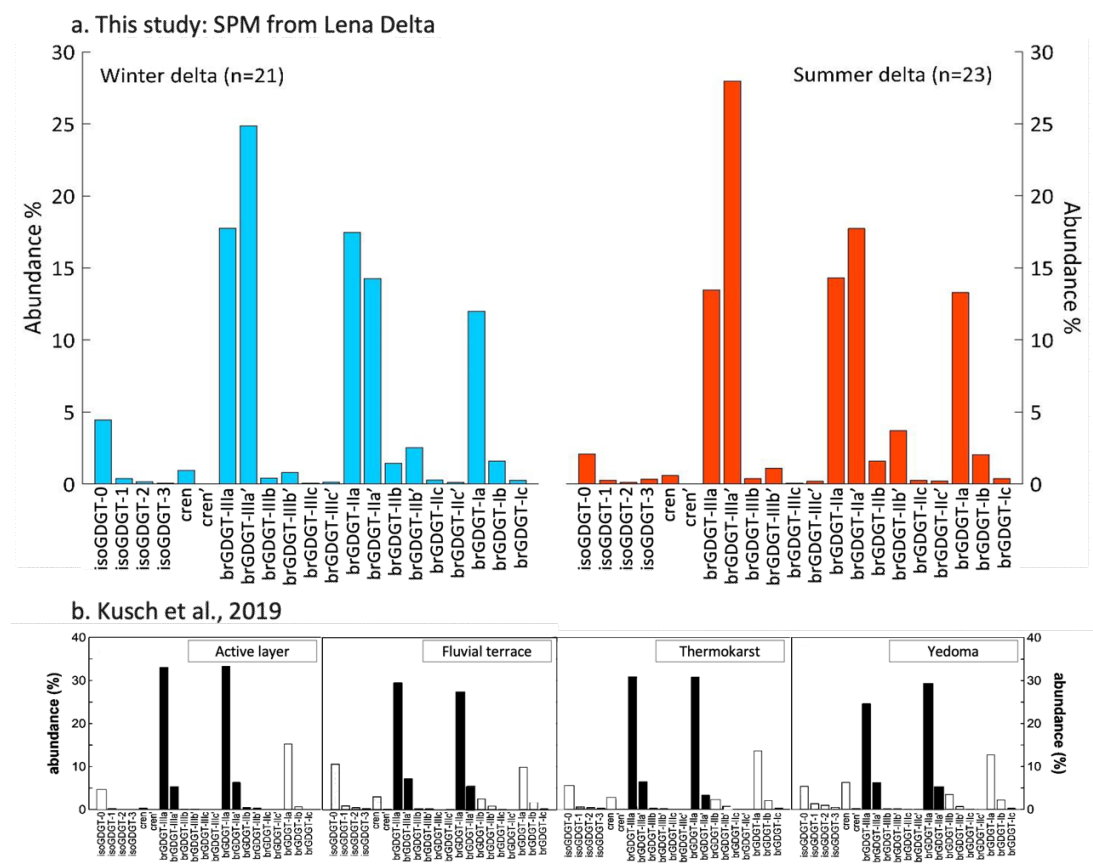


Figure 5-5. a. Abundances of iso- and brGDGTs in suspended particulate matter of the Lena Delta in winter (blue) and summer (red); b. black and white diagrams show the abundances of iso- and brGDGT for different sources in the Lena Delta by Kusch et al., (2019).

The high abundance of 6-methyl brGDGTs (IIla' and IIa') was attributed to in-situ bacterial production under neutral pH conditions. The distinct predominance of these 6-methyl isomers in riverine SPM firstly identified for Arctic rivers by De Jonge et al. (2014b, 2015), was characteristic of neutral to slightly alkaline environments, then was also observed in studies on the Seine River (France) by Zhang et al. (2024), suggesting that microbial production of 6-methyl brGDGTs is a widespread phenomenon in large river systems. As demonstrated by Peterse et al. (2009), microbial processes linked to brGDGT formation in rivers are influenced by factors such as pH and temperature, further

supporting the idea that these compounds are synthesized locally rather than being transported from soils.

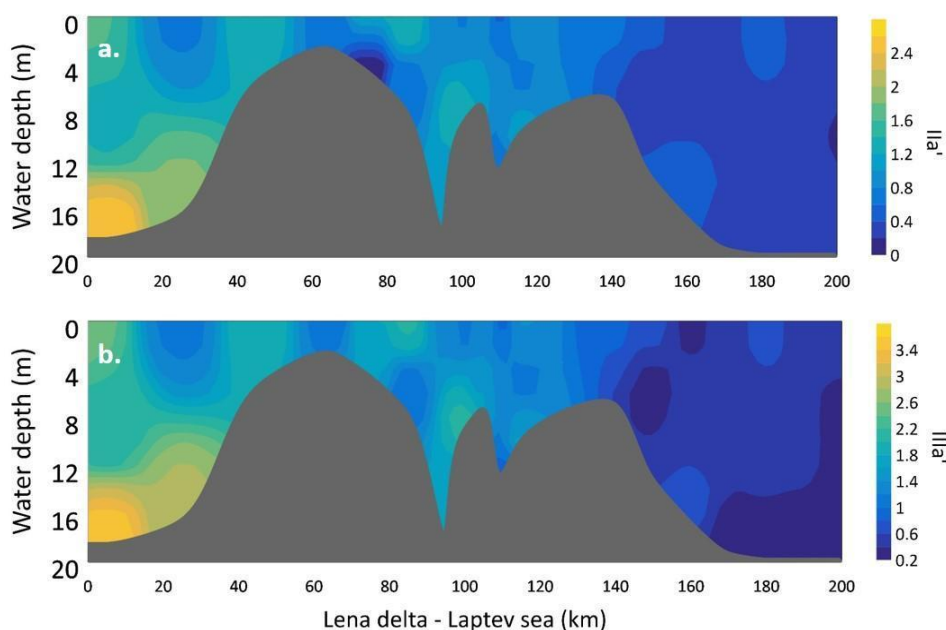


Figure 5-6. Distribution of Ila' (a) and IIIa' (b) brGDGT along the transect from the Lena Delta to the Laptev Nearshore.

Summarizing the characteristics of brGDGTs observed in this study, we suggested that the predominance of both 5-methyl isomers (such as IIIa and IIa), which were typical of Arctic terrestrial ecosystems as demonstrated by Kusch et al. (2019), and 6-methyl isomers (such as IIIa' and IIa'), which had been identified in riverine systems (Zhang et al., 2024; De Jonge et al., 2014b, 2015), represented a unique combination of cold-climate adaptation (5-methyl brGDGTs) and pH-driven riverine responses (6-methyl brGDGTs). This distinct brGDGT signature in Lena Delta SPM may have reflected characteristics not only specific to the Lena Delta but also broadly representative of Arctic suspended particulate matter (SPM).

To better contextualize our findings, we constructed a ternary diagram illustrating the methylation composition of brGDGTs, comparing our data with the comprehensive

dataset compiled by Raberg et al. (2022). We placed particular emphasis on comparing data from northern environments with those from other regions (Figure 5-7). Our results showed the closest alignment with Arctic SPM samples from the Yenisei River (De Jonge et al., 2015) and were also close to Arctic soil samples, meanwhile, they differed notably from non-Arctic SPM data. Based on these observations, we propose that the brGDGT signature, shaped by its sensitivity to environmental factors such as cold temperatures and pH, can serve as a reliable biomarker for distinguishing unique geochemical signatures in East Siberian Arctic SPM.

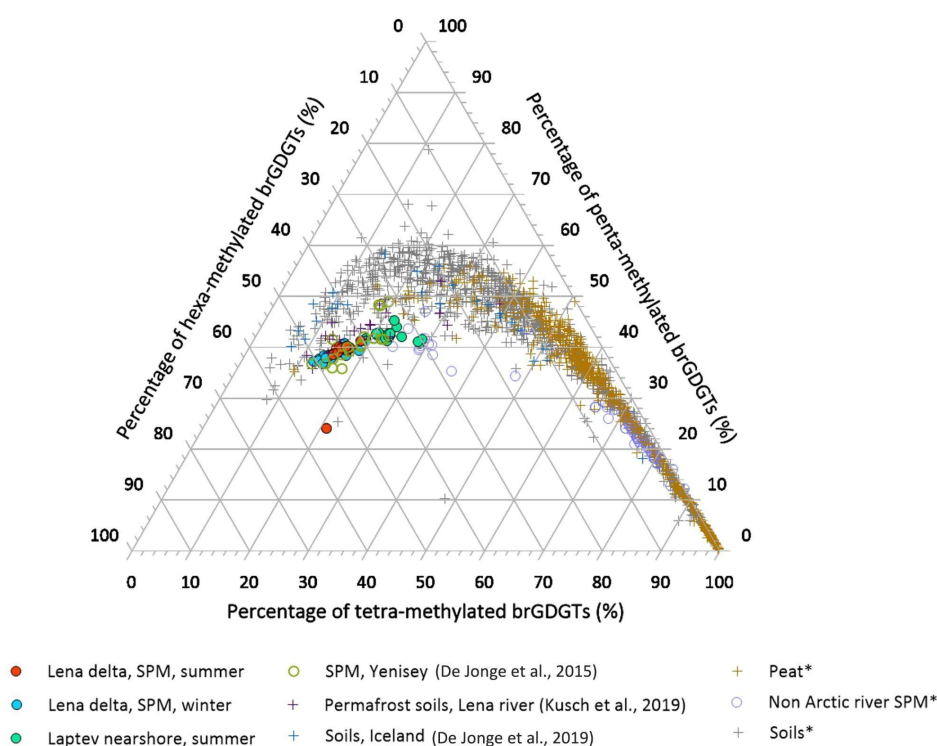


Figure 5-7. Ternary diagram showing the methylation composition of brGDGTs in analysed samples from this research and previously analysed samples from different studies: Kusch et al. 2019, De Jonge et al., 2019, starred (*) samples were taken from the GDGTs source compilation by Raberg et al. (2022) (Peat, soils, non-Arctic river SPM).

5.5 Conclusion

In conclusion, our study offers valuable insights into the biogeochemical processes of Arctic river ecosystems, focusing on the dynamics of glycerol dialkyl glycerol tetraethers (GDGTs) within the Lena Delta and Laptev Sea nearshore.

The distribution pattern of iso- and OH-GDGTs closely mirrors the salinity profile observed along the transect of our study. These compounds are absent within the delta region, becoming more prevalent as we move seaward, with concentrations increasing from the surface to deeper layers. Additionally, TEX₈₆L-derived temperatures align well with in-situ data in marine environments, but show discrepancies in freshwater delta conditions during winter. This is likely due to reduced thaumarchaeal activity and lower salinity.

The distribution of brGDGTs and H-brGDGTs reveals distinct transport and sedimentation patterns from the Lena Delta to the Laptev Sea. While brGDGTs, derived from soil, decrease along the delta, H-brGDGTs, associated with peat, show a secondary peak in the nearshore bottom sediments. We suggest that H-brGDGTs are preferentially transported and deposited in saline environments through flocculation and particle aggregation processes. This contributes to the "estuarine filter" effect that limits the transport of terrigenous material to the open ocean.

We hypothesize that the elevated concentration of POC-normalized brGDGTs during winter reflects a higher relative input of soil-derived organic matter and/or reduced aquatic production. This is supported by the fact that, despite lower overall POC levels in winter, the BrGDGT as soil-derived GDGT compound remained significant. In contrast, summer brGDGT concentrations, while higher in absolute terms, were diluted by increased contributions from vegetation and algae.

The distinct brGDGT signature in Lena Delta suspended particulate matter (SPM) reveals both cold-climate adaptation and pH-dependent microbial processes. While 5-methyl isomers (IIIa, IIa), typical of Arctic terrestrial environments, dominate, the notable presence of 6-methyl isomers (IIIa', IIa') indicates in-situ production in the riverine system under neutral to slightly alkaline conditions. This combination highlights the unique geochemical signature of Arctic river systems, suggesting that brGDGTs can serve as effective biomarkers for environmental conditions such as temperature and pH in East Siberian Arctic SPM.

References

- Bianchi, T. S. (2011). The role of terrestrially derived organic carbon in the coastal ocean: A changing paradigm and the priming effect. *Proceedings of the National Academy of Sciences*, 108(49), 19473-19481. <https://doi.org/10.1073/pnas.1017982108>
- Biskaborn, B. K., Smith, S. L., Noetzi, J., Matthes, H., Vieira, G., Streletskiy, D. A., ... & Lantuit, H. (2019). Permafrost is warming at a global scale. *Nature Communications*, 10(1), 1-11. <https://doi.org/10.1038/s41467-018-08240-4>
- Chalov, S., & Prokopeva, K. (2022). Sedimentation and Erosion Patterns of the Lena River Anabranching Channel. *Water*, 14(23), 3845. <https://doi.org/10.3390/w14233845>
- Cole, J. J., Prairie, Y. T., Caraco, N. F., McDowell, W. H., Tranvik, L. J., Striegl, R. G., ... & Melack, J. M. (2007). Plumbing the global carbon cycle: integrating inland waters into the terrestrial carbon budget. *Ecosystems*, 10(1), 171-184. <https://doi.org/10.1007/s10021-006-9013-8>
- Crimpen, F. C. J., Madaj, L., Whalen, D., Tesi, T., van Genuchten, J. M., Bröder, L., et al. (2024). Traveling light: Arctic coastal erosion releases mostly matrix free, unprotected organic carbon. *Geophysical Research Letters*, 51, e2024GL108622. <https://doi.org/10.1029/2024GL108622>
- Damsté, J. S. S., Weber, Y., Zopfi, J., Lehmann, M. F., & Niemann, H. (2022a). Distributions and sources of isoprenoidal GDGTs in Lake Lugano and other central European (peri-)alpine lakes: Lessons for their use as paleotemperature proxies. *Quaternary Science Reviews*, 277, 107352. <https://doi.org/10.1016/j.quascirev.2021.107352>
- Damsté, J. S. S., Warden, L. A., Berg, C., Jürgens, K., & Moros, M. (2022b). Evaluation of the distributions of hydroxylated glycerol dibiphytanyl glycerol tetraethers (GDGTs) in Holocene Baltic Sea sediments for reconstruction of sea surface temperature: The effect of changing salinity. *Climate of the Past*, 18(10), 2271-2288. <https://doi.org/10.5194/cp-18-2271-2022>
- De Jonge, C., Hopmans, E. C., Zell, C. I., Kim, J. H., Schouten, S., & Sinninghe Damsté, J. S. (2014a). Occurrence and abundance of 6-methyl branched glycerol dialkyl glycerol tetraethers in soils: Implications for palaeoclimate reconstruction. *Geochimica et Cosmochimica Acta*, 141, 97-112. <https://doi.org/10.1016/j.gca.2014.06.013>
- De Jonge, C., Stadnitskaia, A., Hopmans, E. C., Cherkashov, G., Fedotov, A., & Sinninghe Damsté, J. S. (2014b). In situ produced branched glycerol dialkyl glycerol tetraethers in suspended particulate matter

- from the Yenisei River, Eastern Siberia. *Geochimica et Cosmochimica Acta*, 125, 476–491. <https://doi.org/10.1016/j.gca.2013.10.031>
- De Jonge, C., Stadnitskaia, A., Hopmans, E. C., Cherkashov, G., Fedotov, A., Streletskaya, I. D., Vasiliev, A. A., & Sinninghe Damsté, J. S. (2015). Drastic changes in the distribution of branched tetraether lipids in suspended matter and sediments from the Yenisei River and Kara Sea (Siberia): Implications for the use of brGDGT-based proxies in coastal marine sediments. *Geochimica et Cosmochimica Acta*, 165, 200–225. <https://doi.org/10.1016/j.gca.2015.05.044>
- De Jonge, C., Radujković, D., Sigurdsson, B. D., Weedon, J. T., Janssens, I., & Peterse, F. (2019). Lipid biomarker temperature proxy responds to abrupt shift in the bacterial community composition in geothermally heated soils. *Organic Geochemistry*, 137, 103897. <https://doi.org/10.1016/j.orggeochem.2019.07.006>
- Fietz, S., Ho, S. L., & Huguët, C. (2021). Archaeal membrane lipid-based paleothermometry for applications in polar oceans. *Ocean Science*, 9(5), 803–816. <https://doi.org/10.5670/oceanog.2020.207>
- Frey, K. E., & McClelland, J. W. (2009). Impacts of permafrost degradation on Arctic river biogeochemistry. *Hydrological Processes: An International Journal*, 23(1), 169–182. <https://doi.org/10.1002/hyp.7196>
- Fuchs, M., Ogneva, O., Sanders, T., Schneider, W., Polyakov, V., Becker, O. O., Bolshiyarov, D., Mollenhauer, G., and Strauss, J. (2021): CACOON Sea – water sampling along the Sardakhskaya channel and near shore of the Laptev Sea, in: Reports on Polar and Marine Research, Russian-German Cooperation: Expeditions to Siberia in 2019, edited by: Fuchs, M., Bolshiyarov, D., Grigoriev, M. N., Morgenstern, A., and Dill, A., Bremerhaven, Alfred Wegener Institute, chap. 3.26, 141–149, ISBN: 1866-3192, https://doi.org/10.48433/BzPM_0749_2021
- Furukawa, Y., Reed, A.H. & Zhang, G. (2014). Effect of organic matter on estuarine flocculation: a laboratory study using montmorillonite, humic acid, xanthan gum, guar gum and natural estuarine flocs. *Geochem Trans* 15, 1. <https://doi.org/10.1186/1467-4866-15-1>
- Gustafsson, Ö., Semiletov, I., Shakhova, N., Dudarev, O., Vonk, J., Van Dongen, B., Eglinton, T., Tesi, T., Bröder, L., Andersson, A., Wild, B., Matsubara, F., & Martens, J. (2020, March 23). Transport and fate of different components of terrestrial organic matter across the Siberian-Arctic shelves. <https://doi.org/10.5194/egusphere-egu2020-17595>
- Haugk, C., Jongejans, L. L., Mangelsdorf, K., Fuchs, M., Ogneva, O., Palmtag, J., Mollenhauer, G., Mann, P. J., Overduin, P. P., Grosse, G., Sanders, T., Tuerena, R. E., Schirrmeister, L., Wetterich, S., Kizyakov, A., Karger, C., & Strauss, J. (2022). Organic matter characteristics of a rapidly eroding permafrost cliff in NE Siberia (Lena Delta, Laptev Sea region). *Biogeosciences*, 19(7), 2079–2094. <https://doi.org/10.5194/bg-19-2079-2022>
- Holzheimer, M., Sinninghe Damsté, J. S., Schouten, S., Havenith, R. W., Cunha, A. V., & Minnaard, A. J. (2021). Total synthesis of the alleged structure of crenarchaeol enables structure revision. *Angewandte Chemie International Edition*, 60(17). <https://doi.org/10.5194/bg-19-2079-2022>
- Holzheimer, M., Sinninghe Damsté, J. S., Schouten, S., Havenith, R. W., Cunha, A. V., & Minnaard, A. J. (2021). Total synthesis of the alleged structure of crenarchaeol enables structure revision. *Angewandte Chemie International Edition*, 60(17). <https://doi.org/10.1002/anie.202105384>
- Jong, D. J., Bröder, L. M., Keskitalo, K. H., Tesi, T., Zimov, N., Davydova, A., Haghypour, N., Eglinton, T. I., & Vonk, J. E. (2019). Organic matter characterisation along a river delta to shelf transect in eastern Siberia. 29th International Meeting on Organic Geochemistry, IMOG 2019, 1–2. <https://doi.org/10.3997/2214-4609.201902747>
- Jongejans, L. L., Mangelsdorf, K., Karger, C., Opel, T., Wetterich, S., Courtin, J., Meyer, H., Kizyakov, A. I., Grosse, G., Shepelev, A. G., Syromyatnikov, I. I., Fedorov, A. N., & Strauss, J. (2022). Molecular biomarkers in Batagay megaslump permafrost deposits reveal clear differences in organic matter

- preservation between glacial and interglacial periods. *The Cryosphere*, 16(9), 3601–3617. <https://doi.org/10.5194/tc-16-3601-2022>
- Kim, J. H., Schouten, S., Hopmans, E. C., Donner, B., & Sinninghe Damsté, J. S. (2008). Global sediment core-top calibration of the TEX86 paleothermometer in the ocean. *Geochimica et Cosmochimica Acta*, 72(4), 1154–1173. <https://doi.org/10.1016/j.gca.2007.12.010>
- Kim, J. H., van der Meer, J., Schouten, S., Helmke, P., Willmott, V., Sangiorgi, F., Koc, N., Hopmans, E. C., & Sinninghe Damsté, J. S. (2010). New indices and calibrations derived from the distribution of crenarchaeal isoprenoid tetraether lipids: Implications for past sea surface temperature reconstructions. *Geochimica et Cosmochimica Acta*, 74(16), 4639–4654. <https://doi.org/10.1016/j.gca.2010.05.027>
- Knappy, C. S., Nunn, C. E. M., & Morgan, H. W. (2011). The major lipid cores of the archaeon *Ignisphaera aggregans*: Implications for the phylogeny and biosynthesis of glycerol monoalkyl glycerol tetraether isoprenoid lipids. *Extremophiles*, 15(5), 517–528. <https://doi.org/10.1007/s00792-011-0382-3>
- Kusch, S., Winterfeld, M., Mollenhauer, G., Höfle, S. T., Schirrneister, L., Schwamborn, G., & Rethemeyer, J. (2019). Glycerol dialkyl glycerol tetraethers (GDGTs) in high latitude Siberian permafrost: Diversity, environmental controls, and implications for proxy applications. *Organic Geochemistry*, 136, 103888. <https://doi.org/10.1016/j.orggeochem.2019.103888>
- Lü, X., Liu, X.-L., Elling, F. J., Yang, H., Xie, S., Song, J., Li, X., Yuan, H., Li, N., & Hinrichs, K.-U. (2015). Hydroxylated isoprenoid GDGTs in Chinese coastal seas and their potential as a paleotemperature proxy for mid-to-low latitude marginal seas. *Organic Geochemistry*, 89, 31–43. <https://doi.org/10.1016/j.orggeochem.2015.10.004>
- Mann, P. J., Strauss, J., Palmtag, J., Dowdy, K., Ogneva, O., Fuchs, M., Bedington, M., Torres, R., Polimene, L., Overduin, P., Mollenhauer, G., Grosse, G., Rachold, V., Sobczak, W. V., Spencer, R. G. M., & Juhls, B. (2022). Degrading permafrost river catchments and their impact on Arctic Ocean nearshore processes. *Ambio*, 51(2), 439–455. <https://doi.org/10.1007/s13280-021-01666-z>
- Mietta, F., Chassagne, C., & Manning, A. J. (2009). Influence of shear rate, organic matter content, pH, and salinity on mud flocculation. *Ocean Dynamics*, 59(5), 751–763. <https://doi.org/10.1007/s10236-009-0231-4>
- Naafs, B. D. A., Gallego-Sala, A. V., Inglis, G. N., & Pancost, R. D. (2017). Refining the global branched glycerol dialkyl glycerol tetraether (brGDGT) soil temperature calibration. *Organic Geochemistry*, 106, 48–56. <https://doi.org/10.1016/j.orggeochem.2017.01.009>
- Ogneva, O., Mollenhauer, G., Juhls, B., Sanders, T., Palmtag, J., Fuchs, M., Grotheer, H., Mann, P. J., & Strauss, J. (2023). Particulate organic matter in the Lena River and its delta: From the permafrost catchment to the Arctic Ocean. *Biogeosciences*, 20, 1423–1441. <https://doi.org/10.5194/bg-20-1423-2023>
- Park, Y. H., Yamamoto, M., Nam, S. I., Irino, T., Polyak, L., Harada, N., Nagashima, K., Khim, B.K., Chikita, K., & Saitoh, S. I. (2014). Distribution, source and transportation of glycerol dialkyl glycerol tetraethers in surface sediments from the western Arctic Ocean and the northern Bering Sea. *Marine Chemistry*, 165, 10–24. <https://doi.org/10.1016/j.marchem.2014.07.001>
- Peterse, F., Kim, J. H., Schouten, S., Kristensen, D. K., Koç, N., & Sinninghe Damsté, J. S. (2009). Constraints on the application of the MBT/CBT palaeothermometer at high latitude environments (Svalbard, Norway). *Organic Geochemistry*, 40(6), 692–699. <https://doi.org/10.1016/j.orggeochem.2009.03.004>
- Polimene, L., Torres, R., Powley, H. R., Bedington, M., Juhls, B., Palmtag, J., Strauss, J., & Mann, P. J. (2022). Biological lability of terrestrial DOM increases CO₂ outgassing across Arctic shelves. *Biogeochemistry*, 160(3), 289–300. <https://doi.org/10.1007/s10533-022-00961-5>
- Råberg, J. H., Miller, G. H., Geirsdóttir, Á., & Sepúlveda, J. (2022). Near-universal trends in brGDGT distributions in nature. *Science Advances*. <https://doi.org/10.1126/sciadv.abm7625>

- Rantanen, M., Karpechko, A. Y., Lipponen, A., Nordling, K., Hyvärinen, O., Ruosteenoja, K., Vihma, T., & Laaksonen, A. (2022). The Arctic has warmed nearly four times faster than the globe since 1979. *Communications Earth & Environment*, 3, 168. <https://doi.org/10.1038/s43247-022-00498-3>
- Sanders, T., Fiencke, C., Fuchs, M., Haugk, C., Juhls, B., Mollenhauer, G., Ogneva, O., Overduin, P., Palmtag, J., Povazhniy, V., and Strauss, J. (2022): Seasonal nitrogen fluxes of the Lena River Delta, *Ambio*, 51, 423–438, <https://doi.org/10.1007/s13280-021-01665-0>
- Semiletov, I. P., Pipko, I. I., Shakhova, N. E., Dudarev, O. V., Pugach, S. P., Charkin, A. N., McRoy, C. P., Kosmach, D., & Gustafsson, Ö. (2011). Carbon transport by the Lena River from its headwaters to the Arctic Ocean, with emphasis on fluvial input of terrestrial particulate organic carbon vs. Carbon transport by coastal erosion. *Biogeosciences*, 8(9), 2407–2426. <https://doi.org/10.5194/bg-8-2407-2011>
- Schouten, S., Hopmans, E. C., & Sinninghe Damsté, J. S. (2013). The organic geochemistry of glycerol dialkyl glycerol tetraether lipids: A review. *Organic Geochemistry*, 54, 19-61. <https://doi.org/10.1016/j.orggeochem.2012.09.006>
- Schuur, E. A. G., McGuire, A. D., Schädel, C., Grosse, G., Harden, J. W., Hayes, D. J., ... & Vonk, J. E. (2015). Climate change and the permafrost carbon feedback. *Nature*, 520(7546), 171–179. <https://doi.org/10.1038/nature14338>
- Sinninghe Damsté, J. S., Rijpstra, W. I. C., Foesel, B. U., Huber, K. J., Overmann, J., Nakagawa, S., Kim, J. J., Dunfield, P. F., Dedysh, S. N., & Villanueva, L. (2018). An overview of the occurrence of ether- and ester-linked iso-diabolic acid membrane lipids in microbial cultures of the Acidobacteria: Implications for brGDGT paleoproxies for temperature and pH. *Organic Geochemistry*, 124, 63-76. <https://doi.org/10.1016/j.orggeochem.2018.07.008>
- Smith, S. V., Renwick, W. H., Bartley, J. D., & Buddemeier, R. W. (2002). Distribution and significance of small, artificial water bodies across the United States landscape. *Science of the Total Environment*, 348(1-3), 249–259. [https://doi.org/10.1016/s0048-9697\(02\)00222-x](https://doi.org/10.1016/s0048-9697(02)00222-x)
- Strauss, J., Schirrmeister, L., Grosse, G., Fortier, D., Hugelius, G., Knoblach, C., ... & Veremeeva, A. (2017). Deep Yedoma permafrost: A synthesis of depositional characteristics and carbon vulnerability. *Earth-Science Reviews*, 172, 75–86. <https://doi.org/10.1016/j.earscirev.2017.07.007>
- Strauss, J., Fuchs, M., Hugelius, G., Miesner, F., Nitze, I., Opfergelt, S., Schuur, E., Treat, C., Turetsky, M., Yang, Y., Grosse, G., 2024. Organic matter storage and vulnerability in the permafrost domain, in: *Encyclopedia of Quaternary Science*, 3rd Edition. <https://doi.org/10.1016/B978-0-323-99931-1.00164-1>
- Tank, S. E., Raymond, P. A., Striegl, R. G., McClelland, J. W., Holmes, R. M., Fiske, G. J., & Peterson, B. J. (2012). A land-to-ocean perspective on the magnitude, source and flux of organic carbon exports along the freshwater–marine continuum in the Arctic. *Global Biogeochemical Cycles*, 26(4), GD4018. <https://doi.org/10.1029/2011GB004192>
- Tanski, G., Wagner, D., Knoblach, C., Fritz, M., Sachs, T., & Lantuit, H. (2019). Rapid CO₂ release from eroding permafrost in seawater. *Geophysical Research Letters*, 46, 11244-11252. <https://doi.org/10.1029/2019GL084303>
- Tanski, G., Bröder, L., Wagner, D., Knoblach, C., Lantuit, H., Beer, C., Sachs, T., Fritz, M., Tesi, T., Koch, B.P., Haghypour, N., Eglinton, T.I., Strauss, J. and Vonk, J.E. (2021) Permafrost Carbon and CO₂ Pathways Differ at Contrasting Coastal Erosion Sites in the Canadian Arctic. *Front. Earth Sci.* 9:630493. doi: 10.3389/feart.2021.630493
- Terhaar, J., Lauerwald, R., Regnier, P., Gruber, N., and Bopp, L. (2021). Around one third of current Arctic Ocean primary production sustained by rivers and coastal erosion, *Nat. Commun.*, 12, 1–10, <https://doi.org/10.1038/s41467-020-20470-z>
- Turetsky, M. R., Abbott, B. W., Jones, M. C., Anthony, K. W., Olefeldt, D., Schuur, E. A. G., ... & McGuire, A. D. (2020). Carbon release through abrupt permafrost thaw. *Nature Geoscience*, 13(2), 138-143. <https://doi.org/10.1038/s41561-019-0526-0>

- Wang, S., Wang, R., Chen, J., Chen, Z., Cheng, Z., Wang, W., & Huang, Y. (2013). Spatial distribution patterns of GDGTs in the surface sediments from the Bering Sea and Arctic Ocean and their environmental significances. *Advances in Earth Science*, 28(2), 282-296. <https://doi.org/10.11867/j.issn.1001-8166.2013.02.0282>
- Wang, K., Zhang, T., and Yang, D. (2021): Permafrost dynamics and their hydrologic impacts over the Russian Arctic Drainage Basin, *Adv. Clim. Change Res.*, 12, 482–498, <https://doi.org/10.1016/j.accre.2021.03.014>
- Weijers, J. W. H., Schouten, S., Spaargaren, O. C., & Damsté, J. S. S. (2006). Occurrence and distribution of tetraether membrane lipids in soils: Implications for the use of the TEX86 proxy and the BIT index. *Organic Geochemistry*, 37(12), 1680-1690, <https://doi.org/10.1016/j.orggeochem.2006.07.018>
- Wild, B., Andersson, A., Broder, L., Vonk, J. E., Haghypour, N., McClelland, J. W., ... & Gustafsson, Ö. (2019). Rivers across the Siberian Arctic unearth the patterns of carbon release from thawing permafrost. *Proceedings of the National Academy of Sciences*, 116(21), 10280-10285. <https://doi.org/10.1073/pnas.1811797116>
- Zell, C., Kim, J.-H., Balsinha, M., Dorhout, D., Fernandes, C., Baas, M., and Sinninghe Damsté, J. S. (2014): Transport of branched tetraether lipids from the Tagus River basin to the coastal ocean of the Portuguese margin: consequences for the interpretation of the MBT'/CBT paleothermometer, *Biogeosciences*, 11, 5637–5655, <https://doi.org/10.5194/bg-11-5637-2014>
- Zhang, Z.-X., Parlanti, E., Anquetil, C., Morelle, J., Laverman, A. M., Thibault, A., Bou, E., and Huguet, A. (2024): Environmental controls on the distribution of brGDGTs and brGMGTs across the Seine River basin (NW France): implications for bacterial tetraethers as a proxy for riverine runoff, *Biogeosciences*, 21, 2227–2252, <https://doi.org/10.5194/bg-21-2227-2024>

Supplement

Exploring the mysteries of GDGTs in the Arctic: Insights from the Lena Delta and Laptev Sea Nearshore

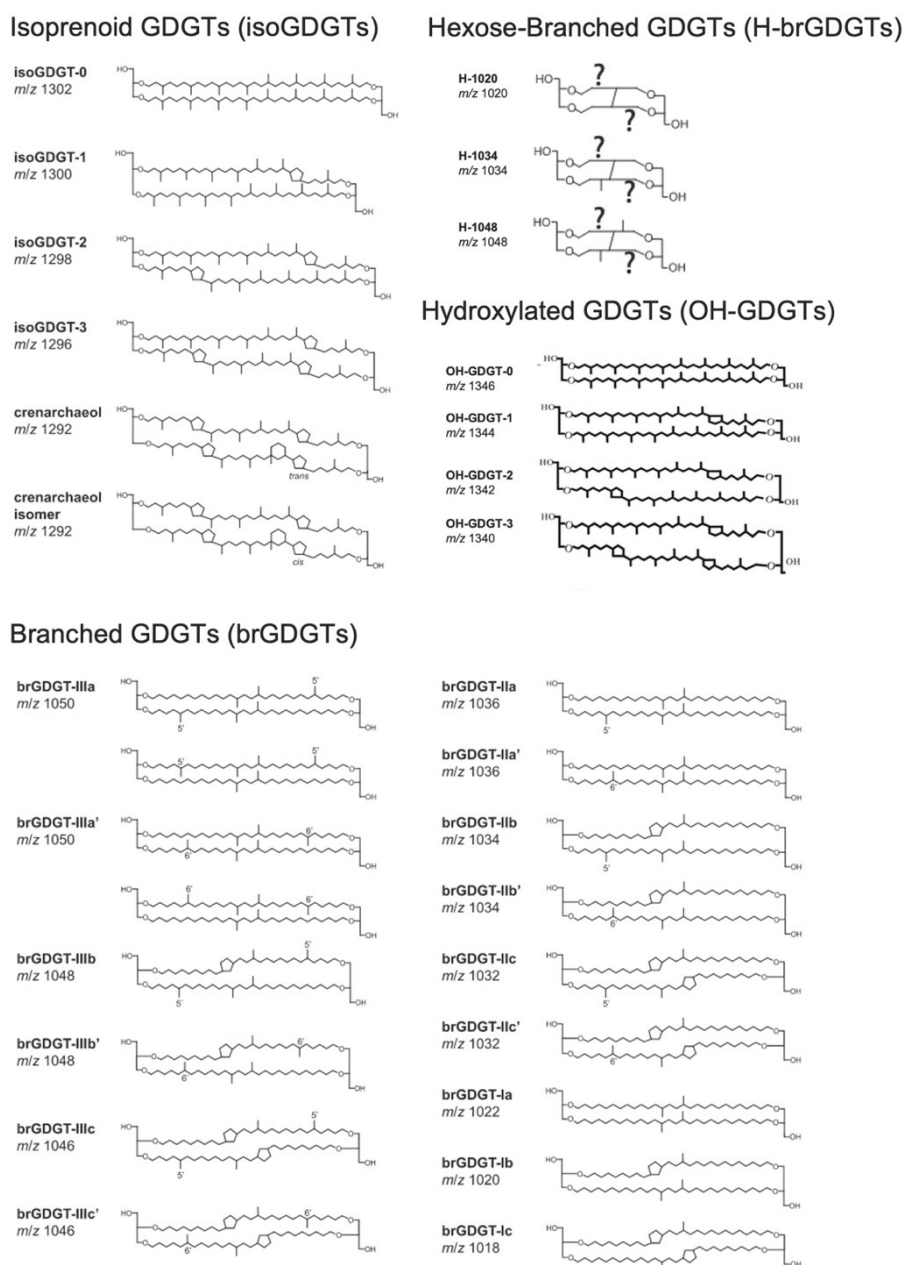


Figure 5-S1. Structures of GDGTs discussed in the text. The exact location of the covalent bond between the two alkyl chains in both H-isoGDGTs and H-brGDGTs is unknown (Naafs et al., 2018).

Table 5-S1. Locations, date, depth and season of sampling collection from different sampling stations.

Station	Latitude	Longitude	Date of sample collection	Depth,m	Sampling area & season
					<i>Winter sampling</i>
CAC19-01	72.50908	129.24791	30.03.2019	11	Lena Delta, 2019
CAC19-02	72.51685	129.54568	29.03.2019	2	Lena Delta, 2019
CAC19-03	72.52538	129.84203	30.03.2019	3	Lena Delta, 2019
CAC19-04	72.52548	129.86385	31.03.2019	3	Lena Delta, 2019
CAC19-23	72.52135	129.69305	31.03.2019	2	Lena Delta, 2019
CAC19-A	72.50127	129.10159	01.04.2019	12	Lena Delta, 2019
CAC19-B	72.47939	128.97108	01.04.2019	5	Lena Delta, 2019
CAC19-C	72.45562	128.84447	02.04.2019	2	Lena Delta, 2019
CAC19-D	72.46153	128.69456	02.04.2019	18	Lena Delta, 2019
CAC19-E	72.50182	128.62968	03.04.2019	3	Lena Delta, 2019
CAC19-F	72.51871	128.49216	03.04.2019	3	Lena Delta, 2019
CAC19-G	72.53542	128.35324	04.04.2019	8	Lena Delta, 2019
CAC19-H	72.56407	128.23865	04.04.2019	3	Lena Delta, 2019
					<i>Summer sampling</i>
LEN19-S-01	72,39936	126.69558	09.08.2019	19	Lena Delta, 2019
LEN19-S-02	72.53733	126.92917	09.08.2019	17	Lena Delta, 2019
LEN19-S-03	72.62711	127.41936	09.08.2019	6	Lena Delta, 2019
LEN19-S-04	72.63353	127.95914	09.08.2019	3	Lena Delta, 2019
LEN19-S-05	72.56378	128.24464	09.08.2019	5	Lena Delta, 2019
LEN19-S-06	72.52108	128.51558	08.08.2019	8	Lena Delta, 2019
LEN19-S-07	72.46139	128.69514	08.08.2019	18	Lena Delta, 2019
LEN19-S-78	72.45311	128.84103	08.08.2019	9	Lena Delta, 2019
LEN19-S-08	72.47706	128.97078	08.08.2019	7	Lena Delta, 2019
LEN19-S-89	72.50167	129.10172	08.08.2019	13	Lena Delta, 2019
LEN19-S-09	72.50897	129.25089	08.08.2019	10	Lena Delta, 2019
CAC19-S-04	72.53014	130.12631	03.08.2019	6	Laptev Sea nearshore, 2019
CAC19-S-05	7253928	130.43433	03.08.2019	12	Laptev Sea nearshore, 2019
CAC19-S-06	7254128	130.72461	03.08.2019	15	Laptev Sea nearshore, 2019

Manuscript 3: Exploring the mysteries of GDGTs in the Arctic: Insights from the Lena Delta and Laptev Sea Nearshore

CAC19-S-07	7255056	131.01814	03.08.2019	18	Laptev Sea nearshore, 2019
CAC19-S-08	72.55447	131.31572	03.08.2019	19	Laptev Sea nearshore, 2019
CAC19-S-09	72.55900	131.60608	03.08.2019	20	Laptev Sea nearshore, 2019
CAC19-S-10	72.55294	131.91447	03.08.2019	20	Laptev Sea nearshore, 2019

Synthesis and Outlook

To synthesize my work, I aim to revisit each manuscript, emphasizing the main findings in the context of the objectives and research questions outlined in Chapter 1.5. Additionally, I will highlight other notable aspects that merit attention. In this chapter, I will draw connections between the three manuscripts presented in this dissertation, exploring their specific nuances while integrating them into a cohesive narrative.

In the first paper, I investigated the transformations of POC during its transport from the Lena River catchment to the delta, focusing on how these processes influence its spatial distribution and concentration. I examined the sources and fate of POC during its transport from the Lena main stem to the delta, highlighting the potentially underexplored role of the delta in POC distribution. This perspective was motivated by the observation that existing studies, such as those relying on ArcticGRO data, are based on stations located far upstream from deltas and estuaries (McClelland et al., 2016; Wild et al., 2019). For example, the ArcticGRO station on the Lena River at Zhigansk is situated approximately 800 km upstream from the delta. I found that POC undergoes significant sedimentation along the river's main stem before it reaches the actual delta. This was not the first time pointing out this dynamic, the part of the Lena River called "Lena pipe" was mentioned in literature before, as well as the Total organic carbon (TOC) decrease downstream the Lena River (Semiletov et al., 2011b), but I have shown how this geomorphological attribute resulted in a substantial decrease in TSM and POC concentrations by the time the water reaches the delta. These reductions, by

approximately 70%, highlight the critical role of sedimentation in shaping the spatial distribution of POC within the system (Q1.1). This finding has provided a strong foundation, helping us to shape hypotheses for subsequent research. In addition to POC dynamics, I also explored the geomorphological characteristics of the Lena River catchment and created a detailed map with its subdivisions (Figure 3-1) being inspired by the study of Kutscher et al. (2017), I analyzed the Lena catchment basins and their varying contributions to TSM within the Lena River system. The main focus of the first paper was to explore the composition of POC in the Lena delta and to compare it with the composition in the river's main stem. Isotopic analyses and its amplification into the end-member model revealed that modern OM, particularly from phytoplankton primary production, dominates in the delta (68%), whereas riverine OM is predominantly derived from Holocene soil OM (56%). My finding on the dominant role of aquatic production in POC aligns with Behnke's (2023) observation, which highlights this phenomenon across major Arctic rivers, reporting a phytoplankton contribution to riverine POM in summer ranging from 46% to 72%. While this data supports my finding that phytoplankton is a key contributor to POC, it also challenges the distinction I observed between the delta and the river, as Behnke's measurements in the river indicate phytoplankton contributions comparable to or exceeding the delta value I reported in 2019 (68%), despite the lower contribution I observed in the river that year (39%).

I showed that deltaic POC was combined with a higher input of ancient permafrost approximately 18%, while in the Lena River main stem, only 5 % of POC was attributed to permafrost-derived organic matter. In the work of Behnke et al., (2023) the contribution of Yedoma to riverine POC (15–30%) significantly exceeded the values reported in my first manuscript. This discrepancy between our works may arise due to several factors: (1) Sampling year—my conclusions are based on data from 2019, emphasizing trends (e.g., the higher contribution of Pleistocene deposits to POC in the

delta compared to the river main stem) rather than absolute values, which can vary from year to year, while Behnke's analysis integrates ArcticGRO data spanning nearly 20 years; (2) Modeling approach—our study used a three-end-member model based on C isotopes, whereas Behnke's study employed Bayesian modeling combining C isotopes and C:N ratios.

Findings from the first manuscript emphasize the dynamic interplay of terrestrial, aquatic, and permafrost-derived sources in shaping the composition of POC as it transitions from the Lena River catchment to the Arctic Ocean (Q1.2). A concrete outcome of our first manuscript was the suggestion that estimating the Lena River's OM discharge to the Arctic coastal zone based solely on data from the river's main stem (e.g., data from the ArcticGRO) may overestimate the load of suspended material while underestimating sedimentation occurring in the lower Lena and its delta. To accurately predict the effects of permafrost changes on coastal waters due to climate change, additional and concurrent sampling from both the river delta and the main stem is essential.

In my second study, I focused on concentrations, sources, and transformation processes of DOC in the Lena delta in winter and summer and additionally demonstrated seasonal differences for POC. I showed that DOC concentrations in winter were higher despite the low-flow conditions (Q2.1). These findings contrast with earlier reports, either Juhls (2020), who observed that DOC concentrations in April (end of the winter season) at Zhigansk and Samoylov Island were the lowest (from 2014 to 2019), or studies reporting similar DOC concentrations in the Lena River in winter and summer (Behnke et al., 2021; Liu et al., 2022). We propose that our results differ from these studies due to the unique hydrology of the Lena Delta, characterised by extensive channel branching and slower water flow (Rachold et al., 1996), which causes spatial variations in DOC concentrations compared to upstream sites like Zhigansk. Furthermore, climatic anomalies in 2019, including warm temperatures and record low water discharge (Arctic GRO, 2024), likely

affected DOC concentrations through reduced flow and enhanced microbial degradation and photo-oxidation (Stolpmann et al., 2022) of permafrost-derived DOC during summer, which is preferentially utilized by microorganisms (Vonk et al., 2013a, b; Mann et al., 2015).

Isotopic composition of winter DOC reflected contributions from deeper soil layers and aged organic matter, as indicated by more depleted in ^{14}C . This observation aligns with some previous studies (Wild et al., 2019; Liu et al., 2022). The unambiguous interpretation of $\Delta^{14}\text{C}$ signals for DOC remains challenging due to the complex mixture of sources shaping the $\Delta^{14}\text{C}$ signature. Specifically, winter depletion may result from contributions of aged groundwater draining permafrost taliks (Amon et al., 2012; Behnke et al., 2021), seasonally pooled waters from the Vilui (Juhls et al., 2020; Tananaev et al., 2016b) reservoir, or a combination of both. In summer, DOC was enriched in ^{14}C and predominantly derived from modern organic carbon sources, such as plant debris from the post-1950s period and active layer inputs during thaw periods (Q2.2). Plants growing during that time were enriched in ^{14}C due to nuclear bomb testing, and $\Delta^{14}\text{C}$ values have remained above 0 until recent days. This pattern should be considered when studying the age and composition of DOC, as the active layer deepens and permafrost thaws, the ^{14}C signatures in DOC leached from these layers may initially increase and only begin to decrease when older permafrost organic matter accumulated before 1950 is released.

POC concentrations, as anticipated based on previous studies and data (McClelland et al., 2016), were significantly higher in summer, driven by greater contributions from suspended particles of terrestrial and aquatic origins, including phytoplankton, influenced by increased water flow and sediment transport (Q2.1). POC also displayed seasonal shifts in composition, with a stronger terrestrial signal in winter compared to summer, which, as known from my previous study, has major contributions from aquatic

productivity. These findings underscore the importance of seasonal sampling to fully capture the complexity of organic carbon dynamics in Arctic deltas.

Finally, in my third study, I investigated the seasonal and spatial distribution patterns of glycerol dialkyl glycerol tetraethers (GDGTs) in the Lena delta and the Laptev Sea nearshore zone. Focusing on their occurrence in POM, I examined how Arctic rivers influence the composition of GDGTs and their response to environmental changes. IsoGDGTs and OH-GDGTs were largely absent in the delta but increased seaward, correlating with salinity (Q3.1) which aligned with previous studies (Park et al., 2014; Damsté et al., 2022). This trend highlights the influence of salinity on their distribution and the transition from freshwater to marine conditions. TEX₈₆L-derived temperatures aligned well with in-situ summer data in the nearshore zone but underestimated winter temperatures in the freshwater delta, indicating limited thaumarchaeal activity under low-salinity conditions.

BrGDGTs and H-brGDGTs showed distinct seasonal and spatial patterns, with brGDGT concentrations decreasing from the delta to the Laptev nearshore zone (Q3.1). Winter samples exhibited higher relative brGDGT concentrations normalized to POC, reflecting enhanced soil-derived contributions under low aquatic production. H-brGDGTs, often associated with peat (Naafs et al., 2018), revealed a secondary accumulation peak in nearshore bottom sediments. This pattern suggests enhanced flocculation and deposition of peat-derived material in saline environments, contributing to the "estuarine filter" effect (Q3.2).

One of the most significant outcomes of my study is a distinct Arctic river signature for GDGTs, particularly in the suspended particulate matter (SPM) of the Lena delta. I observed the predominance of 5-methyl brGDGT isomers and the dominance of 6-methyl brGDGTs isomers in Lena delta SPM. The predominance of (e.g., IIIa and IIa) also

observed by Kusch et al. in the Lena delta soils (Kusch et al., 2019) together with the dominance of 6-methyl brGDGT isomers (e.g., IIIa' and IIa'), both characteristic of Arctic terrestrial environments, together suggest a unique combination of cold-climate adaptation and pH-driven microbial production mechanisms (De Jonge et al., 2014; Peterse et al., 2014; Kusch et al., 2019). This pattern aligns with previous observations from the Yenisei River (De Jonge et al., 2014, 2015), indicating that microbial production of 6-methyl brGDGTs is widespread in large Arctic river systems.

The elevated abundances of 6-methyl brGDGTs in SPM, compared to terrestrial sources such as permafrost deposits, point to in-situ bacterial production within the freshwater system under neutral to slightly alkaline conditions (De Jonge et al., 2014). These results emphasize the influence of riverine processes, particularly in shaping the composition and distribution of GDGTs in Arctic waters as demonstrated in the third manuscript using a ternary diagram (Figure 5-7) that illustrates the methylation composition of brGDGTs in the analyzed samples from this research alongside previously studied samples. The unique brGDGT signature in the Lena delta SPM not only reflects the environmental conditions of the delta but also represents a broader characteristic of Arctic river systems, distinguishing them from non-Arctic environments.

Taken together, the three manuscripts presented in this dissertation, along with the three co-authored publications in the appendix, provide a cohesive exploration of the dynamics of organic matter in the Lena delta. By integrating these findings, this dissertation directly addresses critical questions in permafrost carbon research, particularly regarding the contribution of permafrost to carbon release, sources and the fate of that carbon. The first manuscript identifies the major sources of POC, uncovers the dominance of aquatic primary production as POC source, highlights the elevated contribution of Yedoma-origin OC to POM in the delta compared to the river main stem, and establishes the delta's critical role in sedimentation processes, which controls the

Synthesis and Outlook

distribution of permafrost-derived carbon. The second manuscript demonstrates the seasonal variability of DOC and POC, showing that winter conditions have elevated DOC concentrations. The third manuscript further explores the seasonal dynamics of OM and examines the freshwater-marine transition influence on OM distribution. It reveals a higher relative input of soil-derived organic matter in winter through biomarker analysis and illustrates the complex interactions between temperature, salinity, and organic matter sources in driving the seasonal and spatial distribution of GDGTs. Thus, the isotopic and biomarker evidence presented in this work identifies the distribution and sources of OM in the Lena delta, highlights aged permafrost contributions, and demonstrates the role of microbial indicators in shaping organic carbon fluxes across Arctic aquatic ecosystems.

Together, my studies illuminate the critical role of river deltas (with the Lena Delta as an example), as a biogeochemical transition zone, bridging riverine and coastal ecosystems. These results contribute to a deeper understanding of how deltaic processes mediate the release and transformation of particulate and dissolved organic carbon, offering a more nuanced perspective on carbon cycling and potentially refining predictive models of permafrost carbon release under future climate scenarios. Building on the findings of this dissertation, future research should prioritise multi-site sampling across the river main stem, delta, and nearshore environments to better capture the spatial dynamics of organic matter. This is crucial because relying solely on the main stem data may lead to overestimating TSM load while underestimating sedimentation in the lower course and in the delta. The increased contributions of ancient organic matter, such as Yedoma-derived material, under specific conditions in the deltaic ecosystem further underscore the pivotal role of Arctic deltas in estimating permafrost carbon dynamics. In addition to spatial sampling, future studies should include winter measurements alongside summer observations to better account for seasonal variability. Ignoring winter processes may

Synthesis and Outlook

lead to an incomplete understanding of permafrost carbon discharge. Finally, further research could explore the response of permafrost ecosystems to hydrological and climatic extremes, such as the record-low discharge observed in 2019. This may provide valuable insights into carbon dynamics during crises that are bound to intensify with a changing climate, leaving the fragile Arctic ever more vulnerable to their impact.

Acknowledgements

When I thought about writing my thesis, I always imagined this part. The idea of reflecting on the entire journey motivated me to move forward. And now, here I am—ready to look back and honor the path I've walked. From my arrival on that last night of July in Bremerhaven, through the Arctic's vast expanse, to this last night of autumn in Berlin, as I finish my thesis. With this chapter, I express my deepest appreciation—to the journey itself and to the people who have been part of it.

First of all, I want to express my endless gratitude to my extraordinary supervisors tandem: to Prof. Dr. Gesine Mollenhauer and Dr. Jens Strauss, whose scientific expertise, visionary ideas, constant support on my way and patience fueled my work! Gesine, you are an absolutely inspiring person to me, being exceptionally professional, determined and motivating mentor and deeply caring, guiding and open to Pelmeny in night St. Petersburg, adventurous ally, thank you! Thank you, Jens, for being the greatest "Nachalnic", for your Arctic field spirit and the working group you have built in Potsdam - the bonded community of aspiring young Arctic researchers. During the toughest time of my journey, when I was doubting, my supervisors believed in me.

I want to say a special thanks to Jens Hefter, who can turn the toxic lab environment into warm greenhouse, where we PhDs cultivate our research like flowers. Thanks to the entire Bremerhaven team for assistance and insights sharing: Torben Gentz, Bingbing Wei, Laura Kattein, Hendrik Grotheer, Liz Bonk, Malte Höhn. Many thanks to POLMAR ladies Claudia & Claudia, always willing to help and accompany in the Alps.

I was very lucky to investigate the Arctic ice fields and coast with Matthias Fuchs, Tina Sanders, Juri Palmtag & Jens Strauss. Thank you for this, sometimes wet, sometimes

Acknowledgements

cold, most of the time windy and an absolutely breath-taking experience! Thanks to Volkmar Assmann & Waldemar Schneider for organizing the expeditions to the middle of Nowhere.

I am deeply grateful to Prof. Dr. Cindy De Jonge for agreeing to review my thesis. I truly appreciate your time and effort, as well as the assistance from Uni Bremen for providing the venue for my defence.

I would like to say many many many thanks to the people whose presence made my PhD journey even more meaningful and at times very joyful. Thanks to those with whom I used to split the day into "before" and "after" lunch by eating a cake/chocolate/cookie during my stay at Bremerhaven - thank you "the Lunch Group" (Mariano, Sara, Eduardo, Lukas, Spela, Cote, Onur, Bimo, Mica, Manu and others), thanks to Bremen chikas – JC & Jenna, and Michael Angelopoulos for bringing humour to Potsdam. Special thanks to Mariano Martinez for Amigoschaft, Sara Schlagenhauff for the heat waves in the middle of June and especial thank to Manuel Ruben for the company on trails and beyond.

Thanks so much to my old friends: to Sofiya Bondarenko for being my friend through all of our adulthood, and to Polina, Galina, Anna, Slava, Pasha, Boris, and many more.

With all my heart, thank you to my sister and her husband, Polina and Karim Kanj, for being my warmth and serenity, and for giving me the feeling of home. Thanks to Ayra Ogneva for teaching me patience, acceptance and to listen to my true self. At the end, I want to say thank you to my mom and dad for always being on my side, no matter what, and a loving thank you to my beloved grandmother, who has been my nurturer, my supporter, my advocate, and my dearest companion in childhood and always.

References

This reference list includes the references of the chapters 1,2 and 6. The manuscript's references are given in the respective chapter separately.

- Amon, R. M. W., Rinehart, A. J., Duan, S., Louchouart, P., Prokushkin, A., Guggenberger, G., Bauch, D., Stedmon, C., Raymond, P. A., Holmes, R. M., McClelland, J. W., Peterson, B. J., Walker, S. A., & Zhulidov, A. V. (2012). Dissolved organic matter sources in large Arctic rivers. *Geochimica et Cosmochimica Acta*, 94, 217–237. <https://doi.org/10.1016/j.gca.2012.07.015>
- Atkinson, D. E. (2005). Observed storminess patterns and trends in the circum-Arctic coastal regime. *Geo-Marine Letters*, 25(2–3), 98–109. <https://doi.org/10.1007/s00367-004-0191-0>
- Back, D.-Y., Ha, S.-Y., Else, B., Hanson, M., Jones, S. F., Shin, K.-H., Tatarek, A., Wiktor, J. M., Cicek, N., Alam, S., & Mundy, C. J. (2021). On the impact of wastewater effluent on phytoplankton in the Arctic coastal zone: A case study in the Kitikmeot Sea of the Canadian Arctic. *Science of the Total Environment*, 764, 143861. <https://doi.org/10.1016/j.scitotenv.2020.143861>
- Behnke, M. I., McClelland, J. W., Tank, S. E., Kellerman, A. M., Holmes, R. M., Haghypour, N., Eglinton, T. I., Raymond, P. A., Suslova, A., Zhulidov, A. V., Gurtovaya, T., Zimov, N., Zimov, S., Mutter, E. A., Amos, E., & Spencer, R. G. M. (2021). Pan-Arctic Riverine Dissolved Organic Matter: Synchronous Molecular Stability, Shifting Sources and Subsides. *Global Biogeochemical Cycles*, 35(4), e2020GB006871. <https://doi.org/10.1029/2020GB006871>
- Behnke, M. I., Tank, S. E., McClelland, J. W., Holmes, R. M., Haghypour, N., Eglinton, T. I., Raymond, P. A., Suslova, A., Zhulidov, A. V., Gurtovaya, T., Zimov, N., Zimov, S., Mutter, E. A., Amos, E., & Spencer, R. G. M. (2023). Aquatic biomass is a major source to particulate organic matter export in large Arctic rivers. *Proceedings of the National Academy of Sciences*, 120(12), e2209883120. <https://doi.org/10.1073/pnas.2209883120>
- Bobrovitskaya, N. N., Kokorev, A. V., & Lemeshko, N. A. (2003). Regional patterns in recent trends in sediment yields of Eurasian and Siberian rivers. *Global and Planetary Change*, 39(1–2), 127–146. [https://doi.org/10.1016/S0921-8181\(03\)00021-3](https://doi.org/10.1016/S0921-8181(03)00021-3)
- Bring, Arvid & Shiklomanov, Alexander & Lammers, Richard. (2016). Pan-Arctic river discharge: prioritizing monitoring of future climate change hot spots: Pan-Arctic river discharge monitoring. *Earth's Future*. 5. 10.1002/2016EF000434.
- Bristol, E. M., Behnke, M. I., Spencer, R. G. M., McKenna, A., Jones, B. M., Bull, D. L., & McClelland, J. W. (2024). Eroding Permafrost Coastlines Release Biodegradable Dissolved Organic Carbon to the Arctic Ocean. *Journal of Geophysical Research: Biogeosciences*, 129(7), e2024JG008233. <https://doi.org/10.1029/2024JG008233>
- Charkin, A. N., Dudarev, O. V., Semiletov, I. P., Kruhmalev, A. V., Vonk, J. E., Sánchez-García, L., Karlsson, E., & Gustafsson, Ö. (2011). Seasonal and interannual variability of sedimentation and organic matter distribution in the Buor-Khaya Gulf: The primary recipient of input from Lena River and coastal erosion in the southeast Laptev Sea. *Biogeosciences*, 8(9), 2581–2594. <https://doi.org/10.5194/bg-8-2581-2011>
- Clark, I. D., Lauriol, B., Harwood, L., & Marschner, M. (2001). Groundwater Contributions to Discharge in a Permafrost Setting, Big Fish River, N.W.T., Canada. *Arctic, Antarctic, and Alpine Research*, 33(1), 62–69. <https://doi.org/10.1080/15230430.2001.12003405>

References

- Connolly, C. T., Cardenas, M. B., McClelland, J. W., Burkart, G. A., & Spencer, R. G. M. (n.d.). Groundwater as a major source of dissolved organic matter to Arctic coastal waters. *Nature Communications*, (2020), 1–8. <https://doi.org/10.1038/s41467-020-15250-8>
- Damsté, J. S., Warden, L. A., Berg, C., Jürgens, K., & Moros, M. (2022). Evaluation of the distributions of hydroxylated glycerol dibiphytanyl glycerol tetraethers (GDGTs) in Holocene Baltic Sea sediments for reconstruction of sea surface temperature: The effect of changing salinity. *Climate of the Past*, 18(10), 2271–2288. <https://doi.org/10.5194/cp-18-2271-2022>
- De Jonge, C., Stadnitskaia, A., Hopmans, E. C., Cherkashov, G., Fedotov, A., & Sinninghe Damsté, J. S. (2014). In situ produced branched glycerol dialkyl glycerol tetraethers in suspended particulate matter from the Yenisei River, Eastern Siberia. *Geochimica et Cosmochimica Acta*, 125, 476–491. <https://doi.org/10.1016/j.gca.2013.10.031>
- De Jonge, C., Stadnitskaia, A., Hopmans, E. C., Cherkashov, G., Fedotov, A., Streletskaia, I. D., Vasiliev, A. A., & Sinninghe Damsté, J. S. (2015). Drastic changes in the distribution of branched tetraether lipids in suspended matter and sediments from the Yenisei River and Kara Sea (Siberia): Implications for the use of brGDGT-based proxies in coastal marine sediments. *Geochimica et Cosmochimica Acta*, 165, 200–225. <https://doi.org/10.1016/j.gca.2015.05.044>
- Derrien, M., Cabrera, F. A., Tavera, N. L. V., Kantún Manzano, C. A., & Vizcaino, S. C. (2015). Sources and distribution of organic matter along the Ring of Cenotes, Yucatan, Mexico: Sterol markers and statistical approaches. *Science of The Total Environment*, 511, 223–229. <https://doi.org/10.1016/j.scitotenv.2014.12.053>
- Derrien, M., Kim, M.-S., Ock, G., Hong, S., Cho, J., Shin, K.-H., & Hur, J. (2018). Estimation of different source contributions to sediment organic matter in an agricultural-forested watershed using end member mixing analyses based on stable isotope ratios and fluorescence spectroscopy. *Science of The Total Environment*, 618, 569–578. <https://doi.org/10.1016/j.scitotenv.2017.11.067>
- Dethier, M. N., & Harper, J. (2012). Classes of Nearshore Coasts. In *Treatise on Estuarine and Coastal Science* (Vol. 1). <https://doi.org/10.1016/B978-0-12-374711-2.00105-4>
- Dittmar, T., & Kattner, G. (2003). The biogeochemistry of the river and shelf ecosystem of the Arctic Ocean: A review. *Marine Chemistry*, 83(3–4), 103–120. [https://doi.org/10.1016/S0304-4203\(03\)00105-1](https://doi.org/10.1016/S0304-4203(03)00105-1)
- Ewing, S. A., O'Donnell, J. A., Aiken, G. R., Butler, K., Butman, D., Windham-Myers, L., & Kanevskiy, M. Z. (2015). Long-term anoxia and release of ancient, labile carbon upon thaw of Pleistocene permafrost. *Geophysical Research Letters*, 42(24), 10,730–10,738. <https://doi.org/10.1002/2015GL066296>
- Feng, D., Gleason, C. J., Lin, P., Yang, X., Pan, M., & Ishitsuka, Y. (2021). Recent changes to Arctic river discharge. *Nature Communications*, 12(1), 6917. <https://doi.org/10.1038/s41467-021-27228-1>
- Forbes, D. L. (editor). (2011). State of the Arctic Coast 2010 Scientific Review and Outlook. In *State of the Arctic Coast 2010: Scientific review and outlook*.
- Forryan, A., Bacon, S., Tsubouchi, T., Torres-Valdés, S., & Naveira Garabato, A. C. (2019). Arctic freshwater fluxes: Sources, tracer budgets and inconsistencies. *The Cryosphere*, 13(8), 2111–2131. <https://doi.org/10.5194/tc-13-2111-2019>
- French HM: The periglacial environment. Edited by John Wiley, 3rd edition; 2007
- Brown J, Ferrians OJ, Heginbottom JA, Melnikov ES (Eds): Circum-arctic map of permafrost and ground ice conditions. Circum-pacific map series. Edited by the US Geological Survey; 2001.
- Frey, K. E., & McClelland, J. W. (2009). Impacts of permafrost degradation on arctic river biogeochemistry. *Hydrological Processes*, 23(1), 169–182. <https://doi.org/10.1002/hyp.7196>
- Gordeev, V. V. (2006). Fluvial sediment flux to the Arctic Ocean. *Geomorphology*, 80(1–2), 94–104. <https://doi.org/10.1016/j.geomorph.2005.09.008>

References

- Guay, C. K. H., Falkner, K. K., Muench, R. D., Mensch, M., Frank, M., & Bayer, R. (2001). Wind-driven transport pathways for Eurasian Arctic river discharge. *Journal of Geophysical Research: Oceans*, 106(C6), 11469–11480. <https://doi.org/10.1029/2000jc000261>
- Haugk, C., Jongejans, L. L., Mangelsdorf, K., Fuchs, M., Ogneva, O., Palmtag, J., Mollenhauer, G., Mann, P. J., Overduin, P. P., Grosse, G., Sanders, T., Tuerena, R. E., Schirmeister, L., Wetterich, S., Kizyakov, A., Karger, C., & Strauss, J. (2022). Organic matter characteristics of a rapidly eroding permafrost cliff in NE Siberia (Lena Delta, Laptev Sea region). *Biogeosciences*, 19(7), 2079–2094. <https://doi.org/10.5194/bg-19-2079-2022>
- Holmes, R. M., Peterson, B. J., Gordeev, V. V., Zhulidov, A. V., Meybeck, M., Lammers, R. B., & Vorosmarty, C. J. (2000). Flux of nutrients from Russian rivers to the Arctic Ocean : Can we establish a baseline against which to judge future changes, 2309–2320.
- Holmes, R. M.; Shiklomanov, A. I.; Suslova, A.; Tretiakov, M.; McClelland, J. W.; Scott, L.; Spencer, R. G. M.; Tank, S. E. (2021). River Discharge. NOAA Technical Report OAR ARC ; 21-11, doi: <https://doi.org/10.25923/zevf-ar65>
- Hugelius, G., Strauss, J., Zubrzycki, S., Harden, J. W., Schuur, E. A. G., Ping, C.-L., Schirmeister, L., Grosse, G., Michaelson, G. J., Koven, C. D., O'Donnell, J. A., Elberling, B., Mishra, U., Camill, P., Yu, Z., Palmtag, J., & Kuhry, P. (2014). Estimated stocks of circumpolar permafrost carbon with quantified uncertainty ranges and identified data gaps. *Biogeosciences*, 11(23), 6573–6593. <https://doi.org/10.5194/bg-11-6573-2014>
- ICARP-II. 2007. Arctic Research: a Global Responsibility - An Overview of the Second International Conference on Arctic Research Planning. ICARP II Steering Group, ICARP II Secretariat, Danish Polar Centre, Copenhagen, Denmark. (Summary and Science Plans now available at http://aosb.arcticportal.org/icarp_ii/index.html; accessed 2011-03-31).
- IPCC, 2021: Climate Change 2021: The Physical Science Basis. Contribution of Working Group I to the Sixth Assessment Report of the Intergovernmental Panel on Climate Change [Masson-Delmotte, V., P. Zhai, A. Pirani, S.L. Connors, C. Péan, S. Berger, N. Caud, Y. Chen, L. Goldfarb, M.I. Gomis, M. Huang, K. Leitzell, E. Lonnoy, J.B.R. Matthews, T.K. Maycock, T. Waterfield, O. Yelekçi, R. Yu, and B. Zhou (eds.)]. Cambridge University Press, Cambridge, United Kingdom and New York, NY, USA, 3949 pp. doi:10.1017/9781009157896
- Jones, B. M., Irrgang, A. M., Farquharson, L. M., Lantuit, H., Whalen, D., Ogorodov, S., Grigoriev, M., Tweedie, C., Gibbs, A. E., Strzelecki, M. C., Baranskaya, A., Belova, N., Sinitsyn, A., Kroon, A., Maslakov, A., Vieira, G., Grosse, G., Overduin, P., Nitze, I., ... Romanovsky, V. E. (n.d.). Arctic Report Card 2020: Coastal Permafrost Erosion. Retrieved November 20, 2024, from <https://repository.library.noaa.gov/view/noaa/27897>
- Jong, D., Bröder, L., Tanski, G., Fritz, M., Lantuit, H., Tesi, T., Haghipour, N., Eglinton, T. I., & Vonk, J. E. (2020). Nearshore Zone Dynamics Determine Pathway of Organic Carbon From Eroding Permafrost Coasts. *Geophysical Research Letters*, 47(15), e2020GL088561. <https://doi.org/10.1029/2020GL088561>
- Juhls, B., Stedmon, C. A., Morgenstern, A., Meyer, H., Hölemann, J., Heim, B., Povazhnyi, V., & Overduin, P. P. (2020). Identifying Drivers of Seasonality in Lena River Biogeochemistry and Dissolved Organic Matter Fluxes. *Frontiers in Environmental Science*, 8, 53. <https://doi.org/10.3389/fenvs.2020.00053>
- Krumpen, T., Belter, H.J., Boetius, A. et al. Arctic warming interrupts the Transpolar Drift and affects long-range transport of sea ice and ice-rafted matter. *Sci Rep* 9, 5459 (2019). <https://doi.org/10.1038/s41598-019-41456-y>
- Kusch, S., Winterfeld, M., Mollenhauer, G., Höfle, S. T., Schirmeister, L., Schwamborn, G., & Rethemeyer, J. (2019). Glycerol dialkyl glycerol tetraethers (GDGTs) in high latitude Siberian permafrost: Diversity, environmental controls, and implications for proxy applications. *Organic Geochemistry*, 136, 103888. <https://doi.org/10.1016/j.orggeochem.2019.06.009>

References

- Kutscher, L., Mörth, C., Porcelli, D., Hirst, C., Maximov, T. C., Petrov, R. E., & Andersson, P. S. (2017). Spatial variation in concentration and sources of organic carbon in the Lena River, Siberia. *Journal of Geophysical Research: Biogeosciences*, 122(8), 1999–2016. <https://doi.org/10.1002/2017JG003858>
- Lantuit, H., Overduin, P. P., Couture, N., Wetterich, S., Aré, F., Atkinson, D., Brown, J., Cherkashov, G., Drozdov, D., Forbes, D. L., Graves-Gaylord, A., Grigoriev, M., Hubberten, H.-W., Jordan, J., Jorgenson, T., Ødegård, R. S., Ogorodov, S., Pollard, W. H., Rachold, V., ... Vasiliev, A. (2012). The Arctic Coastal Dynamics Database: A New Classification Scheme and Statistics on Arctic Permafrost Coastlines. *Estuaries and Coasts*, 35(2), 383–400. <https://doi.org/10.1007/s12237-010-9362-6>
- Lewis, K. M., Dijken, G. L. Van, & Arrigo, K. R. (2020). Changes in phytoplankton concentration now drive increased Arctic Ocean primary production. *202(July)*, 198–202.
- Liu, S., Wang, P., Huang, Q., Yu, J., Pozdniakov, S. P., & Kazak, E. S. (2022). Seasonal and spatial variations in riverine DOC exports in permafrost-dominated Arctic river basins. *Journal of Hydrology*, 612, 128060. <https://doi.org/10.1016/j.jhydrol.2022.128060>
- Ma, Q., Jin, H., Yu, C., & Bense, V. F. (2019). Dissolved organic carbon in permafrost regions: A review. *Science China Earth Sciences*, 62(2), 349–364. <https://doi.org/10.1007/s11430-018-9309-6>
- Mann, P. J., Eglinton, T. I., McIntyre, C. P., Zimov, N., Davydova, A., Vonk, J. E., Holmes, R. M., & Spencer, R. G. M. (2015). Utilization of ancient permafrost carbon in headwaters of Arctic fluvial networks. *Nature Communications*, 6(1), 7856. <https://doi.org/10.1038/ncomms8856>
- Mann, P. J., Strauss, J., Palmtag, J., Dowdy, K., Ogneva, O., Fuchs, M., Bedington, M., Torres, R., Polimene, L., Overduin, P., Mollenhauer, G., Grosse, G., Rachold, V., Sobczak, W. V., Spencer, R. G. M., & Juhls, B. (2022). Degrading permafrost river catchments and their impact on Arctic Ocean nearshore processes. *Ambio*, 51(2), 439–455. <https://doi.org/10.1007/s13280-021-01666-z>
- McClelland, J. W., De, S. J., Peterson, B. J., Holmes, R. M., & Wood, E. F. (2006). A pan-arctic evaluation of changes in river discharge during the latter half of the 20th century. *33*, 2–5. <https://doi.org/10.1029/2006GL025753>
- McClelland, J. W., Holmes, R. M., Peterson, B. J., Raymond, P. A., Striegl, R. G., Zhulidov, A. V., Zimov, S. A., Zimov, N., Tank, S. E., Spencer, R. G. M., Staples, R., Gurtovaya, T. Y., & Griffin, C. G. (2016). Particulate organic carbon and nitrogen export from major Arctic rivers. *Global Biogeochemical Cycles*, 30(5), 629–643. <https://doi.org/10.1002/2015GB005351>
- Naafs, B. D. A., McCormick, D., Inglis, G. N., & Pancost, R. D. (2018). Archaeal and bacterial H-GDGTs are abundant in peat and their relative abundance is positively correlated with temperature. *Geochimica et Cosmochimica Acta*, 227, 156–170. <https://doi.org/10.1016/j.gca.2018.02.025>
- National Snow and Ice Data Center (NSIDC), 2023. How does Arctic sea ice loss affect coastlines? Available at: <https://nsidc.org/learn/ask-scientist/how-does-arctic-sea-ice-loss-affect-coastlines>. Accessed 11 November 2024.
- Nielsen, D. M., Dobrynin, M., Baehr, J., Razumov, S., & Grigoriev, M. (2020). Coastal Erosion Variability at the Southern Laptev Sea Linked to Winter Sea Ice and the Arctic Oscillation. *Geophysical Research Letters*, 47(5), e2019GL086876. <https://doi.org/10.1029/2019GL086876>
- Obu, J., Westermann, S., Bartsch, A., Berdnikov, N., Christiansen, H. H., Dashtseren, A., Delaloye, R., Elberling, B., Etzelmüller, B., Kholodov, A., Khomutov, A., Kääb, A., Leibman, M. O., Lewkowicz, A. G., Panda, S. K., Romanovsky, V., Way, R. G., Westergaard-Nielsen, A., Wu, T., ... Zou, D. (2019). Northern Hemisphere permafrost map based on TTOP modelling for 2000–2016 at 1 km² scale. *Earth-Science Reviews*, 193, 299–316. <https://doi.org/10.1016/j.earscirev.2019.04.023>
- Ogneva, O., Mollenhauer, G., Juhls, B., Sanders, T., Palmtag, J., Fuchs, M., Grotheer, H., Mann, P. J., & Strauss, J. (2023). Particulate organic matter in the Lena River and its delta: From the permafrost catchment to the Arctic Ocean. *Biogeosciences*, 20(7), 1423–1441. <https://doi.org/10.5194/bg-20-1423-2023>

References

- Oliva, M., & Fritz, M. (2018). Permafrost degradation on a warmer Earth: Challenges and perspectives. *Current Opinion in Environmental Science & Health*, 5, 14–18. <https://doi.org/10.1016/j.coesh.2018.03.007>
- Opsahl, S., Benner, R., & Amon, R. M. W. (1999). Major flux of terrigenous dissolved organic matter through the Arctic Ocean. *Limnology and Oceanography*, 44(8), 2017–2023. <https://doi.org/10.4319/lo.1999.44.8.2017>
- Osadchiev, A. A., Pisareva, M. N., Spivak, E. A., Shchuka, S. A., & Semiletov, I. P. (2020). Freshwater transport between the Kara , Laptev , and East - Siberian seas. *Scientific Reports*. <https://doi.org/10.1038/s41598-020-70096-w>
- Park, Y.-H., Yamamoto, M., Nam, S.-I., Irino, T., Polyak, L., Harada, N., Nagashima, K., Khim, B.-K., Chikita, K., & Saitoh, S.-I. (2014). Distribution, source and transportation of glycerol dialkyl glycerol tetraethers in surface sediments from the western Arctic Ocean and the northern Bering Sea. *Marine Chemistry*, 165, 10–24. <https://doi.org/10.1016/j.marchem.2014.07.001>
- Peterse, F., Vonk, J. E., Holmes, R. M., Giosan, L., Zimov, N., & Eglinton, T. I. (2014). Branched glycerol dialkyl glycerol tetraethers in Arctic lake sediments: Sources and implications for paleothermometry at high latitudes: Branched GDGTs in Arctic lakes. *Journal of Geophysical Research: Biogeosciences*, 119(8), 1738–1754. <https://doi.org/10.1002/2014JG002639>
- Rachold, V., Alabyan, A., Hubberten, H.-W., Korotaev, V. N., & Zaitsev, A. A. (1996). Sediment transport to the Laptev Sea? hydrology and geochemistry of the Lena River. *Polar Research*, 15(2), 183–196. <https://doi.org/10.1111/j.1751-8369.1996.tb00468.x>
- Rachold, V., Grigoriev, M. N., Are, F. E., Solomon, S., Reimnitz, E., Kassens, H., & Antonow, M. (2000). Coastal erosion vs riverline sediment discharge in the Arctic shelf seas. *International Journal of Earth Sciences*, 89(3), 450–460. <https://doi.org/10.1007/s005310000113>
- Rantanen, M., Karpechko, A. Yu., Lipponen, A., Nordling, K., Hyvärinen, O., Ruosteenoja, K., Vihma, T., & Laaksonen, A. (2022). The Arctic has warmed nearly four times faster than the globe since 1979. *Communications Earth & Environment*, 3(1), 168. <https://doi.org/10.1038/s43247-022-00498-3>
- Schuur, E. A. G., Abbott, B. W., Commane, R., Ernakovich, J., Euskirchen, E., Hugelius, G., ... Turetsky, M. (2022). Permafrost and climate change: Carbon cycle feedbacks from the warming Arctic. *Annual Review of Environment and Resources*, 47, 343–371. <https://doi.org/10.1146/annurev-environ-012220-011847>
- Schuur, E. A. G., McGuire, A. D., Schädel, C., Grosse, G., Harden, J. W., Hayes, D. J., ... Vonk, J. E. (2015). Climate change and the permafrost carbon feedback. *Nature*, 520(7546), 171–179. <https://doi.org/10.1038/nature14338>
- Semiletov, I. P., Pipko, I. I., Shakhova, N. E., Dudarev, O. V., Pugach, S. P., Charkin, A. N., McRoy, C. P., Kosmach, D., & Gustafsson, Ö. (2011). Carbon transport by the Lena River from its headwaters to the Arctic Ocean, with emphasis on fluvial input of terrestrial particulate organic carbon vs. Carbon transport by coastal erosion. *Biogeosciences*, 8(9), 2407–2426. <https://doi.org/10.5194/bg-8-2407-2011>
- Shiklomanov, A., Déry, S., Tretiakov, M., Yang, D., Magritsky, D., Georgiadi, A., & Tang, W. (2021). River Freshwater Flux to the Arctic Ocean. In D. Yang & D. L. Kane (Eds.), *Arctic Hydrology, Permafrost and Ecosystems* (pp. 703–738). Springer International Publishing. https://doi.org/10.1007/978-3-030-50930-9_24
- Stolpmann, L., Mollenhauer, G., Morgenstern, A., Hammes, J. S., Boike, J., Overduin, P. P., & Grosse, G. (2022). Origin and Pathways of Dissolved Organic Carbon in a Small Catchment in the Lena River Delta. *Frontiers in Earth Science*, 9, 759085. <https://doi.org/10.3389/feart.2021.759085>
- Strauss, J., Abbott, B., Hugelius, G., Schuur, E. A. G., Treat, C., Fuchs, M., Schädel, C., Ulrich, M., Turetsky, M. R., Keuschnig, M., Biasi, C., Yang, Y., and Grosse, G. (2021a). Permafrost, in: *Recarbonizing global soils – A technical manual of recommended management practices*, edited by: Food and Agriculture

References

- Organization of the United Nations (FAO), FAO, Rome, Italy, 127–147, ISBN: 978-92-5-134838-3, <https://doi.org/10.4060/cb6386en>
- Strauss, J., Biasi, C., Sanders, T., Abbott, B. W., Von Deimling, T. S., Voigt, C., Winkel, M., Marushchak, M. E., Kou, D., Fuchs, M., Horn, M. A., Jongejans, L. L., Liebner, S., Nitzbon, J., Schirrmeister, L., Walter Anthony, K., Yang, Y., Zubrzycki, S., Laboor, S., ... Grosse, G. (2022). A globally relevant stock of soil nitrogen in the Yedoma permafrost domain. *Nature Communications*, 13(1), 6074. <https://doi.org/10.1038/s41467-022-33794-9>
- Strauss, J., Laboor, S., Schirrmeister, L., Fedorov, A. N., Fortier, D., Froese, D., Fuchs, M., Günther, F., Grigoriev, M., Harden, J., Hugelius, G., Jongejans, L. L., Kanevskiy, M., Kholodov, A., Kunitsky, V., Kraev, G., Lozhkin, A., Rivkina, E., Shur, Y., ... Grosse, G. (2021b). Circum-Arctic Map of the Yedoma Permafrost Domain. *Frontiers in Earth Science*, 9. <https://doi.org/10.3389/feart.2021.758360>
- Strauss, J., Schirrmeister, L., Grosse, G., Wetterich, S., Ulrich, M., Herzsuh, U., , Hubberten, H.-W. (2013). The deep permafrost carbon pool of the Yedoma region in Siberia and Alaska. *Geophysical Research Letters*, 40(23), 6165–6170. <https://doi.org/10.1002/2013GL058088>
- Strauss, Jens , Fuchs, Matthias , Hugelius, Gustaf , Miesner, Frederieke , Nitze, Ingmar , Opfergelt, Sophie , Schuur, Edward , Treat, Claire , Turetsky, Merritt , Yang, Yuanhe , Grosse, Guido. (2024). Organic matter storage and vulnerability in the permafrost domain.
- Tananaev, N. I. (2016a). Hydrological and sedimentary controls over fluvial thermal erosion, the Lena River, central Yakutia. *Geomorphology*, 253, 524–533. <https://doi.org/10.1016/j.geomorph.2015.11.009>
- Tananaev, N. I., Makarieva, O. M., & Lebedeva, L. S. (2016b). Trends in annual and extreme flows in the Lena River basin, Northern Eurasia. *Geophysical Research Letters*, 43(20), 10,764-10,772. <https://doi.org/10.1002/2016GL070796>
- Tanski, G., Wagner, D., Knoblauch, C., Fritz, M., Sachs, T., & Lantuit, H. (2019). Rapid CO₂ Release From Eroding Permafrost in Seawater. *Geophysical Research Letters*, 46(20), 11244–11252. <https://doi.org/10.1029/2019GL084303>
- Turetsky, M. R., Abbott, B. W., Jones, M. C., Anthony, K. W., Olefeldt, D., Schuur, E. A. G., Grosse, G., Kuhry, P., Hugelius, G., Koven, C., Lawrence, D. M., Gibson, C., Sannel, A. B. K., & McGuire, A. D. (2020). Carbon release through abrupt permafrost thaw. *Nature Geoscience*, 13(2), 138–143. <https://doi.org/10.1038/s41561-019-0526-0>
- Vermaire, J. C., Pizaric, M. F. J., Thienpont, J. R., Courtney Mustaphi, C. J., Kokelj, S. V., & Smol, J. P. (2013). Arctic climate warming and sea ice declines lead to increased storm surge activity. *Geophysical Research Letters*, 40(7), 1386–1390. <https://doi.org/10.1002/grl.50191>
- Voigt, C., Marushchak, M. E., Abbott, B. W., Biasi, C., Elberling, B., Siciliano, S. D., Sonnentag, O., Stewart, K. J., Yang, Y., & Martikainen, P. J. (2020). Nitrous oxide emissions from permafrost-affected soils. *Nature Reviews Earth & Environment*, 1(8), 420–434. <https://doi.org/10.1038/s43017-020-0063-9>
- Vonk, J. E., Mann, P. J., Davydov, S., Davydova, A., Spencer, R. G. M., Schade, J., Sobczak, W. V., Zimov, N., Zimov, S., Bulygina, E., Eglinton, T. I., & Holmes, R. M. (2013). High biolability of ancient permafrost carbon upon thaw. *Geophysical Research Letters*, 40(11), 2689–2693. <https://doi.org/10.1002/grl.50348>
- Vonk, J. E., Mann, P. J., Dowdy, K. L., Davydova, A., Davydov, S. P., Zimov, N., Spencer, R. G. M., Bulygina, E. B., Eglinton, T. I., & Holmes, R. M. (2013). Dissolved organic carbon loss from Yedoma permafrost amplified by ice wedge thaw. *Environmental Research Letters*, 8(3), 035023. <https://doi.org/10.1088/1748-9326/8/3/035023>
- Vonk, J. E., Semiletov, I. P., Dudarev, O. V., Eglinton, T. I., Andersson, A., Shakhova, N., Charkin, A., Heim, B., & Gustafsson, Ö. (2014). Preferential burial of permafrost-derived organic carbon in Siberian- Arctic shelf waters. *Journal of Geophysical Research: Oceans*, 119(12), 8410–8421. <https://doi.org/10.1002/2014JC010261>

References

- Vonk, J. E., Tank, S. E., & Walvoord, M. A. (2019). Integrating hydrology and biogeochemistry across frozen landscapes. *Nature Communications*, 10(1), 5377. <https://doi.org/10.1038/s41467-019-13361-5>
- Wang, P., Huang, Q., Pozdniakov, S. P., Liu, S., Ma, N., Wang, T., Zhang, Y., Yu, J., Xie, J., Fu, G., Frolova, N. L., & Liu, C. (2021). Potential role of permafrost thaw on increasing Siberian river discharge. *Environmental Research Letters*, 16(3), 034046. <https://doi.org/10.1088/1748-9326/abe326>
- Wassmann, P. (2015). Overarching perspectives of contemporary and future ecosystems in the Arctic Ocean. *Progress in Oceanography*, 139, 1–12. <https://doi.org/10.1016/j.pocean.2015.08.004>
- Wild, B., Andersson, A., Bröder, L., Vonk, J., Hugelius, G., McClelland, J. W., Song, W., Raymond, P. A., & Gustafsson, Ö. (2019). Rivers across the Siberian Arctic unearth the patterns of carbon release from thawing permafrost. *Proceedings of the National Academy of Sciences*, 116(21), 10280–10285. <https://doi.org/10.1073/pnas.1811797116>
- Ye, B., Yang, D., & Kane, D. L. (2003). Changes in Lena River streamflow hydrology: Human impacts versus natural variations. *Water Resources Research*, 39(7). <https://doi.org/10.1029/2003WR001991>
- Zhang, S., Yin, Y., Yang, P., Yao, C., Tian, S., Lei, P., Jiang, T., & Wang, D. (2023). Using the end-member mixing model to evaluate biogeochemical reactivities of dissolved organic matter (DOM): Autochthonous versus allochthonous origins. *Water Research*, 232, 119644. <https://doi.org/10.1016/j.watres.2023.119644>
- Zhang, T., Barry, R. G., Knowles, K., Heginbottom, J. A., & Brown, J. (2008). Statistics and characteristics of permafrost and ground-ice distribution in the Northern Hemisphere. *Polar Geography*, 31(1–2), 47–68. <https://doi.org/10.1080/10889370802175895>
- Zheng, L., Overeem, I., Wang, K., & Clow, G. D. (2019). Changing Arctic River Dynamics Cause Localized Permafrost Thaw. *Journal of Geophysical Research: Earth Surface*, 124(9), 2324–2344. <https://doi.org/10.1029/2019JF005060>

Versicherung an Eides Statt

Affirmation in lieu of an oath

gem. § 5 Abs. 5 der Promotionsordnung vom 28.04.2021 /

according to § 5 (5) of the Doctoral Degree Rules and Regulations of 28 April, 2021

Ich / I, Olga Ogneva

versichere an Eides Statt durch meine Unterschrift, dass ich die vorliegende Dissertation selbständig und ohne fremde Hilfe angefertigt und alle Stellen, die ich wörtlich dem Sinne nach aus Veröffentlichungen entnommen habe, als solche kenntlich gemacht habe, mich auch keiner anderen als der angegebenen Literatur oder sonstiger Hilfsmittel bedient habe und die zu Prüfungszwecken beigelegte elektronische Version (PDF) der Dissertation mit der abgegebenen gedruckten Version identisch ist. / With my signature I affirm in lieu of an oath that I prepared the submitted dissertation independently and without illicit assistance from third parties, that I appropriately referenced any text or content from other sources, that I used only literature and resources listed in the dissertation, and that the electronic (PDF) and printed versions of the dissertation are identical.

Ich versichere an Eides Statt, dass ich die vorgenannten Angaben nach bestem Wissen und Gewissen gemacht habe und das die Angaben der Wahrheit entsprechen und ich nichts verschwiegen habe. / I affirm in lieu of an oath that the information provided herein to the best of my knowledge is true and complete.

Die Strafbarkeit einer falschen eidesstattlichen Versicherung ist mir bekannt, namentlich die Strafandrohung gemäß § 156 StGB bis zu drei Jahren Freiheitsstrafe oder Geldstrafe bei vorsätzlicher Begehung der Tat bzw. gemäß § 161 Abs. 1 StGB bis zu einem Jahr Freiheitsstrafe oder Geldstrafe bei fahrlässiger Begehung. / I am aware that a false affidavit is a criminal offence which is punishable by law in accordance with § 156 of the German Criminal Code (StGB) with up to three years imprisonment or a fine in case of intention, or in accordance with § 161 (1) of the German Criminal Code with up to one year imprisonment or a fine in case of negligence.

Ort / Place, Datum / Date:

25 Nov 2024, Berlin

Unterschrift / Signature :

Appendix

This appendix includes my three topically relevant co-authorships. The three publications included in their published format.

Organic matter characteristics of a rapidly eroding permafrost cliff in NE
Siberia (Lena Delta, Laptev Sea region)

Haugk, C., Jongejans, L. L., Mangelsdorf, K., Fuchs, M., **Ogneva, O.**, Palmtag, J., Mollenhauer, G., Mann, P. J., Overduin, P. P., Sanders, T., Tuerena, R. E., Schirrmeister, L., Wetterich, S., Kizyakov, A. I., Karger, C. and Strauss, J. (2022)

Published in *Biogeosciences*

<https://doi.org/10.5194/bg-19-2079-2022>



Organic matter characteristics of a rapidly eroding permafrost cliff in NE Siberia (Lena Delta, Laptev Sea region)

Charlotte Haugk^{1,2,a}, Loeka L. Jongejans^{1,2}, Kai Mangelsdorf³, Matthias Fuchs¹, Olga Ogneva^{1,4,5}, Juri Palmtag^{6,b}, Gesine Mollenhauer^{4,5}, Paul J. Mann⁶, P. Paul Overduin¹, Guido Grosse^{1,2}, Tina Sanders⁷, Robyn E. Tuerena⁸, Lutz Schirrmeister¹, Sebastian Wetterich^{1,c}, Alexander Kizyakov⁹, Cornelia Karger³, and Jens Strauss¹

¹Permafrost Research Section, Alfred Wegener Institute, Helmholtz Centre for Polar and Marine Research, 14473 Potsdam, Germany

²Institute of Geosciences, University of Potsdam, 14476 Potsdam, Germany

³Organic Geochemistry Section, Helmholtz Centre Potsdam GFZ German Research Centre for Geosciences, 14473 Potsdam, Germany

⁴Marine Geochemistry Section, Alfred Wegener Institute, Helmholtz Centre for Polar and Marine Research, 27570 Bremerhaven, Germany

⁵Faculty of Geosciences, University of Bremen, 28359 Bremen, Germany

⁶Department of Geography and Environmental Sciences, Northumbria University, Newcastle-upon-Tyne, NE1 8ST, UK

⁷Institute of Carbon Cycles, Helmholtz Centre Hereon, 21502 Geesthacht, Germany

⁸Scottish Association for Marine Science, Oban, PA37 1QA, UK

⁹Cryolithology and Glaciology Department, Faculty of Geography, Lomonosov Moscow State University, Moscow, 119991, Russia

^anow at: Department of Environmental Science and Analytical Chemistry, Stockholm University, Stockholm, 11418, Sweden

^bnow at: Department of Human Geography, Stockholm University, Stockholm, 11418, Sweden

^cnow at: Institute of Geography, Technische Universität Dresden, 01069 Dresden, Germany

Correspondence: Loeka L. Jongejans (loeka.jongejans@awi.de) and Jens Strauss (jens.strauss@awi.de)

Received: 10 December 2021 – Discussion started: 13 December 2021

Revised: 15 March 2022 – Accepted: 15 March 2022 – Published: 14 April 2022

Abstract. Organic carbon (OC) stored in Arctic permafrost represents one of Earth's largest and most vulnerable terrestrial carbon pools. Amplified climate warming across the Arctic results in widespread permafrost thaw. Permafrost deposits exposed at river cliffs and coasts are particularly susceptible to thawing processes. Accelerating erosion of terrestrial permafrost along shorelines leads to increased transfer of organic matter (OM) to nearshore waters. However, the amount of terrestrial permafrost carbon and nitrogen as well as the OM quality in these deposits is still poorly quantified. We define the OM quality as the intrinsic potential for further transformation, decomposition and mineralisation. Here, we characterise the sources and the quality of OM supplied to the Lena River at a rapidly eroding permafrost river shoreline cliff in the eastern part of the delta (Sobo-Sise Island). Our multi-proxy approach captures bulk elemental, molecu-

lar geochemical and carbon isotopic analyses of Late Pleistocene Yedoma permafrost and Holocene cover deposits, discontinuously spanning the last ~ 52 kyr. We showed that the ancient permafrost exposed in the Sobo-Sise cliff has a high organic carbon content (mean of about 5 wt %). The oldest sediments stem from Marine Isotope Stage (MIS) 3 interstadial deposits (dated to 52 to 28 cal ka BP) and are overlaid by last glacial MIS 2 (dated to 28 to 15 cal ka BP) and Holocene MIS 1 (dated to 7–0 cal ka BP) deposits. The relatively high average chain length (ACL) index of *n*-alkanes along the cliff profile indicates a predominant contribution of vascular plants to the OM composition. The elevated ratio of iso- and anteiso-branched fatty acids (FAs) relative to mid- and long-chain ($C \geq 20$) *n*-FAs in the interstadial MIS 3 and the interglacial MIS 1 deposits suggests stronger microbial activity and consequently higher input of bacterial biomass during

these climatically warmer periods. The overall high carbon preference index (CPI) and higher plant fatty acid (HPFA) values as well as high C/N ratios point to a good quality of the preserved OM and thus to a high potential of the OM for decomposition upon thaw. A decrease in HPFA values downwards along the profile probably indicates stronger OM decomposition in the oldest (MIS 3) deposits of the cliff. The characterisation of OM from eroding permafrost leads to a better assessment of the greenhouse gas potential of the OC released into river and nearshore waters in the future.

1 Introduction

Climate warming puts permafrost, especially ice-rich permafrost, in the terrestrial Arctic at risk of thawing (e.g. Strauss et al., 2021b). Permafrost, by definition, is ground that stays below 0°C for 2 or more consecutive years. Terrestrial permafrost ecosystems are affected by ongoing climate warming with consequences for geomorphological, hydrological and biogeochemical processes from a local to regional scale (IPCC, 2019). Almost twice as much carbon is stored in the permafrost region than what is currently contained in the atmosphere (Hugelius et al., 2014; Mishra et al., 2021), making permafrost carbon dynamics a globally relevant issue (Grosse et al., 2011; Schuur et al., 2008; Strauss et al., 2021a; Turetsky et al., 2020). Total estimated soil organic carbon (SOC) storage for the permafrost region is ~ 1100–1600 Gt, of which 181 ± 54 Gt is attributed to deep permafrost (below 3 m depth) of the Yedoma region (Hugelius et al., 2014; Strauss et al., 2021b, 2013).

Warming throughout the Arctic prolongs the season for permafrost thaw and open ice-free water bodies, resulting in increasing erosion of ice- and carbon-rich permafrost sediments exposed at coasts (Günther et al., 2013; Jones et al., 2020). Very ice-rich permafrost deposits (i.e. 50–90 vol % ice) such as the Late Pleistocene Yedoma Ice Complex (Schirrmeyer et al., 2013; Strauss et al., 2017) are particularly vulnerable to rapid thermo-denudation and thermo-erosion processes along river shores (Costard et al., 2014; Kanevskiy et al., 2016; Stettner et al., 2018; Fuchs et al., 2020). Vonk et al. (2013b) showed that Yedoma ice-wedge meltwater can increase the decomposition of organic matter (OM) due to co-metabolising effects. Another potential impact of the decomposition of terrestrial OM and discharge with Arctic river water is the change in biochemical properties that may increase ocean acidification and anthropogenic carbon dioxide uptake from the atmosphere (Semiletov et al., 2016). Furthermore, Semiletov et al. (2016) estimated that 57% of the terrestrial organic carbon in the East Siberian Shelf originates from ancient Pleistocene-age permafrost C, such as Yedoma deposits adjacent to river or coastal zones. Extensive river networks like the Lena River, especially in their delta zones, carry large nutrient OM loads

to the nearshore zone and onto the Arctic Shelf (Mann et al., 2022; Sanders et al., 2022). The Arctic river discharge has increased significantly in recent decades, transporting organic-rich waters to the nearshore area (Holmes et al., 2012, 2021). Increased riverbank erosion of Arctic rivers following warming during the last few decades constitutes an important mechanism of carbon export from land to water (Zhang et al., 2017, 2021; Fuchs et al., 2020). The studies cited here stress the need to better understand the interactions between thawing permafrost and river and nearshore waters.

The study of fossil biomolecules and other OM characteristics provides insights into the composition and level of OM decomposition and hence can greatly improve estimates of the greenhouse gas potential of thaw-mobilised OM from permafrost deposits (Andersson and Meyers, 2012; Sánchez-García et al., 2014). A few studies have previously focused on molecular biomarkers in north-eastern Siberian permafrost deposits (e.g. Zech et al., 2010; Höfle et al., 2013; Strauss et al., 2015; Stapel et al., 2016; Jongejans et al., 2020). In general, the abundance and distribution of *n*-alkanes, which are long-chained, single-bond hydrocarbons, are used for OM characterisation where the chain length of *n*-alkanes indicates OM sources.

In our study, we measure molecular biomarkers (*n*-alkanes, *n*-fatty acids) and use established biomarker proxies and indices such as the average chain length (ACL) of *n*-alkanes, the carbon preference index (CPI) and the higher plant fatty acid (HPFA) index to test whether they mirror the OM degree of decomposition and reflect the OM quality in ancient permafrost deposits. Additionally, analyses of the total organic carbon content (TOC), the stable carbon isotope ratios ($\delta^{13}\text{C}$ of TOC), the total nitrogen (TN) content and TOC/TN (here referred to as the C/N ratio) are applied to our sample set. Hierarchical clustering is used to identify the stratigraphical units along the sample profile based on the major changes in OM composition.

Thus, the OM characteristics of permafrost deposits, rapidly eroding at a cliff site in the eastern Lena Delta, are analysed for the first time for biomarkers. The set of frozen samples was obtained along a 25 m vertical cliff profile with a relatively high sampling density of about 1 m covering all exposed cryostratigraphic units. In this study, we aim (1) to characterise the OM composition of ancient permafrost that accumulated under different climate conditions; (2) to assess the degree of decomposition that the OM already experienced; and (3) to hypothesise, based on the decomposition legacy, the potential of future decomposability and microbial decomposition of the permafrost OM.

2 Study area

The Lena River forms the largest delta in the Arctic, covering an area of $29 \times 10^3 \text{ km}^2$ (Schneider et al., 2009), and discharges the second-highest freshwater load into the Laptev

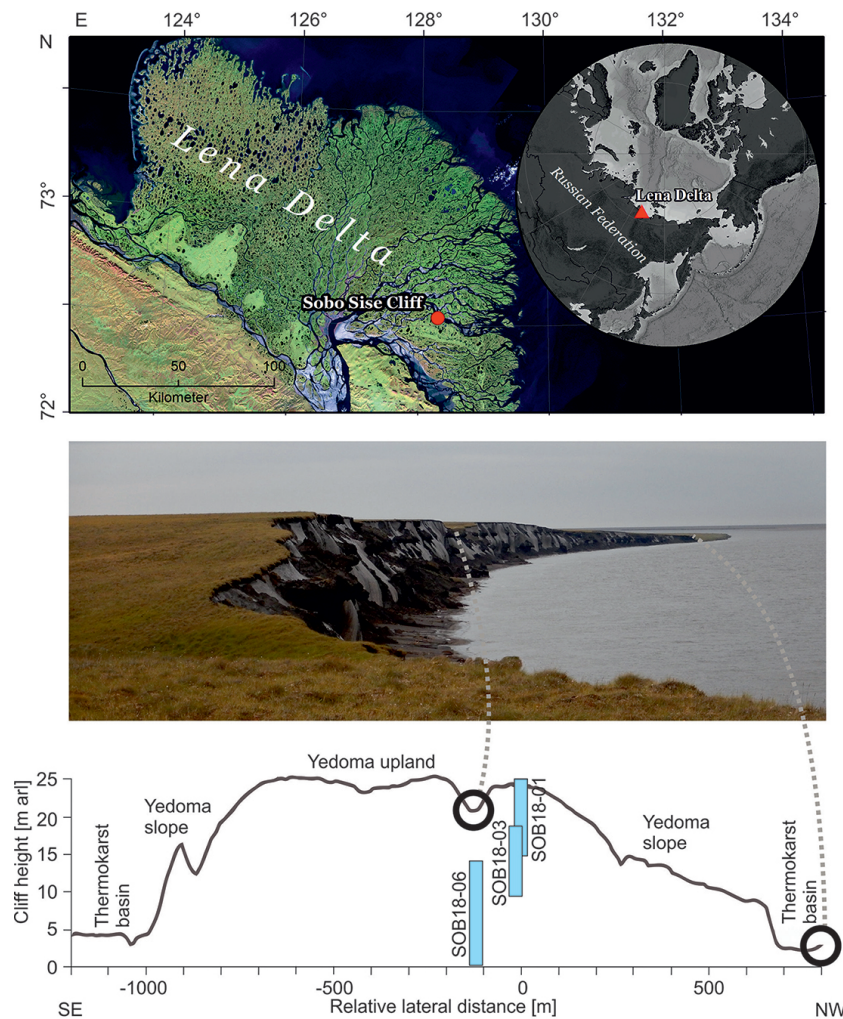


Figure 1. Overview of the Sobo-Sise Yedoma cliff. (a) Location of the Sobo-Sise Yedoma cliff in the Lena Delta in north-eastern Siberia (Landsat 5 mosaic (band combination 5, 4, 3) including scenes from 2009 and 2010; Landsat 5 image courtesy of the US Geological Survey); (b) picture of the Sobo-Sise Yedoma cliff from the east to west; (c) cross-section of the cliff profile (adapted from Wetterich et al., 2020a) indicating the three vertically sampled sections: SOB18-01, SOB18-03 and SOB18-06.

Sea, with a mean annual discharge of $525 \text{ km}^3 \text{ yr}^{-1}$ (Holmes et al., 2021). It also transports summer “heat” from the south to the north (Yang et al., 2005). The study area on Sobo-Sise Island (Fig. 1a–b) is located in the continuous permafrost zone. The island stretches between the Sardakhskaya and Bykovskaya main channels in the eastern part of the delta. In addition to the modern floodplain, there are three geomorphic units in the delta (Grigoriev, 1993; Schwamborn et al., 2002). While the first unit consists of Holocene floodplains and could occur in the whole delta area, the second unit consists of Late Pleistocene and Holocene fluvial deposits that are mostly located in the north-western part of the delta and are cut off from the current delta dynamics (Schirrmeister et al., 2011b). The third geomorphological unit consists of erosional remnants of a Late Pleistocene accumulation plain with ice-rich Yedoma Ice Complex deposits and is present

mainly in the west, south and east of the delta (Schwamborn et al., 2002; Wetterich et al., 2008; Morgenstern et al., 2011). According to a landform classification for Sobo-Sise Island, 43 % of the land surface is occupied by Yedoma uplands and Yedoma slopes and 43 % is thermokarst basins with the remaining 14 % being thermokarst lakes (Fuchs et al., 2018). The terrain is affected by thermokarst processes (Nitze and Grosse, 2016) and surface thaw subsidence (Chen et al., 2018).

The distinct surface morphology of Sobo-Sise Island includes Yedoma uplands intersected by thermo-erosional valleys and thermokarst basins. Syngenetic permafrost formation in polygonal tundra landscapes over long periods in the Late Pleistocene formed thick deposits with large ice wedges that are exposed at the cliff (Schirrmeister et al., 2011b, 2020; Strauss et al., 2015; Jongejans et al., 2018). Schirrmeister

et al. (2011b) attributed parts of the third geomorphological unit in the Lena Delta in the western and southern parts of the delta to remnants of a Yedoma accumulation plain. This formed during the Late Pleistocene when the Lena River had its delta farther north. Radiocarbon ages corroborated that Yedoma deposits on Sobo-Sise Island accumulated during the Late Pleistocene between about 52 and 15 cal ka BP. Substantial hiatuses were found at about 36–29 cal ka BP and at 20 to 17 cal ka BP, which may be related to fluvial erosion and/or changed discharge patterns of the Lena River (Wetterich et al., 2020a). Middle to Late Holocene ages from 6.36 to 2.5 cal kyr BP were found in the uppermost cover deposits of the cliff, which is also in agreement with other cover deposits found on top of Yedoma such as on the nearby Bykovsky Peninsula (Schirrmeister et al., 2002; Grosse et al., 2007).

The Sobo-Sise Yedoma cliff has an average height of 22 m with a maximum height of 27.7 m above the river water level (m a.r.l.) (Fuchs et al., 2020) and is affected by fluvio-thermal erosion. The current average shoreline retreat rate, which was calculated using satellite data, is 15.7 m yr^{-1} (2015–2018), which is remarkably high (Fuchs et al., 2020). In comparison, retreat rates were lower for other Yedoma cliffs such as on Kurungnakh Island in the central Lena Delta ($4.1\text{--}6.9 \text{ m yr}^{-1}$; Stettner et al., 2018) and at the Itkillik exposure in Alaska (11 m yr^{-1} ; Kanevskiy et al., 2016) but even higher for Muostahk Island (29.4 m yr^{-1} ; Günther et al., 2013) and Cape Mamontov Klyk (21 m yr^{-1} ; Günther et al., 2015). The Sobo-Sise Yedoma cliff ($72^{\circ}32' \text{ N}$, $128^{\circ}17' \text{ E}$; Fig. 1c) extends over 1660 m in length and faces north towards the Sardakhskaya Channel. Here, the water discharge amounts to about $8000 \text{ m}^3 \text{ s}^{-1}$ during the summer-low period (Fedorova et al., 2015) and the Lena River is ice-covered for about 8 months per year between October and May. The river ice thickness reaches up to 2 m. Water depth at the beginning of the Sardakhskaya Channel (close to Stolp and Sardakh islands) can reach up to 22 m (Fedorova et al., 2015) and is approximately 11 m in front of the Sobo-Sise Yedoma cliff, allowing for water flow underneath the river ice cover during the winter months (Fuchs et al., 2020).

3 Methods

3.1 Sample collection

The Sobo-Sise Yedoma cliff was sampled in three overlapping vertical sediment profiles (Fig. 1b) covering the entire exposed permafrost section (profile SOB18-01, 24.1 to 15.7 m a.r.l.; profile SOB18-03, 18.2 to 10.2 m a.r.l.; profile SOB18-06, 13.4 to 0.9 m a.r.l.). Each profile was cryolithologically described (see Wetterich et al., 2018, 2020a), and samples were collected at 0.5 m intervals by rappelling down on a rope from the top of the cliff. We used an axe and hammer to extract defined cubes of frozen ground

($\sim 20 \times 10 \times 10 \text{ cm}$) from the cliff wall. Samples were collected after cleaning and scraping off the outermost unfrozen and frozen parts of the cliff wall in order to collect frozen, uncontaminated samples. Then, the samples were lifted upwards, cleaned and subsampled for biomarker analysis. In total, we collected 61 sediment samples, of which 28 were selected for biomarker analysis at about 1 m intervals covering the entire exposed section. The samples were stored frozen in pre-combusted glass jars, apart from 9 samples (SOB18-06-09 to SOB18-06-34) which were initially stored in plastic whirl packs before being transferred in a frozen state to glass containers after transport to the laboratories.

3.2 Sedimentological organic matter parameters

Prior to bulk geochemical analyses, all samples were freeze-dried (Sublimator, ZIRBUS technology), ground and homogenised (Fritsch PULVERISETTE 5 planetary mill; 8 min at 360 rotations per minute). Total elemental carbon (TC) and total nitrogen (TN) content of sediment samples in weight percentage (wt %) were measured with a carbon–nitrogen–sulfur analyser (vario EL III, Elementar) with a detection limit of 0.1 wt % for carbon and nitrogen. Samples below this detection limit were set to 0.05 wt % so that the statistics could be calculated. Total organic carbon (TOC) content in weight percentage (wt %) was measured with a TOC analyser (vario MAX C, Elementar; analytical accuracy of 0.1 wt %). The TOC to TN (C/N) ratio has been used as a rough first indicator of the degree of OM decomposition with decreasing values indicating proceeding decomposition (Palmtag et al., 2015). The stable carbon isotope ratio ($\delta^{13}\text{C}$) of TOC reflects both the initial contribution from different plant species and plant components and OM decomposition processes (Gundelwein et al., 2007). Samples for $\delta^{13}\text{C}$ analyses were treated with hydrochloric acid (20 mL, 1.3 M) to remove carbonates, heated on a hotplate (97.7°C for 3 h) and subsequently washed with distilled water. The samples were filtered (Whatman Grade GF/B, nominal particle retention of $1.0 \mu\text{m}$), after which the residue was dried and ground. All $\delta^{13}\text{C}$ samples were measured using a DELTA V Advantage isotope ratio mass spectrometer (MS) equipped with a Flash 2000 analyser (Thermo Fisher Scientific; analytical accuracy of 0.15 ‰), using helium as a carrier gas. The $\delta^{13}\text{C}$ ($^{13}\text{C}/^{12}\text{C}$) value is reported in per mille (‰) compared to the standard ratio Vienna Pee Dee Belemnite (VPDB).

3.3 Lipid biomarker analyses

Lipid biomarkers provide information on a molecular level about the source of OM, the environmental conditions during deposition and the degree of decomposition. In this study, we focused on *n*-alkanes in the aliphatic OM fraction and *n*-fatty acids in the polar hetero-compound fraction. Changes in their relative abundance can provide an indication of the degree of decomposition (Kim et al., 2005) as outlined below. We anal-

ysed the *n*-alkane distributions of all 28 samples and selected 13 samples for the analysis of *n*-fatty acids. The selection of the *n*-fatty acids was made to cover the entire profile continuously (approximately every 2 m).

3.3.1 Extraction and fraction separation

Following freeze-drying and grinding, biomarker subsamples were transferred into glass jars. Extraction and separation were conducted according to Schulte et al. (2000) and Strauss et al. (2015). Samples were processed in two batches, each containing 14 samples. We weighed between 8 and 11 g in extraction cell bodies fit for the accelerated solvent extractor (ASE 200 Dionex). Dichloromethane / methanol (volume ratio of 99 : 1) was used as a solvent mixture for OM extraction. Each sample was held in a static phase (5 min heating phase, 20 min at 75 °C and 5 MPa). Dissolved compounds were then further concentrated at ~ 42 °C using a closed-cell concentrator (TurboVap 500 Zymark), and the remaining solvent was evaporated under N₂. Afterwards, internal standards were added: 5 α -androstane for the aliphatic fraction, ethylpyrene for the aromatic fraction, 5 α -androstan-17-one for the NSO (nitrogen, sulfur and/or oxygen) neutral polar fraction and erucic acid for the NSO fatty-acid fraction (80 μ L each from respective 100 μ g mL⁻¹ standard solutions). Subsequently, an asphaltene precipitation was performed to remove compounds with higher molecular complexity (asphaltenes) by dissolving the extracts in a small amount of dichloromethane and adding a 40-fold excess of *n*-hexane. Precipitated asphaltenes were removed by filtration through a sodium-sulfate-filled funnel. Subsequently, the *n*-hexane-soluble portion was separated by medium-pressure liquid chromatography (MPLC) (Radke et al., 1980) into three fractions of different polarities: aliphatic hydrocarbons, aromatic hydrocarbons and polar hetero-compounds (NSO compounds). Finally, the NSO fractions of 13 samples were split into an acid and neutral polar (alcohol) fraction using a KOH-impregnated column. While the *n*-fatty-acid potassium salts were attached to the silica gel, the neutral polar compounds were eluted with dichloromethane. After remobilising the *n*-fatty acids by protonation of their salts with formic acid, the *n*-fatty-acid fraction was obtained with dichloromethane.

3.3.2 GC-MS measurements and compound quantification

n-Alkanes and *n*-fatty acids were analysed using gas chromatography coupled with a mass spectrometer (GC-MS; GC – Trace GC Ultra and MS – DSQ, both Thermo Fisher Scientific). Prior to the analyses, *n*-fatty acids were methylated with diazomethane. The GC was equipped with a cold injection system operating in the splitless mode. The injector temperature was programmed from 50 to 300 °C at a rate of 10 °C s⁻¹. Helium was used as carrier gas with a con-

stant flow of 1 mL min⁻¹. After injection, the compounds of interest were separated on an SGE BPX5 fused-silica capillary column (50 m length, 0.22 mm i.d., 0.25 μ m film thickness) using the following temperature conditions: initial temperature of 50 °C (1 min isothermal), heating rate of 3 °C min⁻¹ to 310 °C, held isothermally for 30 min. The MS operated in the electron impact mode at 70 eV. Full-scan mass spectra were recorded from *m/z* 50–600 at a scan rate of 2.5 scans s⁻¹. Using the software Xcalibur (Thermo Fisher Scientific), peaks in the GC-MS run were quantified using the internal standards for *n*-alkanes and *n*-fatty acids. All biomarker concentrations are expressed in micrograms per gram of dry sediment (μ g g⁻¹ sed.) and per gram of TOC (μ g g⁻¹ TOC).

3.4 Lipid biomarker indices

3.4.1 Average chain length

The *n*-alkane average chain length (ACL) is the weighted average number of carbon atoms used for determining OM sources. Long-chain odd-numbered *n*-alkanes ($C \geq 21$) are essential constituents that serve as biomarkers for higher terrestrial plants (Eglinton and Hamilton, 1967; Eglinton and Eglinton, 2008; Schäfer et al., 2016), whereas shorter chain lengths indicate bryophyte, bacterial or algal origin (Cranwell, 1984; Rieley et al., 1991; Kuhn et al., 2010). A change in the ACL can suggest a change in the terrestrial source biota. We used the equation (Eq. 1) first described by Poynter (1989) but with a chain interval from C₂₃ to C₃₃ following Strauss et al. (2015) and Jongejans et al. (2018):

$$\text{ACL} = \frac{\sum i \cdot C_i}{\sum C_i}, \quad (1)$$

where *C* denotes concentration and *i* the carbon number.

3.4.2 Carbon preference index

The CPI (carbon preference index) was originally introduced by Bray and Evans (1961) as the ratio of odd- to even-numbered *n*-alkanes and indicates the level of OM transformation, which decreases with progressing maturation. OM decomposition leading to lower CPI values is a measure of thermal alteration referring to rocks or oils on a geological timescale. However, this ratio, as well as the very similar odd-over-even predominance (OEP) ratio, was previously used in Quaternary permafrost deposits as an indicator for OM decomposition (Zech et al., 2009; Strauss et al., 2015; Struck et al., 2020; Jongejans et al., 2020). Based on these studies, we refer to values over 5 as less degraded OM of high quality. Equation (2) describes the CPI and was modified after Marzi et al. (1993) using C_{23–33} as a chain length interval.

$$\text{CPI}_{23-33} = \frac{(\sum \text{odd } C_{23-31}) + (\sum \text{odd } C_{25-33})}{2(\sum \text{even } C_{22-32})} \quad (2)$$

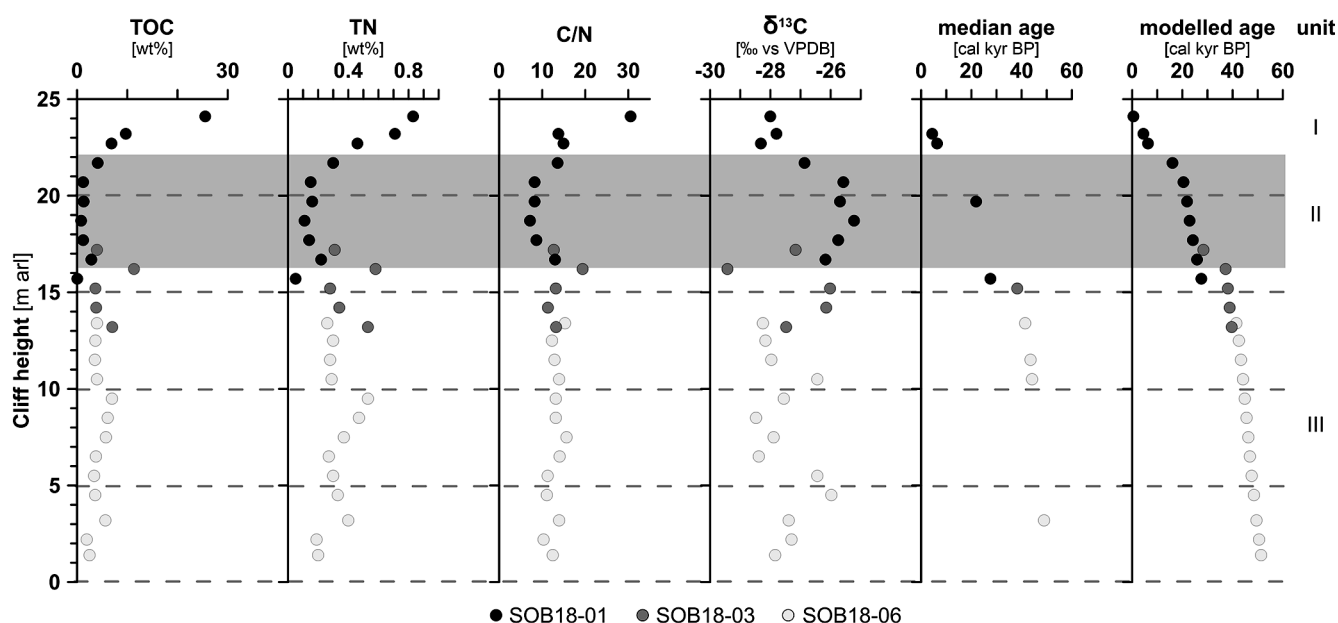


Figure 2. Biogeochemical parameters of the Sobo-Sise Yedoma cliff: total organic carbon (TOC) content, total nitrogen (TN) content, carbon-to-nitrogen (C/N) ratio, bulk stable carbon isotope ratios ($\delta^{13}\text{C}$), radiocarbon ages and modelled age in calibrated kiloyears before present (cal kyr BP). Data points are displayed over cliff height from the cliff top at 25 m above river level (a.r.l.) to cliff bottom at 0 m a.r.l. The three sections of SOB18 are plotted separately for each parameter (black, dark grey and light grey circles). Units I, II (grey rectangle) and III correspond to Marine Isotope Stage (MIS) 1 to 3, respectively. The radiocarbon ages were published in Wetterich et al. (2020a).

3.4.3 Higher plant fatty acids

For each sample, the absolute *n*-fatty-acid (FA) concentration was measured and the most abundant homologue's chain length was identified. In addition, we looked at the share of iso- and anteiso-branched FAs, which are indicators for microbial biomass (Rilfors et al., 1978; Stapel et al., 2016). Furthermore, we calculated the higher plant fatty acid (HPFA) index, which is the relative amount of the long-chain *n*-fatty acids to long-chain *n*-alkanes in the sediments. The HPFA index was introduced by Strauss et al. (2015) following the principles of the HPA index of Poynter (1989), only with using fatty acids instead of wax alcohols (Eq. 3). The HPFA index reflects the degree of preservation of OM due to the higher lability of *n*-fatty acids in relation to *n*-alkanes (Canuel and Martens, 1996). The preferential decomposition of fatty acids is due to their functional group leading to a chemical polarisation within the molecule forming an attack point for geochemical or microbiological decomposition and/or decarboxylation (Killops and Killops, 2013). Therefore, a decrease in the HPFA index indicates increased OM decomposition. We use this index for internal comparison where higher values (above the mean) indicate a comparatively higher-quality OM.

$$\text{HPFA} = \frac{\sum n\text{-fatty acids } C_{24}C_{26}C_{28}}{\sum n\text{-fatty acids } C_{24}C_{26}C_{28} + \sum n\text{-alkanes } C_{27}C_{29}C_{31}} \quad (3)$$

3.5 Data analysis

In order to identify the stratification along the cliff based on the OM characteristics of the permafrost sediments, the data set was clustered using a constrained agglomerative hierarchical clustering of a distance matrix (chclust of the rjoja package, in R version 4.0.4) (Juggins, 2019). We applied the non-parametric Kruskal–Wallis (> two groups) test for statistical analyses of the data to compare all major parameters (TOC, C/N, *n*-alkanes, ACL, CPI, short and long *n*-fatty acids, HPFA index, and (iso- + anteiso-branched) / (mid- and long-chain *n*-fatty acids)) between the identified clusters. In the Results section, we report the *p* values; the correlation coefficients are reported in the Supplement (Table S1).

4 Results

The uppermost sediments of the cliff consisted of Holocene-age sediments (from 24.1 to 22.5 m a.r.l.; upper part of SOB18-01) on top of Late Pleistocene Yedoma sediments from 22.2 m a.r.l. down to the cliff base at the river water level. A detailed cryostratigraphic description is given in Wetterich et al. (2020a).

4.1 Sedimentological organic matter parameters

TOC content was highest in the topmost sample and ranged from < 0.1 wt % (below the detection limit, sample SOB18-01-18 at 15.7 m a.r.l.) to 25.5 wt % (SOB18-01-01 at 24.1 m a.r.l.). Both the minimum and the maximum TOC values were found within profile SOB18-01 (Fig. 2). The average TOC content was 4.9 wt % (standard deviation (SD) 4.7, $n = 28$) and values decreased from the cliff top downwards with two values higher than 10 wt % at 24.1 m a.r.l. (SOB18-01-01; 25.5 wt %) and at 16.2 m a.r.l. (SOB18-03-05; 11.3 wt %). TN content had an average of 0.3 wt % (SD 0.2), and the highest value was also found at 24.1 m a.r.l. (SOB18-01-01; 0.8 wt %) and the lowest at 15.7 m a.r.l. (SOB18-01-18; < 0.1 wt %). C/N ratios ranged from 7.2 to 30.5 (Fig. 2) and displayed, except for the uppermost sample, only little variability over the cliff profile with a mean of 13.2 (SD 4.2). The $\delta^{13}\text{C}$ values ranged from -25.2‰ (SOB18-01-12 at 18.7 m a.r.l.) to -29.4‰ (SOB18-03-05 at 16.2 m a.r.l.) and had an average of -27.2‰ (SD 1.1). There was a significant negative correlation between $\delta^{13}\text{C}$ and C/N values ($r = -0.59$ (Pearson correlation), $p < 0.01$). Radiocarbon ages of selected plant remains were determined on a MICADAS system. These data and a Bayesian age-depth model were published by Wetterich et al. (2020a). The laboratory methods were described in detail by Mollenhauer et al. (2021). The radiocarbon ages ranged from 2.50 (at 23.7 m a.r.l.) to 51.88 cal kyr BP (at 0.9 m a.r.l.).

4.2 Biomarkers

4.2.1 *n*-Alkanes

n-Alkanes were detected in the range between *n*-C₁₄ and *n*-C₃₅ and showed a strong odd-over-even carbon number predominance. The relative *n*-alkane concentration increased in the lower part of the cliff, closer to the river level. Relative *n*-alkane concentrations ranged from 1 to 172 $\mu\text{g g}^{-1}$ TOC (mean 30, SD 42) for the short-chain (C₁₄ to C₂₀) *n*-alkanes and from 119 to 3214 $\mu\text{g g}^{-1}$ TOC (mean 1068, SD 886) for the long-chain (C₂₁ to C₃₃) *n*-alkanes (Fig. 3). The absolute concentrations were also higher in the lower part of the cliff for the short-chain (mean 1 $\mu\text{g g}^{-1}$ sed., SD 1) and long-chain *n*-alkanes (mean 41 $\mu\text{g g}^{-1}$ sed., SD 31). The main dominating *n*-alkane chain length was *n*-C₂₇ in the lower part of the cliff and alternated between *n*-C₂₇ and *n*-C₂₉ in the upper part (Fig. S1). Four samples were dominated by the *n*-C₃₁ *n*-alkane.

The *n*-alkane-based ACL showed variations between 27.1 (SOB18-06-19 at 4.5 m a.r.l.) and 29.0 (SOB18-01-06 at 21.7 m a.r.l.) with a mean of 28.0 across the cliff (SD 0.50; Fig. 3). The CPI of *n*-alkanes (*n*-C₂₃ to *n*-C₃₃) ranged from 5.76 (SOB18-06-15; 6.5 m a.r.l.) to 16.29 (SOB18-06-05; 11.5 m a.r.l.) with a mean value of 9.89 (SD 2.79). Below 7 m a.r.l., the CPI significantly decreased.

4.2.2 *n*-Fatty acids

We found *n*-FAs with carbon numbers between C₈ and C₃₂. The *n*-FAs showed a strong even-over-odd carbon number predominance. Furthermore, hydroxy FAs (C₆ to C₈), iso-branched FAs (C₁₀ to C₁₉), anteiso-branched FAs (C₁₁, C₁₂, C₁₃, C₁₅ and C₁₇), monounsaturated FAs (C₁₆ to C₂₀ and C₂₄), unsaturated iso- and anteiso-branched FAs (C₁₇), cyclopropyl FAs (C₁₇ and C₁₉), di- and triunsaturated FAs (C₁₈), and phytanic acid were detected (Fig. S2, Table S2). Concentration of long-chain *n*-FAs (C₂₄ to C₃₂) ranged from 290 $\mu\text{g g}^{-1}$ TOC at 24.1 m a.r.l. to 2346 $\mu\text{g g}^{-1}$ TOC at 1.4 m a.r.l. (mean 1041 $\mu\text{g g}^{-1}$ TOC, SD 655). The most abundant long-chain *n*-FA was *n*-C₂₄ for all samples, except at 16.7 m a.r.l. (*n*-C₂₆) (Figs. 2 and S2). The mid-chain *n*-FA (C₂₁ to C₂₃) concentration ranged from 121 to 1250 $\mu\text{g g}^{-1}$ TOC (mean 463 $\mu\text{g g}^{-1}$ TOC, SD 314) and was highest at 22.7 m a.r.l. The short-chain *n*-FA concentration (C₈ to C₂₀) ranged from 120 to 968 $\mu\text{g g}^{-1}$ TOC (mean 560 $\mu\text{g g}^{-1}$ TOC, SD 212) and was highest in the bottom sample at 1.4 m a.r.l. Among the short-chain FAs, the *n*-C₁₆ dominated all samples (Fig. S2). The iso- and anteiso-branched FAs were more abundant in the bottom section of the cliff and lowest in the middle section, and the ratio of iso- and anteiso-branched saturated fatty acids (C₁₁, C₁₃, C₁₅ and C₁₇) to mid- and long-chain (C \geq 21) *n*-FAs ranged from 0.03 to 0.32 (mean 0.13, SD 0.09; Figs. 3 and S2). The HPFA index had a mean value of 0.63 (SD 0.11, $n = 13$), a minimum of 0.45 (SOB18-06-17 at 5.5 m a.r.l.) and a maximum of 0.86 (SOB18-01-04 at 22.7 m a.r.l.) close to the cliff top. Overall, HPFA values below 16 m a.r.l. were slightly lower than in the upper section.

4.3 Clustering

We identified three main sub-groups using agglomerative hierarchical clustering (Fig. 4a): unit I from 24.1 to 22.7 m a.r.l. ($n = 3$), unit II from 21.7 to 16.7 m a.r.l. ($n = 7$) and unit III from 16.2 to 1.4 m a.r.l. ($n = 18$). Our clustering matched the three cryostratigraphic units as defined by Wetterich et al. (2020a), which further corresponded to MIS 1, MIS 2 and MIS 3 from the top to the bottom. The TOC content (Fig. 4b) and C/N ratio were significantly the highest in unit I and lowest in unit II ($p < 0.01$ and $p < 0.05$, respectively; Fig. 2 and Table S1). The short-chain (C₁₄ to C₂₀) and long-chain (C₂₁ to C₃₃) *n*-alkane concentration, expressed in $\mu\text{g g}^{-1}$ TOC, was higher in unit III, but the differences were only significant for the short-chain *n*-alkanes ($p < 0.01$) (Fig. 4c). The short-chain (C₈ to C₂₀), mid-chain (C₂₁ to C₂₃) and long-chain (C₂₄ to C₃₂) *n*-fatty-acid concentrations expressed in $\mu\text{g g}^{-1}$ TOC did not differ significantly between the units. The ACL and CPI values were similar for each unit (Fig. 3). The HPFA index was significantly different between the units ($p < 0.05$) with the highest values in unit I and lowest values in unit III (Fig. 4d). The share of iso- and anteiso-branched

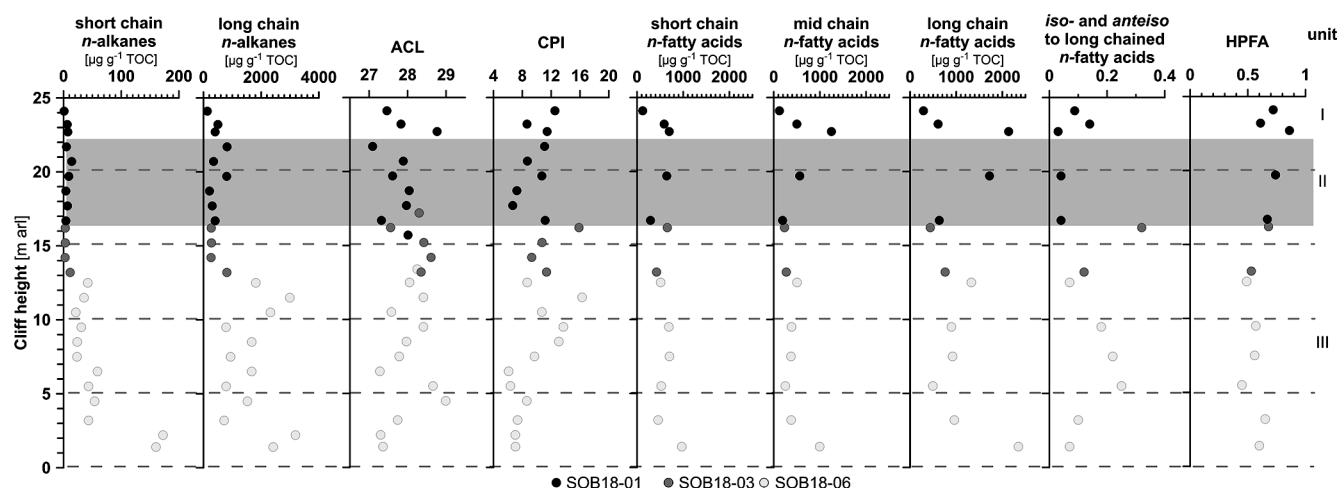


Figure 3. Biomarker parameters of the Sobo-Sise Yedoma cliff. The first four columns show *n*-alkane parameters: short-chain (C_{14} – C_{20}), and long-chain (C_{21} – C_{33}) *n*-alkane concentrations (both in $\mu\text{g g}^{-1}$ TOC), the *n*-alkane average chain length (ACL_{23–33}), and *n*-alkane carbon preference index (CPI_{23–33}). The last five columns show *n*-fatty-acid parameters: short-chain (C_8 – C_{20}), mid-chain (C_{21} – C_{23}) and long-chain (C_{24} – C_{32}) *n*-fatty-acid concentrations (in $\mu\text{g g}^{-1}$ TOC); the ratio of iso- and anteiso-branched saturated fatty acids (C_{11} , C_{13} , C_{15} and C_{17}) to mid- and long-chain ($C \geq 21$) *n*-fatty acids; and the higher plant fatty acid (HPFA) index. Data points are displayed over cliff height from the cliff top at 25 m above river level (a.r.l.) to cliff bottom at 0 m a.r.l. The three sections of SOB18 are plotted separately for each parameter (black, dark grey and light grey circles). Units I, II (grey rectangle) and III correspond to Marine Isotope Stage (MIS) 1 to 3.

FAs compared to mid- and long-chain *n*-FAs was highest in unit III and lowest in unit II (Fig. 4e), but the differences were not significant.

5 Discussion

5.1 Terrestrial organic matter at the interface between permafrost and river

5.1.1 Organic matter source

We found that the *n*-alkane distributions were dominated by the long-chain *n*-alkanes ($C \geq 21$) and that short-chain *n*-alkanes only played a marginal role (Fig. S1). The most abundant *n*-alkane homologues in the entire data set were *n*- C_{27} , *n*- C_{29} and *n*- C_{31} , which indicates that the OM stemmed from higher land plants (Eglinton and Hamilton, 1967). This is confirmed by the dominance of long-chain *n*-FAs (C_{24} – C_{32}) with a strong even-over-odd carbon number predominance (Fig. S2). The relatively high ACL across the cliff (Fig. 3) indicates a predominant contribution of vascular plants, which corroborates the pollen record presented by Wetterich et al. (2021). Their results indicated the presence of tundra–steppe vegetation during MIS 3–2, while MIS 1 pollen spectra of the uppermost three samples indicated a shift from tundra–steppe to shrub–tundra vegetation. Occasional warmer-than-today summers were recorded during the early MIS 3 as well as the presence of low-centre polygons with favourable (stable) aquatic conditions during MIS 3.

Cooler and drier summer conditions as well as unstable (draining and rewetting phases) aquatic conditions were reconstructed for MIS 2 (Wetterich et al., 2021). In our study, the elevated ratio of iso- and anteiso-branched FAs relative to mid- and long-chain ($C \geq 21$) *n*-FAs in unit I (MIS 1) and III (MIS 3) compared to unit II (MIS 2; Figs. 4e and S2) suggests stronger microbial activity during the warmer MIS 3 and MIS 1 periods (Rilfors et al., 1978; Stapel et al., 2016) and points to a higher input of bacterial biomass during that time. Additionally, we found a significant abundance of short-chain FAs, especially *n*- C_{16} in all samples (Fig. S2). However, these FAs are common not only in bacterial but also in eukaryotic microorganisms (Gunstone et al., 2007) and thus represent a mixing signal. Therefore, we focused here on iso- and anteiso-branched FAs as they are more specific biomarkers for bacterial biomass (Kaneda, 1991).

The source and nature of the OM preserved in permafrost influence both its quantity and its quality (Jongejans et al., 2018). TOC, TN, C/N and $\delta^{13}\text{C}$ variations result from changes in biomass productivity and/or decomposition, from different OM sources, from changes in depositional conditions influencing OM preservation, and from different characteristics of Cryosol formation. Generally, enriched $\delta^{13}\text{C}$ and low TOC and C/N values, as we found in unit II and III (Fig. 2), are typical of Yedoma deposits that formed during cold stages (Schirrmeister, 2012). However, climate variations during the last ice age were differentiated into warmer interstadials (e.g. MIS 3) and colder stadial periods (e.g. MIS 2) which climatically triggered changes in vegetation and Cryosol formation. At the Sobo-Sise Yedoma cliff, the

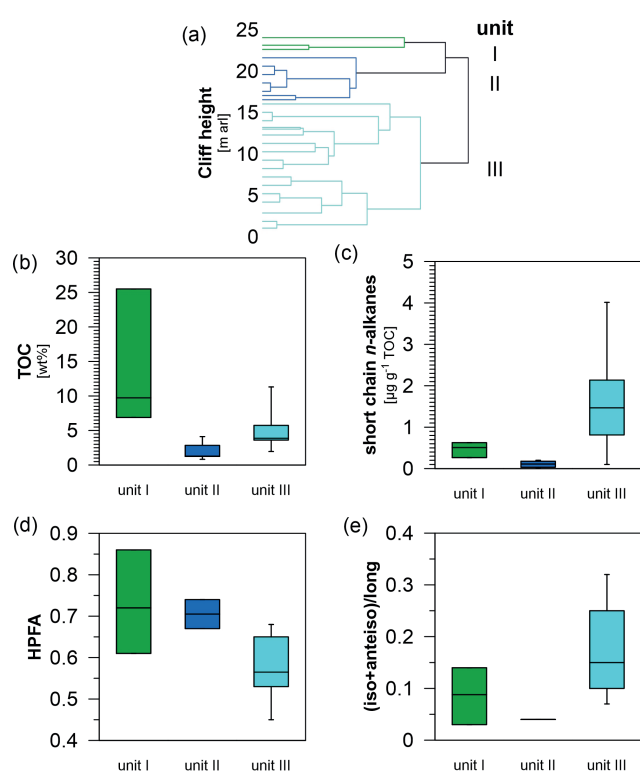


Figure 4. Statistical separation of the Sobo-Sise Yedoma cliff profile and selected carbon parameters of the separated cliff units. **(a)** Clustering of samples with y axis representing cliff height from the cliff top at 25 m above river level (a.r.l.) to cliff bottom at 0 m a.r.l. Unit I corresponds to Marine Isotope Stage (MIS) 1, unit II to MIS 2 and unit III to MIS 3. Resulting box plots allow better visualisation of the OM distribution along the Sobo-Sise Yedoma cliff profile: **(b)** total organic carbon (TOC) content (in wt %), **(c)** short-chain *n*-alkane concentration (in $\mu\text{g g}^{-1}$ TOC), **(d)** higher plant fatty acid (HPFA) index, and **(e)** ratio of iso- and anteiso-branched saturated fatty acids (C_{11} , C_{13} , C_{15} and C_{17}) to mid- and long-chain ($C \geq 21$) *n*-fatty acids.

TOC values were higher during MIS 1 and 3 compared to the last glacial (MIS 2) deposits, suggesting higher OM accumulation, which was presumably triggered by higher biomass production. The TOC values from the MIS 3 and MIS 2 sediments of the Sobo-Sise Yedoma cliff (< 0.1 wt %–11.3 wt %, mean 4.0 wt %) were significantly higher ($p < 0.01$) than those of other Siberian Yedoma sites (< 0.1 wt %–27 wt %, mean 3.0 wt %; 17 study sites, 719 samples) but very similar to data from Kurungnakh Island (mean 3.8 wt %) which is located about 70 km west-south-west of Sobo-Sise Island in the central Lena Delta (Strauss et al., 2012, 2020). Likely, the high TOC values in the Sobo-Sise record are a result of past wetter conditions leading to the formation of peat layers. Comparably to the Kurungnakh Island Yedoma record, the Sobo-Sise Yedoma cliff is characterised by silty sediments with multiple layers enriched in peat pointing to palaeosol formation during permafrost aggradation. The MIS 3 de-

posits contained rather less decomposed twigs and grass remains as well as single peaty lenses (15–20 cm in diameter) and peat layers (10–20 up to 130 cm thick). A similar occurrence of single-twig remains (2–4 mm in diameter), dark brown spots, finely dispersed organic remains and peaty lenses (5–25 cm in diameter) was found in MIS 2 deposits, while MIS 1 deposits contained many more peaty components, i.e. numerous peaty lenses (2–25 cm in diameter), which was reflected in higher TOC values compared to MIS 3 and MIS 2 deposits (Wetterich et al., 2020a).

At 16.2 m a.r.l., we found a peak in TOC (11.3 wt %, SOB18-03-05) and a simultaneously depleted $\delta^{13}\text{C}$ value (-29.4‰). High TOC and low $\delta^{13}\text{C}$ values have been found to be indicative for peat accumulation and low decomposition under wetter conditions in a more anaerobic regime (Wetterich et al., 2009; Schirrmeister et al., 2011a; Strauss et al., 2012). These peat layers can form by moss accumulation which is hardly decomposed and/or incorporated soon upon accumulation. From a biomarker perspective, this sample was not much different regarding the biomolecular composition, indicating a similar organic biomass (Fig. S2). The higher relative abundance of iso- and anteiso-FAs relative to mid- and long-chain FAs in this sample may point to increased microbial activity and thus microbial decomposition during the time of deposition in this OM-rich sample. Considering palaeoenvironmental studies from Kurungnakh Island in the central Lena Delta, palaeosol formation was intensified by relatively warm and wet summers during the climate optimum of the interstadial MIS 3 between 40 and 32 ka BP (Wetterich et al., 2008, 2014). Therefore, it is very likely that this layer is a buried palaeosol layer containing peaty material.

5.1.2 Organic matter quality

OM from different vegetation types was incorporated from the active layer into the permafrost during and after different phases of decomposition. The biogeochemical and biomarker proxies outlined in the previous section mainly describe the sources and composition of permafrost OM. In addition, biomarker ratios provide information on the decomposition level of the OM and, with that, the potential “decomposability” (quality) of the respective permafrost OM upon thaw. The OM assessment of this study via agglomerative clustering found an overall high OM quality of the Sobo-Sise Yedoma deposits with high CPI values (mean 9.89) and higher C/N ratios (mean 13.24) compared to the other Yedoma deposits such as those on the Buor Khaya Peninsula (central Laptev Sea) with mean C/N values of about 10 (Strauss et al., 2015). The elevated C/N value in the top sample of the Sobo-Sise record likely results from the influence of modern plants rooted in the active layer. For the rest of the profile, the C/N ratios were rather uniform. The high CPI in our study is comparable to other Yedoma sites as reported by Strauss et al. (2015) for the Buor Khaya Peninsula (mean

11.6) and Jongejans et al. (2018) for the Baldwin Peninsula (western Alaska; 12.2). At the Sobo-Sise Yedoma cliff, the CPI values scattered around a mean of 9.89 and decreased in the lowermost 7 m of the cliff profile. This could probably indicate a higher level of OM decomposition for the lower cliff part but can also be influenced by the vegetation type and species prevailing during the early MIS 3 with stagnant water and partly warmer-than-today summer climate conditions (Wetterich et al., 2021). The HPFA values (0.45–0.86, median 0.61) are a bit higher compared to Yedoma deposits investigated by Strauss et al. (2015) on the Buor Khaya Peninsula (0.15–0.69, median 0.54). Overall, the HPFA significantly decreased downwards (Fig. 4d; $p < 0.05$), especially below unit II, which suggests that the OM is further decomposed downwards. This fits the assumption that there was more time for OM decomposition for the older lower cliff parts of the palaeo-active layer. A higher decomposition for the lower cliff part is also supported by the highest ratio of the iso- and anteiso-branched FAs vs. mid- and long-chain FAs in the MIS 3 deposits (Fig. 4e), indicating a higher relative amount of microbial biomass and suggesting higher microbial activity during this warmer interval.

Previous studies showed that mineral-associated OM can make up a substantial fraction of the OM in permafrost soils, which protects the OM from decomposition (Dutta et al., 2006; Mueller et al., 2015). We found that the biomarker concentrations are negatively correlated with the mean grain size published by Wetterich et al. (2020b) (Fig. S3). Especially the negative correlation between the grain size and the short- ($p < 0.01$), mid- and long-chain n -FA concentrations ($p < 0.05$) are significant. This suggests that, even though the n -FAs are generally vulnerable with respect to decomposition, the n -FAs might to some extent be protected from OM decomposition upon mobilisation and transport. On top of the preferred decomposition of short-chain n -alkanes over their long counterpart (Elias et al., 2007), the stronger negative correlation (even though not significant) between the grain size and the long-chain n -alkanes compared to their short-chain counterpart could suggest that the latter might be more vulnerable to decomposition or might reflect the different sources of these biomolecules. While long-chain n -alkanes are derived from higher land plants and enter the soil by deposition, short-chain n -alkanes might contain a significant portion of microbial biomass, whose abundance depends on the availability of appropriate substrates.

As outlined above, three stages of permafrost aggradation on Sobo-Sise Island linked to climatic variability were identified according to Wetterich et al. (2020a). OM preservation during these stages is strongly impacted by the duration of freezing and thawing periods, the associated presence and absence of oxygen in the soil, the related level of microbial activity, and/or physical protection of the OM by the inorganic matrices (e.g. Fe complexation) (Freeman et al., 2001; Hedges and Keil, 1995; Lützow et al., 2006). As these factors are all closely interlinked, it is almost impossible to decipher

the control of these processes on the finally preserved OM biomarker signatures.

5.2 Implications

Nitzbon et al. (2020) found that terrestrial permafrost-locked OC will be significantly thaw-affected by 2100, and it could even be up to 3-fold (12-fold) more under warming scenario RCP4.5 (RCP8.5) compared to previous estimates if including thermokarst-inducing processes. Deep OM as characterised in our study can be released by deep disturbance processes such as thermokarst development, thermal erosion or riverbank erosion. Our findings show that freshly thawed and high-quality OM was frozen in the cliff sediments and is now being mobilised rapidly as is shown by the high annual erosion rates of 15.7 m yr^{-1} as reported by Fuchs et al. (2020) (2015–2018, in the long term 9 m yr^{-1}). Furthermore, we suggest that the very ice-rich cliff wall sections are not exposed to aerobic conditions for very long time periods before being eroded into the Lena River. Thus, aerobic microbial decomposition of the OM at the cliff front is presumably playing only a minor role. Additionally, cliff erosion is mainly driven by thermo-erosion and niche formation at the base of the ice-rich Yedoma cliff, resulting in block failure instead of slow gradual cliff retreat (Fuchs et al., 2020). Accordingly, some of the OM in the cliff may not even become exposed to the air and thaw at all before being eroded into the river. Fuchs et al. (2020) showed an average loss of $5.2 \times 10^6 \text{ kg OC yr}^{-1}$ and $0.4 \times 10^6 \text{ kg N yr}^{-1}$ (2015–2018). For the OC flux sourced from permafrost and peat deposits (and in particular from erosive locations like our study site on Sobo-Sise Island), Wild et al. (2019) estimated $0.9 \times 10^8 \text{ kg C yr}^{-1}$.

By using a biomarker approach (e.g. n -alcohols, n -fatty acids, n -alkanes) on sub-aquatic sediments, van Dongen et al. (2008) found a lower degree of decomposition of the old terrestrial OM released by the great eastern Arctic rivers, including the Lena River, compared to the western Eurasian Arctic. Thus, they predicted greater remineralisation rates and release of carbon dioxide and methane. Our biomarker findings of terrestrial permafrost fit well into this scenario. Winterfeld et al. (2015) studied the lignin phenol composition of the Lena River, Lena Delta and Laptev Sea nearshore zones and proposed that OM decomposition is considerable after permafrost thawing on land and during transport and sedimentation in the water. The present study on the OM origin and the annual OC erosion rates at the Sobo-Sise Yedoma cliff complements ongoing research on mobilisation of permafrost-locked carbon from Late Pleistocene Yedoma deposits, while thermal erosion is a widespread and climate-sensitive phenomenon in the Yedoma domain, covering nearly $5 \times 10^5 \text{ km}^2$ in Siberia and Alaska (Strauss et al., 2021b). This indicates the high potential of thermal erosion for mobilisation and release upon thaw of not only large amounts of carbon but also well-preserved OM into

the aquatic system of the Lena Delta and nearshore Laptev Sea and Arctic Ocean areas, which will affect local but likely also regional biogeochemical cycles in the marine realm (Grotheer et al., 2020; Tanski et al., 2021; Mann et al., 2022) and the shelf seas. Once mobilised and transported into inland waters, permafrost-derived OC can be rapidly used by aquatic microorganisms, increasing OM decomposition in riverine and coastal Arctic waters (Vonk et al., 2012, 2013a, 2015; Drake et al., 2015; Mann et al., 2015). Vonk et al. (2012) studied the organic matter exported from the fast-eroding Yedoma cliff of Muostakh Island, which is located about 120 km south-east of the Sobo-Sise Yedoma cliff. They found that decomposition of Yedoma OM prior to delivery to the ocean was substantial. In their study of OM mobilisation by retrogressive thaw slumps in Canada, Bröder et al. (2021) found that the majority of the exported OC was derived from permafrost deposits. However, they also found that Pleistocene permafrost deposits mostly contained less labile, slowly cycling permafrost OC. Similarly, Bröder et al. (2019) showed that more than half of the carbon transported and deposited on the shelf sea floor likely resists decomposition on a centennial scale while the rest decays relatively slowly. Furthermore, OM mobilised from Pleistocene or Holocene permafrost by rapid thermokarst and mass-wasting processes contribute different shares of particulate and dissolved organic matter (Kokelj et al., 2021; Shakil et al., 2020), which has implications for decomposition and transport. In addition, Karlsson et al. (2011) hypothesised that Yedoma OC, associated with mineral-rich matter from coastal erosion, is ballasted and thus quickly settles to the bottom. Increasing thermokarst and mass-wasting processes, as well as river and coastal erosion, will continue to mobilise both labile and recalcitrant OM from Pleistocene permafrost deposits, and it is still largely unknown what short- and long-term effects this will have on the release of greenhouse gases and alteration of biochemical processes in nearshore waters.

6 Conclusions

Sedimentological and biogeochemical analyses showed that the sediments exposed at the Sobo-Sise Yedoma cliff contain a high TOC content (mean 5 wt %) and well-preserved OM (C/N mean 13.2, mean CPI 9.89) in comparison to other Yedoma permafrost sites. Our study corroborated the palaeoenvironmental data from the Sobo-Sise Yedoma cliff from previous research which suggested that Yedoma formation during the interstadial MIS 3 and the accumulation of the topmost Holocene deposits (MIS 1) were associated with more microbial activity than during the stadial MIS 2. In addition, our findings suggest that mainly high-quality OM has been freeze-locked perennially into permafrost during the Late Pleistocene to Holocene. Although the OM quality seems to be overall fairly high (TOC, C/N and CPI), biomarker parameters indicate a higher level of OM decom-

position for the bottom 7 m (CPI) or even for the bottom 15 m (HPFA) of the cliff profile of MIS 3 age, and less OM accumulation during MIS 2 in contrast to the warmer MIS 3 and 1 sequences is assumed. At the Sobo-Sise Yedoma cliff, representing an example of rapidly eroding permafrost shorelines in the Lena Delta, OM with a high decomposition potential is being mobilised from almost all sections of the cliff profile. This material is suggested to rapidly enter the fluvial and probably also the offshore aquatic ecosystem. Thus, OM mobilisation at the Sobo-Sise Yedoma cliff and similarly eroding permafrost sites bear the potential to impact the carbon dynamics, the biogeochemistry, and the riverine and nearshore marine ecosystems.

Data availability. The data presented in this study are freely available in the PANGAEA data repository (<https://doi.org/10.1594/PANGAEA.935672>, Haugk et al., 2022). Cryolithological and geochronological data from the Sobo-Sise Yedoma cliff are available in PANGAEA (<https://doi.org/10.1594/PANGAEA.919470>, Wetterich et al., 2020b).

Supplement. The supplement related to this article is available online at: <https://doi.org/10.5194/bg-19-2079-2022-supplement>.

Author contributions. CH and JS designed this study and drafted a first version of the manuscript. CH carried out the lipid biomarker analyses and interpretation, with help from LLJ, CK and KM. SW, LS and AK conducted the sampling and field studies. CH, JS and LLJ led the manuscript writing. All co-authors contributed to the manuscript writing process.

Competing interests. The contact author has declared that neither they nor their co-authors have any competing interests.

Disclaimer. Publisher's note: Copernicus Publications remains neutral with regard to jurisdictional claims in published maps and institutional affiliations.

Acknowledgements. This study was carried out within the CACOON project and the joint Russian–German expeditions Lena 2018 and Sobo-Sise 2018 supported by the Samoylov Research Station. We thank Michael Fritz (AWI Potsdam) and Aleksey Aksenov (Arctic and Antarctic Research Institute, St Petersburg) for supporting the permafrost sampling on Sobo-Sise in August 2018. We thank Justin Lindemann (AWI Potsdam) and Anke Sobotta (German Research Centre for Geoscience) as well as Hanno Meyer and Mikaela Weiner (AWI ISOLAB Facility) for support with laboratory analysis.

Financial support. This research has been supported by the Bundesministerium für Bildung und Forschung (grant no. 03F0806A), UK Research and Innovation (grant no. NE/R012806/1) and the Deutsche Forschungsgemeinschaft (grant no. WE4390/7-1).

The article processing charges for this open-access publication were covered by the Alfred Wegener Institute, Helmholtz Centre for Polar and Marine Research (AWI).

Review statement. This paper was edited by Sebastian Naeher and reviewed by two anonymous referees.

References

- Andersson, R. A. and Meyers, P. A.: Effect of climate change on delivery and degradation of lipid biomarkers in a Holocene peat sequence in the Eastern European Russian Arctic, *Org. Geochem.*, 53, 63–72, <https://doi.org/10.1016/j.orggeochem.2012.05.002>, 2012.
- Bray, E. E. and Evans, E. D.: Distribution of n-paraffins as a clue to recognition of source beds, *Geochim. Cosmochim. Ac.*, 22, 2–15, [https://doi.org/10.1016/0016-7037\(61\)90069-2](https://doi.org/10.1016/0016-7037(61)90069-2), 1961.
- Bröder, L., Andersson, A., Tesi, T., Semiletov, I., and Gustafsson, Ö.: Quantifying Degradative Loss of Terrigenous Organic Carbon in Surface Sediments Across the Laptev and East Siberian Sea, *Glob. Biogeochem. Cy.*, 33, 85–99, <https://doi.org/10.1029/2018GB005967>, 2019.
- Canuel, E. A. and Martens, C. S.: Reactivity of recently deposited organic matter: Degradation of lipid compounds near the sediment-water interface, *Geochim. Cosmochim. Ac.*, 60, 1793–1806, [https://doi.org/10.1016/0016-7037\(96\)00045-2](https://doi.org/10.1016/0016-7037(96)00045-2), 1996.
- Chen, J., Günther, F., Grosse, G., Liu, L., and Lin, H.: Sentinel-1 InSAR Measurements of Elevation Changes over Yedoma Uplands on Sobo-Sise Island, Lena Delta, *Remote Sens.*, 10, 1152, <https://doi.org/10.3390/rs10071152>, 2018.
- Costard, F., Gautier, E., Fedorov, A., Konstantinov, P., and Dupeyrat, L.: An Assessment of the Erosion Potential of the Fluvial Thermal Process during Ice Breakups of the Lena River (Siberia), *Permafrost Perigl. Proc.*, 25, 162–171, <https://doi.org/10.1002/ppp.1812>, 2014.
- Cranwell, P. A.: Lipid geochemistry of sediments from Upton Broad, a small productive lake, 7, 25–37, [https://doi.org/10.1016/0146-6380\(84\)90134-7](https://doi.org/10.1016/0146-6380(84)90134-7), 1984.
- Drake, T. W., Wickland, K. P., Spencer, R. G., McKnight, D. M., and Striegl, R. G.: Ancient low-molecular-weight organic acids in permafrost fuel rapid carbon dioxide production upon thaw, *P. Natl. Acad. Sci. USA*, 112, 13946–13951, <https://doi.org/10.1073/pnas.1511705112>, 2015.
- Dutta, K., Schuur, E. A. G., Neff, J. C., and Zimov, S. A.: Potential carbon release from permafrost soils of Northeastern Siberia, *Glob. Change Biol.*, 12, 2336–2351, <https://doi.org/10.1111/j.1365-2486.2006.01259.x>, 2006.
- Eglinton, G. and Hamilton, R. J.: Leaf Epicuticular Waxes, *Science*, 156, 1322–1335, <https://doi.org/10.1126/science.156.3780.1322>, 1967.
- Eglinton, T. I. and Eglinton, G.: Molecular proxies for paleoclimatology, 275, 1–16, <https://doi.org/10.1016/j.epsl.2008.07.012>, 2008.
- Fedorova, I., Chetverova, A., Bolshiyarov, D., Makarov, A., Boike, J., Heim, B., Morgenstern, A., Overduin, P. P., Wegner, C., Kashina, V., Eulenburg, A., Dobrotina, E., and Sidorina, I.: Lena Delta hydrology and geochemistry: long-term hydrological data and recent field observations, *Biogeosciences*, 12, 345–363, <https://doi.org/10.5194/bg-12-345-2015>, 2015.
- Freeman, C., Evans, C. D., Monteith, D. T., Reynolds, B., and Fenner, N.: Export of organic carbon from peat soils, *Nature*, 412, 785–785, <https://doi.org/10.1038/35090628>, 2001.
- Fuchs, M., Grosse, G., Strauss, J., Günther, F., Grigoriev, M., Maximov, G. M., and Hugelius, G.: Carbon and nitrogen pools in thermokarst-affected permafrost landscapes in Arctic Siberia, *Biogeosciences*, 15, 953–971, <https://doi.org/10.5194/bg-15-953-2018>, 2018.
- Fuchs, M., Nitze, I., Strauss, J., Gunther, F., Wetterich, S., Kizyakov, A., Fritz, M., Opel, T., Grigoriev, M. N., Maksimov, G. T., and Grosse, G.: Rapid Fluvio-Thermal Erosion of a Yedoma Permafrost Cliff in the Lena River Delta, *Front. Earth Sci.*, 8, 336, <https://doi.org/10.3389/feart.2020.00336>, 2020.
- Fuchs, M., Ogneva, O., Sanders, T., Schneider, W., Polyakov, V., Becker, O. O., Bolshiyarov, D., Mollenhauer, G., and Strauss, J.: CACOON Sea – water sampling along the Sardakhskaya channel and near shore of the Laptev Sea (chapter 3.26) in: Reports on Polar and Marine Research – Russian-German Cooperation: Expeditions to Siberia in 2019, edited by: Fuchs, M., Bolshiyarov, D., Grigoriev, M. N., Morgenstern, A., Pestryakova, L. A., Tsi-bizov, L., and Dill, A., Alfred Wegener Institute, Bremerhaven, https://doi.org/10.48433/BzPM_0749_2021, 2021.
- Grigoriev, M. N.: Cryomorphogenesis in the Lena Delta, Permafrost Institute Press, Yakutsk, 1993.
- Grosse, G., Schirrmeister, L., Siegert, C., Kunitsky, V. V., Slogoda, E. A., Andreev, A. A., and Dereviagn, A. Y.: Geological and geomorphological evolution of a sedimentary periglacial landscape in Northeast Siberia during the Late Quaternary, *Geomorphology*, 86, 25–51, <https://doi.org/10.1016/j.geomorph.2006.08.005>, 2007.
- Grosse, G., Harden, J., Turetsky, M., McGuire, A. D., Camill, P., Tarnocai, C., Frolking, S., Schuur, E. A. G., Jorgenson, T., Marchenko, S., Romanovsky, V., Wickland, K. P., French, N., Waldrop, M., Bourgeau-Chavez, L., and Striegl, R. G.: Vulnerability of high-latitude soil organic carbon in North America to disturbance, *J. Geophys. Res.-Biogeo.*, 116, G00K06, <https://doi.org/10.1029/2010jg001507>, 2011.
- Grotheer, H., Meyer, V., Riedel, T., Pfalz, G., Mathieu, L., Hefter, J., Gentz, T., Lantuit, H., Mollenhauer, G., and Fritz, M.: Burial and Origin of Permafrost-Derived Carbon in the Nearshore Zone of the Southern Canadian Beaufort Sea, *Geophys. Res. Lett.*, 47, e2019GL085897, <https://doi.org/10.1029/2019GL085897>, 2020.
- Gundelwein, A., Muller-Lupp, T., Sommerkorn, M., Haupt, E. T. K., Pfeiffer, E. M., and Wiechmann, H.: Carbon in tundra soils in the Lake Labaz region of arctic Siberia, *Europ. J. Soil Sci.*, 58, 1164–1174, <https://doi.org/10.1111/j.1365-2389.2007.00908.x>, 2007.
- Gunstone, F. D. and Harwood, J. L.: Occurrence and characterisation of oils and fats, in: *The lipid handbook*, edited by: Gunstone,

- F. D., Harwood, J. L., and Dijkstra, A. J., CRC press (Taylor Francis Group), 51–156, 2007.
- Günther, F., Overduin, P. P., Sandakov, A. V., Grosse, G., and Grigoriev, M. N.: Short- and long-term thermo-erosion of ice-rich permafrost coasts in the Laptev Sea region, *Biogeosciences*, 10, 4297–4318, <https://doi.org/10.5194/bg-10-4297-2013>, 2013.
- Günther, F., Overduin, P. P., Yakshina, I. A., Opel, T., Baranskaya, A. V., and Grigoriev, M. N.: Observing Muostakh disappear: permafrost thaw subsidence and erosion of a ground-ice-rich island in response to arctic summer warming and sea ice reduction, *The Cryosphere*, 9, 151–178, <https://doi.org/10.5194/tc-9-151-2015>, 2015.
- Haugk, C., Jongejans, L. L., Mangelsdorf, K., Fuchs, M., Ogneva, O., Palmtag, J., Mollenhauer, G., Mann, P. J., Overduin, P. P., Grosse, G., Sanders, T., Tuerena, R. E., Schirrmeister, L., Wetterich, S., Kizyakov, A., Karger, C., and Strauss, J.: Organic matter characteristics using lipid biomarker analysis of a rapidly eroding permafrost cliff, PANGAEA [data set], <https://doi.org/10.1594/PANGAEA.935672>, 2022.
- Hedges, J. I. and Keil, R. G.: Sedimentary organic matter preservation: an assessment and speculative synthesis, *Mar. Chem.*, 49, 81–115, [https://doi.org/10.1016/0304-4203\(95\)00008-F](https://doi.org/10.1016/0304-4203(95)00008-F), 1995.
- Höfle, S., Rethemeyer, J., Mueller, C. W., and John, S.: Organic matter composition and stabilization in a polygonal tundra soil of the Lena Delta, *Biogeosciences*, 10, 3145–3158, <https://doi.org/10.5194/bg-10-3145-2013>, 2013.
- Holmes, R. M., McClelland, J. W., Peterson, B. J., Tank, S. E., Buluygina, E., Eglinton, T. I., Gordeev, V. V., Gurtovaya, T. Y., Raymond, P. A., Repeta, D. J., Staples, R., Striegl, R. G., Zhulidov, A. V., and Zimov, S. A.: Seasonal and Annual Fluxes of Nutrients and Organic Matter from Large Rivers to the Arctic Ocean and Surrounding Seas, *Estuar. Coasts*, 35, 369–382, <https://doi.org/10.1007/s12237-011-9386-6>, 2012.
- Holmes, R. M., Shiklomanov, A. I., Suslova, A., Tretiakov, M., McClelland, J. W., Scott, L., Spencer, R. G. M., and Tank, S. E.: River Discharge: <https://arctic.noaa.gov/Report-Card/Report-Card-2021/ArtMID/8022/ArticleID/953/River-Discharge> (last access: 14 March 2022), 2021.
- Hugelius, G., Strauss, J., Zubrzycki, S., Harden, J. W., Schuur, E. A. G., Ping, C.-L., Schirrmeister, L., Grosse, G., Michaelson, G. J., Koven, C. D., O'Donnell, J. A., Elberling, B., Mishra, U., Camill, P., Yu, Z., Palmtag, J., and Kuhry, P.: Estimated stocks of circumpolar permafrost carbon with quantified uncertainty ranges and identified data gaps, *Biogeosciences*, 11, 6573–6593, <https://doi.org/10.5194/bg-11-6573-2014>, 2014.
- IPCC: Special Report on the Ocean and Cryosphere in a Changing Climate, Intergov, Panel on Climate Change, Monaco, <https://doi.org/10.1017/9781009157964>, 2019.
- Jongejans, L. L., Strauss, J., Lenz, J., Peterse, F., Mangelsdorf, K., Fuchs, M., and Grosse, G.: Organic matter characteristics in yedoma and thermokarst deposits on Baldwin Peninsula, west Alaska, *Biogeosciences*, 15, 6033–6048, <https://doi.org/10.5194/bg-15-6033-2018>, 2018.
- Jongejans, L. L., Mangelsdorf, K., Schirrmeister, L., Grigoriev, M. N., Maksimov, G. M., Biskaborn, B. K., Grosse, G., and Strauss, J.: *n*-Alkane Characteristics of Thawed Permafrost Deposits Below a Thermokarst Lake on Bykovsky Peninsula, Northeastern Siberia, *Front. Environ. Sci.*, 8, 118, <https://doi.org/10.3389/fenvs.2020.00118>, 2020.
- Juggins, S.: Package: rioja: Analysis of Quaternary Science Data, 2019.
- Kaneda, T.: Iso- and anteiso-fatty acids in bacteria: biosynthesis, function, and taxonomic significance, *Microbiol. Rev.*, 55, 288–302, <https://doi.org/10.1128/mr.55.2.288-302.1991>, 1991.
- Kanevskiy, M., Shur, Y., Strauss, J., Jorgenson, T., Fortier, D., Stephani, E., and Vasiliev, A.: Patterns and rates of riverbank erosion involving ice-rich permafrost (yedoma) in northern Alaska, *Geomorphology*, 253, 370–384, <https://doi.org/10.1016/j.geomorph.2015.10.023>, 2016.
- Karlsson, E. S., Charkin, A., Dudarev, O., Semiletov, I., Vonk, J. E., Sánchez-García, L., Andersson, A., and Gustafsson, Ö.: Carbon isotopes and lipid biomarker investigation of sources, transport and degradation of terrestrial organic matter in the Buor-Khaya Bay, SE Laptev Sea, *Biogeosciences*, 8, 1865–1879, <https://doi.org/10.5194/bg-8-1865-2011>, 2011.
- Killops, S. D. and Killops, V. J.: Introduction to organic geochemistry, John Wiley & Sons, New York, 393 pp., 2013.
- Kim, S., Stanford, L., Rodgers, R., Marshall, A., Walters, C., Qian, K., Wenger, L., and Mankiewicz, P.: Microbial Alteration of the Acidic and Neutral Polar NSO Compounds Revealed by Fourier Transform Ion Cyclotron Resonance Mass Spectrometry, *Org. Geochem.*, 36, 1117–1134, <https://doi.org/10.1016/j.orggeochem.2005.03.010>, 2005.
- Kokelj, S. V., Kokoszka, J., van der Sluijs, J., Rudy, A. C. A., Tunnicliffe, J., Shakil, S., Tank, S. E., and Zolkos, S.: Thaw-driven mass wasting couples slopes with downstream systems, and effects propagate through Arctic drainage networks, *The Cryosphere*, 15, 3059–3081, <https://doi.org/10.5194/tc-15-3059-2021>, 2021.
- Kuhn, T. K., Krull, E. S., Bowater, A., Grice, K., and Gleixner, G.: The occurrence of short chain n-alkanes with an even over odd predominance in higher plants and soils, 41, 88–95, doi:10.1016/j.orggeochem.2009.08.003, 2010.
- Lützow, M. v., Kögel-Knabner, I., Ekschmitt, K., Matzner, E., Guggenberger, G., Marschner, B., and Flessa, H.: Stabilization of organic matter in temperate soils: mechanisms and their relevance under different soil conditions – a review, *Europ. J. Soil Sci.*, 57, 426–445, <https://doi.org/10.1111/j.1365-2389.2006.00809.x>, 2006.
- Mann, P. J., Eglinton, T. I., McIntyre, C. P., Zimov, N., Davydova, A., Vonk, J. E., Holmes, R. M., and Spencer, R. G.: Utilization of ancient permafrost carbon in headwaters of Arctic fluvial networks, *Nat. Commun.*, 6, 7856, <https://doi.org/10.1038/ncomms8856>, 2015.
- Mann, P. J., Strauss, J., Palmtag, J., Dowdy, K., Ogneva, O., Fuchs, M., Bedington, M., Torres, R., Polimene, L., Overduin, P., Mollenhauer, G., Grosse, G., Rachold, V., Sobczak, W. V., Spencer, R. G. M., and Juhls, B.: Degrading permafrost river catchments and their impact on Arctic Ocean nearshore processes, *Ambio*, 51, 439–455, <https://doi.org/10.1007/s13280-021-01666-z>, 2022.
- Marzi, R., Torkelson, B. E., and Olson, R. K.: A Revised Carbon Preference Index, *Org. Geochem.*, 20, 1303–1306, [https://doi.org/10.1016/0146-6380\(93\)90016-5](https://doi.org/10.1016/0146-6380(93)90016-5), 1993.
- Mishra, U., Hugelius, G., Shelef, E., Yang, Y., Strauss, J., Lupachev, A., Harden, J. W., Jastrow, J. D., Ping, C. L., Riley, W. J., Schuur, E. A. G., Matamala, R., Siewert, M., Nave, L. E., Koven, C.

- D., Fuchs, M., Palmtag, J., Kuhry, P., Treat, C. C., Zubrzycki, S., Hoffman, F. M., Elberling, B., Camill, P., Veremeeva, A., and Orr, A.: Spatial heterogeneity and environmental predictors of permafrost region soil organic carbon stocks, *Sci. Adv.*, 7, eaz5236, <https://doi.org/10.1126/sciadv.aaz5236>, 2021.
- Mollenhauer, G., Grotheer, H., Torben, G., Bonk, E., and Hefter, J.: Standard operation procedures and performance of the MICADAS radiocarbon laboratory at Alfred Wegener Institute (AWI), Germany, *Nuclear Instruments and Methods in Physics Research Section B: Beam Interactions with Materials and Atoms*, 496, 45–51, <https://doi.org/10.1016/j.nimb.2021.03.016>, 2021.
- Morgenstern, A., Grosse, G., Gunther, F., Fedorova, I., and Schirrmeyer, L.: Spatial analyses of thermokarst lakes and basins in Yedoma landscapes of the Lena Delta, *Cryosphere*, 5, 849–867, <https://doi.org/10.5194/tc-5-849-2011>, 2011.
- Mueller, C. W., Rethemeyer, J., Kao-Kniffin, J., Löppmann, S., Hinkel, K. M., and G Bockheim, J.: Large amounts of labile organic carbon in permafrost soils of northern Alaska, *Global Change Biol.*, 21, 2804–2817, <https://doi.org/10.1111/gcb.12876>, 2015.
- Nitzbon, J., Westermann, S., Langer, M., Martin, L. C. P., Strauss, J., Laboor, S., and Boike, J.: Fast response of cold ice-rich permafrost in northeast Siberia to a warming climate, *Nat. Commun.*, 11, 2201, <https://doi.org/10.1038/s41467-020-15725-8>, 2020.
- Nitze, I. and Grosse, G.: Detection of landscape dynamics in the Arctic Lena Delta with temporally dense Landsat time-series stacks, *Remote Sens. Environ.*, 181, 27–41, <https://doi.org/10.1016/j.rse.2016.03.038>, 2016.
- Palmtag, J., Hugelius, G., Lashchinskiy, N., Tamstorf, M. P., Richter, A., Elberling, B., and Kuhry, P.: Storage, Landscape Distribution, and Burial History of Soil Organic Matter in Contrasting Areas of Continuous Permafrost, *Arct. Antarct. Alp. Res.*, 47, 71–88, <https://doi.org/10.1657/AAAR0014-027>, 2015.
- Poynter, J. G.: Molecular stratigraphy: The recognition of palaeoclimatic signals in organic geochemical data, PhD, School of Chemistry, University of Bristol, Bristol, 324 pp., 1989.
- Radke, M., Willsch, H., and Welte, D. H.: Preparative hydrocarbon group type determination by automated medium pressure liquid chromatography, *Anal. Chem.*, 52, 406–411, <https://doi.org/10.1021/ac50053a009>, 1980.
- Rieley, G., Collier, R., Jones, D., and Eglinton, G.: The biogeochemistry of Ellesmere Lake, UK – I: source correlation of leaf wax inputs to the sedimentary lipid record, *Org. Geochem.*, 17, 901–912, [https://doi.org/10.1016/0146-6380\(91\)90031-E](https://doi.org/10.1016/0146-6380(91)90031-E), 1991.
- Rilfors, L., Wieslander, A., and Ståhl, S.: Lipid and protein composition of membranes of *Bacillus megaterium* variants in the temperature range 5 to 70°C, *J. Bacteriol.*, 135, 1043–1052, <https://doi.org/10.1128/jb.135.3.1043-1052.1978>, 1978.
- Sánchez-García, L., Vonk, J. E., Charkin, A. N., Kosmach, D., Dudarev, O. V., Semiletov, I. P., and Gustafsson, Ö.: Characterisation of three regimes of collapsing Arctic Ice Complex deposits on the SE Laptev Sea coast using biomarkers and dual carbon isotopes, *Permafrost Periglac.*, 25, 172–183, <https://doi.org/10.1002/ppp.1815>, 2014.
- Sanders, T., Fiencke, C., Fuchs, M., Haugk, C., Juhls, B., Mollenhauer, G., Ogneva, O., Overduin, P., Palmtag, J., Povazhnyi, V., Strauss, J., Tuerena, R., Zell, N., and Dähnke, K.: Seasonal nitrogen fluxes of the Lena River Delta, *Ambio*, 51, 423–438, <https://doi.org/10.1007/s13280-021-01665-0>, 2022.
- Schäfer, I. K., Lanny, V., Franke, J., Eglinton, T. I., Zech, M., Vysloužilová, B., and Zech, R.: Leaf waxes in litter and topsoils along a European transect, *SOIL*, 2, 551–564, <https://doi.org/10.5194/soil-2-551-2016>, 2016.
- Schirrmeyer, L., Siegert, C., Kuznetsova, T., Kuzmina, S., Andreev, A., Kienast, F., Meyer, H., and Bobrov, A.: Paleoenvironmental and paleoclimatic records from permafrost deposits in the Arctic region of Northern Siberia, *Quat. Int.*, 89, 97–118, [https://doi.org/10.1016/S1040-6182\(01\)00083-0](https://doi.org/10.1016/S1040-6182(01)00083-0), 2002.
- Schirrmeyer, L., Grosse, G., Wetterich, S., Overduin, P. P., Strauss, J., Schuur, E. A. G., and Hubberten, H.-W.: Fossil organic matter characteristics in permafrost deposits of the north-east Siberian Arctic, *J. Geophys. Res.-Bioge.*, 116, G00M02, <https://doi.org/10.1029/2011jg001647>, 2011a.
- Schirrmeyer, L., Kunitsky, V., Grosse, G., Wetterich, S., Meyer, H., Schwamborn, G., Babiy, O., Derevyagin, A., and Siegert, C.: Sedimentary characteristics and origin of the Late Pleistocene Ice Complex on north-east Siberian Arctic coastal lowlands and islands – A review, *Quat. Int.*, 241, 3–25, <https://doi.org/10.1016/j.quaint.2010.04.004>, 2011b.
- Schirrmeyer, L.: Late Glacial to Holocene landscape dynamics of Arctic coastal lowlands in NE Siberia, *Quat. Int.*, 279, p. 434, <https://doi.org/10.1016/j.quaint.2012.08.1413>, 2012.
- Schirrmeyer, L., Froese, D. G., Tumskey, V., Grosse, G., and Wetterich, S.: Yedoma: Late Pleistocene ice-rich syngenetic permafrost of Beringia, in: *Encyclopedia of Quaternary Sciences*, 2 Edn., edited by: Elias, S. A., Elsevier, Amsterdam, 542–552, 2013.
- Schirrmeyer, L., Dietze, E., Matthes, H., Grosse, G., Strauss, J., Laboor, S., Ulrich, M., Kienast, F., and Wetterich, S.: The genesis of Yedoma Ice Complex permafrost – grain-size endmember modeling analysis from Siberia and Alaska, *Quat. Sci. J.*, 69, 33–53, <https://doi.org/10.5194/egqsj-69-33-2020>, 2020.
- Schneider, J., Grosse, G., and Wagner, D.: Land cover classification of tundra environments in the Arctic Lena Delta based on Landsat 7 ETM+ data and its application for upscaling of methane emissions, *Remote Sens. Environ.*, 113, 380–391, <https://doi.org/10.1016/j.rse.2008.10.013>, 2009.
- Schulte, S., Mangelsdorf, K., and Rullkötter, J.: Organic matter preservation on the Pakistan continental margin as revealed by biomarker geochemistry, *Org. Geochem.*, 31, 1005–1022, [https://doi.org/10.1016/S0146-6380\(00\)00108-X](https://doi.org/10.1016/S0146-6380(00)00108-X), 2000.
- Schuur, E. A. G., Bockheim, J., Canadell, J. G., Euskirchen, E., Field, C. B., Goryachkin, S. V., Hagemann, S., Kuhry, P., Laflour, P. M., and Lee, H.: Vulnerability of permafrost carbon to climate change: Implications for the global carbon cycle, *BioScience*, 58, 701–714, <https://doi.org/10.1641/B580807>, 2008.
- Schwamborn, G., Rachold, V., and Grigoriev, M. N.: Late Quaternary sedimentation history of the Lena Delta, *Quat. Int.*, 89, 119–134, [https://doi.org/10.1016/S1040-6182\(01\)00084-2](https://doi.org/10.1016/S1040-6182(01)00084-2), 2002.
- Semiletov, I., Pipko, I., Gustafsson, Ö., Anderson, L. G., Sergienko, V., Pugach, S., Dudarev, O., Charkin, A., Gukov, A., Bröder, L., Andersson, A., Spivak, E., and Shakhova, N.: Acidification of East Siberian Arctic Shelf waters through addition of freshwater and terrestrial carbon, *Nat. Geosci.*, 9, 361–365, <https://doi.org/10.1038/ngeo2695>, 2016.

- Shakil, S., Tank, S. E., Kokelj, S. V., Vonk, J. E., and Zolkos, S.: Particulate dominance of organic carbon mobilization from thaw slumps on the Peel Plateau, NT: Quantification and implications for stream systems and permafrost carbon release, *Environ. Res. Lett.*, 15, 114019, <https://doi.org/10.1088/1748-9326/abac36>, 2020.
- Stapel, J. G., Schirrmeister, L., Overduin, P. P., Wetterich, S., Strauss, J., Horsfield, B., and Mangelsdorf, K.: Microbial lipid signatures and substrate potential of organic matter in permafrost deposits – implications for future greenhouse gas production, *J. Geophys. Res.-Biogeo.*, 121, 2652–2666, <https://doi.org/10.1002/2016JG003483>, 2016.
- Stettner, S., Beamish, A. L., Bartsch, A., Heim, B., Grosse, G., Roth, A., and Lantuit, H.: Monitoring Inter- and Intra-Seasonal Dynamics of Rapidly Degrading Ice-Rich Permafrost Riverbanks in the Lena Delta with TerraSAR-X Time Series, *Remote Sens.*, 10, 51, <https://doi.org/10.3390/rs10010051>, 2018.
- Strauss, J., Schirrmeister, L., Wetterich, S., Borchers, A., and Davydov, S. P.: Grain-size properties and organic-carbon stock of Yedoma Ice Complex permafrost from the Kolyma lowland, northeastern Siberia, *Glob. Biogeochem. Cy.*, 26, GB3003, <https://doi.org/10.1029/2011GB004104>, 2012.
- Strauss, J., Schirrmeister, L., Grosse, G., Wetterich, S., Ulrich, M., Herzschuh, U., and Hubberten, H.-W.: The deep permafrost carbon pool of the Yedoma region in Siberia and Alaska, *Geophys. Res. Lett.*, 40, 6165–6170, <https://doi.org/10.1002/2013GL058088>, 2013.
- Strauss, J., Schirrmeister, L., Mangelsdorf, K., Eichhorn, L., Wetterich, S., and Herzschuh, U.: Organic-matter quality of deep permafrost carbon – a study from Arctic Siberia, *Biogeosciences*, 12, 2227–2245, <https://doi.org/10.5194/bg-12-2227-2015>, 2015.
- Strauss, J., Schirrmeister, L., Grosse, G., Fortier, D., Hugelius, G., Knoblauch, C., Romanovsky, V., Schädel, C., Schneider von Deimling, T., Schuur, E. A. G., Shmelev, D., Ulrich, M., and Veremeeva, A.: Deep Yedoma permafrost: A synthesis of depositional characteristics and carbon vulnerability, *Earth-Sci. Rev.*, 172, 75–86, <https://doi.org/10.1016/j.earscirev.2017.07.007>, 2017.
- Strauss, J., Laboor, S., Schirrmeister, L., Grosse, G., Fortier, D., Hugelius, G., Knoblauch, C., Romanovsky, V. E., Schädel, C., Schneider von Deimling, T., Schuur, E. A. G., Shmelev, D., Ulrich, M., and Veremeeva, A.: Geochemical, lithological, and geochronological characteristics of sediment samples from Yedoma and thermokarst deposits in Siberia and Alaska 1998–2016, *PANGAEA*, <https://doi.org/10.1594/PANGAEA.919062>, 2020.
- Strauss, J., Abbott, B., Hugelius, G., Schuur, E. A. G., Treat, C., Fuchs, M., Schädel, C., Ulrich, M., Turetsky, M. R., Keuschnig, M., Biasi, C., Yang, Y., and Grosse, G.: Permafrost, in: *Recarbonizing global soils – A technical manual of recommended management practices*, edited by: Food and Agriculture Organization of the United Nations (FAO), and Intergovernmental Technical Panel on Soils (ITPS), Food and Agriculture Organization of the United Nations, Rome, Italy, 127–147, 2021a.
- Strauss, J., Laboor, S., Schirrmeister, L., Fedorov, A. N., Fortier, D., Froese, D., Fuchs, M., Günther, F., Grigoriev, M., Harden, J., Hugelius, G., Kanevskiy, M., Kholodov, A., Kunitsky, V., Kraev, G., Lozhkin, A., Rivkina, E., Shur, Y., Siegert, C., Spektor, V., Streletskaya, I., Ulrich, M., Vartanyan, S., Veremeeva, A., Walter Anthony, K., Zimov, N., and Grosse, G.: Circum-Arctic Map of the Yedoma Permafrost Domain, *Front. Earth Sci.*, 758360, <https://doi.org/10.3389/feart.2021.758360>, 2021b.
- Struck, J., Bliedtner, M., Strobel, P., Schumacher, J., Bazarradnaa, E., and Zech, R.: Leaf wax *n*-alkane patterns and compound-specific $\delta^{13}\text{C}$ of plants and topsoils from semi-arid and arid Mongolia, *Biogeosciences*, 17, 567–580, <https://doi.org/10.5194/bg-17-567-2020>, 2020.
- Tanski, G., Bröder, L., Wagner, D., Knoblauch, C., Lantuit, H., Beer, C., Sachs, T., Fritz, M., Tesi, T., Koch, B. P., Haghypour, N., Eglinton, T. I., Strauss, J., and Vonk, J. E.: Permafrost Carbon and CO₂ Pathways Differ at Contrasting Coastal Erosion Sites in the Canadian Arctic, *Front. Earth Sci.*, 9, 630493, <https://doi.org/10.3389/feart.2021.630493>, 2021.
- Turetsky, M. R., Abbott, B. W., Jones, M. C., Anthony, K. W., Olefeldt, D., Schuur, E. A. G., Grosse, G., Kuhry, P., Hugelius, G., Koven, C., Lawrence, D. M., Gibson, C., Sannel, A. B. K., and McGuire, A. D.: Carbon release through abrupt permafrost thaw, *Nat. Geosci.*, 13, 138–143, <https://doi.org/10.1038/s41561-019-0526-0>, 2020.
- van Dongen, B. E., Semiletov, I., Weijers, J. W. H., and Gustafsson, O. R.: Contrasting lipid biomarker composition of terrestrial organic matter exported from across the Eurasian Arctic by the five great Russian Arctic rivers, *Global Biogeochem. Cy.*, 22, GB1011, <https://doi.org/10.1029/2007gb002974>, 2008.
- Vonk, J. E., Sánchez-García, L., Dongen, B. E. van, Alling, V., Kosmach, D., Charkin, A., Semiletov, I. P., Dudarev, O. V., Shakhova, N., Roos, P., Eglinton, T. I., Andersson, A., and Gustafsson, Ö.: Activation of old carbon by erosion of coastal and subsea permafrost in Arctic Siberia, *Nature*, 489, 137–140, <https://doi.org/10.1038/nature11392>, 2012.
- Vonk, J. E., Mann, P. J., Davydov, S., Davydova, A., Spencer, R. G. M., Schade, J., Sobczak, W. V., Zimov, N., Zimov, S., Bulygina, E., Eglinton, T. I., and Holmes, R. M.: High biolability of ancient permafrost carbon upon thaw, *Geophys. Res. Lett.*, 40, 2689–2693, <https://doi.org/10.1002/grl.50348>, 2013a.
- Vonk, J. E., Mann, P. J., Dowdy, K. L., Davydova, A., Davydov, S. P., Zimov, N., Spencer, R. G. M., Bulygina, E. B., Eglinton, T. I., and Holmes, R. M.: Dissolved organic carbon loss from Yedoma permafrost amplified by ice wedge thaw, *Environ. Res. Lett.*, 8, 035023, <https://doi.org/10.1088/1748-9326/8/3/035023>, 2013b.
- Vonk, J. E., Tank, S. E., Bowden, W. B., Laurion, I., Vincent, W. F., Alekseychik, P., Amyot, M., Billet, M. F., Canário, J., Cory, R. M., Deshpande, B. N., Helbig, M., Jammet, M., Karlsson, J., Larouche, J., MacMillan, G., Rautio, M., Walter Anthony, K. M., and Wickland, K. P.: Reviews and syntheses: Effects of permafrost thaw on Arctic aquatic ecosystems, *Biogeosciences*, 12, 7129–7167, <https://doi.org/10.5194/bg-12-7129-2015>, 2015.
- Wetterich, S., Kuzmina, S., Andreev, A. A., Kienast, F., Meyer, H., Schirrmeister, L., Kuznetsova, T., and Sierralta, M.: Palaeoenvironmental dynamics inferred from late Quaternary permafrost deposits on Kurungnakh Island, Lena Delta, Northeast Siberia, Russia, *Quat. Sci. Rev.*, 27, 1523–1540, <https://doi.org/10.1016/j.quascirev.2008.04.007>, 2008.
- Wetterich, S., Schirrmeister, L., Andreev, A. A., Pudenz, M., Plessen, B., Meyer, H., and Kunitsky, V. V.: Eemian and Late Glacial/Holocene palaeoenvironmental records from permafrost sequences at the Dmitry Laptev Strait

- (NE Siberia, Russia), *Palaeogeogr. Palaeoclimatol.*, 279, 73–95, <https://doi.org/10.1016/j.palaeo.2009.05.002>, 2009.
- Wetterich, S., Tumskov, V., Rudaya, N., Andreev, A. A., Opel, T., Meyer, H., Schirrmeister, L., and Hüls, M.: Ice Complex formation in Arctic East Siberia during the MIS3 Interstadial, *Quat. Sci. Rev.*, 84, 39–55, <https://doi.org/10.1016/j.quascirev.2013.11.009>, 2014.
- Wetterich, S., Kizyakov, A., Fritz, M., Aksenov, A., Schirrmeister, L., and Opel, T.: Expedition Report: Permafrost research on Sobo-Sise Island (Lena Delta), Reports on Polar and Marine Research, 102–113, https://doi.org/10.2312/BzPM_0734_2019, 2018.
- Wetterich, S., Kizyakov, A., Fritz, M., Wolter, J., Mollenhauer, G., Meyer, H., Fuchs, M., Aksenov, A., Matthes, H., Schirrmeister, L., and Opel, T.: The cryostratigraphy of the Yedoma cliff of Sobo-Sise Island (Lena delta) reveals permafrost dynamics in the central Laptev Sea coastal region during the last 52 kyr, *The Cryosphere*, 14, 4525–4551, <https://doi.org/10.5194/tc-14-4525-2020>, 2020a.
- Wetterich, S., Meyer, H., Fritz, M., Opel, T., and Schirrmeister, L.: Cryolithology of the Sobo-Sise Yedoma cliff (eastern Lena Delta), PANGAEA [data set], <https://doi.org/10.1594/PANGAEA.919470>, 2020b.
- Wetterich, S., Rudaya, N., Nazarova, L., Strykh, L., Pavlova, M., Palagushkina, O., Kizyakov, A., Wolter, J., Kuznetsova, T., Aksenov, A., Stoof-Leichsenring, K. R., Schirrmeister, L., and Fritz, M.: Paleo-Ecology of the Yedoma Ice Complex on Sobo-Sise Island (Eastern Lena Delta, Siberian Arctic), *Front. Earth Sci.*, 9, 681511, <https://doi.org/10.3389/feart.2021.681511>, 2021.
- Wild, B., Andersson, A., Bröder, L., Vonk, J., Hugelius, G., McClelland, J. W., Song, W., Raymond, P. A., and Gustafsson, Ö.: Rivers across the Siberian Arctic unearth the patterns of carbon release from thawing permafrost, *P. Natl. Acad. Sci. USA*, 116, 10280–10285, <https://doi.org/10.1073/pnas.1811797116>, 2019.
- Winterfeld, M., Goñi, M. A., Just, J., Hefter, J., and Mollenhauer, G.: Characterization of particulate organic matter in the Lena River delta and adjacent nearshore zone, NE Siberia – Part 2: Lignin-derived phenol compositions, *Biogeosciences*, 12, 2261–2283, <https://doi.org/10.5194/bg-12-2261-2015>, 2015.
- Yang, D., Liu, B., and Ye, B.: Stream temperature changes over Lena River Basin in Siberia, *Geophys. Res. Lett.*, 32, L05401, <https://doi.org/10.1029/2004GL021568>, 2005.
- Zech, M., Bugge, B., Leiber-Sauheitl, K., Markovic, S., Glaser, B., Hambach, U., Huwe, B., Stevens, T., Sümegi, P., Wiesenberg, G., and Zöller, L.: Reconstructing Quaternary vegetation history in the Carpathian Basin, SE Europe, using *n*-alkane biomarkers as molecular fossils, *Eiszeitalter und Gegenwart, Quat. Sci.*, 58, 148–155, <https://doi.org/10.5167/uzh-76606>, 2009.
- Zech, M., Andreev, A., Zech, R., Müller, S., Hambach, U., Frechen, M., and Zech, W.: Quaternary vegetation changes derived from a loess-like permafrost palaeosol sequence in northeast Siberia using alkane biomarker and pollen analyses, *Boreas*, 39, 540–550, <https://doi.org/10.1111/j.1502-3885.2009.00132.x>, 2010.
- Zhang, X., Bianchi, T., Cui, X., Rosenheim, B., Ping, C.-L., Hanna, A., Kanevskiy, M., Schreiner, K., and Allison, M.: Permafrost Organic Carbon Mobilization From the Watershed to the Colville River Delta: Evidence From ¹⁴C Ramped Pyrolysis and Lignin Biomarkers: Permafrost OC Transport in Coville River, *Geophys. Res. Lett.*, 44, 11491–11500, <https://doi.org/10.1002/2017GL075543>, 2017.
- Zhang, X., Bianchi, T. S., Hanna, A. J. M., Shields, M. R., Izon, G., Hutchings, J. A., Ping, C.-L., Kanevskiy, M., Haghypour, N., and Eglinton, T. I.: Recent Warming Fuels Increased Organic Carbon Export From Arctic Permafrost, *AGU Adv.*, 2, e2021AV000396, <https://doi.org/10.1029/2021AV000396>, 2021.


Degrading permafrost river catchments and their impact on Arctic
Ocean nearshore processes

Mann, P. J., Strauss, J., Palmtag, J., Dowdy, K., **Ogneva, O.**, Fuchs, M., Bedington, M., Torres, R., Polimene, L., Overduin, P. P., Mollenhauer, G., Grosse, G., Rachold, V., Sobczak, W., Spencer, R. G. and Juhls, B. (2022)

Published in *Ambio*

<https://doi.org/1007/s13280-021-01666-z>

Degrading permafrost river catchments and their impact on Arctic Ocean nearshore processes

Paul J. Mann , Jens Strauss, Juri Palmtag, Kelsey Dowdy, Olga Ogneva, Matthias Fuchs, Michael Bedington, Ricardo Torres, Luca Polimene, Paul Overduin, Gesine Mollenhauer, Guido Grosse, Volker Rachold, William V. Sobczak, Robert G. M. Spencer, Bennet Juhls

Received: 12 May 2021 / Revised: 15 October 2021 / Accepted: 1 November 2021 / Published online: 30 November 2021

Abstract Arctic warming is causing ancient perennially frozen ground (permafrost) to thaw, resulting in ground collapse, and reshaping of landscapes. This threatens Arctic peoples' infrastructure, cultural sites, and land-based natural resources. Terrestrial permafrost thaw and ongoing intensification of hydrological cycles also enhance the amount and alter the type of organic carbon (OC) delivered from land to Arctic nearshore environments. These changes may affect coastal processes, food web dynamics and marine resources on which many traditional ways of life rely. Here, we examine how future projected increases in runoff and permafrost thaw from two permafrost-dominated Siberian watersheds—the Kolyma and Lena, may alter carbon turnover rates and OC distributions through river networks. We demonstrate that the unique composition of terrestrial permafrost-derived OC can cause significant increases to aquatic carbon degradation rates (20 to 60% faster rates with 1% permafrost OC). We compile results on aquatic OC degradation and examine how strengthening Arctic hydrological cycles may increase the connectivity between terrestrial landscapes and receiving nearshore ecosystems, with potential ramifications for coastal carbon budgets and ecosystem structure. To address the future challenges Arctic coastal communities will face, we argue that it will become essential to consider how nearshore ecosystems will respond to changing coastal inputs and identify how these may affect the resiliency and availability of essential food resources.

Keywords Arctic rivers · Carbon cycle · Carbon fluxes · Erosion

INTRODUCTION

The Arctic region is experiencing unprecedented change to its physical environment in response to global climate disruptions, causing a multitude of social, geopolitical and ecosystem instabilities. One of the greatest challenges facing the region is due to the loss of permafrost-perennially frozen ground that remains at or below 0 °C for at least two consecutive years (Van Everdingen 2005). Almost five million people live and rely on permafrost ground across the Arctic (4.9 million in 2017; Ramage et al. 2021) and are susceptible to on-going surface permafrost thaw in response to warming Arctic air temperatures (Biskaborn et al. 2019). Loss of terrestrial permafrost causes direct damage to essential infrastructure and impacts upon the livelihoods and culture of local people (Ford and Pearce 2010; Fig. 1). Food and water security have been, and will be, negatively impacted by changes in lake, river and shore-fast ice, as well as permafrost in many Arctic regions (Strauss et al. 2021a). These changes have disrupted access to herding, hunting, and fishing grounds (Fig. 1), and caused the instability of agricultural land (IPCC 2019).

Terrestrial permafrost thaw across river catchments can liberate peat and permafrost-derived OC from soils to inland aquatic ecosystems (Frey and Smith 2005; Wild et al. 2019), modifying stream food web dynamics by changing nutrient or carbon availabilities to aquatic microorganisms (Slavik et al. 2004). Permafrost, specifically ice- and organic-rich Yedoma permafrost (Fig. 2 insets, Yedoma definition in Strauss et al. 2021a, b), has been shown to be of 'high quality' for microbial

Supplementary Information The online version contains supplementary material available at <https://doi.org/10.1007/s13280-021-01666-z>.

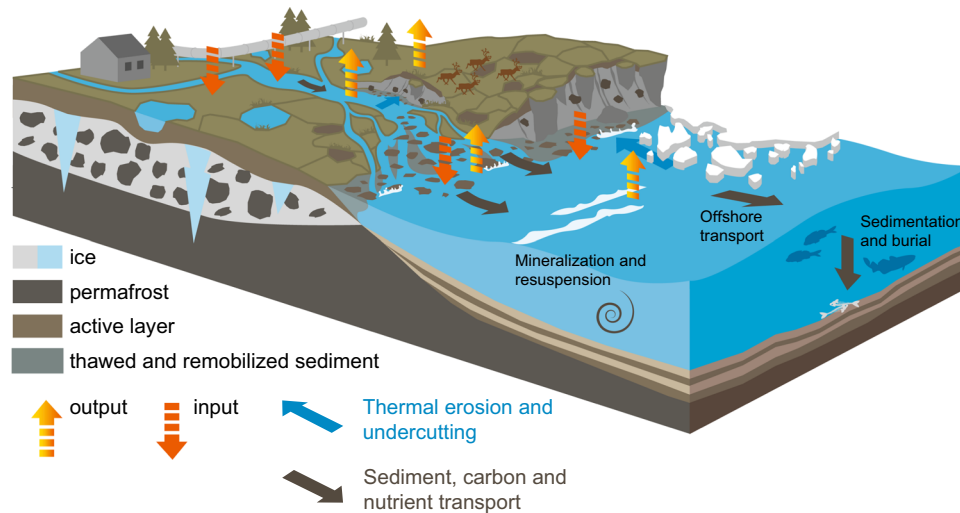


Fig. 1 Future response of nearshore environments to climate change, and potential impacts to ecosystem processes and coastal biogeochemistry. Terrestrial permafrost thaw causes landscape collapse and changing resources, affecting terrestrial infrastructure (drawn as house and pipeline) and distributions of food and traditional lands (represented by reindeer on land). Permafrost thaw on land can affect terrestrial gas fluxes, or be mobilised into freshwaters, affecting OC reactivity and carbon budgets from the river, delta or gulf regions (input/output arrows). Changing terrestrial OC supply (black arrows) may influence nearshore carbon, nutrient budgets, and food web dynamics, altering air-sea gas fluxes (coastal inputs/outputs/processes) or essential coastal food resources (represented as fish/whale). Drawn by Yves Nowak (AWI)



Fig. 2 Permafrost (after Obu et al. 2019) and Yedoma permafrost (Strauss et al. 2021a, b) distribution (map) with two sites of rapidly eroding cliffs as examples. Site 1: Mamontovy Khayata cliff on the Bykovsky Peninsula near the coast of the Lena Delta (credit: P.P. Overduin) and, Site 2: the Duvanny Yar exposure (site 2) on the Kolyma river (credit: A. Stubbins). Freshwater discharge measurement stations at Kusr (Lena) and Kolymskoye (Kolyma) are shown (orange dots). Drawn by S. Laboor

communities (Strauss et al. 2015, 2017, 2021a, b; Jongejans et al. 2018; Haugk et al. in review) likely due to its rapid formation limiting prior processing during the Late Pleistocene. Once mobilised into inland waters, permafrost-derived OC can be rapidly utilized by aquatic microorganisms, increasing bulk OC degradation rates in riverine and coastal Arctic water incubations (Vonk et al. 2013; Drake et al. 2015; Mann et al. 2015) and potentially enhancing riverine CO₂ losses from river basins (Vonk and Gustafsson 2013; Drake et al. 2018a, b; Fig. 1).

Permafrost OC inputs to Arctic headwaters have been shown to be preferentially utilised by aquatic microorganisms, leading to patterns of decreased permafrost contributions in OC pools with increased water residence times (Mann et al. 2015). In addition, a general pattern of decreasing dissolved OC (DOC) reactivity has been demonstrated with increasing retention time of waters across diverse global river catchments, highlighting a universal decline in DOC reactivity along the aquatic-ocean continuum (Catalán et al. 2016; Soares et al. 2019). Any hydrologic changes, such as increases to river discharge or extreme flow events, causing shorter transit times would therefore result in OC bypassing headwater streams and being metabolized in mainstream and nearshore coastal waters, in agreement with the pulse-shunt concept (Raymond et al. 2016).

Arctic hydrological cycles are already intensifying. Pan-Arctic freshwater runoff rates to the Arctic Ocean have increased from $3900 \pm 390 \text{ km}^3$ in 1980–2000 to $4200 \pm 420 \text{ km}^3$ by 2000–2010 (Haine et al. 2015). Global climate model projections indicate that future freshwater runoff will continue to increase and that the rate of increase may accelerate over much of the Arctic during the coming decades (Haine et al. 2015; Brown et al. 2019). Combined hydrologic models informed using climate projections estimate freshwater discharge increases of ~ 25 to 50% to the Laptev and East Siberian Shelf by 2100 (Arnell 2005; Shiklomanov et al. 2013; van Vliet et al. 2013; Koirala et al. 2014; Andreson et al. 2020; Wang et al. 2021). Higher rates of continental freshwater runoff patterns will alter the distribution of terrestrial OC within river networks, and likely deliver greater quantities of OC from degrading river catchments to the coastal ocean. This has the potential to alter the availability of nutrients and carbon across the nearshore and modify the physiochemical environment (e.g., light penetration or carbonate system).

Here, we examine how future projected increases in runoff and permafrost thaw from two permafrost-dominated Siberian watersheds—the Kolyma and Lena, may alter carbon turnover rates and OC distributions through river networks. We present experimental results from the Kolyma River examining how rates of OC degradation in riverine carbon pools will shift with compositional changes

associated with permafrost thaw OC. We then explore potential for future permafrost thaw and hydrological intensification in these basins to alter terrestrial OC loads to East Siberian Arctic Shelf (ESAS) nearshore waters, by scaling our findings to the Lena River. We finally explore potential for future permafrost thaw and hydrological intensification in these basins to alter terrestrial OC loads to East Siberian Shelf nearshore waters. We conclude that there is a substantial paucity of information on how the rapidly changing terrestrial environment may affect coastal ecosystems and processes, and that future research and modelling work is needed to predict how ecosystem functioning and essential food webs may change under future scenarios.

MATERIALS AND METHODS

Study region

Our study focused on the Lena and Kolyma River catchments, two great watersheds that together comprise 19% of the pan-Arctic watershed and drain a watershed area of 3.11 million km² from the permafrost-dominated continental region into the ESAS. The shallow ESAS (average depth 58 m; Jakobsson 2002) represents a quarter of the Arctic shelf area (Shakhova et al. 2010) and is particularly vulnerable to changing inputs of terrestrial OC, with extreme regional climate warming already causing these Siberian terrestrial permafrost-rich watersheds to thaw (Graversen et al. 2008; Shakhova et al. 2010).

The Lena and Kolyma rivers account for a combined annual terrestrial OC flux of 7.0 to 9.4 TgC year⁻¹ (Holmes et al. 2012; McClelland et al. 2016; Juhls et al. 2020), which is approximately 17 to 28% of total terrestrial OC loads to the Arctic Ocean (Raymond et al. 2007). Large quantities of permafrost OC are stored in Pleistocene Yedoma deposits (Strauss et al. 2017), which when degraded or eroded, can represent hotspots of old terrestrial OC release to river catchments (Wetterich et al. 2020). Both the Kolyma and Lena River watersheds contain relatively similar coverage in Yedoma deposits, representing 7.7% of the watershed area in the Kolyma watershed area, and 3.5% of the Lena. Examples of such rapidly eroding Yedoma riverbanks include the Sobo-Sise cliff on the Lena River (Fuchs et al. 2020) and the Duvanny Yar cliff (Fig. 2 inset) on the Kolyma River (e.g., Strauss et al. 2012). Riverine OC loads to coastal waters from both rivers are predominantly (> 80%) in the dissolved form. The composition of the dissolved OC pools in the Kolyma and Lena Rivers are similar with comparable fractions of hydrophobic acids, transphilic acids, and hydrophilic organic matter as a percentage of total OC concentrations

Table 1 First-order OC degradation rates (day^{-1}) and OC lifetimes for each fraction determined in our experiments (Rapid OC) and in previous literature (Slow OC)

	OC degradation rate (day^{-1})	OC lifetime (year^{-1})
Rapid OC fraction ($n = 34$)		
Mean	0.0139	0.20
Median	0.0095	0.29
Stdev	0.0152	0.18
Min	0.0022	1.25
Max	0.0632	0.04
Slow OC fraction ($n = 18$)		
Mean	0.0029	0.95
Median	0.0024	1.14
Stdev	0.0021	1.34
Min	0.0013	2.11
Max	0.0098	0.04

(Table 1; Mann et al. 2016). Additionally, the overall aromaticity of the OC pools are comparable, as inferred from organic matter absorbance measurements (specific ultraviolet absorbance; Mann et al. 2016). The two river catchments differ significantly in the type and morphometry of their estuaries, with the Lena River feeding into an extensive delta before reaching the coastal ocean. The Kolyma, by contrast, runs directly through a gulf feeding directly onto the East Siberian Sea shelf (Fig. 2). Coastal erosion also delivers large amounts of OC into the near-shore, for example from the Mamontovy Khayata coastal cliff on the Bykovsky Peninsula (Fig. 2) (Lantuit et al. 2011; Rolph et al. 2021) or other Yedoma coastal segments along the Laptev Sea coast (Günther et al. 2013; Strauss et al. 2021b).

Contemporary river OC degradation rates

We measured river OC degradation rates ($n = 34$) using oxygen loss measurements on Kolyma lower mainstem waters (within 100 km of river mouth), collected during the summers of 2011 and 2012 (Table S1). Water samples were also collected from under-ice (May) and during the spring freshet (June) during 2012 from the Kolyma mainstem. Unamended biological oxygen demand (BOD) assays (i.e., waters were not seeded or primed) were run over a 5-day period on unfiltered waters at room temperature ($\sim 20^\circ\text{C}$; Jiao et al. 2021). Waters were slowly decanted into triplicate 300 mL glass BOD bottles and total oxygen concentrations measured using self-stirring optical optode oxygen probes (YSI, ProOBOD, $\pm 0.1 \text{ mg L}^{-1}$) after 0, 1 and 5 days. BOD assays measure the amount of dissolved oxygen used by microbial communities during

degradation of OC and are converted to OC carbon concentrations using a commonly applied respiratory quotient of 1 (assuming a ratio of 1 between CO_2 production and O_2 consumption). BOD assays are sensitive to small changes in the OC pool and are suitable for capturing OC rates associated with rapidly available and fast turnover OC pools. As such, rates determined using this method are henceforth considered to represent a *rapid OC pool*.

To supplement our OC degradation measurements, we collated our results with previously published rates determined in Kolyma River mainstem waters (Mann et al. 2012, 2015; $n = 18$, Table S1). Samples from these studies were collected in the Kolyma River across a similar region of the lower river catchment (approximately 100 km of the mouth: site locations Table S1), during the freshet and late autumn periods. These studies calculated OC degradation rates using direct dissolved OC (DOC) losses measured over a 28-day incubation period to provide insights into a slower OC fraction turn over approximately monthly timescales. Rates determined using this method are henceforth considered to represent a *slow OC pool*.

Direct and inferred OC loss measurements from all studies were fitted to an exponential decay to determine OC degradation rates (k) from incubation experiments:

$$\text{OC}_t = \text{OC}_{\text{init}} e^{-kt} \quad (1)$$

where OC_t represents the OC concentration at time (t in days), OC_{init} represents the initial OC concentration and k the degradation rate (day^{-1}).

OC degradation rates (k) were corrected to the in-situ water temperature measured at the study site during sampling (or other as stated below), using a form of the Arrhenius equation:

$$k_T = \frac{k_{20}}{q_{10}^{\frac{20-\text{Temp}}{10}}} \quad (2)$$

where k_T is the corrected OC degradation rate (day^{-1}), k_{20} the degradation rate in incubations at 20°C (from Eq. 1) and Temp the measured in-situ water temperature ($^\circ\text{C}$) at the time of sampling. q_{10} is the temperature coefficient which was assumed to be 2.0 (following estimates from Wickland et al. 2012; Catalán et al. 2016). To allow direct comparisons with other studies which present terrestrial OC lifetimes in reciprocal time units (the time by which an OC pool $[X]$ is degraded to a value equal to $[X]/k_T$) as per Hansell (2013) we additionally present these alongside measured rates (day^{-1}).

Freshwater discharge measurements

River discharges associated with degradation experiments (Table S1) were determined using data from the Arctic

Great Rivers Observatory website (Shiklomanov et al. 2021). Discharge measurements from gauging stations at Kolymskoe, located approximately 160 km upstream of our sampling sites were used (Fig. 2). Adjustments were made to account for the transit time of water between the gauging station and our lower Kolyma River sites by assuming river velocities of 1.5 m s^{-1} as in Holmes et al. (2012).

To assess past trends and contemporary discharge rates for the Kolyma and Lena rivers, we analysed discharge measurements from gauging stations at Kolymskoe (1978–2020) and Srednekolymsk (1927–2016, with gaps) from the Kolyma River basin, and at Kyusur (1936–2020) on the Lena river (Fig. 2). Both were monitored by the Russian Federal Service for Hydrometeorology and Environmental Monitoring (Roshydromet). Climate projections estimate mean annual runoff increases of $\sim 50\%$ ($\pm 25\%$) in the Kolyma River and 25% ($+ 25\%/ - 20\%$) for the Lena River by the end of the twenty-first century (Arnell 2005; Shiklomanov et al. 2013; van Vliet et al. 2013; Koirala et al. 2014). To estimate future discharge rates, we applied these projected increases relative to a baseline period of 1971–2000 from both rivers.

Impact of permafrost thaw OC on freshwater degradation rates

We conducted an experiment to assess if inputs of permafrost thaw OC, and the associated change in aquatic carbon composition, cause changes to bulk OC degradation rates. We specifically examined if the compositional changes alone, independent from concentration changes, cause changes to carbon turnover.

Frozen ice-wedge samples were collected from the Duvanny Yar exposure within the Kolyma River Basin during early September 2013 (Fig. 2). Yedoma deposits at Duvanny Yar accumulated between ~ 40 and 13 ky BP (Vasil'chuk et al. 2001) and are believed to be of polygenetic origin (Strauss et al. 2012). Total average ice content is approximately 75% by volume (35 wt% for ground ice, plus about 50 vol% for ice wedges) and total OC content averages $1.5 \pm 1.4 \text{ wt}\%$ (Strauss et al. 2012). Ice wedge thaw waters carry old terrestrial OC from Yedoma exposures (19,350 to 29,400 years; Vonk et al. 2013; Spencer et al., 2015) directly into the Kolyma River mainstem.

Combined ice-wedge and permafrost samples were chiselled from the cliff and kept cool and dark until laboratory preparation ($< 48 \text{ h}$). A bulk Kolyma River water sample was collected upstream of the exposure, representing mainstem waters unaffected by Duvanny Yar permafrost thaw subsidies in our experiment. In the laboratory, ice-wedge and permafrost were thawed in a double acid-rinsed glass container, before filtration through glass fibre filters (pre combusted Whatman GF/F, nominal

pore size of $0.7 \mu\text{m}$). Filtration removes a proportion of the microbial community, but this approach has been shown to provide comparable results to degradation experiments using a starting inoculum (Vonk et al. 2015). Kolyma mainstem waters were filtered in an identical manner. DOC concentrations were then measured (as below) in the Kolyma River ($4.8 \pm 0.5 \text{ mg/L}$; $n = 6$) and ice-wedge mix waters ($86.4 \pm 2.1 \text{ mg/L}$; $n = 6$), and the ice-wedge waters diluted with Milli-Q waters to match the DOC concentration of the Kolyma River waters.

A series of sample mixtures were then produced containing 0, 1, 10, 25, 50, 75, 99% final contributions of ice-wedge Kolyma River waters (Average initial concentrations = $5.8 \pm 0.7 \text{ mg/L}$; $n = 27$). A minimum of two incubations were run per mixture. Samples were stored dark at room temperature (approximately $20 \text{ }^\circ\text{C}$) and agitated daily to ensure sample mixing. Duplicate vials were sacrificed after 14 and 28-days, filtered as above and then acidified with H_3PO_4 until pH 1–2 and kept in the dark at $4 \text{ }^\circ\text{C}$ until analysis. DOC concentrations were measured using the combustion catalytic oxidation method (Shimadzu TOC-L, $\pm 0.1 \text{ mg/L}$). The differences in DOC concentrations over 28-days were calculated and assigned to turnover rates of the *slow* OC pool as above. The differences in DOC concentrations over 14-days were used to determine a separate *fast* OC pool.

To supplement our permafrost experimental results, we collated published OC degradation measurements from Arctic River waters amended with Yedoma additions to examine the impact of permafrost thaw on inland waters ($n = 39$; Table S2).

RESULTS

Terrestrial OC degradation rates in Arctic freshwaters

Natural mean degradation rates in the rapid OC fraction measured using short-term oxygen loss measurements were 0.0139 day^{-1} (s.d. $\pm 0.0152 \text{ day}^{-1}$), corresponding to lifetime estimates of 0.20 year^{-1} ($\pm 0.18 \text{ year}^{-1}$; Table 1) for this fraction. Mean degradation rates in the slow turnover OC pool were lower ($0.0029 \pm 0.0021 \text{ day}^{-1}$), with correspondingly longer lifetime estimates of 0.95 year^{-1} ($\pm 1.34 \text{ year}^{-1}$; Table 1) for this fraction. Our mean (0.0029 day^{-1}) and median (0.0024 day^{-1}) bioactivity rates in the slow OC pool compare closely yet slightly lower than the median k value of $0.0034 \pm 0.0219 \text{ day}^{-1}$ reported from 46 separate global river systems (Catalán et al. 2016).

River hydrology patterns

The overall load and timing of freshwater discharge from the Kolyma and Lena Rivers have varied over the observational periods available (Fig. 3). Spring river break-up occurs earlier in the season and clear patterns of increased winter discharge are apparent across both river catchments (Fig. 3a, b). Overall mean annual freshwater discharge has increased over the last decade (2010–2020) by 27.7% for the Kolyma River (94.6 to 120.7 km³ year⁻¹) and 9.9% in the Lena River (626.9 to 689.1 km³ year⁻¹) compared to a baseline period of 1971–2000 (black lines—Fig. 3).

Assuming climate projections of mean annual runoff increases of ~ 50% (± 25%) in the Kolyma River and 25% (+ 25%/– 20%) for the Lena River (Arnell, 2005; Shiklomanov et al. 2013; van Vliet et al. 2013; Koirala et al. 2014), we applied projections up to 2100 (Fig. 3c, d). A rapid increase in freshwater discharge since the 1971–2000 baseline meant future projections of + 25% on the Kolyma, or + 5% in the Lena, now represent a reduction in discharge relative to the freshwater loads observed over the last two decades (Fig. 3).

By 2100, we estimate annual mean discharge rates under these assumptions of 141.8 km³ year⁻¹ (± 28.7 km³ year⁻¹) and 783.6 km³ year⁻¹ (± 81.9 km³ year⁻¹) in the Kolyma and Lena Rivers, respectively.

Role of permafrost OC composition on OC degradation rates

Mean OC degradation rates in both the slow and fast OC pools increased relative to Kolyma mainstem rates (0% permafrost input: Fig. 4), with additions of permafrost-derived terrestrial OC (Fig. 4). Terrestrial OC degradation rates increased almost linearly with increasing permafrost OC contributions to the total DOC pool, up to approximately a 25% subsidy (Fig. 4). After approximately 25% of the total OC pool had been replaced by permafrost-derived OC, no further increases in bulk OC degradation rates were observed, and at very high permafrost-OC contributions (95%), degradation rates appeared to decline.

Our results demonstrate that increased OC degradation rates will be observed in waters receiving permafrost-thaw-derived OC, and that these increases were definitively due to compositional shifts in organic matter composition and

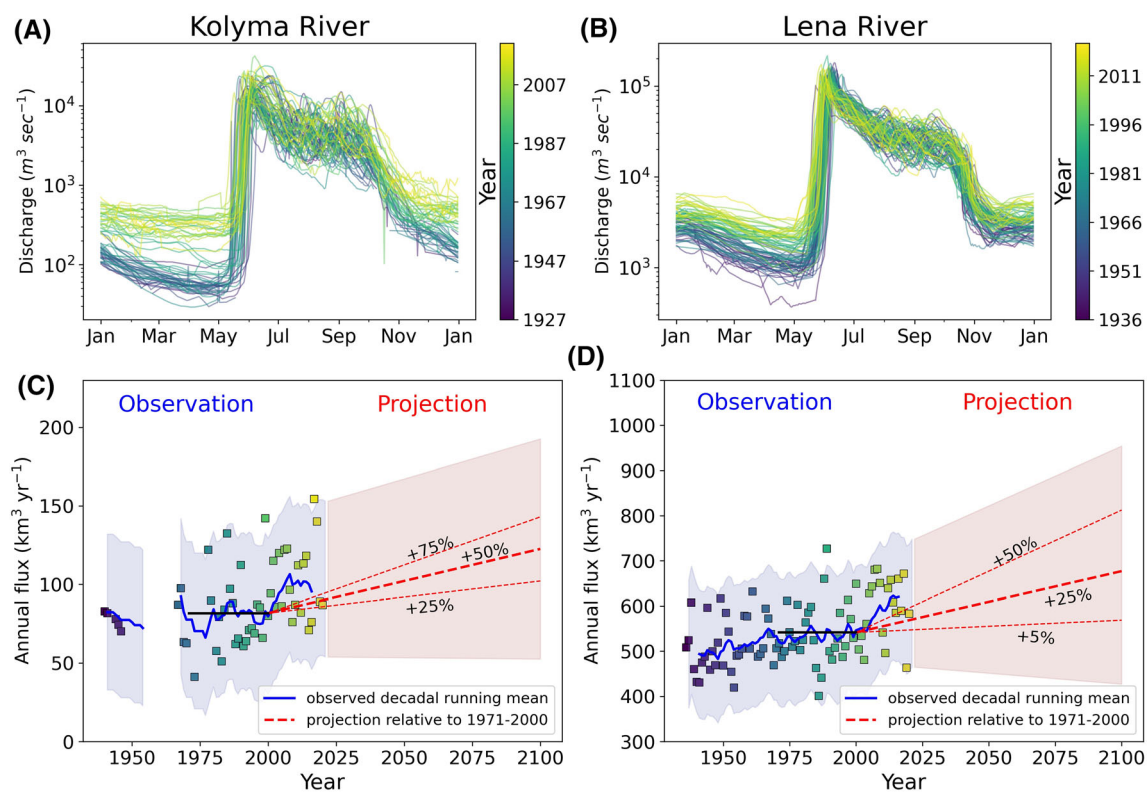


Fig. 3 Upper panel: Hydrograph of **a** Kolyma River for all years from 1927 to 2020 and **b** Lena River from 1936 to 2020. Lower panel: Observed and projected freshwater discharge (km³ year⁻¹) for **c** the Kolyma and, **d** Lena Rivers. Blue line on each plot represents the decadal running mean and filled blue colour the second standard deviation of the observed discharge. Red dashed lines show different projection scenarios to 2100 against the baseline period from 1971 to 2000 (black line). Filled red colour indicates the observed second standard deviation applied on chosen minimum and maximum projection scenarios

not simply by concomitant increases in DOC concentrations. The levelling off and potential decline in OC degradation with permafrost-OC contributions greater than 25%, suggests additional constraints such as limited nutrient availability acted to limit faster terrestrial OC rates.

OC degradation with permafrost subsidies and changing runoff

To combine our permafrost-OC experimental results above with previous studies, we collated and pooled data from published literature (Vonk et al. 2013; Mann et al. 2014, Table S3). To ensure data were comparable across studies, rates were binned into OC pools as above (rapid, fast, slow) and all normalised to 15 °C, an approximate nominal summer Kolyma mainstem surface water temperature.

Mean OC degradation rates measured in all terrestrial pools were substantially faster with increasing permafrost-derived OC contributions (Table 2). Mean OC degradation rates increased by a factor of ten in the rapid OC pool (0.0093 to 0.1029 day⁻¹) and doubled in the fast OC fraction (0.0046 to 0.0093 day⁻¹), with a 10% subsidy to bulk OC pools. Small relative contributions of permafrost-derived OC (e.g., 1% of total OC) decreased overall OC lifetimes between 250% in the rapid OC pool to 125% in the fast OC fraction. Significant linear relationships (simple regression; $p < 0.001$) were found between increased

permafrost-OC contributions up to 25%, and OC degradation rates in each OC fraction (Fig. 5a; $n = 85$; nominal 15 °C).

To examine if changing hydrologic patterns influence bulk OC degradation rates within river catchments, we compare natural OC degradation rates reported above for the rapid (this study) and slow OC pools (Mann et al. 2012, 2015) with river discharge on that sample date. No relationship between OC rates in the slow turnover pool and discharge were found, but discharge was shown to be significantly and positively correlated with OC degradation rates of the rapid turnover pool (Fig. 5b; $R^2 = 0.82$; Table S4).

This relationship most closely fit the equation:

$$\log k = 0.00013 \times \text{discharge} - 5.51246 \quad (3)$$

where $\log k$ represents the log OC degradation rate in the rapid OC pool (day⁻¹) and discharge Kolyma River discharge (m³ s⁻¹). The relationship was strongly influenced by extreme higher and lower OC rates measured in freshet waters (sampled during very high discharge) and under-ice waters (very low discharge conditions), respectively. This likely reflects the substantial shift in OC composition across the hydrograph (Mann et al. 2012).

DISCUSSION

Terrestrial permafrost thaw and landscape evolution

The source and quantity of terrestrial OC mobilised from Arctic catchments will change in response to widespread landscape evolution due to climate warming. Both gradual and abrupt processes are taking place across river basins (Fuchs et al. 2020) releasing old permafrost-derived OC for decomposition and enabling its mobilisation and potential utilization within nearshore waters (Vonk and Gustafsson 2013). However, the rate of permafrost OC release to waters is dependent upon still uncertain projections of terrestrial permafrost thaw. The ice-rich permafrost across northeastern Siberia has been projected to remain relatively stable beyond 2100 even under extreme climate warming (RCP 8.5) (Koven et al. 2011, 2015), yet these estimates did not incorporate landforms such as thermokarst resulting from permafrost thaw, which are known to accelerate OC release substantially (Schneider von Deimling et al. 2015; Turetsky et al. 2020). A recent study has shown that substantial quantities of additional permafrost-derived OC thaw could occur in NE Siberia under future warming scenarios (Nitzbon et al. 2020). They show that when thermokarst-related permafrost thaw processes are included in models, a three-fold (RCP4.5) to 12-fold (RCP8.5)

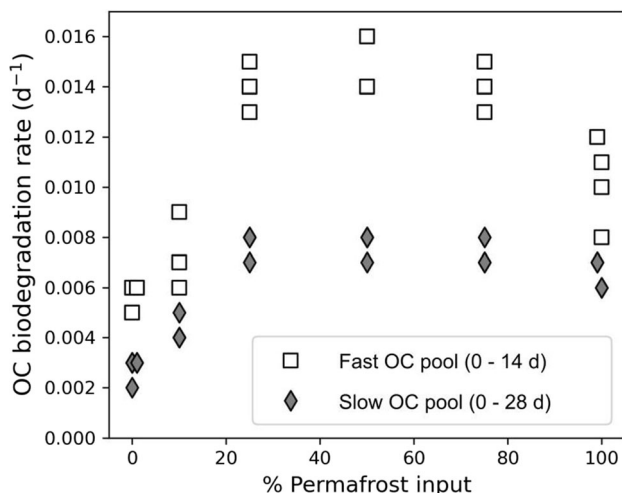


Fig. 4 OC degradation rates in carbon-normalised Kolyma River waters with increasing percent permafrost-derived OC contributions. Fast and slow rates relate to OC losses measured over 14 and 28-day incubation periods, respectively. 0% permafrost input (= 100% Kolyma) represents contemporary mainstem waters, whereas 100% permafrost are permafrost and thaw stream derived waters. OC degradation rates have been normalised to September Kolyma mainstem in situ water temperature of 7.3 °C

Table 2 OC degradation rates in experimental incubations of waters with up to 25% permafrost-thaw OC. Rapid OC fraction determined using oxygen loss measurements over 5-days. Fast and Slow OC pools are determined via dissolved OC loss over 14 or 28-days, respectively. All degradation rates were normalised to 15 °C, enabling comparison between experiments

Permafrost OC (%)	OC biodegradation rate (day ⁻¹)	OC lifetime (year ⁻¹)
Rapid OC pool		
0	0.0093 ± 0.0008	0.30 ± 0.02
1	0.0223 ± 0.0010	0.12 ± 0.01
10	0.1029 ± 0.0056	0.03 ± 0.001
Fast OC pool		
0	0.0091 ± 0.0010	0.31 ± 0.03
0.5	0.0103 ± 0.0003	0.27 ± 0.01
1	0.0112 ± 0.0007	0.25 ± 0.02
10	0.0163 ± 0.0047	0.18 ± 0.06
25	0.0239 ± 0.0020	0.11 ± 0.01
Slow OC pool		
0	0.0046 ± 0.0005	0.60 ± 0.06
0.5	0.0056 ± 0.0008	0.50 ± 0.08
1	0.0058 ± 0.0007	0.48 ± 0.06
10	0.0093 ± 0.0025	0.31 ± 0.09
25	0.0132 ± 0.0004	0.21 ± 0.01

increase (compared to over previous projections) more OC can be thaw-affected to OC (Nitzbon et al. 2020).

Terrestrial OC collected from Pleistocene Yedoma permafrost have been found to be of good quality for future biological degradation (Haugk et al. in review). Both our studied rivers cut into extensive Yedoma deposits, like at the Sobo Sise cliff (Fuchs et al. 2020) and the Kurungnakh cliff (Stettner et al. 2018) on the Lena River, and the Duvanny Yar cliff (Strauss et al. 2012; Vonk et al. 2013) on the Kolyma River indicating that future landscape degradation or increased erosion and thermokarst in these

catchments will liberate permafrost OC to nearshore environments.

Permafrost thaw enhances aquatic OC degradation

Greater subsidies of permafrost-derived OC from land will increase mean degradation rates of OC in inland waters. We demonstrated that this was due to compositional shifts in the bulk OC pool, and irrespective of total DOC concentrations (Fig. 4). Our experimental results from waters collected during autumn months (e.g., 1% permafrost OC lifetime 0.38 year⁻¹ at 7.3 °C) compare well with those previously reported in summer samples (1% permafrost OC lifetime 0.31 year⁻¹ at 16.9 °C; Vonk et al. 2013), suggesting an enhanced degradation to OC from permafrost supply could be expected over the entire open water season.

Contrary to previous studies, OC degradation rates did not increase with additional permafrost-thaw contributions > 25% (Fig. 4) indicating that additional regulatory factors such as nutrient availability began to limit additional reactivity enhancements (Frey et al. 2009; Mann et al. 2014; Reyes and Lougheed 2015; Fouché et al. 2020). Associated enrichment of aquatic systems with nutrients from permafrost-derived OC additions could also therefore play an important role in determining future OC degradation rates. Linear increases in OC degradation rates with permafrost thaw contributions up to one-quarter of the total OC pool (Table 2), show that permafrost-derived OC additions will significantly enhance inland OC turnover over upcoming decades. Future thaw impacts may potentially be modelled using simple empirical relationships such as those we found (Fig. 5a), although additional research is needed across other Arctic catchments to confirm if similar relationships exist, especially across basins containing different permafrost types and formation histories.

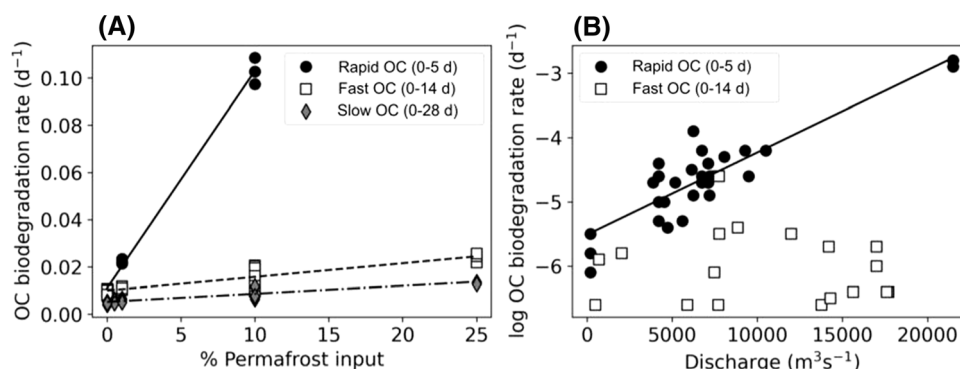


Fig. 5 OC degradation rates in Kolyma River waters **a** calculated across all permafrost addition experiments with contributions up to and including 25% permafrost contributions ($n = 55$; normalised to 15 °C), and **b** determined in unamended waters and plotted on a log scale against river discharge. All rates have been corrected to in-situ temperature on sample date and discharge normalised to site location. All linear relationships shown are significant ($R^2 > 0.8$, $p < 0.0001$). Full detail on linear regression fits provided in Table S4)

Despite highly uncertain estimates for future terrestrial permafrost thaw, evidence is emerging to suggest the release of permafrost-derived OC to inland waters is underway (Mann et al. 2015; Abbott et al., 2015; Wickland et al., 2018; Wild et al. 2019; O'Donnell et al. 2020; Walvoord et al. 2020; Kokelj et al. 2020). Contemporary permafrost contributions to bulk Kolyma mainstem OC calculated using dual-isotopic ($\Delta^{14}\text{C}/\delta^{13}\text{C}$) signatures are estimated to be $0.7 \pm 0.1\%$ during August–September (Mann et al. 2015), and between 0.8 and 7.7% in late summer via a combination of ultrahigh-resolution mass spectrometry and ramped pyrolysis oxidation techniques (Rogers et al. 2021). The fraction of permafrost and peat deposits to total DOC within the Kolyma and Lena Rivers have also been estimated using $\Delta^{14}\text{C}$ and source apportionment across seasons (Table S8 in Wild et al. 2019). Kolyma mainstem waters were estimated to contain between 4.6 to 18.7% (best estimate of 7.9%) of peat and permafrost during Spring, but up between 9.8 to 34.5% (16.3%) during winter months. Lena waters were estimated to contain 3.2 to 13.3% (best estimate of 5.6%) in spring and 6.9 to 25.4% (11.6%) during winter. The large differences in estimates between these studies demonstrate the difficulties in identifying permafrost contributions within river waters, although highlights relatively small current contributions, and suggest younger peat deposits contribute substantially to the bulk OC pool.

Using the relationship, we report between permafrost OC supply and increased OC degradation rates (Fig. 5a), we test the sensitivity of river OC to increased future permafrost supply. Assuming a conservative doubling of permafrost-derived OC to bulk river carbon pools (i.e., a further 0.7% permafrost contribution), we suggest mean OC degradation rates would increase from 0.0175 to 0.0240 day^{-1} in the rapid OC fraction and from 0.0055 to 0.0057 day^{-1} in the slow OC pool (Fig. 5a). These biolability rate increases translate to reductions in terrestrial OC lifetimes from 0.16 to 0.11 year^{-1} and 0.50 to 0.48 year^{-1} , respectively. Increasing freshwater runoff will additionally transport terrestrial OC from upstream headwaters to mainstem river and coastal waters more rapidly (Catalán et al. 2016). Headwater catchments have an intimate link with the landscape and currently receive significantly greater proportions of permafrost-derived OC. For example, smaller streams within the Kolyma River were shown to contain $13 \pm 4\%$ of permafrost-derived OC and those affected by erosional processes $43 \pm 21\%$ (Table 1 in Mann et al. 2015). This material is currently rapidly processed within river networks reducing observed permafrost-derived OC contributions downstream (Mann et al. 2015; Spencer et al. 2015). More efficient delivery of permafrost-derived enriched OC from headwaters and tributaries may therefore significantly increase downstream

degradation rates. As an example, if mainstem waters were to contain OC with 5.7% permafrost-derived OC as currently present within Kolyma minor tributaries ($5.7 \pm 3.5\%$ permafrost contributions; Mann et al. 2015), degradation rates in the slow OC pool would increase from rates of 0.0055 day^{-1} (lifetime of 0.50 year^{-1} ; assuming current 0.7% permafrost subsidy), to 0.0072 day^{-1} (lifetime of 0.38 year^{-1}). Associated increases in terrestrial OC degradation rates in upstream tributaries would also be expected, as they in turn receive greater subsidies from smaller headwater streams. It is however highly uncertain if mainstem waters will ever receive such subsidies, or how much they may make up of the bulk OC pool. Accurately constraining the amount of permafrost OC being released to headwaters, and improved methods for tracing permafrost OC through Arctic networks will be essential in understanding how permafrost underlain river catchments may adapt in response to future permafrost thaw and thermokarst events.

Enhanced freshwater runoff increases aquatic OC degradation rates

Increasing freshwater runoff rates delivered greater quantities of terrestrial OC that could be rapidly degraded in aquatic ecosystems over the order of a few days (i.e., Rapid turnover OC; Fig. 5b). No comparable relationships between the rates measured in the ‘slow’ OC pools and discharge were identified (Fig. 5b). Increased freshwater discharge rates therefore appear to be associated with greater delivery of highly reactive OC from the landscape, likely fueling higher OC degradation rates in receiving stream and river waters. The lack of an empirical relationship between discharge and ‘fast’ or ‘slow’ OC pools suggest that the changing hydrologic runoff will not directly alter their degradation rates.

Assuming the relationship between rapid OC pool degradation rates and discharge holds under future scenarios (Eq. 3), we apply this equation to discharge records from the Kolyma River (Fig. 3) to project how rapid OC pool degradation rates may change under future runoff patterns (Fig. 6). As noted above, OC pools in the Kolyma and Lena rivers are similar in composition (Mann et al. 2016) and thus we expect them to display comparable degradation rates as those reported in the Kolyma River. We therefore also examined how Lena River OC degradation rates may alter in response to increasing discharge but note that future studies are needed to test that these assumptions are valid. We scaled the Lena discharge to that of the Kolyma, using a scaling factor of 0.164 which was determined by dividing the mean annual Lena and Kolyma Rivers discharge. We then applied the scaled Lena River discharge to Eq. 3. Despite the many assumptions present

in such calculations—especially in Lena River waters, it seems likely that an enhanced hydrological system will promote OC pools in river catchment that can be rapidly utilized by microorganisms.

Increased OC degradation rates in the ‘rapid’ turnover OC pool under future enhanced runoff conditions will likely fuel greater greenhouse gas emissions from Arctic catchments. For example, the Kolyma River mainstem is supersaturated in dissolved CH₄ (15,300% relative to atmosphere) and CO₂ (235%) fueling significant gas exchange fluxes from the river and gulf regions (Palmtag et al. 2021). Using a simple box model incorporating present-day runoff rates and field gas measurements, the authors estimate mean CH₄ loads of 9.5×10^5 kg CH₄ year⁻¹ enters the lower reach of the Kolyma River (ca. 100 km upstream of river mouth) during the open water period (1 Jun–1 Nov). Of these loads, they calculate losses of 49% (-4.7×10^5 kg CH₄ year⁻¹) to the atmosphere via gas exchange in the gulf, with total fluxes to the coastal ocean of 6.0×10^5 kg CH₄ year⁻¹ (with net oxidation accounting for small variations). Assuming conservative increases in freshwater discharge of 25% and identical water gas concentrations, CH₄ loads would be expected to increase to 11.9×10^5 kg CH₄ year⁻¹, with gas exchange losses of 50% (-6.0×10^5 kg CH₄ year⁻¹) and fluxes to the ocean of 7.2×10^5 kg CH₄ year⁻¹. These findings suggest that higher discharge rates have the potential to strengthen both greenhouse emissions from Arctic catchments as well as dissolved gas loads to coastal waters. Future work is therefore needed to understand how constituent river loads will increase under freshwater intensification.

Future decreasing ice thickness and broader sub-ice pathways will further increase the connectivity of Arctic rivers. This connectivity could account for increased winter runoff signals (Juhls et al. 2021) as observed here (Fig. 3a, b). Active layer thickening and Talik formations caused by warming may also cause increased connectivity and

groundwater flow (Frey and McClelland 2009). This will lead to increasing subsurface water flow and greater leaching and contributions of old reactive permafrost-derived OC.

How could future increases in the supply of OC from land impact coastal biogeochemistry?

Future changes in the quantity or composition of terrestrial OC delivered to the Arctic Ocean nearshore may play a significant role in shaping nearshore processes, largely through the supply of nutrients and terrestrial OC to coastal oceans. Increasing river discharge and coastal erosion across the Siberian Arctic is not only increasing terrestrial OC loads to coastal waters but is also likely to substantially alter its composition with greater subsidies of permafrost-derived OC translocated from river catchments (described above), and enhanced erosion of permafrost-rich coastlines (Günther et al. 2013). The future impact of terrestrial permafrost thaw and enhanced runoff rates on Arctic Ocean nearshore processes are however strongly influenced by estuarine removal processes, such as flocculation processes or biological or photochemical degradation before reaching the shelf. For example, only 5–15% of the particulate OC measured within the river mainstem is estimated to leave the Lena River delta (Semiletov et al. 2016). By contrast, a minimal removal of DOC (< 5%) was reported for a boreal river using a simple box model parameterized with river inputs, settling fluxes, advective export and solved for degradation (Gustafsson et al. 2000). This is in good agreement with the apparently linear and conservative mixing trends for DOC extending from the Lena River and into nearshore regions (Köhler et al. 2003; Amon 2004; Juhls et al. 2019), although these studies have historically only focused on late summer seasons. Further offshore, the inner and outer Lena-Laptev Sea plume has been shown to contain riverine DOC that is approximately two months old, having lost approximately 10% of the

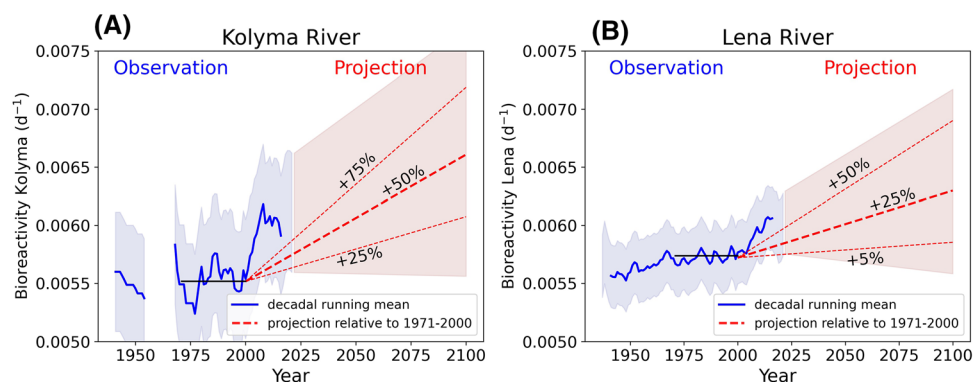


Fig. 6 Observed and projected OC degradation rates (day^{-1}) calculated using Eq. 2 for: **a** the Kolyma River and, **b** Lena River. OC degradation rates for the Lena River are scaled by calculating a scale factor (0.164) correcting for relative differences in discharge

initial DOC (Alling et al. 2010). Substantial losses of DOC (ca. 10–20%) delivered by the Kolyma River into the East Siberian Sea have also been reported (Alling et al. 2010). Increasing exports of terrestrial OC therefore have the potential to be reflected in coastal nearshore environments and play a crucial role in affecting nearshore degradation rates.

Terrestrial lifetime estimates for the entire OC pool over the Laptev and East Siberian Shelf have previously been estimated from field dissolved OC measurements across the shelf, indicating lifetimes on the order of 3.3 year^{-1} (Alling et al. 2010) and 10 year^{-1} derived from ocean waters and used across the entire Arctic from a modelling study (Manniza et al. 2009). These are significantly longer than the lifetimes in contemporary Kolyma River mainstem waters calculated here which were on the order of $0.95 \pm 1.3 \text{ year}^{-1}$ (Slow OC pool; Table 1). Our results compare well with previous estimates of 0.7 year^{-1} in Alaskan rivers (Holmes et al. 2008). Increasing lifetime estimates reported from waters moving offshore are consistent with expected decreases in OC degradation rates across the aquatic-ocean continuum (Catalán et al. 2016). These changes appear not to be driven by the capabilities of the coastal microbial community, as parallel OC degradation rates measured in Kolyma River and coastal waters containing their natural microbial communities showed highly similar OC loss rates (Vonk et al. 2013). Future studies need to consider implementing different degradation rates for terrestrial OC throughout the nearshore, with faster rates within and near river mouths, and higher removal rate constants in Arctic shelf waters relative to the Arctic interior (Alling et al. 2010). The role of particulates across the nearshore also needs to be further understood, as adsorption and flocculation processes have the potential to change biodegradation rates and the ultimate fate of DOC (Keskitalo et al. in review).

Future contributions of permafrost-derived OC to coastal waters will additionally exacerbate reductions in bulk OC lifetimes across shelf waters. Rapid losses of fluvial permafrost OC within river catchments may cause limited quantities of permafrost OC to be exported to the nearshore, but as river catchments continue to degrade, and catchment OC residence times continue to decline, it is possible the composition of exported OC will shift. Direct inputs of particulate and dissolved permafrost-OC from increased coastal erosion may also increase (Jones et al. 2020). Here, we show that relatively small subsidies of permafrost could significantly increase degradation rates, with an additional 1% contribution to mainstem waters increasing OC loss rates by 20 to 60%, depending on the OC pool studied (Table 2). Enhanced coastal OC degradation could result in CO_2 accumulation in coastal waters slowing or potentially reversing annual Arctic Ocean sea-

air uptake and acting as positive feedback upon Arctic climate change. The Arctic Ocean is currently considered a small net sink of atmospheric CO_2 , with uptake estimates ranging between 0.1 to $0.2 \text{ Pg C year}^{-1}$ (McGuire et al. 2009; Arrigo et al. 2010; Jeansson et al. 2011; Manizza et al. 2013; Schuster et al. 2013). Model estimates of coastal nearshore environments however often use only a single OC degradation rate to represent degradation rates across the entire Arctic Ocean (e.g., Manniza et al. 2009). Recent modelling efforts using a biogeochemical model incorporating terrestrial OC dynamics identifies the degradation rate of terrestrial OC as a critical parameter in projecting the strength and direction of future CO_2 emissions from shelf waters (Polimene et al. submitted). The authors examined a range of OC lifetimes spanning 0.3 to 10 year^{-1} under changing terrestrial OC supply scenarios (+ 0 to 100% discharge) to the Laptev Sea and found that either increased OC loads or changing composition (reductions in OC degradation rates) significantly affected net shelf CO_2 budgets. Furthermore, changes to terrestrial OC loads or composition to coastal waters had profound impacts upon light penetration, and in turn rates of primary production, as well as phytoplankton community dynamics. Recent suggestions that the riverine and erosional supply of terrestrial dissolved nitrogen may strengthen the Arctic shelf as a net CO_2 sink (McGuire et al. 2010; Terhaar et al. 2021) may be optimistic. Changes to net primary production rates and phytoplankton community dynamics in shelf waters may also modify essential food webs and their distributions across changing Arctic coasts. Coastal food webs may also need to respond to enhanced rates of ocean acidification. The Arctic Ocean is particularly sensitive to ocean acidification due to the greater quantities of CO_2 that can dissolve in cold waters and the changing alkalinity load received from Arctic Rivers (Drake et al. 2018a, b). Ocean acidification across the ESAS has been attributed to degradation of terrestrial organic matter and addition of CO_2 rich waters from river runoff, rather than atmospheric CO_2 uptake (Semiletov et al. 2016). Greater delivery of terrestrial materials, or any enhancement in OC degradation rates caused by increasing freshwater discharge or permafrost supply will, therefore, likely also cause a worsening of ocean acidification across coastal waters.

CONCLUSION

We propose that nearshore regions across the Arctic are hotspots for environmental change requiring concerted and co-ordinated sampling efforts across river, estuary, coastal and shelf regions. An intensification of the hydrological cycle across the nearshore is underway and expected to continue well into the twenty-first century, with a range of

complex and non-mutually exclusive impacts and greater dissolved organic carbon loads to coastal waters. Greater freshwater discharge rates may cause a lateral shift in terrestrial OC concentration and composition, efficiently translocating more biodegradable OC to mainstem and coastal waters for biodegradation or storage. Permafrost and peat-derived OC will be mobilised more rapidly into river networks from headwaters or via enhanced river erosion supplying an additional source of highly available OC to aquatic organisms, subsidising higher atmospheric greenhouse gas emissions during river transit and greater loads of dissolved concentrations to coastal waters. Coastal erosion will further increase permafrost OC pools in shelf waters. The rapidity of changes across the Arctic nearshore will require studies that incorporate new and existing observations with improved modelling efforts that can capture changing hydrology and coastal freshwater dynamics, as well as a range of terrestrial OC degradation rates. There is an explicit need to capture seasonal variability more effectively across all seasons, especially in underrepresented areas such as the Russian Arctic. Effective use of in-situ monitoring platforms and remote sensing products could aid in delivering spatially consistent data on OC fluxes, but it remains a challenge to “observe” permafrost OC mobilisation to the nearshore. Monitoring changes in bulk DOC degradation may prove a useful, and fundamentally viable metric to help monitor any shifts in fluvial and coastal OC amount and composition. Future increased quantities of terrestrial OC within coastal waters will cause a suite of physical and biogeochemical changes including in the availability of light and nutrients, patterns of ocean acidification and ultimately coastal productivity and fisheries.

SOCIETAL AND POLICY IMPLICATIONS

Approximately, 10% of the 4 million people who live in the Arctic are Indigenous. The Arctic has been their home for thousands of years and over the millennia they have developed the skills to survive in areas of harshest living conditions and to adapt to changes. However, the rapid and unprecedented climatic and environmental changes that we are seeing in the Arctic today are the biggest long-term challenge that the Indigenous Peoples are facing. These changes are affecting indigenous practices such as reindeer herding, hunting, fishing, and gathering, ultimately challenging food security (Plate et al. 2021). Hydrological changes and permafrost degradation in the river catchments are affecting reindeer herding indigenous peoples who are dependent on the migration routes and pasture lands of the herd to maintain food security. Additionally, permafrost thaw related changes in riverine carbon and nutrient supply

could affect fish stocks both in rivers and nearshore marine waters. Changes to the amount and type of marine plants (phytoplankton) may cause changes to the distribution, availability and biomass of coastal fish and higher mammals. Increased coastal erosion and permafrost inputs also has the potential to increase the concentration of contaminants—such as inorganic and methyl mercury, in inland and potentially coastal waters (St Pierre et al. 2018; Zolkos et al. 2020). This may result in greater loads of contaminants within coastal foods and accumulating up the food chain to higher species, resulting in greater risk to local peoples’ who rely on nearshore marine resources.

The Russian Arctic Rivers are important transportation routes both to supply the cities and settlements in the hinterland and to ship raw materials to the coastal zone and further via the Northern Sea Route. Port facilities and other infrastructure along the rivers and in the coastal and nearshore zone are vulnerable to an intensification of the hydrological cycle and to amplified permafrost degradation. Loss of nearshore sea-ice can be exacerbated by increasing coastal runoff and terrestrial loads (for instance through altering heat absorption into coastal waters). Greater volumes of shipping across Arctic coastal waters increases the risks of accidents and spillages across the nearshore, with the potential for long-term damage to coastal ecosystems and loss (or contamination) of essential species.

We, therefore, believe that this study’s topic is highly relevant for Arctic policymakers, in particular for the Arctic Council which promotes the cooperation between Arctic States, indigenous peoples and other Arctic residents with regard to sustainable development and environmental protection. The three Arctic Council working groups Conservation of Arctic Flora and Fauna (CAFF), Protection of the Arctic Marine Environments (PAME) and Sustainable Development Working Group (SDWG) as well as the Arctic Indigenous Peoples organizations, represented on the Council as Permanent Participants, are potential users of this study.

Acknowledgements This work is embedded into the Changing Arctic Ocean (CAO) program (lead by the NERC-BMBF project CACOON [NE/R012806/1 (UKRI NERC) and #03F0806A (BMBF)]). This work was partly funded by the U.S. NSF (National Science Foundation, ANT-1203885/PLR-1500169) grants to RGMS. We thank the NSF POLARIS project (<https://www.thepolarisproject.org>; 0732944 and 1044610) and participants for Kolyma bioreactivity measurements and sample collection. Figure 1 was drawn by Yves Nowak (AWI), Fig. 2 by Sebastian Laboor (AWI). For fieldwork support, we want to thank the Samoylov Research Station and the Northeast Science Station and teams, especially Sergei and Nikita Zimov.

Open Access This article is licensed under a Creative Commons Attribution 4.0 International License, which permits use, sharing, adaptation, distribution and reproduction in any medium or format, as

long as you give appropriate credit to the original author(s) and the source, provide a link to the Creative Commons licence, and indicate if changes were made. The images or other third party material in this article are included in the article's Creative Commons licence, unless indicated otherwise in a credit line to the material. If material is not included in the article's Creative Commons licence and your intended use is not permitted by statutory regulation or exceeds the permitted use, you will need to obtain permission directly from the copyright holder. To view a copy of this licence, visit <http://creativecommons.org/licenses/by/4.0/>.

REFERENCES

- Abbott, B.W., J.B. Jones, S.E. Godsey, J.R. Larouche, and W.B. Bowden. 2015. Patterns and persistence of hydrologic carbon and nutrient export from collapsing upland permafrost. *Biogeochemistry* 12: 3725–3740. <https://doi.org/10.5194/bg-12-3725-2015>.
- Alling, V., L. Sanchez-Garcia, D. Porcelli, S. Pugach, J.E. Vonk, B. van Dongen, C.-M. Mörth, L.G. Anderson, et al. 2010. Nonconservative behavior of dissolved organic carbon across the Laptev and East Siberian seas. *Global Biogeochemical Cycles*. <https://doi.org/10.1029/2010GB003834>.
- Amon, R.M.W. 2004. The role of dissolved organic matter for the organic carbon cycle in the Arctic Ocean. In *The organic carbon cycle in the Arctic Ocean*, ed. R.S. Stein and R.W. Macdonald, 83–99. New York: Springer.
- Andresen, C.G., D.M. Lawrence, C.J. Wilson, A.D. McGuire, C. Koven, K. Schaefer, E. Jafarov, S. Peng, et al. 2020. Soil moisture and hydrology projections of the permafrost region – A model intercomparison. *The Cryosphere* 14: 445–459. <https://doi.org/10.5194/tc-14-445-2020>.
- Arnell, N.W. 2005. Implications of climate change for freshwater inflows to the Arctic Ocean. *Journal of Geophysical Research: Atmospheres*. <https://doi.org/10.1029/2004JD005348>.
- Arrigo, K.R., S. Pabi, G.L. van Dijken, and W. Maslowski. 2010. Air-sea flux of CO₂ in the Arctic Ocean, 1998–2003. *Journal of Geophysical Research: Biogeosciences*. <https://doi.org/10.1029/2009JG001224>.
- Biskaborn, B.K., S.L. Smith, J. Noetzi, H. Matthes, G. Vieira, D.A. Streletskiy, P. Schoeneich, V.E. Romanovsky, et al. 2019. Permafrost is warming at a global scale. *Nature Communications* 10: 264. <https://doi.org/10.1038/s41467-018-08240-4>.
- Brown, N.J., J. Nilsson, and P. Pemberton. 2019. Arctic Ocean freshwater dynamics: Transient response to increasing river runoff and precipitation. *Journal of Geophysical Research: Oceans* 124: 5205–5219. <https://doi.org/10.1029/2018JC014923>.
- Catalán, N., R. Marcé, D.N. Kothawala, and L.J. Tranvik. 2016. Organic carbon decomposition rates controlled by water retention time across inland waters. *Nature Geoscience* 9: 501–504. <https://doi.org/10.1038/ngeo2720>.
- Drake, T.W., F. Guillemette, J.D. Hemingway, J.P. Chanton, D.C. Podgorski, N.S. Zimov, and R.G.M. Spencer. 2018. The ephemeral signature of permafrost carbon in an Arctic fluvial network. *Journal of Geophysical Research: Biogeosciences* 123: 1475–1485. <https://doi.org/10.1029/2017JG004311>.
- Drake, T.W., S.E. Tank, A.V. Zhulidov, R.M. Holmes, T. Gurtovaya, and R.G.M. Spencer. 2018. Increasing alkalinity export from large Russian Arctic rivers. *Environmental Science & Technology* 52: 8302–8308. <https://doi.org/10.1021/acs.est.8b01051>.
- Drake, T.W., K.P. Wickland, R.G.M. Spencer, D.M. McKnight, and R.G. Striegl. 2015. Ancient low-molecular-weight organic acids in permafrost fuel rapid carbon dioxide production upon thaw. *Proceedings of the National Academy of Sciences* 112: 13946–13951. <https://doi.org/10.1073/pnas.1511705112>.
- Ford, J.D., and T. Pearce. 2010. What we know, do not know, and need to know about climate change vulnerability in the western Canadian Arctic: A systematic literature review. *Environmental Research Letters* 5: 14008.
- Fouché, J., C.T. Christiansen, M.J. Lafrenière, P. Grogan, and S.F. Lamoureux. 2020. Canadian permafrost stores large pools of ammonium and optically distinct dissolved organic matter. *Nature Communications* 11: 4500. <https://doi.org/10.1038/s41467-020-18331-w>.
- Frey, K.E., and J.W. McClelland. 2009. Impacts of permafrost degradation on arctic river biogeochemistry. *Hydrological Processes* 23: 169–182. <https://doi.org/10.1002/hyp.7196>.
- Frey, K.E., and L.C. Smith. 2005. Amplified carbon release from vast West Siberian peatlands by 2100. *Geophysical Research Letters*. <https://doi.org/10.1029/2004GL022025>.
- Fuchs, M., I. Nitze, J. Strauss, F. Günther, S. Wetterich, A. Kizyakov, T. Opel, M.N. Grigoriev, et al. 2020. Rapid fluvio-thermal erosion of a yedoma permafrost cliff in the Lena River Delta. *Frontiers in Earth Science*. <https://doi.org/10.3389/feart.2020.00336>.
- Graversen, R.G., T. Mauritsen, M. Tjernstrom, E. Kallen, and G. Svensson. 2008. Vertical structure of recent Arctic warming. *Nature* 451: 53–56. <https://doi.org/10.1038/nature06502>.
- Günther, F., P.P. Overduin, A.V. Sandakov, G. Grosse, and M.N. Grigoriev. 2013. Short- and long-term thermo-erosion of ice-rich permafrost coasts in the Laptev Sea region. *Biogeosciences* 10: 4297–4318. <https://doi.org/10.5194/bg-10-4297-2013>.
- Gustafsson, Ö., A. Widerlund, P. Andersson, J. Ingri, P. Roos, and A. Ledin. 2000. Colloid dynamics and transport of major elements through a boreal river — brackish bay mixing zone. *Marine Chemistry* 71: 1–21.
- Haine, T.W.N., B. Curry, R. Gerdes, E. Hansen, M. Karcher, C. Lee, B. Rudels, G. Spreen, et al. 2015. Arctic freshwater export: Status, mechanisms, and prospects. *Global and Planetary Change* 125: 13–35. <https://doi.org/10.1016/j.gloplacha.2014.11.013>.
- Hansell, D.A. 2013. Recalcitrant dissolved organic carbon fractions. *Annual Review of Marine Science* 5: 421–445. <https://doi.org/10.1146/annurev-marine-120710-100757>.
- Haugk, C., L. L. Jongejans, K. Mangelsdorf, M. Fuchs, O. Ogneva, J. Palmtag, G. Mollenhauer, P. J. Mann, et al. in review. Organic matter characteristics using lipid biomarker analysis of a rapidly eroding permafrost cliff. *Frontiers in Earth Science*.
- Holmes, R.M., J.W. McClelland, B.J. Peterson, S.E. Tank, E. Bulygina, T.I. Eglinton, V.V. Gordeev, T.Y. Gurtovaya, et al. 2012. Seasonal and annual fluxes of nutrients and organic matter from large rivers to the Arctic Ocean and surrounding seas. *Estuaries and Coasts* 35: 369–382. <https://doi.org/10.1007/s12237-011-9386-6>.
- Holmes, R.M., J.W. McClelland, P.A. Raymond, B.B. Frazer, B.J. Peterson, and M. Stieglitz. 2008. Lability of DOC transported by Alaskan rivers to the Arctic Ocean. *Geophysical Research Letters*. <https://doi.org/10.1029/2007GL032837>.
- IPCC. 2019. Special Report on the Ocean and Cryosphere in a Changing Climate. Monaco: Intergov. Panel on Climate Change.
- Jakobsson, M. 2002. Hypsometry and volume of the Arctic Ocean and its constituent seas. *Geochemistry, Geophysics, Geosystems* 3: 1–18. <https://doi.org/10.1029/2001GC000302>.
- Jeansson, E., A. Olsen, T. Eldevik, I. Skjelvan, A.M. Omar, S.K. Lauvset, J.E.Ø. Nilsen, R.G.J. Bellerby, et al. 2011. The Nordic Seas carbon budget: Sources, sinks, and uncertainties. *Global Biogeochemical Cycles*. <https://doi.org/10.1029/2010GB003961>.
- Jiao, N., J. Liu, B. Edwards, Z. Lv, R. Cai, Y. Liu, X. Xiao, J. Wang, et al. 2021. Correcting a major error in assessing organic carbon

- pollution in natural waters. *Science Advances* 7: eabc7318. <https://doi.org/10.1126/sciadv.abc7318>.
- Jones, B. M., A. M. Irrgang, L. M. Farquharson, H. Lantuit, D. Whalen, S. Ogorodov, M. Grigoriev, C. Tweedie, et al. 2020. Arctic report card: Update for 2020 - The sustained transformation to a warmer, less frozen and biologically changed Arctic remains clear. <https://arctic.noaa.gov/Report-Card/Report-Card-2020/ArtMID/7975/ArticleID/904/Coastal-Permafrost-Erosion>.
- Jongejans, L.L., J. Strauss, J. Lenz, F. Peterse, K. Mangelsdorf, M. Fuchs, and G. Grosse. 2018. Organic matter characteristics in yedoma and thermokarst deposits on Baldwin Peninsula, west Alaska. *Biogeosciences* 15: 6033–6048. <https://doi.org/10.5194/bg-15-6033-2018>.
- Juhls, B., S. Antonova, M. Angelopoulos, N. Bobrov, M. Grigoriev, M. Langer, G. Maksimov, F. Miesner, and P.P. Overduin. 2021. Serpentine (floating) ice channels and their interaction with riverbed permafrost in the Lena River Delta, Russia. *Frontiers in Earth Science*. <https://doi.org/10.3389/feart.2021.689941>.
- Juhls, B., P.P. Overduin, J. Hölemann, M. Hieronymi, A. Matsuoka, B. Heim, and J. Fischer. 2019. Dissolved organic matter at the fluvial–marine transition in the Laptev Sea using in situ data and ocean colour remote sensing. *Biogeosciences* 16: 2693–2713. <https://doi.org/10.5194/bg-16-2693-2019>.
- Juhls, B., C.A. Stedmon, A. Morgenstern, H. Meyer, J. Hölemann, B. Heim, V. Povazhnyi, and P.P. Overduin. 2020. Identifying drivers of seasonality in Lena river biogeochemistry and dissolved organic matter fluxes. *Frontiers in Environmental Science*. <https://doi.org/10.3389/fenvs.2020.00053>.
- Keskitalo, K., L. Bröder, D. Jong, N. Zimov, A. Davydova, S. Davydov, T. Tesi, P. J. Mann, et al. *Environmental Research Letters*. in review.
- Köhler, H., B. Meon, V.V. Gordeev, A. Spitzky, and R.M.W. Amon. 2003. Dissolved organic matter (DOM) in the estuaries of Ob and Yenisei and the adjacent Kara Sea, Russia. In *Siberian river run-off in the Kara Sea: Characterization, quantification, variability, and environmental significance*, ed. R. Stein, et al., 281–308. New York: Elsevier.
- Koirala, S., Y. Hirabayashi, R. Mahendran, and S. Kanae. 2014. Global assessment of agreement among streamflow projections using CMIP5 model outputs. *Environmental Research Letters* 9: 064017. <https://doi.org/10.1088/1748-9326/9/6/064017>.
- Kokelj, S.V., J. Kokoszka, J. van der Sluijs, A.C.A. Rudy, J. Tunnicliffe, S. Shakil, S. Tank, and S. Zolkos. 2020. Permafrost thaw couples slopes with downstream systems and effects propagate through Arctic drainage networks. *The Cryosphere Discuss* 2020: 1–43. <https://doi.org/10.5194/tc-2020-218>.
- Koven, C.D., B. Ringeval, P. Friedlingstein, P. Ciais, P. Cadule, D. Khvorostyanov, G. Krinner, and C. Tarnocai. 2011. Permafrost carbon-climate feedbacks accelerate global warming. *Proceedings of the National Academy of Sciences* 108: 14769–14774. <https://doi.org/10.1073/pnas.1103910108>.
- Koven, C.D., E.A.G. Schuur, C. Schädel, T.J. Bohn, E.J. Burke, G. Chen, X. Chen, P. Ciais, et al. 2015. A simplified, data-constrained approach to estimate the permafrost carbon–climate feedback. *Philosophical Transactions of the Royal Society A: Mathematical, Physical & Engineering Sciences* 373: 20140423. <https://doi.org/10.1098/rsta.2014.0423>.
- Lantuit, H., D. Atkinson, P. Paul Overduin, M. Grigoriev, V. Rachold, G. Grosse, and H.-W. Hubberten. 2011. Coastal erosion dynamics on the permafrost-dominated Bykovsky Peninsula, north Siberia, 1951–2006. *Polar Research* 30: 7341. <https://doi.org/10.3402/polar.v30i0.7341>.
- Manizza, M., M.J. Follows, S. Dutkiewicz, J.W. McClelland, D. Menemenlis, C.N. Hill, A. Townsend-Small, and B.J. Peterson. 2009. Modeling transport and fate of riverine dissolved organic carbon in the Arctic Ocean. *Global Biogeochemical Cycles*. <https://doi.org/10.1029/2008GB003396>.
- Manizza, M., M.J. Follows, S. Dutkiewicz, D. Menemenlis, C.N. Hill, and R.M. Key. 2013. Changes in the Arctic Ocean CO₂ sink (1996–2007): A regional model analysis. *Global Biogeochemical Cycles* 27: 1108–1118. <https://doi.org/10.1002/2012GB004491>.
- Mann, P.J., A. Davydova, N. Zimov, R.G.M. Spencer, S. Davydov, E. Bulygina, S. Zimov, and R.M. Holmes. 2012. Controls on the composition and lability of dissolved organic matter in Siberia’s Kolyma River basin. *Journal of Geophysical Research: Biogeosciences*. <https://doi.org/10.1029/2011JG001798>.
- Mann, P.J., T.I. Eglinton, C.P. McIntyre, N. Zimov, A. Davydova, J.E. Vonk, R.M. Holmes, and R.G.M. Spencer. 2015. Utilization of ancient permafrost carbon in headwaters of Arctic fluvial networks. *Nature Communications*. <https://doi.org/10.1038/ncomms8856>.
- Mann, P.J., W.V. Sobczak, M.M. LaRue, E. Bulygina, A. Davydova, J.E. Vonk, J. Schade, S. Davydov, et al. 2014. Evidence for key enzymatic controls on metabolism of Arctic river organic matter. *Global Change Biology* 20: 1089–1100. <https://doi.org/10.1111/gcb.12416>.
- Mann, P.J., R.G.M. Spencer, P.J. Hernes, J. Six, G.R. Aiken, S.E. Tank, J.W. McClelland, K.D. Butler, et al. 2016. Pan-Arctic trends in terrestrial dissolved organic matter from optical measurements. *Frontiers in Earth Science* 4: 18. <https://doi.org/10.3389/feart.2016.00025>.
- McClelland, J.W., R.M. Holmes, B.J. Peterson, P.A. Raymond, R.G. Striegl, A.V. Zhulidov, S.A. Zimov, N. Zimov, et al. 2016. Particulate organic carbon and nitrogen export from major Arctic rivers. *Global Biogeochemical Cycles* 30: 629–643. <https://doi.org/10.1002/2015GB005351>.
- McGuire, A.D., L.G. Anderson, T.R. Christensen, S. Dallimore, L. Guo, D.J. Hayes, M. Heimann, T.D. Lorenson, et al. 2009. Sensitivity of the carbon cycle in the Arctic to climate change. *Ecological Monographs* 79: 523–555. <https://doi.org/10.1890/08-2025.1>.
- McGuire, A.D., D.J. Hayes, D.W. Kicklighter, M. Manizza, Q. Zhuang, M. Chen, M.J. Follows, K.R. Gurney, et al. 2010. An analysis of the carbon balance of the Arctic Basin from 1997 to 2006. *Tellus b: Chemical and Physical Meteorology* 62: 455–474. <https://doi.org/10.1111/j.1600-0889.2010.00497.x>.
- Nitzbon, J., S. Westermann, M. Langer, L.C.P. Martin, J. Strauss, S. Laboor, and J. Boike. 2020. Fast response of cold ice-rich permafrost in northeast Siberia to a warming climate. *Nature Communications* 11: 2201. <https://doi.org/10.1038/s41467-020-15725-8>.
- O’Donnell, J.A., M.P. Carey, J.C. Koch, X. Xu, B.A. Poulin, J. Walker, and C.E. Zimmerman. 2020. Permafrost hydrology drives the assimilation of old carbon by stream food webs in the Arctic. *Ecosystems* 23: 435–453. <https://doi.org/10.1007/s10021-019-00413-6>.
- Obu, J., S. Westermann, A. Bartsch, N. Berdnikov, H.H. Christiansen, A. Dashtseren, R. Delaloye, B. Elberling, et al. 2019. Northern Hemisphere permafrost map based on TTOP modelling for 2000–2016 at 1 km² scale. *Earth-Science Reviews* 193: 299–316. <https://doi.org/10.1016/j.earscirev.2019.04.023>.
- Palmtag, J., C. Manning, M. Bedington, M. Fuchs, M. Göckede, G. Grosse, B. Juhls, P. Lefebvre, et al. 2021. Seasonal methane and carbon dioxide emissions from the coastal nearshore of the Kolyma river, Siberia. EGU General Assembly. <https://doi.org/10.5194/egusphere-egu21-9535>.
- Plate, S., S. Israellson, H. Midleja, G.-B. Retter, and V. Rachold. 2021. Arctic indigenous peoples. <https://www.arctic-office.de/en/publications/arctic-indigenous-peoples/>
- Polimene, L., R. Torres, H. R. Powley, M. Bedington, B. Juhls, J. Palmtag, J. Strauss, and P. J. Mann. submitted. Biological

- lability of terrigenous DOC increases CO₂ outgassing across Arctic shelves. *Geophysical Research Letters*.
- Ramage, J., L. Jungsberg, S. Wang, S. Westermann, H. Lantuit, and T. Heleniak. 2021. Population living on permafrost in the Arctic. *Population and Environment* 43: 22–38. <https://doi.org/10.1007/s11111-020-00370-6>.
- Raymond, P.A., J.W. McClelland, R.M. Holmes, A.V. Zhulidov, K. Mull, B.J. Peterson, R.G. Striegl, G.R. Aiken, et al. 2007. Flux and age of dissolved organic carbon exported to the Arctic Ocean: A carbon isotopic study of the five largest arctic rivers. *Global Biogeochemical Cycles*. <https://doi.org/10.1029/2007GB002934>.
- Raymond, P.A., J.E. Saiers, and W.V. Sobczak. 2016. Hydrological and biogeochemical controls on watershed dissolved organic matter transport: Pulse-shunt concept. *Ecology* 97: 5–16.
- Reyes, F.R., and V.L. Loughheed. 2015. Rapid nutrient release from permafrost thaw in arctic aquatic ecosystems. *Arctic, Antarctic, and Alpine Research* 47: 35–48.
- Rogers, J.A., V. Galy, A.M. Kellerman, J.P. Chanton, N. Zimov, and R.G.M. Spencer. 2021. Limited presence of permafrost dissolved organic matter in the Kolyma River, Siberia revealed by ramped oxidation. *Journal of Geophysical Research: Biogeosciences* 126: e2020JG005977. <https://doi.org/10.1029/2020JG005977>.
- Rolph, R., P.P. Overduin, T. Ravens, H. Lantuit, and M. Langer. 2021. ArcticBeach v1.0: A physics-based parameterization of pan-Arctic coastline erosion. *Geoscientific Model Development* 2021: 1–26. <https://doi.org/10.5194/gmd-2021-28>.
- Schneider von Deimling, T., G. Grosse, J. Strauss, L. Schirrmeister, A. Morgenstern, S. Schaphoff, M. Meinshausen, and J. Boike. 2015. Observation-based modeling of permafrost carbon fluxes with accounting for deep carbon deposits and thermokarst activity. *Biogeosciences* 12: 3469–3488. <https://doi.org/10.5194/bg-12-3469-2015>.
- Schuster, U., G.A. McKinley, N. Bates, F. Chevallier, S.C. Doney, A.R. Fay, M. González-Dávila, N. Gruber, et al. 2013. An assessment of the Atlantic and Arctic sea–air CO₂ fluxes, 1990–2009. *Biogeosciences* 10: 607–627. <https://doi.org/10.5194/bg-10-607-2013>.
- Semiletov, I., I. Pipko, Ö. Gustafsson, L.G. Anderson, V. Sergienko, S. Pugach, O. Dudarev, A. Charkin, et al. 2016. Acidification of East Siberian Arctic Shelf waters through addition of freshwater and terrestrial carbon. *Nature Geoscience* 9: 361–365. <https://doi.org/10.1038/ngeo2695>.
- Shakhova, N., I. Semiletov, A. Salyuk, V. Yusupov, D. Kosmach, and Ö. Gustafsson. 2010. Extensive methane venting to the atmosphere from sediments of the East Siberian Arctic Shelf. *Science* 327: 1246–1250. <https://doi.org/10.1126/science.1182221>.
- Shiklomanov, A. I., R. M. Holmes, J. W. McClelland, S. E. Tank, and R. G. M. Spencer. 2021. Arctic great rivers observatory. Discharge Dataset, Version 20210319.
- Shiklomanov, A., R. Lammers, D. Lettenmaier, M. Polischuk Yu, O. Savichev, and L. Smith. 2013. 4. Hydrological changes: Historical analysis, contemporary status, and future projections. In *Regional environmental changes in Siberia and their global consequences*, ed. P. Groisman and G. Gutman. New York: Springer.
- Slavik, K., B.J. Peterson, L.A. Deegan, W.B. Bowden, A.E. Hershey, and J.E. Hobbie. 2004. Long-term responses to the Kuparuk river ecosystem to phosphorus enrichment. *Ecology* 85: 939–954.
- Soares, A.R.A., J.-F. Lapierre, B.P. Selvam, G. Lindström, and M. Berggren. 2019. Controls on dissolved organic carbon bioreactivity in river systems. *Scientific Reports* 9: 14897. <https://doi.org/10.1038/s41598-019-50552-y>.
- Spencer, R.G.M., P.J. Mann, T. Dittmar, T.I. Eglinton, C. McIntyre, R.M. Holmes, N. Zimov, and A. Stubbins. 2015. Detecting the signature of permafrost thaw in Arctic rivers. *Geophysical Research Letters* 42: 2830–2835. <https://doi.org/10.1002/2015GL063498>.
- St Pierre, K.A., S. Zolkos, S. Shakil, S.E. Tank, V.L. St Louis, and S.V. Kokelj. 2018. Unprecedented increases in total and methyl mercury concentrations downstream of retrogressive thaw slumps in the Western Canadian Arctic. *Environmental Science & Technology* 52: 14099–14109.
- Stettner, S., A.L. Beamish, A. Bartsch, B. Heim, G. Grosse, A. Roth, and H. Lantuit. 2018. Monitoring inter- and intra-seasonal dynamics of rapidly degrading ice-rich permafrost riverbanks in the Lena Delta with TerraSAR-X time series. *Remote Sensing* 10: 51. <https://doi.org/10.3390/rs10010051>.
- Strauss, J., B. Abbott, G. Hugelius, E.A.G. Schuur, C. Treat, M. Fuchs, C. Schädel, M. Ulrich, et al. 2021a. Permafrost. In *Recarbonizing global soils – A technical manual of recommended management practices*, ed. J. Strauss, B. Abbott, and Food and Agriculture Organization of the United Nations (FAO), and Intergovernmental Technical Panel on Soils (ITPS), 127–147. Rome: Food and Agriculture Organization of the United Nations.
- Strauss, J., S. Laboor, L. Schirrmeister, A. N. Fedorov, D. Fortier, D. Froese, M. Fuchs, F. Günther, et al. 2021b. Circum-Arctic Map of the Yedoma permafrost domain. *Frontiers in Earth Science*.
- Strauss, J., L. Schirrmeister, G. Grosse, D. Fortier, G. Hugelius, C. Knoblauch, V. Romanovsky, C. Schädel, et al. 2017. Deep Yedoma permafrost: A synthesis of depositional characteristics and carbon vulnerability. *Earth-Science Reviews* 172: 75–86. <https://doi.org/10.1016/j.earscirev.2017.07.007>.
- Strauss, J., L. Schirrmeister, K. Mangelsdorf, L. Eichhorn, S. Wetterich, and U. Herzschuh. 2015. Organic matter quality of deep permafrost carbon - A study from Arctic Siberia. *Biogeosciences* 12: 2227–2245. <https://doi.org/10.5194/bg-12-2227-2015>.
- Strauss, J., L. Schirrmeister, S. Wetterich, A. Borchers, and S.P. Davydov. 2012. Grain-size properties and organic-carbon stock of Yedoma Ice Complex permafrost from the Kolyma lowland, northeastern Siberia. *Global Biogeochemical Cycles* 26: GB3003. <https://doi.org/10.1029/2011GB004104>.
- Terhaar, J., R. Lauerwald, P. Regnier, N. Gruber, and L. Bopp. 2021. Around one third of current Arctic Ocean primary production sustained by rivers and coastal erosion. *Nature Communications* 12: 169. <https://doi.org/10.1038/s41467-020-20470-z>.
- Turetsky, M.R., B.W. Abbott, M.C. Jones, K.W. Anthony, D. Olefeldt, E.A.G. Schuur, G. Grosse, P. Kuhry, et al. 2020. Carbon release through abrupt permafrost thaw. *Nature Geoscience* 13: 138–143. <https://doi.org/10.1038/s41561-019-0526-0>.
- Van Everdingen, R.O. 2005. *Multi-language glossary of permafrost and related ground-ice*. International Permafrost Association, Terminology Working Group.
- van Vliet, M.T.H., W.H.P. Franssen, J.R. Yearsley, F. Ludwig, I. Haddeland, D.P. Lettenmaier, and P. Kabat. 2013. Global river discharge and water temperature under climate change. *Global Environmental Change* 23: 450–464. <https://doi.org/10.1016/j.gloenvcha.2012.11.002>.
- Vasil'chuk, Y.K., A.C. Vasil'chuk, D. Rank, W. Kutschera, and J.C. Kim. 2001. Radiocarbon dating of $\delta^{18}\text{O}$ - δD plots in Late Pleistocene ice-wedges of the Duvanny Yar (Lower Kolyma River, Northern Yakutia). *Radiocarbon* 43: 541–553. <https://doi.org/10.1017/S0033822200041199>.
- Vonk, J.E., and Ö. Gustafsson. 2013. Permafrost-carbon complexities. *Nature Geoscience* 6: 675–676. <https://doi.org/10.1038/ngeo1937>.
- Vonk, J.E., P.J. Mann, S. Davydov, A. Davydova, R.G.M. Spencer, J. Schade, W.V. Sobczak, N. Zimov, et al. 2013. High biolability

- of ancient permafrost carbon upon thaw. *Geophysical Research Letters* 40: 2689–2693. <https://doi.org/10.1002/grl.50348>.
- Vonk, J.E., S.E. Tank, P.J. Mann, R.G.M. Spencer, C. Treat, R.G. Striegl, B.W. Abbott, and K.P. Wickland. 2015. Biodegradability of dissolved organic carbon in permafrost soils and aquatic systems: A meta-analysis. *Biogeosciences* 12: 6915–6930. <https://doi.org/10.5194/bg-12-6915-2015>.
- Wang, P., Q. Huang, S.P. Pozdniakov, S. Liu, N. Ma, T. Wang, Y. Zhang, J. Yu, et al. 2021. Potential role of permafrost thaw on increasing Siberian river discharge. *Environmental Research Letters* 16: 034046. <https://doi.org/10.1088/1748-9326/abe326>.
- Wetterich, S., A. Kizyakov, M. Fritz, J. Wolter, G. Mollenhauer, H. Meyer, M. Fuchs, A. Aksenov, et al. 2020. The cryostratigraphy of the Yedoma cliff of Sobo-Sise Island (Lena delta) reveals permafrost dynamics in the central Laptev Sea coastal region during the last 52 kyr. *The Cryosphere* 14: 4525–4551. <https://doi.org/10.5194/tc-14-4525-2020>.
- Wickland, K.P., G.R. Aiken, K. Butler, M.M. Dornblaser, R.G.M. Spencer, and R.G. Striegl. 2012. Biodegradability of dissolved organic carbon in the Yukon River and its tributaries: Seasonality and importance of inorganic nitrogen. *Global Biogeochemical Cycles*. <https://doi.org/10.1029/2012GB004342>.
- Wickland, K.P., M.P. Waldrop, G.R. Aiken, J.C. Koch, M.T. Jorgenson, and R.G. Striegl. 2018. Dissolved organic carbon and nitrogen release from boreal Holocene permafrost and seasonally frozen soils of Alaska. *Environmental Research Letters* 13: 065011. <https://doi.org/10.1088/1748-9326/aac4ad>.
- Wild, B., A. Andersson, L. Bröder, J. Vonk, G. Hugelius, J.W. McClelland, W. Song, P.A. Raymond, et al. 2019. Rivers across the Siberian Arctic unearth the patterns of carbon release from thawing permafrost. *Proceedings of the National Academy of Sciences* 116: 10280–10285. <https://doi.org/10.1073/pnas.1811797116>.
- Zolkos, S., D.P. Krabbenhoft, A. Suslova, S.E. Tank, J.W. McClelland, R.G.M. Spencer, A. Shiklomanov, A.V. Zhulidov, et al. 2020. Mercury export from Arctic Great rivers. *Environmental Science & Technology* 54: 4140–4148. <https://doi.org/10.1021/acs.est.9b07145>.

Publisher's Note Springer Nature remains neutral with regard to jurisdictional claims in published maps and institutional affiliations.

AUTHOR BIOGRAPHIES

Paul J. Mann (✉) is an Associate Professor at the Department of Geography and Environmental Sciences at Northumbria University, Newcastle-Upon-Tyne, UK. His research interests include the degradation, transport and fate of thawing permafrost matter in the aquatic and marine environment.
Address: Dept of Geography & Environmental Sciences, Northumbria University, Newcastle upon Tyne NE1 8ST, UK.
e-mail: paul.mann@northumbria.ac.uk

Jens Strauss is a geoecologist who heads the working group on Permafrost Biogeochemistry of the Permafrost Research Section at the Alfred Wegener Institute (AWI) in Potsdam. He has specialized in deep ice-rich permafrost (Yedoma) and his research strives to determine the size of the organic carbon pool frozen in Yedoma, the quality of this carbon, and the speed at which it may be broken down by microorganisms and released in the form of greenhouse gases if it thaws.
Address: Alfred Wegener Institute Helmholtz Centre for Polar and Marine Research, Telegrafenberg A45, 14473 Potsdam, Germany.
e-mail: jens.strauss@awi.de

Juri Palmtag is a research fellow at the Department of Geography and Environmental Sciences at Northumbria University. His research interests range from the spatial distribution of terrestrial soil organic carbon and nitrogen in permafrost-affected soils to carbon dioxide and methane fluxes from nearshore environments.
Address: Dept of Geography & Environmental Sciences, Northumbria University, Newcastle upon Tyne NE1 8ST, UK.
e-mail: juri.palmtag@northumbria.ac.uk

Kelsey Dowdy is a doctoral candidate at the Department for Ecology, Evolution, and Marine Biology at the University of California, Santa Barbara. She is an ecosystem ecologist interested in connections both within nature and between nature and humans. Her Ph.D. studies focus on Ecology with an emphasis in Ethnomusicology.
Address: University of California, Santa Barbara, UCEN Rd, Goleta, CA 93117, USA.
e-mail: kelsey.dowdy@lifesci.ucsb.edu

Olga Ogneva is a doctoral candidate at the Alfred Wegener Institute in Bremerhaven, Germany. Her research interests include investigation of stable and radiocarbon composition of organic matter derived from permafrost into the Arctic deltaic ecosystems.
Address: Alfred Wegener Institute Helmholtz Centre for Polar and Marine Research, Am Handelshafen 12, 27570 Bremerhaven, Germany.
e-mail: Olga.Ogneva@awi.de

Matthias Fuchs is a Postdoc at the Alfred Wegener Institute Helmholtz Centre for Polar and Marine Research, Potsdam, Germany. His research interests include permafrost research, biogeochemistry, Arctic coastal wetlands.
Address: Alfred Wegener Institute Helmholtz Centre for Polar and Marine Research, Telegrafenberg A45, 14473 Potsdam, Germany.
e-mail: matthias.fuchs@awi.de

Michael Bedington is a numerical modeller at Plymouth Marine Laboratory. His research uses high resolution models of coastal systems to understand problems in coastal oceanography and biogeochemistry under global change.
Address: Plymouth Marine Laboratory, Prospect Place, Plymouth PL1 3DH, UK.
e-mail: mbe@pml.ac.uk

Ricardo Torres is physical oceanographer at Plymouth Marine Laboratory. His research focuses on the physical–biological interactions that mediate shelf, coastal and estuarine ecosystem responses to natural variability, anthropogenic interventions and climate change combining modelling and observational approaches.
Address: Plymouth Marine Laboratory, Prospect Place, Plymouth PL1 3DH, UK.
e-mail: rito@pml.ac.uk

Luca Polimene is a marine ecosystem modeller at Plymouth Marine Laboratory. His research focuses on the cycle of dissolved and particulate organic carbon in the ocean and the physical–biological interactions driving the planktonic ecosystem.
Address: Plymouth Marine Laboratory, Prospect Place, Plymouth PL1 3DH, UK.
e-mail: luca@pml.ac.uk

Paul Overduin is a senior scientist who heads the working group on Subsea Permafrost of the Permafrost Research Section at the Alfred Wegener Institute (AWI) in Potsdam. He has specialized in submarine and terrestrial permafrost, Arctic coastal geomorphodynamics and in geophysical methods.

Address: Alfred Wegener Institute Helmholtz Centre for Polar and Marine Research, Telegrafenberg A45, 14473 Potsdam, Germany.
e-mail: Paul.Overduin@awi.de

Gesine Mollenhauer is a marine organic geochemist at the Alfred Wegener Institute in Bremerhaven, Germany. She uses a combination of organic geochemical methods and radiocarbon dating to investigate transport of organic matter and carbon cycling in a land–ocean continuum, the fate of terrestrial organic matter delivered to aquatic systems and the ocean, and glacial–interglacial changes in these processes.

Address: Alfred Wegener Institute Helmholtz Centre for Polar and Marine Research, Am Handelshafen 12, 27570 Bremerhaven, Germany.

e-mail: Gesine.mollenhauer@awi.de

Guido Grosse is a Professor for Permafrost in the Earth System at University of Potsdam and the Alfred Wegener Institute Helmholtz Centre for Polar and Marine Research, Germany. His research interests include permafrost landscape dynamics in the Arctic and its feedbacks with hydrology and carbon cycling.

Address: Alfred Wegener Institute Helmholtz Centre for Polar and Marine Research, Telegrafenberg A45, 14473 Potsdam, Germany.

Address: Institute of Geosciences, University of Potsdam, Potsdam, Germany.

e-mail: guido.grosse@awi.de

Volker Rachold is the Head of the German Arctic Office at the Alfred Wegener Institute (AWI), which serves as an information and cooperation platform between German stakeholders from science, politics and industry. Before he served as the Executive Secretary of the International Arctic Science Committee (IASC) in Stockholm and

Potsdam since 2006. His research as a graduated geochemist at AWI was focussed on land–ocean interactions in the Siberian Arctic. He led several land- and ship-based Russian-German expeditions.

Address: Alfred Wegener Institute Helmholtz Centre for Polar and Marine Research, Telegrafenberg A45, 14473 Potsdam, Germany.

e-mail: Volker.Rachold@arctic-office.de

William V. Sobczak is a Professor in the Biology Department at the College of the Holy Cross. His research interests span aquatic and ecosystem ecology, biogeochemistry and watershed hydrology.

Address: Department of Biology, College of the Holy Cross, 1 College St, Worcester, MA 01610, USA.

e-mail: wsobczak@holycross.edu

Robert G. M. Spencer is a Professor of Oceanography in the department of Earth, Ocean and Atmospheric Science at Florida State University, USA. His research interests are focused on the understanding of the chemical composition of Earth's major carbon reservoirs and dissolved organic matter in marine and terrestrial ecosystems.

Address: Florida State University, 303 Oceanography Building, Tallahassee, FL 32306, USA.

e-mail: rgspencer@fsu.edu

Bennet Juhls is a Postdoctoral Scientist at the Alfred Wegener Institute Helmholtz Centre for Polar and Marine Research. His research interests include land–ocean matter fluxes in the Arctic, aquatic biogeochemistry, and optical and radar remote sensing.

Address: Alfred Wegener Institute Helmholtz Centre for Polar and Marine Research, Telegrafenberg A45, 14473 Potsdam, Germany.

e-mail: bjuhls@awi.de


Seasonal nitrogen fluxes of the Lena River Delta

By Sanders, T., Fiencke, C., Fuchs, M., Haugk, C., Juhls, B., Mollenhauer, G., **Ogneva, O.**, Overduin, P. P., Palmtag, J., Povazhniy, V., Strauss, J., Tuerena, R. E., Zell, N. and Dähnke, K. (2022)

Published in *Ambio*

<https://doi.org/10.1007/s13280-021-01665-0>

Seasonal nitrogen fluxes of the Lena River Delta

Tina Sanders , Claudia Fiencke, Matthias Fuchs, Charlotte Haugk, Bennet Juhls, Gesine Mollenhauer, Olga Ogneva, Paul Overduin, Juri Palmtag, Vasily Povazhniy, Jens Strauss, Robyn Tuerena, Nadine Zell, Kirstin Dähnke

Received: 5 May 2021 / Revised: 7 September 2021 / Accepted: 1 November 2021 / Published online: 16 December 2021

Abstract The Arctic is nutrient limited, particularly by nitrogen, and is impacted by anthropogenic global warming which occurs approximately twice as fast compared to the global average. Arctic warming intensifies thawing of permafrost-affected soils releasing their large organic nitrogen reservoir. This organic nitrogen reaches hydrological systems, is remineralized to reactive inorganic nitrogen, and is transported to the Arctic Ocean via large rivers. We estimate the load of nitrogen supplied from terrestrial sources into the Arctic Ocean by sampling in the Lena River and its Delta. We took water samples along one of the major deltaic channels in winter and summer in 2019 and sampling station in the central delta over a one-year cycle. Additionally, we investigate the potential release of reactive nitrogen, including nitrous oxide from soils in the Delta. We found that the Lena transported nitrogen as dissolved organic nitrogen to the coastal Arctic Ocean and that eroded soils are sources of reactive inorganic nitrogen such as ammonium and nitrate. The Lena and the Deltaic region apparently are considerable sources of nitrogen to nearshore coastal zone. The potential higher availability of inorganic nitrogen might be a source to enhance nitrous oxide emissions from terrestrial and aquatic sources to the atmosphere.

Keywords Arctic Ocean · Lena Delta · Nitrogen · Nitrous oxide

INTRODUCTION

The Arctic is warming at twice the rate of the global average (Smith et al. 2019). In the Arctic Ocean, for instance, sea ice, especially multi-year ice, is being lost at an unprecedented rate (Overland and Wang 2013). Longer ice-free periods result in potentially higher productivity and changes of food webs (Lewis et al. 2020). At the same time, increasing air temperatures are thawing permafrost around the Arctic Ocean (Biskaborn et al. 2019), which then release organic matter including nitrogen to river and further on to the Arctic Ocean.

The permafrost-affected soils store a globally large amount of organic matter, including organic carbon (OC) and nitrogen (N). It is estimated that more than half of the global soil organic matter (SOM) are stored within the northern permafrost region. Hugelius et al. (2014) estimated a total SOC stocks in the northern circumpolar permafrost region of $\sim 1300 \text{ Pg} \pm 200 \text{ Pg}$. A recent publication by Mishra et al. (2021) based on > 2700 soil profiles estimated a total SOC stock of 1000 (– 170 to + 186 Pg) to 300 cm. Circumpolar estimate for N ranged between 40 and 67 Pg N (Weintraub and Schimel 2003; Harden et al. 2012). Compared to SOC stocks, we know little about the N stocks in the permafrost zone, which are therefore a subject of ongoing debate. For instance, based on typical soil C:N ratios of 10–50 and scaled to the amount of SOC, the actual N stock in permafrost-affected soils could reach 130 Pg N (Voigt et al. 2020). Abbott and Jones (2015) suggest that globally relevant quantities of N are stored in permafrost soils.

These stocks are prone to be reactivated by thawing ground ice, which leads to a suite of mass wasting and subsidence processes such as thermokarst. The release of N stocks also results from fluvial (Kanevskiy et al. 2016;

Supplementary Information The online version contains supplementary material available at <https://doi.org/10.1007/s13280-021-01665-0>.

Fuchs et al. 2020) and coastal erosion (Günther et al. 2013). In order to understand N release and its utilization as a consequence of permafrost thaw, we need studies that combine investigations of soil N cycling with soil erosion, soil release of reactive nitrogen to the rivers, and transport to the Arctic Ocean. Reactive nitrogen are components (dissolved inorganic N (DIN) and dissolved organic N (DON)), which are available for primary producers such as plants and microorganisms.

There are some studies on N cycling in permafrost-affected soils (e.g., Biasi et al. 2005; Stewart et al. 2014; Sanders et al. 2019; Horn and Hetz 2021). Recent newer studies focus on the potential nitrous oxide (N₂O) emissions from permafrost-affected soils (reviewed by Voigt et al. (2020)) and the input of C and N into the fluvial system (Hugelius et al. 2020; Pastor et al. 2020). While most N turnover occurs during summer, winter N mineralization may provide an important N source upon thaw in spring, when a pulse of nitrate (NO₃⁻) in soil solution has been observed in studies of Arctic ecosystems (Schimel and Bennett 2004; Buckeridge et al. 2013; Rasmussen et al. 2020). Inorganic dissolved nitrogen or small dissolved organic N compounds such as urea or amino acids can contribute to primary productivity in soils (Schimel and Bennett 2004) and nevertheless, nitrogen and phosphorus are limiting nutrients in the Arctic ecosystems such as soils and rivers (Shaver et al. 1986; Beermann et al. 2014; Schade et al. 2016; Hobbie et al. 2021).

Other studies have investigated N fluxes in Arctic rivers (Dittmar and Kattner 2003; Frey and McClelland 2009; Holmes et al. 2012); rivers receive a large portion of N from soils during the spring freshet, which is consumed during summer (Buckeridge et al. 2010; Abbott and Jones 2015). N is mainly transported to the Arctic Ocean as DON and NO₃⁻ (Holmes et al. 2012). The mean riverine NO₃⁻ contribution to ocean primary production in the Arctic is generally low and is approx. 5% for the Laptev Sea (Le Fouest et al. 2015). Both nitrite (NO₂⁻) and ammonium (NH₄⁺) are rapidly converted into NO₃⁻ or assimilated by plants or phytoplankton. However, rapid uptake of DIN, coupled with relatively quick regeneration of dissolved organic nitrogen (DON) in N-limited nearshore regions, could potentially lead to high local rates of riverine-supported photosynthesis (Tank et al. 2012). Arctic rivers annually carry ~ 13% of the freshwater transported globally from land to ocean, though the Arctic Ocean only makes up approximately 1% of the total global ocean volume. (Aagaard and Carmack 1989; Anderson et al. 1998). Throughout the Eurasian Shelf region, rapid summertime depletion of NO₃⁻ across the full fluvial–marine transition in the Laptev Sea indicates N limitation (Kattner

et al. 1999; Dittmar and Kattner 2003; Reyes and Loughheed 2015).

Across the entire Arctic, the influx of DON to the Arctic shelf waters from rivers is five times greater compared to the influx of NO₃⁻ (Dittmar and Kattner 2003) and also 70% of the DON is removed in shelf waters before even reaching the open marine environment (Thibodeau et al. 2017). In the nearshore regions, the riverine nutrients (organic and inorganic) have the greatest influence on productivity (Dunton et al. 2006). However, Tank et al. (2012) found that riverine nutrients are not sufficient to explain a large proportion of primary production in the Arctic Ocean. Although, Terhaar et al (2021) reported recently that riverine inputs indeed fuels primary production, but that satellite-based primary production rates might be overestimated especially for the Laptev and East Siberian Seas. It is important, therefore, to understand how much permafrost degradation may impact N forms and amounts from delta to nearshore environments, and the potential changes to the riverine and coastal nitrogen cycle and the ratio between its organic and inorganic N components. Generally, estuarine and deltaic regions are filters for riverine inputs to the coastal waters and the open ocean (Smith et al. 2005). They can also be a considerable source of N₂O emissions (Seitzinger and Kroeze 1998; Dunton et al. 2006; Marzadri et al. 2021), nevertheless, N₂O emissions from Arctic rivers and deltas are as yet poorly investigated.

In this study, we want to assess the amount of nitrogen which is released and transported from terrestrial sources to the Lena River and further through its delta towards the nearshore Laptev Sea. Based on our findings, we discuss the implications that thawing permafrost and release of reactive nitrogen may have on the ecosystem and the nitrogen cycle. In addition, we explore whether the increasing availability of reactive inorganic nitrogen in soils and rivers can potentially cause increasing N₂O emissions.

MATERIALS AND METHODS

In this study, we present nutrient data focusing on N from two cruises in winter and summer 2019 from the inner Lena Delta to the nearshore Laptev Sea and a one-year monitoring data set from the Research Station Samoylov in 2018 and 2019 (see (Juhls et al. 2020)). Furthermore, in order to estimate soil release of organic matter including C and N, soil incubation experiments were conducted. We measured the release of inorganic N forms by remineralization and nitrification and potential nitrous oxide (N₂O) production.

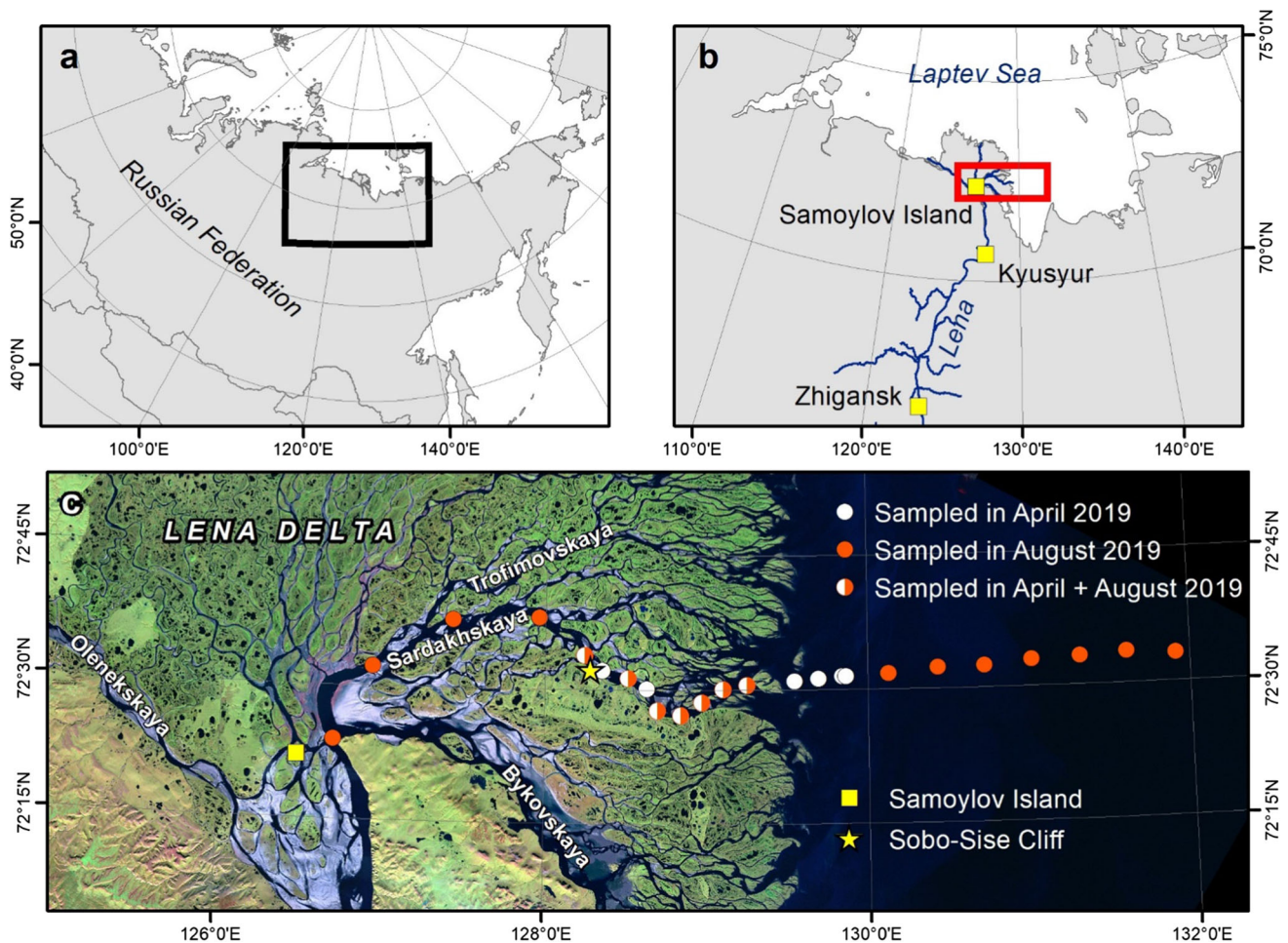


Fig. 1 Study site area of the Lena Delta in Northeast Siberia (a). Lena River and Delta including the ArcticGRO station in Zhigansk, the gauge station in Kyusyur, and the Samoylov Station (b). Transect and sampling sites of the cruises in winter (white dots) and summer (red dots), Samoylov Island, sampling site for soil incubations and the one-year data set, Sobe-Sibe Cliff (c)

River study site and cruises

The Lena Delta is located in northeastern Siberia, where the Lena River cuts through the Verkhoyansk Mountains range and discharges into the Laptev Sea, a shallow shelf sea in the Arctic Ocean. The Lena is divided in three major channels, the Olenekskaya flowing to the western Laptev Sea and the Trofimovskaya, which bifurcates into the Sardakhskaya and Bykovskaya channels, both flowing into the eastern Laptev Sea (Fig. 1) (Fedorova et al. 2015). Samples were collected along the Sardakhskaya Channel in late winter (March/April 2019) and summer (August 2019). The Sardakhskaya Channel has a water discharge of $\sim 8000 \text{ m}^3 \text{ s}^{-1}$, which represent up to 40% of the discharge of the Lena main channel (Fedorova et al. 2015). The Lena River is ice-covered for about 8 months a year between October and May with an ice thickness of up to 2 m. Water depth at the beginning of the Sardakhskaya Channel can reach 22 m (Fedorova et al. 2015) and is approximately

11 m in front of Sobo-Sise cliff (Fuchs et al. 2020), so that water flows underneath the river ice cover during the winter months (Fuchs et al. (in review)).

Water, suspended particulate matter (SPM), and surface sediment samples were collected. Overall, 24 stations were sampled: at seven sites were sampled in both winter and summer, with an extra six sites sampled in winter only, and an extra 11 sites sampled in summer only (Fig. 1C).

In winter, water samples were collected from beneath the ice, if possible, additional on the halfway down and above the sediment through holes drilled through the river ice (ca. 2 m thickness) using an UWITEC water sampler. Holes were drilled at 5-km intervals until approximately 30 km offshore. Conductivity, temperature, and depth (CTD) were measured at each station using a SontekTM CastAway CTD sensor. Water samples were filtered directly in the field through pre-combusted GF/F glass fiber filters ($0.7 \mu\text{m}$, Whatman) and stored frozen in HDPE bottles until thawed for further analysis.

In summer, the transect was sampled in two short campaigns: (1) from offshore to the nearshore in the Laptev Sea with the marine vessel *Anatoliy Zhilinskiy* and (2) from the board of the river ship *Merzlotoved* along the Sardakhsaya channel. In the Laptev Sea, we sampled the water column at three different depths, 1 m below the water surface, halfway down the water column, and just above the riverbed or seabed. In the Lena Delta, one to three water samples were taken depending on the water depth. Additionally, sediment samples were taken using a gravity corer (from which the overlying bottom water was sampled).

121 river water samples were collected at the Samoylov research station from September 2018 to September 2019. The sampling procedure is described in detail in Juhls et al. (2020). Water samples were collected from just below the river surface in the center of the Olenekskaya Channel near Samoylov Island in a pre-rinsed HDPE bottle. Samples were collected from a boat during the ice-free period and from the ice during the winter. When ice break-up or freeze-up made access dangerous, samples were taken from the shore of Samoylov Island.

Soil study site and incubations

Soil was sampled from different soil types and geomorphologic units on Samoylov Island. The soils of Samoylov represent the main Holocene soil types in the younger part of the Lena Delta. The island can be divided into two major geomorphological units (Sanders et al. 2010), which vary in moisture regime and in SOM (Boike et al. 2013) (Fig. 2). The western part of Samoylov Island represents a relatively young floodplain up to 4 m above river level (a.r.l.), which is flooded in spring. The eastern part of Samoylov Island is an elevated (10–16 m a.r.l.) river terrace of late Holocene age. The river terrace is flooded only during extreme flooding events (Kutzbach et al. 2004). Soil types and characteristics are described in detail elsewhere (Sanders et al. 2010; Zubrzycki et al. 2013).

Soils were sampled from the floodplain and elevated river terrace. For the measurement of the OM content, extractable DIN, and the incubation setups, soil was sampled from polygonal tundra, cliff, and beach at seven sites (Fig. 2). Permafrost was sampled from the cliff face of Samoylov Island on the river terrace (K1 and K3). The cliff was exposed by ongoing thawing and erosion. At K1, soil was sampled from a former polygon center in a depth of

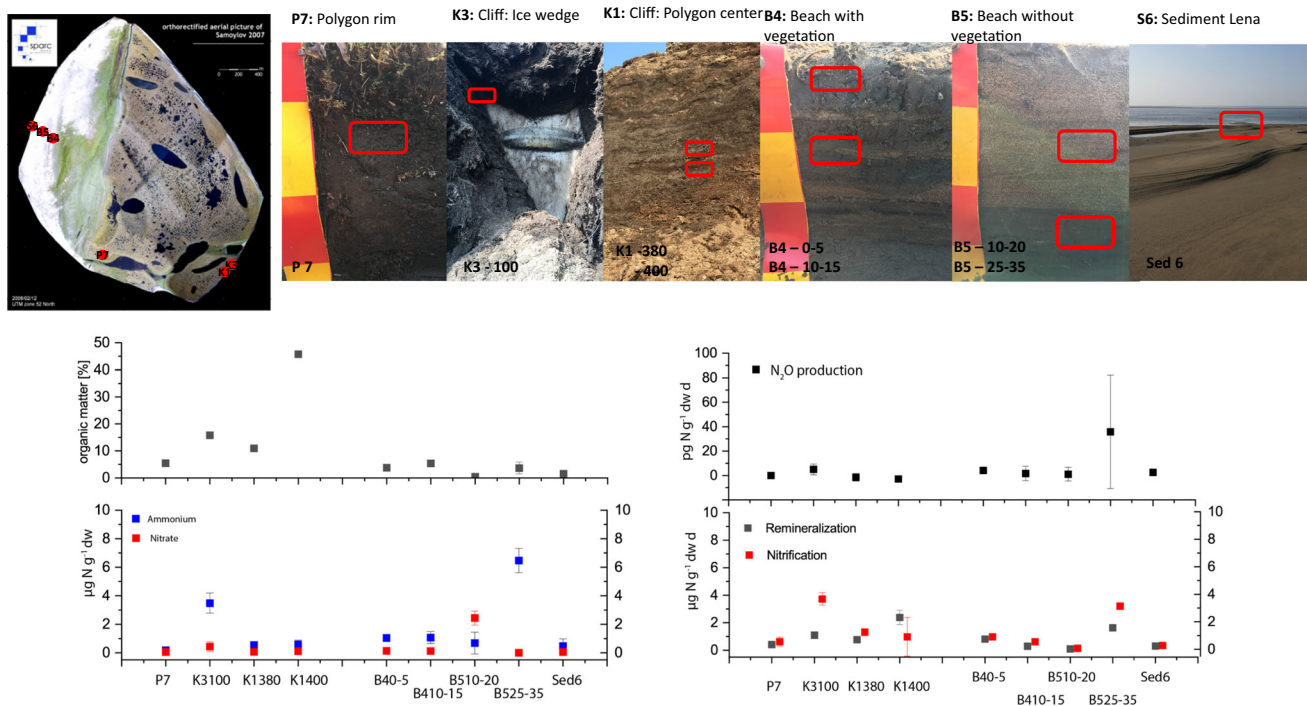


Fig. 2 Properties of investigated soils and their remineralization, nitrification and N_2O production rates. Soil samples were taken at 6 different sites: K1 (cliff, former polygon center) in two depth 3.8 and 4.0 m below the ground surface, K2 (cliff, former polygon wall, close to the ice wedge), 1.0 m below the ground surface, P7 (polygon wall), depth 10–20 cm, B4 (beach, primary vegetation cover), 0–5 cm and 10–20 cm, B5 (beach without vegetation cover), 10–20 cm and 25–35 cm, Sed6 (sediment in the Lena) as surface sediment. Organic matters were measured by combustion at 550 °C; NO_3^- and NH_4^+ were extracted by 0,0125 M KCl; remineralization and nitrification rates were measured by incubation of soil in Lena water; N_2O production rates were measured after soil samples were transported to Germany

3.8 and 4 m below the ground surface. In addition, the polygonal tundra (P7) were sampled at a polygon rim in 10–20 cm. At K3 soils were sampled next to an ice wedge and originated from a former polygon rim in 1 m below the ground surface. Furthermore, a transect was sampled from the floodplain to the beach into the Lena River sediment at different depths (B4: 0–5 cm and 10–15 cm, B5: 10–20 cm and 25–35 cm, and S6: surface sediment). Primary vegetation was present only at sampling site B4. The other sites were bare soil (Fig. 2).

Soil samples were incubated in Lena water to quantify the remineralization and nitrification of organic N to inorganic N (NH_4^+ and NO_3^-). We followed two different approaches for sample analysis: (1) Analyses during the field campaign in 2019 in the laboratory of the Samoylov Island Research Station to measure the net N-remineralization and net nitrification rates; (2) Analyses of frozen soil samples and Lena River water at the University of Hamburg to measure potential N_2O production.

For the first analysis, 15–20 g of wet soils and 130 ml unfiltered Lena water were incubated on a shaker (14 days, 110 rpm) at room temperature (20–25 °C). Subsamples of mixed overlying water were taken every 2–3 days. At the end of the incubation, the remaining soil/sediment and the overlying water were sampled. To calculate net N remineralization and net nitrification, DIN was measured over time, and sediment and soil TN were determined at the end of the incubations.

In another incubation, we measured potential aerobic nitrous oxide production rates. 1 g fresh weight of homogenized soil was weighed in 100 ml serum bottles. 20 ml Lena River water was added and the bottles were sealed air-tight with rubber septa. Soil samples were incubated in 18 replicates at 5 °C, without shaking in the dark. 3×1 ml gas samples were taken after 1, 2, 8, 11, and 18 weeks, and N_2O concentration was determined by gas chromatography (GC, Agilent Technologies 7890 A, Santa Clara, CA, USA).

Laboratory analyses

For this study, water, suspended particulate matter (SPM), and sediment were sampled. Soil samples were taken for incubation experiments. Dissolved nutrients (NH_4^+ , NO_2^- , NO_3^-), phosphate and silicate, total dissolved organic nitrogen and phosphorus (TDN and TDP), and dissolved carbon (DOC) were measured in filtered water samples. Total nitrogen and phosphorus (TN and TP) were measured in unfiltered water samples. SPM was analyzed for C and N content and $\delta^{15}\text{N}$. Sediment samples were analyzed for grain size, C and N content and $\delta^{15}\text{N}$. Soil and sediment samples from Samoylov Island were analyzed for their OM, C, N, $\delta^{15}\text{N}$ and extractable dissolved inorganic N

contents. A detailed description of the analytical methods is provided in the [Supplementary Information](#).

Estimation of nitrogen loads from the Lena River to the nearshore Laptev Sea

We used the Samoylov monitoring data of 121 samples from September 2018 to August 2019 to calculate the annual N-NO_3^- and TN flux to the Arctic Ocean. We linearly interpolated between sampling days to obtain daily concentrations. To calculate discharge, we corrected the Lena River discharge data from the Roshdyromet gauge station at Kyusyur (Shiklomanov et al. 2021.) for the travel time to the sampling station Samoylov Island (Juhls et al. 2020) Fig. 6). Daily concentration was multiplied with corrected daily discharge values and summed to calculate annual fluxes.

RESULTS

Hydrographic properties from land to ocean

During the winter cruises, we investigated a transect just in the Sardakhskaya channel. Water depth varied between 2 and 18 m. Water temperature and salinity profiles showed little variation, with range from 0.05 to 0.18 °C and 0.19 to 0.21 PSU (excluding site CAC19-F) (Fig. 3a + b). Measurements from site CAC19-F were anomalously warm (2.17 °C) with higher salinity values (0.25 PSU) relative to all other samples.

During the summer cruises, we investigated a longer transect from the center of the delta to approx. 80 km outside the delta in the nearshore Laptev Sea. The water depth ranged from 20 m in the main channel, to less than 0.5 m at the edge of the delta. In the coastal Laptev Sea, water depths gradually increased to 22 m. The temperature and salinity were homogenous in the water column within the delta compared to a strongly stratified water column in the coastal Laptev Sea. Salinity ranged from 0.1 in the delta to 30 in the deeper Arctic shelf water. Temperature ranged from 16 °C in the delta to – 1.0 °C in the bottom water. (Fig. 4a + b).

The data of the winter and summer cruises are accessible in the Pangaea data base (<https://doi.pangaea.de/10.1594/PANGAEA.933187>) (Fuchs et al. (in review)).

Sediment properties from land to ocean

The riverbed of the main channels near Samoylov and in the Sardakhskaya Channel consists of mostly sandy sediments with a sand content of over 98%. The sediments in the nearshore Laptev Sea are muddier with a sand content

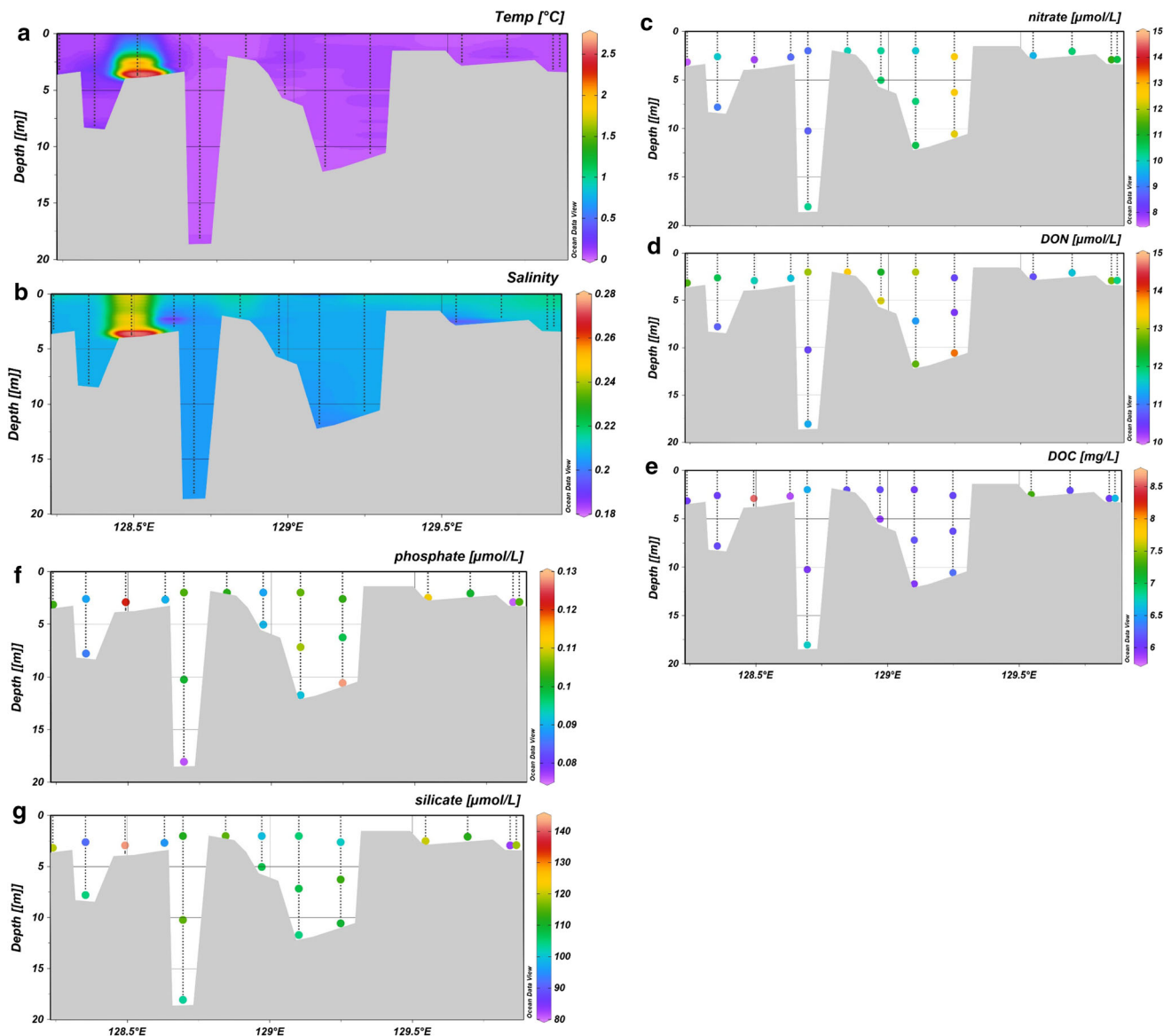


Fig. 3 Water properties and nutrient concentrations from the winter cruise. (a) temperature (°C), (b) salinity (PSU), (c) nitrate ($\mu\text{mol/L}$), (d) dissolved organic nitrogen (DON) ($\mu\text{mol/L}$), (e) dissolved organic carbon (DOC) (mg/L), (f) phosphate ($\mu\text{mol/L}$), and (g) silicate ($\mu\text{mol/L}$)

below 10% and a silt content of over 50%. The organic matter content of sediments in the delta is very low ($< 0.2\%$). In the Laptev Sea, OC was between 2 and 3% and $\delta^{15}\text{N}$ values were slightly enriched in relation to the soils within the delta and ranged from 3.0 to 3.7‰ (Table 1).

Nutrients from land to ocean

Nutrient concentrations differed considerably between the winter and summer sampling campaigns. In winter, NO_3^-

and DON were present along the transect. In summer, NO_3^- was near the detection limit, DON and particulate N are dominant forms of N in the study region.

In winter, NO_3^- concentrations increased from the delta interior to the nearshore by $\sim 3 \mu\text{mol L}^{-1}$ from 7.5 to $10.5 \mu\text{mol L}^{-1}$. DON remained relatively constant through the transect ($10 \pm 1 \mu\text{mol L}^{-1}$), contributing approximately 50% of the dissolved N pool. NH_4^+ concentrations were below $1.5 \mu\text{mol L}^{-1}$ in all samples apart from CAC19-F ($14.6 \mu\text{mol L}^{-1}$), suggesting that this sample may have been influenced by riverbed sediments.

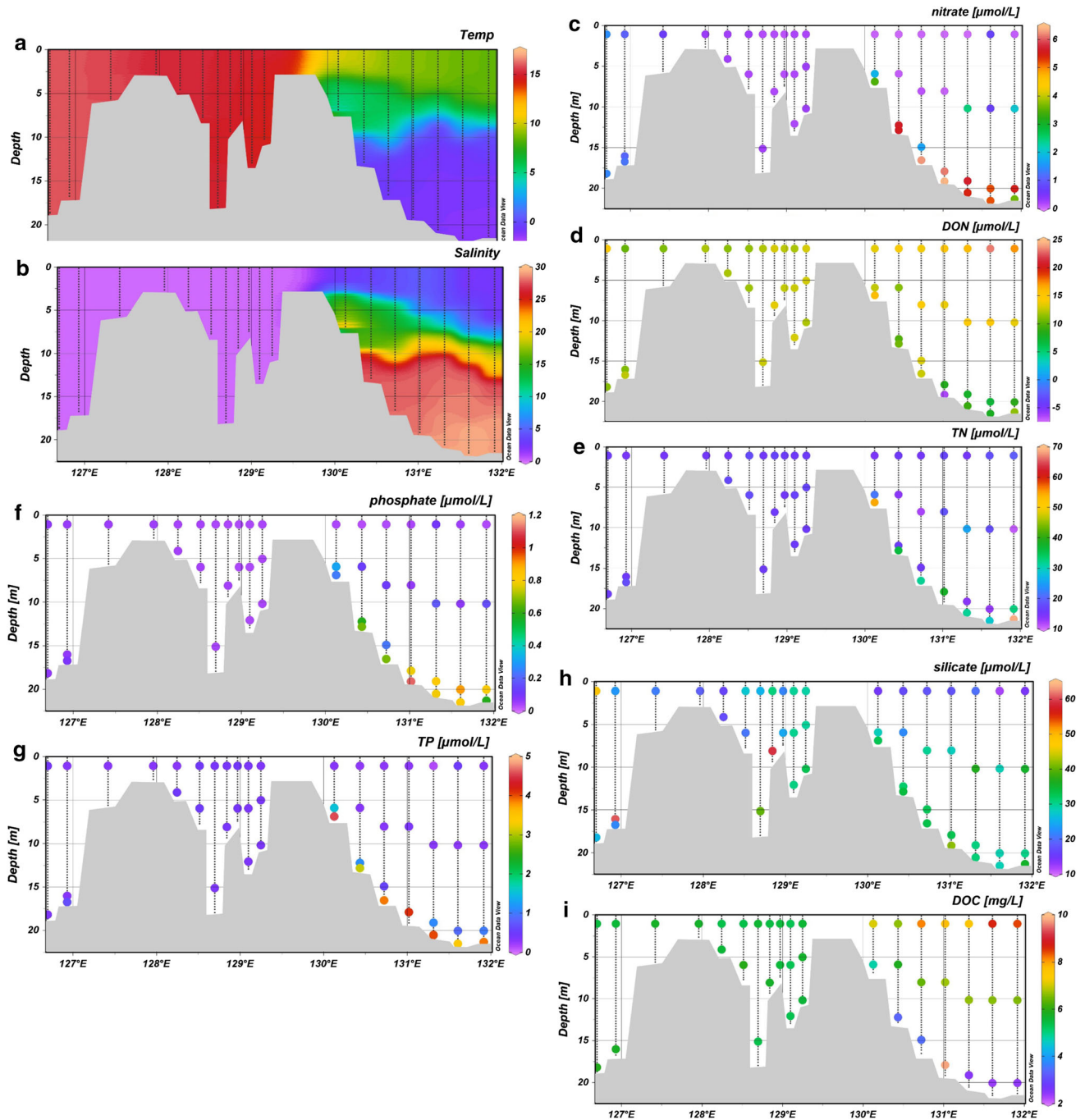


Fig. 4 Water properties and nutrient concentrations from the summer cruise. (a) Temperature (°C), (b) salinity (PSU), (c) nitrate ($\mu\text{mol/L}$), (d) dissolved organic nitrogen (DON) ($\mu\text{mol/L}$), (e) total nitrogen (TN) ($\mu\text{mol/L}$), (f) phosphate ($\mu\text{mol/L}$), (g) total phosphate (TP) ($\mu\text{mol/L}$), (h) silicate ($\mu\text{mol/L}$), and (i) dissolved organic carbon (DOC) (mg/)

DOC concentrations were generally constant along the river-to-sea transect for all winter samples (except CAC19-F), with a mean value of 6.2 mg L^{-1} and a minimum of 5.8 mg L^{-1} (Fig. 3).

In summer, the NO_3^- concentration was considerably lower than in winter. There was a decrease in NO_3^- (1.4 to

$0.2 \mu\text{mol L}^{-1}$) from the delta interior and in the beginning of the Sardakhskeya channel and a slight increase in DON (10 to $13 \mu\text{mol L}^{-1}$). The bottom water in the Laptev Sea had a NO_3^- concentration of approx. $5 \mu\text{mol L}^{-1}$ (Fig. 4).

Table 1 Sediment properties during the summer cruises in August 2019

Sample ID	Longitude	Latitude	Sand (%)	Silt (%)	Clay (%)	Total nitrogen (%)	Total nitrogen ($\mu\text{g/g}$)	Total carbon (%)	Total carbon ($\mu\text{g/g}$)	$\delta^{15}\text{N}$ (‰)	C/N
Lena delta											
CAC19-Lena 1	126.69564	72.39938	99.7	0.2	0.1	0.01	0.06	0.1	1.1	n.d.	18.7
CAC19-Lena 2	126.92899	72.53734	99.6	0.3	0.1	0.01	0.08	0.2	2.2	n.d.	27.1
CAC19-Lena 3	127.41932	72.62705	99.6	0.3	0.1	0.01	0.06	0.1	0.8	n.d.	13.8
CAC19-Lena 4	127.95918	72.63351	99.5	0.4	0.0	0.01	0.06	0.1	1.1	n.d.	18.5
CAC19-Lena 5	128.24466	72.56380	n.d.	n.d.	n.d.	n.d.	n.d.	n.d.	n.d.	n.d.	n.d.
CAC19-Lena 6	128.51548	72.52111	n.d.	n.d.	n.d.	n.d.	n.d.	n.d.	n.d.	n.d.	n.d.
CAC19-Lena 7	128.69504	72.46133	97.8	1.0	1.2	0.01	0.07	0.1	0.8	n.d.	11.3
CAC19-Lena 7/8	128.84105	72.45303	99.0	0.4	0.6	0.00	0.04	0.1	1.1	n.d.	27.3
CAC19-Lena 8	128.97076	72.47704	98.4	0.8	0.8	0.01	0.07	0.1	1.1	n.d.	16.1
CAC19-Lena 8/9	129.09922	72.50168	n.d.	n.d.	n.d.	n.d.	n.d.	n.d.	n.d.	n.d.	n.d.
CAC19-Lena 9	129.24841	72.50904	98.3	0.8	0.9	0.01	0.06	0.1	0.6	n.d.	10.0
Laptev sea											
CAC19-S-04	130.12630	72.53012	1.7	83.2	15.0	0.1	1.4	2.3	22.5	3.0	15.7
CAC19-S-05	130.43350	72.53983	10.1	67.5	22.4	0.2	1.6	2.3	23.4	3.3	14.4
CAC19-S-06	130.72248	72.54118	2.9	68.7	28.4	0.2	1.6	2.3	22.9	3.1	14.6
CAC19-S-07	131.01836	72.55056	2.3	66.1	31.6	0.2	1.6	2.2	22.1	3.2	13.9
CAC19-S-08	131.31468	72.55446	5.1	55.4	39.5	0.2	2.0	2.7	26.5	3.6	13.1
CAC19-S-09	131.60606	72.55886	0.6	56.7	42.8	0.2	2.2	2.8	28.0	3.7	12.8
CAC19-S-10	131.91480	72.55320	2.7	58.6	38.7	0.2	1.8	2.2	22.0	3.6	12.0

n.d. not determined. *CN* ratio of TN and TC

Nutrients at the Samoylov monitoring station

At the Samoylov monitoring station, nutrient concentrations were measured from September 2018 to September 2019, including nitrate + nitrite (herein presented as NO_3^-), NH_4^+ , phosphate (PO_4^{3-}), silicate, and TN (Figs. 5, 6). NO_3^- was detectable during periods of ice cover from October to June, reached highest concentration during the spring flood and then dropped below the detection limit. The NH_4^+ concentrations ranged from below detection limit up to $12 \mu\text{mol L}^{-1}$. There was a clear increase in NH_4^+ when the Lena ice cover built up from October to December. The phosphate⁻ concentrations ranged from below the detection limit up to $0.4 \mu\text{mol L}^{-1}$, during the spring flood the concentration increased to more than $1.0 \mu\text{mol L}^{-1}$. The silicate concentration showed a clear seasonal cycle with an increase during the ice-covered months from approx. $50 \mu\text{mol L}^{-1}$ to slightly above $100 \mu\text{mol L}^{-1}$. The TN (DIN + DON + particulate N) values (Fig. 6) showed a similar pattern with higher but more variable concentrations in winter and lower concentration in summer. From September 2018 to August 2019, we estimated an annual N- NO_3^- load of $24.5 \text{ Gg year}^{-1}$ and a total N load of $242.1 \text{ Gg year}^{-1}$.

Nutrient and potential N_2O release and transport from soils to river

We incubated two types of soil samples: firstly, organic-rich and peaty soils of the polygonal tundra which can enter the Lena River after thawing and erosion at the cliffs of the Samoylov Island, and secondly, soils and sediment from the floodplain, which are regularly flooded by the Lena River and contain mostly allochthonous organic matter from the river.

The soil samples differed mainly in SOM, which ranged from 0.5 to 45.7%. SOM of the polygonal tundra and the cliff was generally higher (above 5%) than in soils from the floodplain (0.5–5.8%) (Table 2).

The NH_4^+ content of the soils ranged between 0.1 and $6.5 \mu\text{g N g}^{-1} \text{ dw}$. The highest concentration was found in the peat containing cliff and the organic-rich layer of the beach. A considerable amount of NO_3^- was detected in the sandier layer of the beach.

The soil and sediment samples from the floodplain were sandy to silty with a sand content between 50 and 98%. Silt content increased with distance from the water line of the river. The soils from the river terrace contained less sand, whereas SOM was higher than in the floodplain samples. The $\delta^{15}\text{N}$ values of river terrace soils were lower than those

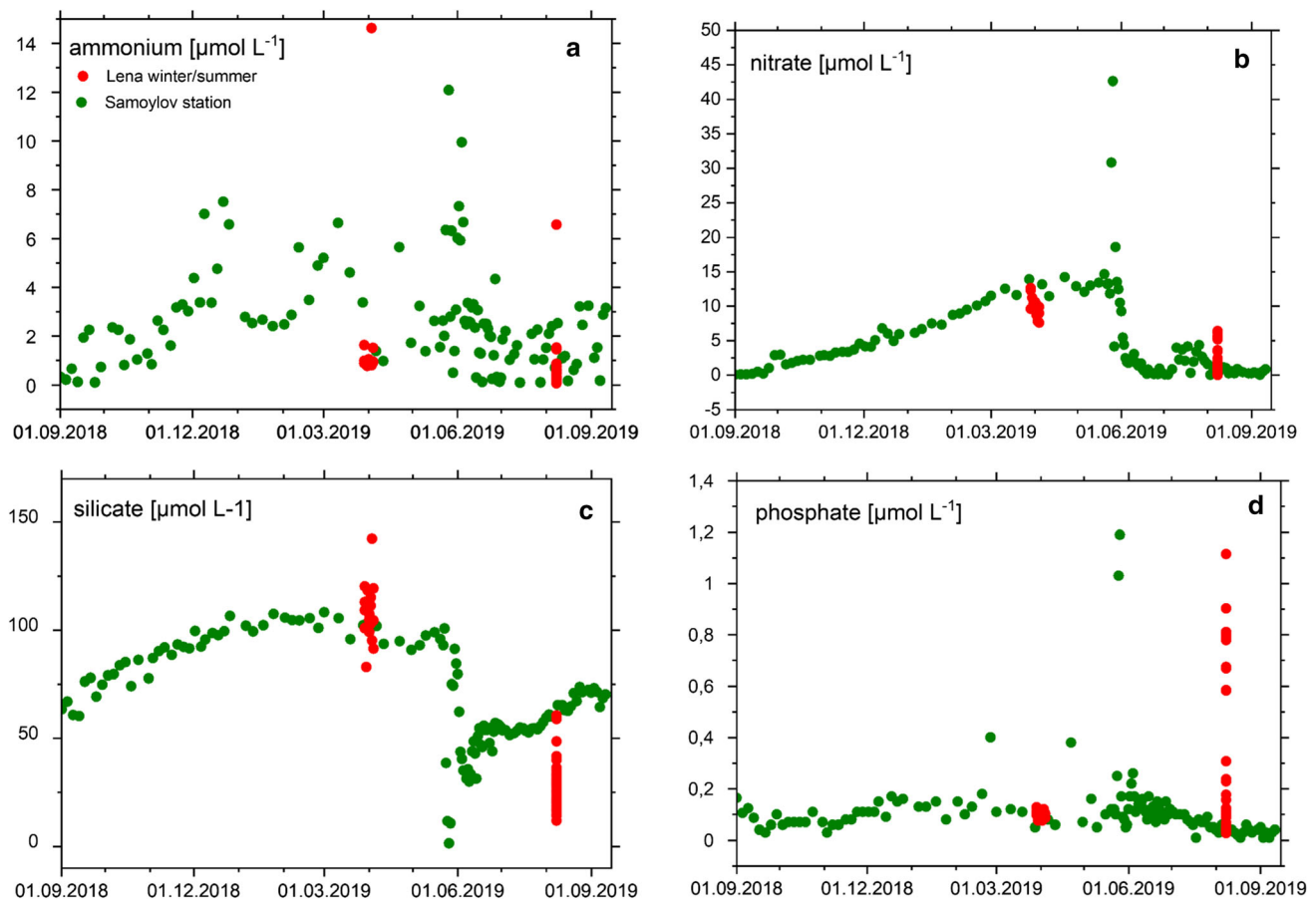


Fig. 5 Nutrient data from Samoylov Monitoring station September 2018–September 2019 (green) and data from the two Lena cruises in winter and summer 2019 in this study (red). **a** Ammonium ($\mu\text{mol/L}$), **b** nitrate ($\mu\text{mol/L}$), **c** silicate ($\mu\text{mol/L}$), and **d** phosphate ($\mu\text{mol/L}$)

found in the floodplain (Table 2) and ranged between 0.6 and 1.6 ‰, which is close to the average of the atmospheric N_2 of 0‰ (Kendall 1998).

In all soil incubations, DIN production occurred. The samples with high NH_4^+ concentrations such as K3 near the ice wedge and the deeper sample from the beach (B5 25–35) also had higher NH_4^+ concentrations during the incubation and showed an increase of NO_3^- after a maximum of five days. The net N-remineralization rates ranged between 0.1 and 1.7 $\mu\text{g N g}^{-1} \text{d}^{-1}$ and they correlated with the organic matter content (R^2 of 0.72) and OC (R^2 of 0.65) (Fig. 2).

The net nitrification rates ranged between 0.1 and 5.0 $\mu\text{g N g}^{-1} \text{day}^{-1}$ (Fig. 2). The highest rates were observed in the organic- and ammonium-rich cliff and beach soils. The nitrification rates correlated (R^2 of 0.92) with the NH_4^+ concentration.

We also investigated the potential N_2O production of soils from the delta region. A considerable N_2O production was only detected in the incubations after 8 weeks at 5 °C in the non-vegetated subsoil samples of the floodplain,

containing higher SOM than the topsoil, with mean N_2O production rate of $35.7 \pm 46.5 \text{ pg N-N}_2\text{O g dw}^{-1} \text{ day}^{-1}$ (Fig. 2). In all the other incubations, the N_2O formation was near the detection limit.

DISCUSSION

Nitrogen signal in the Lena Delta

Dissolved N was exported mostly as DON and NO_3^- during the winter, whereas DON prevailed in the delta in summer. These results corroborate observations from the Arctic GRO data from Zhigansk in the south (Holmes et al. 2012, 2021).

In winter (October to May), DON, NH_4^+ , and NO_3^- were continuously released to the aquatic environment, resulting in relatively high and uniform concentrations of NO_3^- and DON in the water column (Fig. 3C, D and 5). After the growing season, when the active layer freezes, we observed a clear increase of NO_3^- and NH_4^+ at the

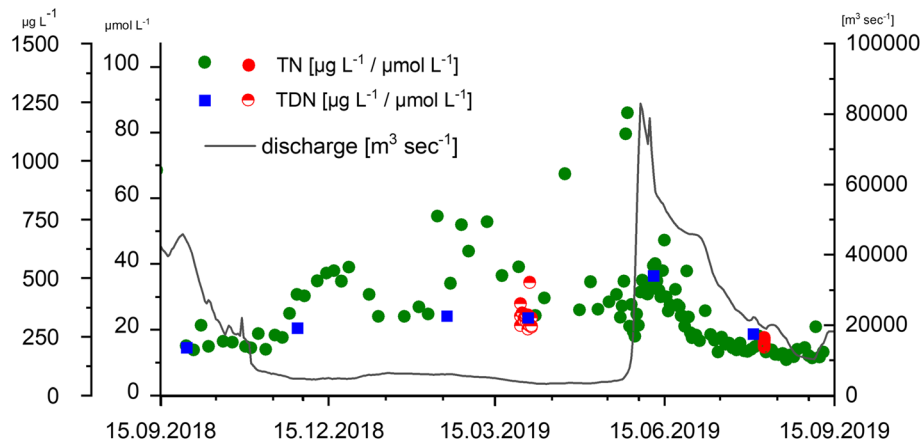


Fig. 6 Total N ($\mu\text{g L}^{-1}$ and $\mu\text{mol L}^{-1}$) concentration at the Samoylov Monitoring (green) from 15.9.2018 to 15.9.2019 and from the summer cruises (red, sites inside the delta). TDN ($\mu\text{g L}^{-1}$ and $\mu\text{mol L}^{-1}$) concentration from the winter cruises (half-red circles) and from the ArcticGRO station (blue square, Holmes et al. 2021) from 15.9.2018 to 15.9.2019. Discharge (black line) in $\text{m}^3 \text{sec}^{-1}$ at the gauge station Kyusyur

Table 2 Soil properties of samples from Samoylov Island

Sample ID	Depth (cm)	Sample site	Sand (%)	Silt (%)	Clay (%)	SOM (%)	Total Nitrogen (%)	Total Nitrogen ($\mu\text{g/g}$)	Total Carbon (%)	Total Carbon ($\mu\text{g/g}$)	$\delta^{15}\text{N}$ (‰)	C/N
Polygonal tundra												
LD19P7	10–20	P7	55.9	37.2	6.9	6.0	0.1	1.4	2.5	25.4	0.7	18.4
LD19K3	100	K3	31.9	56.2	11.9	15.8	0.4	3.9	8.9	88.8	0.6	22.8
LD19K1	380	K1	15.7	69.9	14.4	10.9	0.3	2.7	5.5	54.9	1.0	20.3
LD19K2	400	K1	n.d	n.d	n.d	45.7	0.4	3.9	16.2	162.1	0.8	41.3
Floodplain												
LD19B4 0–5	0–5	B4 0–5	49.9	43.1	7.1	3.5	0.1	0.9	1.4	13.7	1.6	15.7
LD19B4 10–15	10–15	B4 10–15	51.5	40.6	7.9	5.8	0.1	1.0	1.6	16.2	1.4	15.9
LD19B5 10–20	10–20	B5 10–20	97.6	1.7	0.7	0.5	0.0	0.1	0.1	1.10	n.d	7.3
LD19B5	25–35	B5 25–35	74.2	21.0	4.7	5.2	0.1	1.0	2.0	19.6	0.9	19.2
LD19Sed6	0–5	Sed 6	91.6	7.4	1.0	2.0	0.0	0.2	0.4	3.8	n.d	16.3

n.d. not determined. *CN* ratio of TN and TC

Samoylov station. This allochthonous, terrestrial DIN was not consumed by plants, but rather leached to the river.

With warming and active layer deepening into mineral horizons with low C/N ratios, the hydrological flow path penetrates deeper, intensifying NO_3^- and NH_4^+ leaching to the river (Harms and Jones 2012). In soils with vegetation cover, plants and microbial communities will compete for remineralized DON and DIN (Stark and Kytöviita 2006). By the end of the growing season or in unvegetated soils, mineralization and nitrification will be the dominant processes. Therefore, winter N export from soils to rivers in the unfrozen active layer will be in the form of NH_4^+ , NO_3^- , and DON. Especially, because by the end of the

vegetation period, NO_3^- was enriched in soils without vegetation cover (Sanders et al. 2010).

In summer, the main N export from soils takes place via DON and NH_4^+ , which is consistent with former studies in permafrost-affected soils (Harms and Jones 2012). In the river, NH_4^+ and NO_3^- are consumed immediately (Dittmar and Kattner 2003), again either by primary producers or oxidized to nitrate. This was confirmed by our own results that NH_4^+ was not detectable in the Lena transect (Table S1) and nitrate dropped down from $1.5 \mu\text{mol L}^{-1}$ to close to the detection limit during the first stations in the inner Delta (Fig. 4C). We speculate that phytoplankton, likely diatoms, are responsible for this uptake (Hawkings

et al. 2017). This is backed up by the low silicate concentration in summer (Fig. 5), we found up to $60 \mu\text{mol L}^{-1}$ in summer and more than $100 \mu\text{mol L}^{-1}$ in winter. The SPM values, with high N percentage and low C/N ratios, further support this, as they indicate the production of fresh biomass (Supplementary Table S1).

We do not have direct evidence for DON uptake in summer, but according to Redfield ratios, silicate uptake must be backed up by approximately equimolar N uptake. N is limited in the delta, and must either stem from rapid recycling or from direct DON uptake as is known from permafrost-affected soils (Schimel and Bennett 2004) and also in aquatic environments (Wheeler et al. 1974).

Overall, we conclude that soils and pore water can be sources of NO_3^- to the Lena Delta in winter, even though in low concentration (Heikoop et al. 2015) and that nitrate can also stem from in-situ nitrification. In summer, DIN overall is less important in the Delta, because it is used immediately, and we hypothesize that active DON uptake supports primary production in the water column of the Lena.

Implications of thaw for the ecosystem

The flux of C and N from the Lena River has been estimated previously: Hugelius et al. (2020) estimated losses into aquatic systems (dissolved and particulate organic matter) to be $0.022 \pm 0.02 \text{ Pg C}\cdot\text{year}^{-1}$ and $0.7 \pm 0.5 \text{ Tg N}\cdot\text{year}^{-1}$. Wild et al. (2019) estimated an OC flux of $0.9 \text{ Tg C year}^{-1}$ coming from permafrost and peat deposits. Based on the TDN data from the ArcticGRO Station, an annual flux of approx. 170 Gg year^{-1} were estimated by Holmes et al (2012) for the year 2008 to 2012. In our single-year study from September 2018 to September 2019, we estimate an annual TN flux of $242.1 \text{ Gg year}^{-1}$. This is higher than the average of the ArcticGRO data.

Comparisons between years and between different locations along the Lena River are challenging due to the two factors as follows: (1) The differences that can be accounted to strongly varying seasonal differences and (2) geographical differences, e.g., sources of different regions of the catchment.

Additionally some issues have to be considered and discussed, for instance, the particulate nitrogen is missing in the ArcticGRO data. Based on data from the cruises in this study, approximately one-fifth of the TN is particulate N, (average TN $16.0 \mu\text{mol L}^{-1}$, average TDN $12.9 \mu\text{mol L}^{-1}$) so this can partly explain the higher annual fluxes, we found. However, if we added 20 percent of N to the ArcticGRO data, the results still fall below our estimate of annual N flux by about 15% (approx.. 36 Gg), even though the N-NO_3^- load is comparable (24.2 Gg in our study compared to 24.0 Gg , Holmes et al. 2012). It is possible

that this deviation merely represents inter-annual variability because we compare one single annual cycle to a long-term data set. However, our Samoylov Island monitoring data were collected at higher temporal resolution and closer to the mouth of the Lena than the ArcticGRO data. In particular, the higher temporal resolution improved flux estimates by capturing the higher nutrient concentrations during peak discharge in spring and short hydrological events.

Additionally, 2019, our year of study, was a dry year and the summer discharge was low. There was no correlation of TN concentration with discharge (Fig. 6). Especially during the ice-covered period, higher concentrations of TN were measured during relatively low discharge. During winter, TN values varied strongly and ranged between 20 and $90 \mu\text{mol L}^{-1}$. Under ice, the higher velocity and pressure can re-suspend materials from the sediment. The TN concentrations during the summer cruise in the delta were slightly higher than our annual station data, which could be an evidence that the delta itself adds a considerable N load to the Lena River (Fig. 6). Fuchs et al. (2020) calculated an annual eroded N amount to the Lena River from the Sobe-Sise Cliff (Fig. 1C) of $0.4 \times 10^6 \text{ kg}$ in the period of 2015–2018. The island is located downstream from Samoylov Island. Our soil incubations highlight that intense input can occur upon remineralization. Especially soils that were recently exposed by erosion are organic-rich and can release high amounts of DIN and DON.

This eroded soil material partly settled in the delta, in regions with low flow velocities, like on the beach of Samoylov Island. In the main channel, flow velocity is too high to allow for settling of organic-rich SPM. Instead, it is transported to the Laptev Sea, where it can be remineralized. However, only a minor part of the sediments transported by the Lena River enters the Laptev Sea shelf through the main channels of the delta, while the rest is dispersed within the network of the Lena Delta (Rachold et al. 1996).

Thibodeau et al. (2017) showed that the Lena River discharge mostly affects Laptev Sea surface water, while the bottom water is influenced by modified Atlantic-derived water flowing along the continental slope and branching onto the shelf. Consequently, most ecosystem implications of nutrient supply from the Lena River affect the upper shelf waters. Secondary advective processes by currents can be responsible for along-shore drift of suspended OM once it discharges into the shelf area. Although our study and other previously published work identify high N:P export from the Lena Delta, these high N:P ratios are quickly lost and replaced with lower marine N:P ratios (Tuerena et al. 2022). This suggests biological uptake and sedimentary denitrification that lead to a loss of N on the Laptev Sea shelf.

Potential N₂O production in deposited and former eroded material

To investigate the potential N₂O production and further emission to the atmosphere, we incubated samples from different soil types in Lena water over 8 weeks. In most of our incubations, the N₂O concentrations were close to the detection limit but one incubation was a significant exception. From the sample of an organic-rich buried layer on the beach of the floodplain of Samoylov Island, significant amounts of N₂O were produced with approximately 36 pg N-N₂O g dw⁻¹ day⁻¹. Taking soil density into account, this corresponds to approximately 1000 µg N₂O-N m⁻² day⁻¹. In this calculation, we ignored potential consumption of N₂O. Actual emissions require chamber measurements, and we acknowledge that this single measurement may estimate potential N₂O emission. However, higher N₂O production rates of 1080 to 10,030 µg N₂O-N m⁻² day⁻¹ were determined in unvegetated permafrost peat soils (Marushchak et al. 2011). Voigt et al (2020) summarized that unvegetated soils generally show highest N₂O. Assuming that bare soils contribute to N₂O emissions, the unvegetated floodplain in the delta, which contains layers of organic-rich deposits is a potential source of N₂O emissions. Higher erosion rates, organic matter depositions within the delta, and higher NH₄⁺ and NO₃⁻ load in the water column can trigger the N₂O emissions in the future.

CONCLUSIONS

We found the Lena Delta region to play an important role as a source of reactive nitrogen stemming from the soil active layer and from thawing permafrost. Eroded soil materials release reactive, inorganic nitrogen and show significant rates of remineralization and nitrification. The inorganic nitrogen is almost completely utilized in the summer month and output to the coastal ocean is mainly organic nitrogen. Our estimate of nitrogen inputs in 2019 was 15% above the average data from the ArcticGRO stations further upstream in the Lena River. Though based on one annual cycle, this points towards additional N-sources downstream of the ArcticGRO station. We attribute this difference to an underestimation of the particulate nitrogen flux from eroded soil material in summer and due to resuspension of sediments, particularly important in winter.

Despite these high N fluxes, the effect of N on primary production on the shelf to date appears limited. However, the erosion and especially input of organic-rich material, and its subsequent remineralization from organic matter

over DON to DIN, potentially may increase the N₂O production and emissions from permafrost-affected soils and in permafrost-influenced aquatic environments, though this must be affirmed by future measurements.

Potentially, the changes in release of organic and inorganic nitrogen from thawing permafrost might alleviate the nitrogen limitations, in soils, the river, and consequently also in the coastal water of the Arctic Ocean causing higher productivity at the primary producer level and across food webs.

SOCIETAL AND POLICY IMPLICATIONS

The Arctic is heavily impacted by climate change. Its air temperature increase is twice that of temperate regions (Smith et al. 2019). This increase in temperature is tied to extended thaw of permafrost-affected soils and increased soil organic matter decomposition. This increases the ubiquitous input of nutrients to the coastal ecosystem and enhances biogeochemical processes and availability of reactive nitrogen in the river and adjacent ocean. On a global scale, anthropogenic input of reactive nitrogen to the natural nitrogen cycle mainly by fertilization and industrial emission had imbalanced the cycle and these already exceed planetary boundaries (Steffen et al. 2011). That does not apply only to the over-fertilized temperate regions, but also to more pristine and oligotrophic ecosystems like the Arctic. Nonetheless, new data (Tuerena et al. 2022) suggest that the effect may be limited to the shelf region due to limited export to the open Arctic Ocean. Changing nutrient inputs potential increases coastal productivity, but temperature changes will also change the species composition in the coastal region. With possible increase in productivity, the ecosystem will be exposed to the increase in anthropogenic pressure, likely from fisheries.

The permafrost region is indicated as one tipping point regarding green-house gas emission of carbon dioxide and methane for the global climate system (Lenton et al. 2019). The main focus is usually put on methane and CO₂ emissions, but it is yet unclear whether nitrous oxide production in Arctic soils and possibly in the rivers may intensify in the future and maybe contributed in particular to the tipping point. Global N₂O emissions are increasing. Although atmospheric N₂O is less concentrated than CO₂ and CH₄, it traps around 300 times more heat as a green-house gas. The N₂O emissions from Arctic ecosystems could be one missing source in the global estimation.

The changing natural N cycle in the Arctic and the anthropogenic changed N cycle have to be considered together in the future.

Acknowledgements This work is embedded into the Changing Arctic Ocean (CAO) program (lead by the NERC-BMBF Project EISPAC [#03F0809A] and supported by the CACOON [#03F0806A] and ARISE CAO projects. BJ was funded by the European Space Agency (ESA) as part of the Climate Change Initiative (CCI) fellowship (ESA ESRIN/Contract No. 4000133761/21/I-NB). We thank the Trofimuk Institute of Petroleum Geology and Geophysics, Siberian Branch of the Russian Academy of Sciences (IPGG SB RAS), Novosibirsk, Russia, for their efforts to run the Research Station Samoylov Island. We thank the captain and crew of the *Anatoliy Zhilinskiy* and the *Merzlotoved* for hosting us.

Funding Open Access funding enabled and organized by Projekt DEAL.

Open Access This article is licensed under a Creative Commons Attribution 4.0 International License, which permits use, sharing, adaptation, distribution and reproduction in any medium or format, as long as you give appropriate credit to the original author(s) and the source, provide a link to the Creative Commons licence, and indicate if changes were made. The images or other third party material in this article are included in the article's Creative Commons licence, unless indicated otherwise in a credit line to the material. If material is not included in the article's Creative Commons licence and your intended use is not permitted by statutory regulation or exceeds the permitted use, you will need to obtain permission directly from the copyright holder. To view a copy of this licence, visit <http://creativecommons.org/licenses/by/4.0/>.

REFERENCES

- Aagaard, K., and E.C. Carmack. 1989. The role of sea ice and other fresh water in the Arctic circulation. *Journal of Geophysical Research: Oceans* 94: 14485–14498.
- Abbott, B.W., and J.B. Jones. 2015. Permafrost collapse alters soil carbon stocks, respiration, CH₄, and N₂O in upland tundra. *Global Change Biology* 21: 4570–4587.
- Anderson, L.G., K. Olsson, and M. Chierici. 1998. A carbon budget for the Arctic Ocean. *Global Biogeochemical Cycles* 12: 455–465.
- Beermann, F., A. Teltewskoi, C. Fiencke, E.-M. Pfeiffer, and L. Kutzbach. 2014. Stoichiometric analysis of nutrient availability (N, P, K) within soils of polygonal tundra. *Biogeochemistry*. <https://doi.org/10.1007/s10533-014-0037-4>.
- Biasi, C., W. Wanek, O. Rusalimova, C. Kaiser, H. Meyer, P. Barsukov, and A. Richter. 2005. Microtopography and plant-cover controls on nitrogen dynamics in hummock tundra ecosystems in Siberia. *Arctic, Antarctic, and Alpine Research* 37: 435–443.
- Biskaborn, B.K., S.L. Smith, J. Noetzli, H. Matthes, G. Vieira, D.A. Streletskiy, P. Schoeneich, V.E. Romanovsky, et al. 2019. Permafrost is warming at a global scale. *Nature Communications* 10: 1–11.
- Boike, J., B. Kattenstroth, K. Abramova, N. Bornemann, A. Chetverova, I. Fedorova, K. Fröb, M. Grigoriev, M. et al. 2013. Baseline characteristics of climate, permafrost and land cover from a new permafrost observatory in the Lena River Delta, Siberia (1998–2011). *Biogeosciences* 10: 2105–2128.
- Buckeridge, K., E. Zufelt, H. Chu, and P. Grogan. 2010. Soil nitrogen cycling rates in low arctic shrub tundra are enhanced by litter feedbacks. *Plant and Soil* 330: 407–421.
- Buckeridge, K.M., S. Banerjee, S.D. Siciliano, and P. Grogan. 2013. The seasonal pattern of soil microbial community structure in mesic low arctic tundra. *Soil Biology and Biochemistry* 65: 338–347.
- Dittmar, T., and G. Kattner. 2003. The biogeochemistry of the river and shelf ecosystem of the Arctic Ocean: A review. *Marine Chemistry* 83: 103–120.
- Dunton, K.H., T. Weingartner, and E.C. Carmack. 2006. The nearshore western Beaufort Sea ecosystem: Circulation and importance of terrestrial carbon in arctic coastal food webs. *Progress in Oceanography* 71: 362–378.
- Fedorova, I., A. Chetverova, D. Bolshiyarov, A. Makarov, J. Boike, B. Heim, A. Morgenstern, P.P. Overduin, et al. 2015. Lena Delta hydrology and geochemistry: Long-term hydrological data and recent field observations. *Biogeosciences* 12: 345–363.
- Frey, K.E., and J.W. McClelland. 2009. Impacts of permafrost degradation on arctic river biogeochemistry. *Hydrological Processes* 23: 169–182.
- Fuchs, M., I. Nitze, J. Strauss, F. Günther, S. Wetterich, A. Kizyakov, M. Fritz, T. Opel, et al. 2020. Rapid fluvio-thermal erosion of a yedoma permafrost cliff in the Lena River Delta. *Frontiers in Earth Science*. <https://doi.org/10.3389/feart.2020.00336>.
- Fuchs, M., J. Palmtag, B. Juhls, P.P. Overduin, G. Grosse, A. Abdelwahab, M. Bedington, T. Sanders, et al. 2021. High-resolution bathymetry models for the Lena Delta and Kolyma Gulf coastal zones. *Earth System Science Data*. <https://doi.org/10.5194/essd-2021-256>.
- Günther, F., P.P. Overduin, A.V. Sandakov, G. Grosse, and M.N. Grigoriev. 2013. Short-and long-term thermo-erosion of ice-rich permafrost coasts in the Laptev Sea region. *Biogeosciences* 10: 4297–4318.
- Harden, J.W., C.D. Koven, C.-L. Ping, G. Hugelius, A. David McGuire, P. Camill, T. Jorgenson, P. Kuhry, et al. 2012. Field information links permafrost carbon to physical vulnerabilities of thawing. *Geophysical Research Letters* 39: L15704.
- Harms, T.K., and J.B. Jones. 2012. Thaw depth determines reaction and transport of inorganic nitrogen in valley bottom permafrost soils. *Global Change Biology* 18: 2958–2968.
- Hawkings, J.R., J.L. Wadham, L.G. Benning, K.R. Hendry, M. Tranter, A. Tedstone, P. Nienow, and R. Raiswell. 2017. Ice sheets as a missing source of silica to the polar oceans. *Nature Communications* 8: 14198.
- Heikoop, J.M., H.M. Throckmorton, B.D. Newman, G.B. Perkins, C.M. Iversen, T. Roy Chowdhury, V. Romanovsky, D.E. Graham, et al. 2015. Isotopic identification of soil and permafrost nitrate sources in an Arctic tundra ecosystem. *Journal of Geophysical Research: Biogeosciences* 120: 1000–1017.
- Hobbie, J., G.R. Shaver, T.T. Høge, and J. Bowden. 2021. Arctic Tundra. In *Arctic Ecology*, ed. D. Thomas. New York: Wiley.
- Holmes, R.M., J.W. McClelland, B.J. Peterson, S.E. Tank, E. Bulygina, T.I. Eglinton, V.V. Gordeev, T.Y. Gurtovaya, et al. 2012. Seasonal and annual fluxes of nutrients and organic matter from large rivers to the Arctic Ocean and surrounding seas. *Estuaries and Coasts* 35: 369–382.
- Holmes, R.M., J.W. McClelland, S.E. Tank, R.G.M. Spencer, and A.I. Shiklomanov. 2021. Arctic great rivers observatory. Water quality dataset, version 20210421. <https://www.arcticgreatrivers.org/data>.
- Horn, M.A., and S.A. Hetz. 2021. Microbial nitrogen cycling in permafrost soils: implications for atmospheric chemistry. In *Microbial Life in the Cryosphere and its Feedback on Global Change*, ed. S. Liebner and L. Ganzert, 53–112. Berlin: De Gruyter.
- Hugelius, G., J. Loisel, S. Chadburn, R.B. Jackson, M. Jones, G. MacDonald, M. Marushchak, D. Olefeldt, et al. 2020. Large stocks of peatland carbon and nitrogen are vulnerable to

- permafrost thaw. *Proceedings of the National Academy of Sciences* 117: 20438–20446.
- Hugelius, G., J. Strauss, S. Zubrzycki, J.W. Harden, E. Schuur, C.-L. Ping, L. Schirmer, G. Grosse, et al. 2014. Estimated stocks of circumpolar permafrost carbon with quantified uncertainty ranges and identified data gaps. *Biogeosciences* 11: 6573–6593.
- Juhls, B., C.A. Stedmon, A. Morgenstern, H. Meyer, J. Hölemann, B. Heim, V. Povazhnyi, and P.P. Overduin. 2020. Identifying drivers of seasonality in Lena River biogeochemistry and dissolved organic matter fluxes. *Frontiers in Environmental Science* 8: 53.
- Kanevskiy, M., Y. Shur, J. Strauss, T. Jorgenson, D. Fortier, E. Stephani, and A. Vasiliev. 2016. Patterns and rates of riverbank erosion involving ice-rich permafrost (yedoma) in northern Alaska. *Geomorphology* 253: 370–384.
- Kattner, G., J. Lobbes, H. Fitznar, R. Engbrodt, E.-M. Nöthig, and R. Lara. 1999. Tracing dissolved organic substances and nutrients from the Lena River through Laptev Sea (Arctic). *Marine Chemistry* 65: 25–39.
- Kendall, C. 1998. Tracing nitrogen sources and cycles in catchments. In *Isotope Tracers in Catchment Hydrology*, ed. C. Kendall and J.J. McDonnell, 519–576. Amsterdam: Elsevier.
- Kutzbach, L., D. Wagner, and E.-M. Pfeiffer. 2004. Effect of microrelief and vegetation on methane emission from wet polygonal tundra, Lena Delta, Northern Siberia. *Biogeochemistry* 69: 341–362.
- Le Fouest, V., M. Manizza, B. Tremblay, and M. Babin. 2015. Modelling the impact of riverine DON removal by marine bacterioplankton on primary production in the Arctic Ocean. *Biogeosciences* 12: 3385–3402.
- Lenton, T.M., J. Rockström, O. Gaffney, S. Rahmstorf, K. Richardson, W. Steffen, and H.J. Schellnhuber. 2019. Climate tipping points—too risky to bet against. *Nature* 575: 592–595.
- Lewis, K., G. Van Dijken, and K.R. Arrigo. 2020. Changes in phytoplankton concentration now drive increased Arctic Ocean primary production. *Science* 369: 198–202.
- Marushchak, M., A. Pitkämäki, H. Koponen, C. Biasi, M. Seppälä, and P. Martikainen. 2011. Hot spots for nitrous oxide emissions found in different types of permafrost peatlands. *Global Change Biology* 17: 2601–2614.
- Marzadri, A., G. Amatulli, D. Tonina, A. Bellin, L.Q. Shen, G.H. Allen, and P.A. Raymond. 2021. Global riverine nitrous oxide emissions: The role of small streams and large rivers. *Science of The Total Environment* 776: 145148.
- Mishra, U., G. Hugelius, E. Shelef, Y. Yang, J. Strauss, A. Lupachev, J.W. Harden, J.D. Jastrow, et al. 2021. Spatial heterogeneity and environmental predictors of permafrost region soil organic carbon stocks. *Science advances* 7: eaaz5236.
- Overland, J.E., and M. Wang. 2013. When will the summer Arctic be nearly sea ice free? *Geophysical Research Letters* 40: 2097–2101.
- Pastor, A., S. Poblador, L.J. Skovsholt, and T. Riis. 2020. Microbial carbon and nitrogen processes in high-Arctic riparian soils. *Permafrost and Periglacial Processes* 31: 223–236.
- Rachold, V., A. Alabyan, H.W. Hubberten, V. Korotaev, and A. Zaitsev. 1996. Sediment transport to the Laptev Sea—hydrology and geochemistry of the Lena River. *Polar Research* 15: 183–196.
- Rasmussen, L.H., A. Michelsen, P. Ladegaard-Pedersen, C.S. Nielsen, and B. Elberling. 2020. Arctic soil water chemistry in dry and wet tundra subject to snow addition, summer warming and herbivory simulation. *Soil Biology and Biochemistry* 141: 107676.
- Reyes, F.R., and V.L. Loughheed. 2015. Rapid nutrient release from permafrost thaw in arctic aquatic ecosystems. *Arctic, Antarctic, and Alpine Research* 47: 35–48.
- Sanders, T., C. Fiencke, J. Hüpeden, E.M. Pfeiffer, and E. Spieck. 2019. Cold adapted *Nitrosospira* sp: A potential crucial contributor of ammonia oxidation in cryosols of permafrost-affected landscapes in Northeast Siberia. *Microorganisms* 7: 699.
- Sanders, T., C. Fiencke, and E.M. Pfeiffer. 2010. Small-scale variability of dissolved inorganic nitrogen (DIN), C/N ratios and ammonia oxidizing capacities in various permafrost affected soils of Samoylov Island, Lena River Delta, Northeast Siberia. *Polarforschung* 80: 23–35.
- Schade, J.D., E.C. Seybold, T. Drake, S. Spawn, W.V. Sobczak, K.E. Frey, R.M. Holmes, and N. Zimov. 2016. Variation in summer nitrogen and phosphorus uptake among Siberian headwater streams. *Polar Research* 35: 24571.
- Schimmel, J.P., and J. Bennett. 2004. Nitrogen mineralization: Challenges of a changing paradigm. *Ecology* 85: 591–602.
- Seitzinger, S.P., and C. Kroeze. 1998. Global distribution of nitrous oxide production and N inputs in freshwater and coastal marine ecosystems. *Global Biogeochemical Cycles* 12: 93–113.
- Shaver, G., F. Chapin III., and B.L. Gartner. 1986. Factors limiting seasonal growth and peak biomass accumulation in *Eriophorum vaginatum* in Alaskan tussock tundra. *The Journal of Ecology* 74: 257–278.
- Shiklomanov, A.I., R.M. Holmes, J.W. McClelland, S.E. Tank, and R.G.M. Spencer. 2021. Arctic Great Rivers Observatory. Discharge Dataset, Version 20210319. <https://www.arcticrivers.org/data>.
- Smith, D.M., J.A. Screen, C. Deser, J. Cohen, J.C. Fyfe, J. García-Serrano, T. Jung, V. Kattsov, et al. 2019. The polar amplification model intercomparison project (PAMIP) contribution to CMIP6: Investigating the causes and consequences of polar amplification. *Geoscientific Model Development* 12: 1139–1164.
- Smith, S.V., R.W. Buddemeier, F. Wulff, and D.P. Swaney. 2005. C, N, P fluxes in the coastal zone. In *Coastal Fluxes in the Anthropocene*, ed. C.J. Crossland, H.H. Kremer, H.J. Lindeboom, J.I. Marshall Crossland, and M.D.A. Le Tisser, 95–141. Berlin: Springer.
- Stark, S., and M.-M. Kytöviita. 2006. Simulated grazer effects on microbial respiration in a subarctic meadow: Implications for nutrient competition between plants and soil microorganisms. *Applied Soil Ecology* 31: 20–31.
- Steffen, W., Å. Persson, L. Deutsch, J. Zalasiewicz, M. Williams, K. Richardson, C. Crumley, P. Crutzen, et al. 2011. The anthropocene: From global change to planetary stewardship. *Ambio* 40: 739.
- Stewart, K.J., P. Grogan, D.S. Coxson, and S.D. Siciliano. 2014. Topography as a key factor driving atmospheric nitrogen exchanges in arctic terrestrial ecosystems. *Soil Biology and Biochemistry* 70: 96–112.
- Tank, S.E., M. Manizza, R.M. Holmes, J.W. McClelland, and B.J. Peterson. 2012. The processing and impact of dissolved riverine nitrogen in the Arctic Ocean. *Estuaries and Coasts* 35: 401–415.
- Terhaar, J., R. Lauerwald, P. Regnier, N. Gruber, and L. Bopp. 2021. Around one third of current Arctic Ocean primary production sustained by rivers and coastal erosion. *Nature Communications* 12: 1–10.
- Thibodeau, B., D. Bauch, and M. Voss. 2017. Nitrogen dynamic in Eurasian coastal Arctic ecosystem: Insight from nitrogen isotope. *Global Biogeochemical Cycles* 31: 836–849.
- Tuerena, R.E., C. Mahaffey, S.F. Henley, C. de la Vega, L. Norman, T. Brand, T. Sanders, M. Debyser, et al. 2022. Nutrient pathways and their susceptibility to past and future change in the Eurasian Arctic Ocean. *Ambio*. <https://doi.org/10.1007/s13280-021-01673-0>.
- Voigt, C., M.E. Marushchak, B.W. Abbott, C. Biasi, B. Elberling, S.D. Siciliano, O. Sonnentag, K.J. Stewart, et al. 2020. Nitrous

oxide emissions from permafrost-affected soils. *Nature Reviews Earth & Environment* 1: 420–434.

- Weintraub, M.N., and J.P. Schimel. 2003. Interactions between carbon and nitrogen mineralization and soil organic matter chemistry in arctic tundra soils. *Ecosystems* 6: 129–143.
- Wheeler, P.A., B.B. North, and G.C. Stephens. 1974. Amino acid uptake by marine phytoplankters 1, 2. *Limnology and Oceanography* 19: 249–259.
- Wild, B., A. Andersson, L. Bröder, J. Vonk, G. Hugelius, J.W. McClelland, W. Song, P.A. Raymond, et al. 2019. Rivers across the Siberian Arctic unearth the patterns of carbon release from thawing permafrost. *Proceedings of the National Academy of Sciences* 116: 10280–10285.
- Zubrzycki, S., L. Kutzbach, G. Grosse, A. Desyatkin, and E.M. Pfeiffer. 2013. Organic carbon and total nitrogen stocks in soils of the Lena River Delta. *Biogeosciences* 10: 3507–3524.

Publisher's Note Springer Nature remains neutral with regard to jurisdictional claims in published maps and institutional affiliations.

AUTHOR BIOGRAPHIES

Tina Sanders (✉) is a Senior Scientist at the Helmholtz-Zentrum Hereon. Her research interests include aquatic nutrient cycles and nitrogen stable isotopes.
Address: Institute for Carbon Cycles, Helmholtz-Zentrum Hereon, Geesthacht, Germany.
 e-mail: tina.sanders@hereon.de

Claudia Fiencke is Senior Scientist at the University of Hamburg, Institute of Soil Science. Her research interests include microbial terrestrial nitrogen turnover with focus on nitrification, ecological soil evaluation.
Address: Institute of Soil Science, Universität Hamburg, Allende-Platz 2, 20146 Hamburg, Germany.
Address: Center for Earth System Research and Sustainability, Universität Hamburg, Allende-Platz 2, 20146 Hamburg, Germany.
 e-mail: Claudia.Fiencke@uni-hamburg.de

Matthias Fuchs is a PostDoc at the Alfred Wegener Institute Helmholtz Centre for Polar and Marine Research, Potsdam, Germany. His research interests include permafrost research, biogeochemistry, arctic coastal wetlands.
Address: Permafrost Research Section, Helmholtz Centre for Polar and Marine Research, Alfred Wegener Institute, Telegrafenberg A 45, Potsdam, Germany.
 e-mail: matthias.fuchs@awi.de

Charlotte Haugk is a Doctoral candidate at the Stockholm University. Her research interest include the organic matter release from permafrost-affected soils
Address: Department of Environmental Science and Analytical Chemistry, Stockholm University, Svante Arrhenius Väg 8, 11418 Stockholm, Sweden.
 e-mail: charlotte.haugk@aces.su.se

Bennet Juhls is a Postdoc at the Alfred Wegener Institute Helmholtz Centre for Polar and Marine Research. His research interests include land-ocean matter fluxes in the Arctic, aquatic biogeochemistry, and optical and radar remote sensing.
Address: Permafrost Research Section, Helmholtz Centre for Polar and Marine Research, Alfred Wegener Institute, Telegrafenberg A 45, Potsdam, Germany.
 e-mail: bjuhls@awi.de

Gesine Mollenhauer is a marine organic geochemist at the Alfred Wegener Institute in Bremerhaven, Germany. She uses a combination of organic geochemical methods and radiocarbon dating to investigate transport of organic matter and carbon cycling in a land-ocean continuum, the fate of terrestrial organic matter delivered to aquatic systems and the ocean, and glacial-interglacial changes in these processes.

Address: Marine Geochemistry Section, Helmholtz Centre for Polar and Marine Research, Alfred Wegener Institute, Am Handelshafen 12, 27570 Bremerhaven, Germany.
 e-mail: Gesine.mollenhauer@awi.de

Olga Ogneva is a Doctoral Candidate at the Alfred Wegener Institute in Bremerhaven, Germany. Her research interest include investigation of stable composition of organic carbon.

Address: Marine Geochemistry Section, Helmholtz Centre for Polar and Marine Research, Alfred Wegener Institute, Am Handelshafen 12, 27570 Bremerhaven, Germany.
 e-mail: Olga.Ogneva@awi.de

Paul Overduin studies permafrost as a Senior Scientist at the Alfred Wegener Institute Helmholtz Centre for Polar and Marine Research in Potsdam, Germany. He focusses especially on permafrost beneath the Arctic shelf seas and on interaction between permafrost and surface waters.

Address: Permafrost Research Section, Helmholtz Centre for Polar and Marine Research, Alfred Wegener Institute, Telegrafenberg A 45, Potsdam, Germany.
 e-mail: Paul.Overduin@awi.de

Juri Palmtag is a Research Fellow at the Department of Geography and Environmental Sciences at Northumbria University. His research interests range from the spatial distribution of terrestrial soil organic carbon and nitrogen in permafrost-affected soils to carbon dioxide and methane fluxes from nearshore environments.

Address: Department of Geography and Environmental Sciences, Northumbria University, Newcastle-upon-Tyne NE1 8ST, UK.
 e-mail: juri.palmtag@northumbria.ac.uk

Vasily Povazhnyi is a Co-Head of German-Russian Otto-Schmidt Laboratory for Polar and Marine Research in Arctic and Antarctic Research Institute. He is a water ecologist and biogeochemist, studying nutrients and carbon cycling in Siberian Shelf Seas and Lena River delta.

Address: Otto Schmidt Laboratory for Polar and Marine Research, Arctic and Antarctic Research Institute, Beringa 38, Saint Petersburg, Russia 199397.
 e-mail: povazhnyi@aari.ru

Jens Strauss is a Geoecologist who heads the working group on Permafrost Biogeochemistry of the Permafrost Research Section at the Alfred Wegener Institute (AWI) in Potsdam. He has specialized in deep ice-rich permafrost (Yedoma) and his research strives to determine the size of the organic carbon pool frozen in Yedoma, the quality of this carbon, and the speed at which it may be broken down by microorganisms and released in the form of greenhouse gases if it thaws.

Address: Permafrost Research Section, Helmholtz Centre for Polar and Marine Research, Alfred Wegener Institute, Telegrafenberg A 45, Potsdam, Germany.
 e-mail: jens.strauss@awi.de

Robyn Tuereña is a Lecturer in Nutrient Biogeochemistry at the Scottish Association for Marine Science. Her research interests include carbon and nutrient cycling in open ocean and Arctic environments.

Address: Scottish Association for Marine Science, Dunstaffnage, Oban PA37 1QA, UK.
e-mail: robyn.tuerena@sams.ac.uk

Nadine Zell is Master Student at the University of Hamburg. Her master thesis investigate the nitrogen turn-over in Cryosols.
Address: Institute of Soil Science, Universität Hamburg, Allende-Platz 2, 20146 Hamburg, Germany.
Address: Center for Earth System Research and Sustainability, Universität Hamburg, Allende-Platz 2, 20146 Hamburg, Germany.
e-mail: Nadine.zell@uni-hamburg.de

Kirstin Dähnke is Head of the Department for Aquatic nutrient cycles in the institute of Carbon Cycles at Helmholtz Zentrum Hereon. Her research interests include coastal and marine nutrient cycles and stable isotope applications.

Address: Institute for Carbon Cycles, Helmholtz-Zentrum Hereon, Geesthacht, Germany.
e-mail: kirstin.daehnke@hereon.de